DEVELOPMENT OF A MODEL FOR SIMULTANEOUS MEASUREMENT OF RHEOLOGY AND DISSOLUTION FOR *IN SITU* GEL FORMING DRUG DELIVERY SYSTEMS

FARIA GIAS SENJOTI

A thesis submitted to the University of Huddersfield in partial fulfilment of the requirements for
the degree of Doctor of Philosophy

The University of Huddersfield

Submission date: February 2020

Copyright Statement

The following notes on copyright and the ownership of intellectual property rights must be included as written below:

i. The author of this thesis (including any appendices and/ or schedules to this thesis) owns any copyright in it (the "Copyright") and s/he has given The University of Huddersfield the right to use such copyright for any administrative, promotional, educational and/or teaching purposes.

ii. Copies of this thesis, either in full or in extracts, may be made only in accordance with the regulations of the University Library. Details of these regulations may be obtained from the Librarian. Details of these regulations may be obtained from the Librarian. This page must form part of any such copies made.

iii. The ownership of any patents, designs, trademarks and any and all other intellectual property rights except for the Copyright (the "Intellectual Property Rights") and any reproductions of copyright works, for example graphs and Tables ("Reproductions"), which may be described in this thesis, may not be owned by the author and may be owned by third parties. Such Intellectual Property Rights and Reproductions cannot and must not be made available for use without permission of the owner(s) of the relevant Intellectual Property Rights and/or Reproductions. "

Abstract

In situ gel forming drug delivery systems utilize the concept of undergoing sol-gel transitions on exposure to physiological fluids in response to changes in temperature, pH and/or ionic environment. Gelation in response to the changes in pH/ionic contents are particularly difficult to measure in a biorelevant manner as gelation is often too rapid for adequate mixing of physiological fluids with the polysaccharides prior to loading on to a rheometer. Although, several modifications have been applied to conventional rheometers to facilitate changing environmental conditions, modifications that can change the chemical environment of a sample and simultaneously measure release of active ingredients from *in sit*u gelling formulations has yet to be developed. To address this problem a novel method has been demonstrated using a 3D printed rheo-dissolution cell to simultaneously measure the rheological behaviour and dissolution of drug from the *in situ* gelling systems on exposure to physiological fluids. The technique was validated and then used to understand the behaviour of a range of *in situ* gelling formulations.

An *in situ* gel forming ophthalmic formulation of low acyl gellan gum (gellan) (0.4%) and timolol maleate (TM) (6.8 mg/ml) was prepared based on commercial Timoptol LA®. Rheological evaluation and a drug release study were performed separately using the rheo-dissolution device. This study also highlighted the importance of drug-polymer interaction by indicating electrostatic interactions between the positively charged TM and negatively charged gellan. The concept of rheo-dissolution was further explored with the full experimental set up of the rheo-dissolution cell integrated with a rheometer. An *in situ* gelling ophthalmic (gellan-TM) and an oral formulation (alginate- metronidazole) were prepared to evaluate the novel technique. The ophthalmic formulations of gellan-TM

showed rapid onset of gelation on exposure to simulated lacrimal fluid (SLF) (pH 7.5) and release slowed down with increased gellan concentrations (0.6% to 0.8% w/v). Rheo-dissolution experiments performed on the oral formulation of revealed the formation of a strong gel with rapid gelation on exposure to simulated gastric fluid (pH 1.2). Rapid release was observed while the gel was structuring, which then slowed down (~53% in 7h) once gelation was complete. The pH of the media was increased to 8.0, which resulted in a dramatic increase of MNZ release (~96% in 7h) and degradation of the alginate gel. Finally, an *in situ* gelling ophthalmic formulation of gellan was prepared using flurbiprofen (FBP) (a poorly soluble drug) and 2-hydroxypropyl-β-cyclodextrin (HβCD) inclusion complex. This work highlighted the difficulties of incorporating the sodium salt form FBP in *in situ* gelling systems prepared using gellan because of the tendency of gellan to cross link with salts. Besides the rheo-dissolution study, *ex-vivo* permeation study was performed which showed higher percentage of FBP permeation (~55% in 6h) in the inclusion complex formulation compared with FBP sodium in the commercial product Ocufen® (~37% in 6h).

Acknowledgements

I would like to express my gratitude to my supervisor Professor Alan M. Smith for his continuous support throughout my PhD. I appreciate all his guidance, encouragement and constant feedback during the research work. I would like to thank my co supervisor Professor Barbara R. Conway for supporting me with her immense knowledge during the course of my research. I greatly appreciate them for spending their time to respond to my queries so promptly.

I would like to extend my appreciation to Dr Muhammad Ghori for his support for developing and modifying the rheo-dissolution cell. Additionally, I would like to thank the technicians particularly James Rooney, Ibrahim George and Hayley Markham for all their technical support and assistance in the lab. Many thanks to the biopolymer research group for making the biopolymer lab an enjoyable place to work.

Also, I would like to thank each member of my family for their on-going support specially my parents for their irreplaceable encouragement and blessings over all these years. A great appreciation for Barsan who stood by my side during the whole period of the research no matter how hard the time was. It would not been possible to do my PhD without the inspirations from all of them. Thanks to Arisha and Areeb for their long distance love and cheering.

Table of Contents

List of Figures

List of Tables

List of Abbreviations

Å	Angstrom
ABS	Acrylonitrile Butadiene Styrene
ANOVA	Analysis of Variance,
AUC	Area Under the Curve
$CaCl_2$	Calcium Chloride
CAD	Computer Aided Design
DSC	Differential Scanning Calorimetry
ERD	Electro-Rheological Devices
FBP	Flurbiprofen
FTIR	Fourier-Transform Infrared Spectroscopy
GIT	Gastrointestinal Tract
G′	Elastic Modulus
G″	Viscous Modulus
HβCD	Hydroxypropyl-β-Cyclodextrin
HPMC	Hydroxypropyl Methylcellulose
H_2SO_4	Sulfuric Acid
HCl	Hydrochloric Acid
H. Pylori	*Helicobacter Pylori*
LOD	Limit of Detection
LOQ	Limit of Quantification
LVR	Linear Viscoelastic Region
LC	Liquid Chromatography
M	Molar
mM	Millimolar
MC	Methyl Cellulose
MNZ	Metronidazole
MWCO	Molecular Weight Cut-Off
$NaHCO_3$	Sodium Bicarbonate
NaCl	Sodium Chloride
NaOH	Sodium Hydroxide
NSAID	Nonsteroidal Anti-Inflammatory Drug
Pa	Pascal
PSA	Phenol-Sulfuric Acid
R^2	Correlation coefficient
RPM	Revolutions Per Minute
RSD	Relative Standard Deviation
RP-HPLC	Reversed Phase High Performance Liquid Chromatography
SAXS	Small Angle X-Ray Scattering
SGF	Simulated Gastric Fluid
SLF	Simulated Lacrimal Fluid
Stl	Stereolithography
TM	Timolol Maleate
UCST	Upper Critical Solution Temperature
UV/VIS	Ultraviolet–Visible

Chapter 1: Rheology

1.1 Introduction

Controlled drug delivery systems often use synthetic polymers as carriers for the drugs which have been extensively exploited over many decades (Liechty et al., 2010). Among several polymeric drug delivery platforms, *in situ* gel forming drug delivery systems are particularly attractive with increasing demands for the development of easy to use drug delivery platforms (Kang and Majd, 2016). These systems are formulated as free flowing liquids which then undergo sol-gel transition upon administration and convert to gel in contact with the target sites of the body. To effectively design such delivery systems, a thorough understanding of the rheology of the gelation system (gelation kinetics and gel strength) and drug release kinetics are required. An important part of the work in this thesis therefore, involves rheological characterisation of *in situ* gelling formulations using rheological techniques. This chapter outlines fundamental principles of the rheological methods used in this thesis.

The term 'Rheology' was invented by Professor Bingham of Lafayette College, Easton, Pennsylvania; which means the study of the deformation and flow of matter. This definition was accepted in 1929 when the American Society of Rheology was founded. The word ‘rheology’ is derived from the Greek words “rheo” (to flow) and “logos” (science). Rheology describes the deformation of material under the influence of stress (Barnes et al., 1989; Schramm, 1994). The stress applied to a material is defined as the force per unit of area and strain is the deformation as a result of the applied stress.

When stress is applied to a material, two extreme behaviours may result which is either solid or liquid. These extremes are basis for two broad categories into which the materials can be

divided and these are ‘liquid-like’ and ‘solid-like’ corresponding to a perfect (Newtonian) liquid or and a perfect (Hookean) solid. From the rheological point of view, ‘solid-like’ behaviour is described as elastic and ‘liquid-like’ behaviour is described as viscous. There are some materials, such as polysaccharides, that have both elastic and viscous behaviour and are referred as ‘viscoelastic’, (Ibarz et al., 2002; Mezger, 2006; Marriott, 2007).

The rheological measurement of a product during the development stage often serves as a control of quality for the product. However more detailed information about the microstructure of a product can be revealed from rheological measurements. Rheological techniques and methods have been employed for many decades for the characterization of polymers which plays a significant role in designing polymer based products (Ibarz et al., 2002). Most of the experimental work in this thesis is based on the rheological measurement of *in situ* gelling polymers on exposure to the crosslinking ions. So the basic concepts of rheology are discussed in this chapter. To understand the basic concept of rheology, it is necessary to understand the principle of rheology and some basic terms that are used for rheological analysis.

1.2 Stress and Strain

A force has to act on a material for a deformation to occur. Stress is the intensity factor of force, expressed as force (F) per unit area (A) and can be determined by using Equation 2.1.

$$Stress\ (Pa) = {}^{F}/_{A} \qquad \textbf{\textit{Equation 2.1}}$$

Stress can be categorized in three ways according to the way it is applied. These are compressive/tensile stress, shear stress and bulk stress. Compressive stress acts towards the plane in which it is acting and resulting in shortening an object. Tensile stress acts away from the plane in which it is acting resulting in lengthening an object. Shear stress acts

tangentially to the plane and in bulk stress; and force is applied from all areas. Figure 2.1 illustrates the forces applied in longitudinal, lateral and isotopic direction on a solid material. When the material is stressed, a deformation occurs which is expressed as strain (unit less). Strain can be calculated using Equation 2.2.

$$Strain = {}^{\Delta L}/_{L} \quad \textbf{\textit{Equation 2.2}}$$

Where L is the length of the material which is subjected to stress and ΔL is the change in length.

The mechanical properties of a material can be determined by the relationship between stress and strain which is also called modulus. In case of liquid material, the change in strain is another important parameter which is expressed as strain rate or shear rate (s^{-1}) and can be determined by Equation 2.3.

$$\dot{\gamma} = {}^{d\gamma}/_{dt} \quad \textbf{\textit{Equation 2.3}}$$

Where $\dot{\gamma}$ is the strain rate and dγ/dt is the change in strain with time (Harnett, 1989).

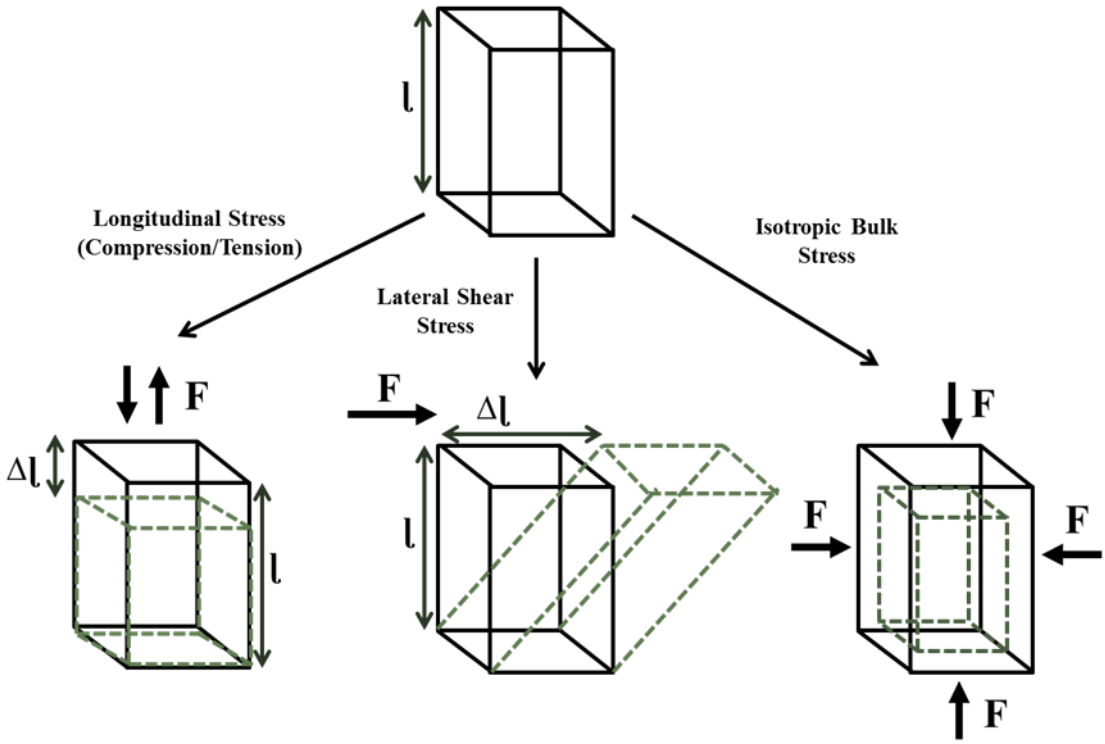

Figure 1.1: Schematic diagram of deformation when a solid material is subjected to forces applied in longitudinal, lateral and isotopic direction (Mahdi, 2016)

1.3 Young's Modulus

Hooke's law by Hooke (Hooke, 1678) states that in deformation of solids, stress is proportional to strain and independent of strain rate. A material exhibiting Hookean behaviour is defined as; when stress is applied to the material it deforms and the material returns to its original shape and size instantly upon removal of the stress, for example, a spring. In case of Hookean solids, stress and strain maintain an instantaneous relationship which means if the stress component is doubled, its contribution to each of the strain components will also be doubled. There will be no time lag between stress and strain change (Barnes et al., 1989).

The coefficient of proportionality of Hooke's law is called Young's modulus. It is useful to analyse the relative strength of a solid material which has defined size and shape and having

self-supporting capabilities. When a perpendicular force is applied to that solid material, energy is stored and the material returns to the original form upon releasing the force. Young's modulus (Pa) is calculated by dividing the extensional (tensile) stress by the corresponding extensional strain of the solid material and expressed in Equation 2.4.

$$E = {}^{\tau}/_{\varepsilon} \quad \textbf{\textit{Equation 1.4}}$$

Where, E is the Young's modulus, τ is stress and ε is strain. (Barnes, 2000).

1.4 Shear Modulus

The shear modulus is used for the deformation which takes place when a material is subjected to parallel force (shear stress) and it deforms through a specific angle. Shear modulus is useful for the materials which are not self-supporting, for example viscoelastic materials. It is used to determine the rigidity of a material. Shear modulus (Pa) can be expressed as a ratio of shear stress and shear strain. The shear stress can be expressed by the equation 2.5.

$$\sigma = {}^{F}/_{A} \quad \textbf{\textit{Equation 1.5}}$$

Where σ is the shear stress (Pa), F is parallel force and A is the area. The resulting shear strain can be expressed by equation 2.6.

$$\gamma = {}^{\Delta l}/_{l} = tan(\theta) = \theta \quad \textbf{\textit{Equation 1.6}}$$

Where γ is the shear strain, Δl is the tangential displacement; l is the material thickness and θ is the angle of deformation.

So the shear modulus (G) can be defined by the equation 2.7.

$$G\ (Pa) = {}^{\sigma}/_{\gamma} = {}^{\frac{F}{A}}/_{\frac{\Delta l}{l}} = {}^{Fl}/_{A\Delta l} \quad \textbf{\textit{Equation 1.7}}$$

Larger shear moduli represent more rigidity because more shear stress is required for the same tangential deformation (shear strain). This is why the shear modulus is also called the modulus of rigidity (Mahdi, 2016; Moxon, 2016).

1.5 Bulk Relaxation Modulus

Bulk relaxation modulus is the modulus of volume expansion. It is defined as the ratio of the isotropic stress to the relative strain in volume. When a solid material is subjected to isotropic stress, relative change of volume is observed and it can be expressed by the Equation 2.8.

$$K\ (Pa) = {}^{\sigma_v}/_{\varepsilon_v} \quad \textbf{\textit{Equation 1.8}}$$

Where K is the bulk relaxation modulus, σ_v is the bulk stress and ε_v is the volumetric strain. Bulk relaxation modulus is rarely used for the characterization of viscoelastic materials such as biopolymer gels. It is used in operating hydraulic systems at high pressure to measure the resistance of the substance to compression.

1.6 Rheological Analysis

To understand the flow behaviour of a material, it is necessary to understand the basic rheological measurements; for example, viscosity and oscillation. The basic measurement techniques provide an idea whether the material is ‘elastic’, ‘viscous’ or ‘viscoelastic’. Rheology is extremely important for polymers because to process and fabricate the polymers, it is necessary to understand their flow behaviour (Al-Fariss and Al-Zahranl, 1993). However, it is necessary to understand the basic principle of a commercial rheometer before explaining the common rheological analysis.

1.6.1 Rheometer

An oscillatory controlled stress rheometer is used for rheological analysis. The essential features of this type of rheometer consists of a vertically mounted motor, geometry and Peltier plate (Figure 2.2). The motor is usually attached to the upper fixture. A top surface is attached to the motor which is called the geometry. The geometry can be of several types depending on the type of samples; for example, parallel plate, cone/plate and serrated plate geometry.

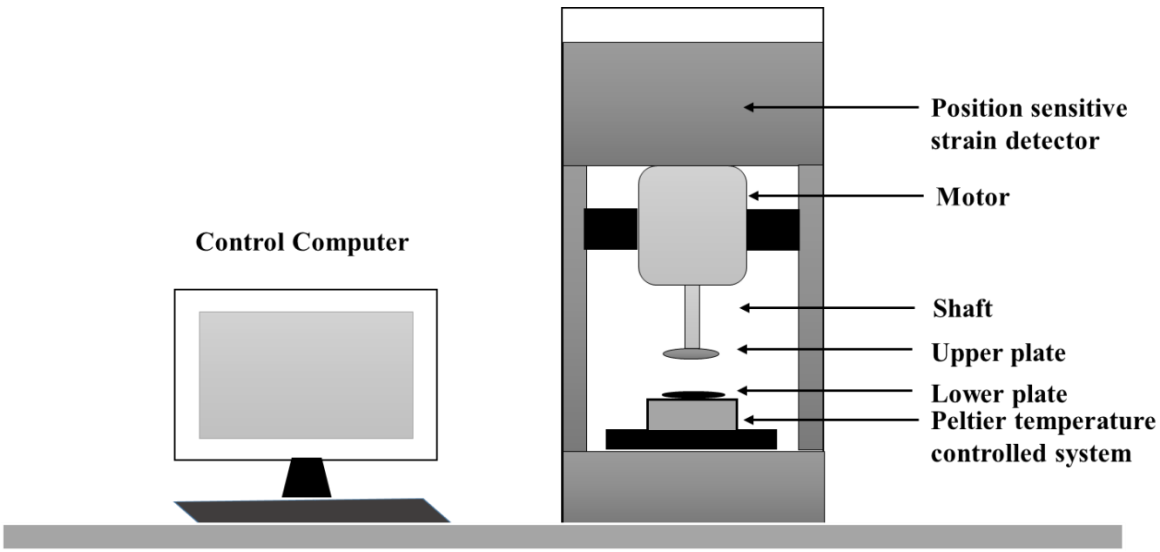

Figure 1.2: Schematic diagram of a typical controlled stress rheometer

In the controlled stress rheometer, the lower surface is fixed and is capable of controlling the temperature. The test material is placed between the upper and lower surface. A computer-generated voltage is applied to the motor to produce stress. The induced strain can be measured using an optical encoder or radial positions transducers which are connected to a control computer.

The chosen geometry directly impacts upon the rheological analysis because stress is transmitted to the sample in different way through different geometries. Parallel plate (Figure 2.3A) and cone-plate (Figure 2.3B) are the most common types of geometries.

Parallel plate geometry offers the advantage of adjusting the gap size and can be used to test a wide range of materials especially when there are small particles in the samples. It is also useful when there is need to change the shear rate range. Larger strain can be applied when using parallel plate geometry and it is widely used in industry due to its flexibility. However, the shear stress is much greater at the outer radius than the inner radius, which results in the generation of non-uniform strain field. When using a cone-plate geometry, the gap is fixed during the experiments which limits the range of shear rates. It is suitable for small sample size (0.5-2.0 ml) which ensures rapid temperature equilibration. The shear rate and shear stress are constant through the gap which results in uniform strain field (Song et al., 2017). It is used in the rheological measurements of single phase liquids.

When rheological measurements are carried out on structured liquids (*e.g.* suspensions, foams, or emulsions), a phenomenon can occur which is called 'slippage'. This happens due to local depletion of the dispersed phase near the geometry surface which causes formation of a lubrication layer at the surface. To avoid this, serrated or roughened plates (Figure 2.3C) are used for rheological measurements.

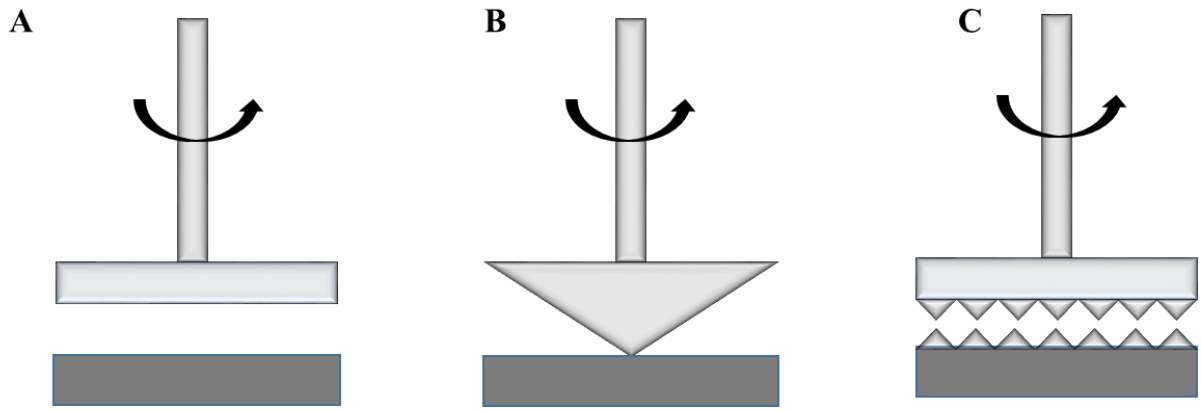

Figure 1.3: Schematic illustration of different types of geometry (A) parallel plate (B) cone-plate (C) serrated plate

Geometry diameter is another factor by which the measurements can vary. To analyse stiffer materials, small diameter geometries are more suitable whereas large geometries (having large surface contact) are better suited for weak or low viscosity materials because these materials can spread over a large surface area upon applying stress.

1.6.2 Viscosity

The term viscosity came from the Latin viscum, the mistletoe, which exudes a gelatinous juice when squeezed (Barnes, 2000). It can be defined as resistance to flow which is a result of internal friction of the molecules within a fluid. This is an important property in controlling the quality of products that are expected to be of particular consistency, such as paste, cream (Lewis, 1996). Viscosity can be expressed by the Equation 2.9 which is based on Isaac Newton's principle stating the flow of liquid is directly proportional to the applied stress.

$$\eta = {}^{\sigma}/_{\dot{\gamma}} \qquad \textbf{\textit{Equation 2.9}}$$

Where η is the viscosity (Pa), σ is shear stress and $\dot{\gamma}$ is rate of shear.

1.6.3 Newtonian and Non-Newtonian Systems

A Newtonian fluid's viscosity is independent of shear rate. The viscosity of Newtonian fluid remains constant, no matter the amount of shear stress applied. Some materials, such as oil and water can behave as Newtonian fluids under certain environmental conditions. In the case of Newtonian fluids, shear stress is linearly proportional to the shear strain rate. Non Newtonian fluids are opposite of Newtonian fluids and viscosity changes when shear is applied to these fluids (Steffe, 1996; Marriott, 2007).

1.6.3.1 *Shear Thinning and Shear Thickening Fluids*

There are several classes of non-Newtonian fluids which can be characterised by flow curves as a plot of shear stress and shear rate (Figure 2.4). Shear thinning fluids are most widely encountered type of non-Newtonian fluid behaviour. Shear thinning fluids exhibit the viscosity which gradually decreases with increasing shear rate. These are also called pseudoplastic fluids; for example paint. There is another class of non-Newtonian fluids where viscosity increases with increasing shear rate, these are called shear thickening or dilatant fluids; such as wet sand, corn starch suspensions or ceramic suspensions. Newtonian, shear thinning and shear thickening behaviour of fluids can be expressed by a single mathematical equation (Equation 2.10).

$$\sigma\ (Pa) = K\ \dot{\gamma}^{n} \qquad \textbf{\textit{Equation 2.10}}$$

Where K is the consistency index and n is the flow index. n = 1 in Newtonian fluids, n > 1 in shear thinning (pseudoplastic) fluids and n < 1 in shear thickening (dilatant) fluid (Barnes et al., 1989).

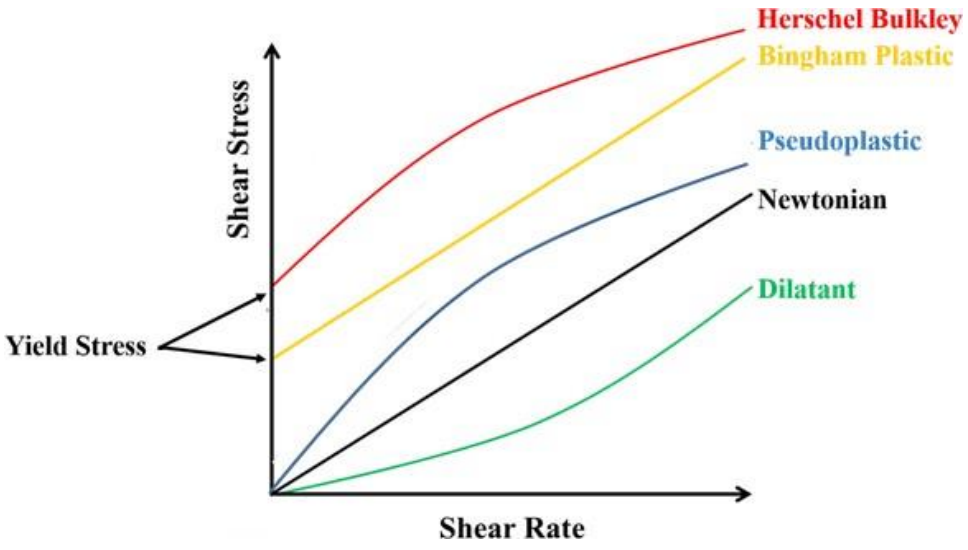

Figure 1.4: Different types of flow behaviour of Newtonian and Non-Newtonian Systems (Tagha, 2011)

1.6.3.2 *Plasticity and Yield stress*

Yield stress is defined as minimum shear stress to be exceeded for flow of a fluid to begin. Materials that begin to flow in a Newtonian manner once the yield stress is exceeded are termed Bingham plastic materials. This behaviour can be expressed by Equation 2.11.

$$\sigma\ (Pa) = \sigma_0 + \eta\dot{\gamma} \qquad \textbf{\textit{Equation 2.11}}$$

Where σ_0 is the yield stress.

If a material reaches its yield stress and the system then starts to flow in a shear thinning manner, it is classified as a Herschel Bulkley fluid. Materials that have Herschel Bulkley flow behaviour therefore, have shear thinning and yield stress properties (Barnes et al., 1989; Mahdi, 2016). This type of flow behaviour can be expressed by Equation 2.12.

$$\sigma\ (Pa) = \sigma_0 + K\,\dot{\gamma}^n \qquad \textbf{\textit{Equation 2.12}}$$

Biopolymer solutions generally show shear thinning behaviour. There are some factors which directly influence the shear thinning behaviour, such as molecular weight, charge and concentration. Biopolymer solutions follow a Newtonian behaviour when dis-entanglement and re-entanglement occurs at the same rate. When there is a disruption of entanglements with shear rate and the rate of dis-entanglement is greater than the rate of re-entanglement, the viscosity of the solutions start to decrease as a result of reduced entanglement density (Koliandris et al., 2008).

1.6.4 Intrinsic Viscosity

Intrinsic viscosity is one of the most essential properties of polymer and is extensively used to determine the size, structure and molecular weight of polymers. It can be defined as a measure of a solute's contribution to the viscosity of a solution in which it is dispersed. It

provides an insight to the interaction between the molecular weight of the polymeric molecule and the solution (Lee and Tripathi, 2005; Lu et al., 2013). Because molecular weight has a direct impact on molecular entanglement, viscosity and degree of crosslinking between polymer molecules.

1.6.5 Rheological Measurements of Biopolymer Gels

The conventional industry approach for characterising the rheological properties of liquid products is mainly through the use of destructive rheological techniques using viscometer or a rheometer. Using this technique can irreversibly alter the flow behaviour and structure of the sample, which may not represent the actual quality of the product (Seman et al., 2009). Using destructive rheological techniques, the system is under the shear stress until the elasticity (G') breaks which is inappropriate for biopolymer gel samples. However, non-destructive rheological techniques allow assessment of the processes that take place at the molecular level of the sample, which is necessary to understand for developing polymeric gelling formulations. In these tests, the elasticity (G') is independent of shear stress and measurements are performed using fixed or increased oscillatory frequency (Mendoza, 1998). The non-destructive technique is also called an oscillatory dynamic test (Ozer et al., 1997) and it does not irreversibly deform or alter the structure of the sample. Therefore, viscoelastic behaviours of biopolymer gels are widely performed using non-destructive rheological techniques. All rheological measurements in this work have been conducted using non-destructive techniques.

1.6.6 Viscoelasticity and Oscillation

The word 'viscoelastic' refers to the simultaneous existence of viscous and elastic properties in a material. Viscoelasticity is the property of materials that exhibit both viscous and elastic characteristics when undergoing deformation. (Barnes et al., 1989; Papanicolaou and Zaoutsos, 2011). It is one of the most important properties of biopolymer materials. To characterize both ‘solid like’ and ‘liquid like’ behaviour of viscoelastic materials, oscillatory measurements are generally used which allow simultaneous analysis of both responses on applied stress (Picout and Ross-Murphy, 2003)

During oscillatory measurements, the viscoelastic samples are subjected to oscillating stress or oscillating strain instead of constant stress. The stress (or strain) is usually applied as a sinusoidal time function to a sample immobilised on a geometry of a rheometer and the rheometer then measures the result as a strain (Schramm, 1994).

If the material is perfectly elastic and the stress is proportional to strain, the stress wave will be exactly in phase with the strain wave where the phase angle (δ) will be 0º. In contrast, the resultant stress wave will be exactly 90º out of phase for purely viscous systems. For a viscoelastic material, the stress wave will have a phase difference and δ will be between 0º and 90º (Picout and Ross-Murphy, 2003). Figure 2.5 represents the stress wave resulting from the applied strain for elastic, viscoelastic and viscous material.

The viscoelastic behaviour of the system is characterised by the modulus, which is defined as the ratio of stress and strain. The solid-like (elastic) and the liquid-like contributions (viscous) of a viscoelastic material are represented by the elastic modulus (G′) and viscous modulus (G") respectively (Weitz et al., 2007).

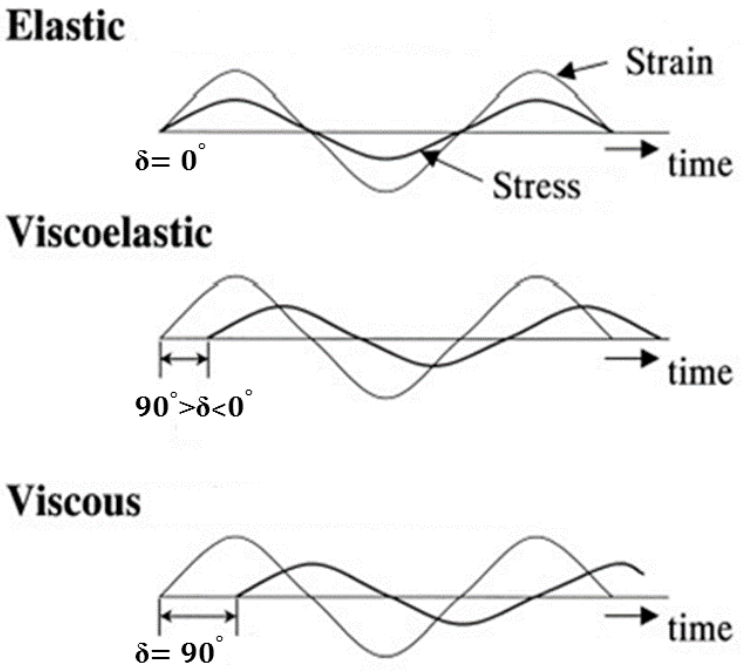

Figure 1.5: Illustration of relationship between stress and strain during a sinusoidal oscillating strain for elastic material where the phase difference between stress and strain (δ) is 0°, viscoelastic material where 90°>δ< 0°, and viscous material where δ=90° (Tanaka et al., 2003)

The elastic modulus (G′) is defined as the ratio of in phase stress and strain under sinusoidal conditions. It is also known as the storage modulus. It indicates the elastic (solid) characteristic of the material under deformation. It can be calculated using Equation 2.13.

$$G'\,(Pa) = \left(\sigma^{\circ}/_{\gamma^{\circ}}\right) cos\,\delta \qquad \textbf{\textit{Equation 2.13}}$$

The viscous modulus (G") is defined as the ratio of out of phase stress and strain under sinusoidal conditions. It is also known as the loss modulus. It indicates the viscous (liquid) characteristic of the material under deformation. It can be calculated using Equation 2.14.

$$G"\,(Pa) = (\,\sigma^{\circ}/_{\gamma^{\circ}})\ sin\,\delta \qquad \textbf{\textit{Equation 2.14}}$$

Complex modulus (G^{*}) is another parameter of viscoelastic system which is defined as overall stress response to the strain regardless of whether the response is elastic or viscous.

It can be calculated using Equation 2.15.

$$G^* = \sqrt{(G')^2 + (G'')^2} \qquad \textbf{\textit{Equation 2.15}}$$

Complex dynamic viscosity (η^*) is derived from complex modulus. This is defined as the ratio between complex modulus (G^*) and frequency of oscillation (ω) and it can be calculated using Equation 2.16.

$$\eta^* = {}^{G^*}/_{\omega} \qquad \textbf{\textit{Equation 2.16}}$$

This is an important parameter of the Cox-Merz rule which is based on the relationship between the rheological response of destructive and non-destructive deformation of biopolymer solutions. If the biopolymer solutions are free from physical interaction and aggregation (only simple entanglement), the solutions follow the Cox-Merz rule according to which, η^* should be almost similar to the shear viscosity (as a function of $\dot{\gamma}$) (Picout and Ross-Murphy, 2003).

1.6.6.1 *Linear Viscoelastic Region*

Identification of the linear viscoelastic region (LVR) is necessary to determine the rheological properties of a viscoelastic material. An applied stress produces a proportional stress response within the LVR; as a result, for example, doubling the stress will double the strain response. The amplitude of stress is increased gradually at a constant temperature until the deformation occurs and the modulus start to decline. G′ and G" are the parameters that are used to determine this region.

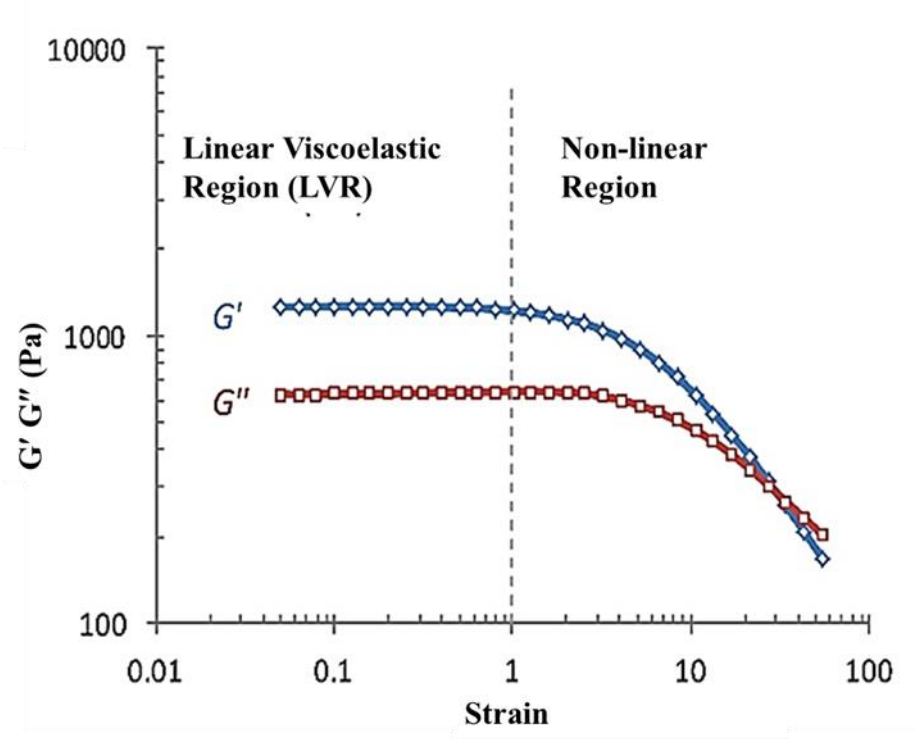

Figure 1.6: An example of amplitude sweep test for the assessment of viscoelastic region of a sample at 1 Hz (6.28 rad/s) frequency (Krishnaiah et al., 2014)

When the deformation occurs as a result of excessive stress, the testing enters the non-linear range. The determined LVR is used for other rheological analysis, for example; measurements of the elastic and viscus modulus on changing oscillatory frequency to determine the characteristic of polymer solutions with constant stress. The simple and convenient method of determining the LVR is by performing amplitude sweep measurements. Figure 2.6 illustrates a typical example of the identification of viscoelastic region of a sample at a frequency of 1 Hz (6.28 rad/s).

1.6.6.2 *Frequency Sweeps*

The variation of G′ and G" with the frequency is known as a frequency sweep or the mechanical spectrum of a viscoelastic material (Morris et al. 2012). Frequency sweeps are determined by changing the oscillatory frequency at a constant stress or strain. The

temperature is kept constant during the test. Complex dynamic viscosity (η^*) is also included in the determination of frequency sweeps and normally plotted on logarithmic axes against a range of oscillation frequencies. Frequency dependence of a material is an important parameter that can help determine the characteristic of polysaccharide samples.

The frequency sweep of dilute polymer solution is characterised by predominance of viscous modulus (G") over elastic modulus (G′). The moduli increases with increased frequency of oscillation (ω) but the complex dynamic viscosity (η*) is independent of frequency (Figure 2.7A)**.** Because, polymer molecules are free to move and do not entangle with each other in dilute solutions, so there is no resistance to deformation which mainly derives from flow of molecules (Morris et al., 2012).

At high polymer concentration, polymer molecules form an entangled network by interpenetrating with each other (Graessley, 1974). At low frequency, the concentrated polymer solutions behave like liquid (dominancy of G" over G′) and η^* is independent of ω; because there is sufficient time for disentanglements of the polymer molecules within the period of oscillation. At high frequency, the polymer samples exhibit solid like behaviour (dominancy of G′ over G") and η* decreases as the frequency increases (Figure 2.7B). Because, there is less time for disentanglement within the period of oscillation and the elastic behaviour become predominance for the entangled network (Morris et al., 2012).

The term ‘weak gel’ or structured fluid refers to the free-flowing polymer solutions which exhibit predominant elastic behaviour (G′ is higher than G") and can be stirred, poured like other normal solutions. These polymer solutions show elastic response to small deformation and are unable to self- support.

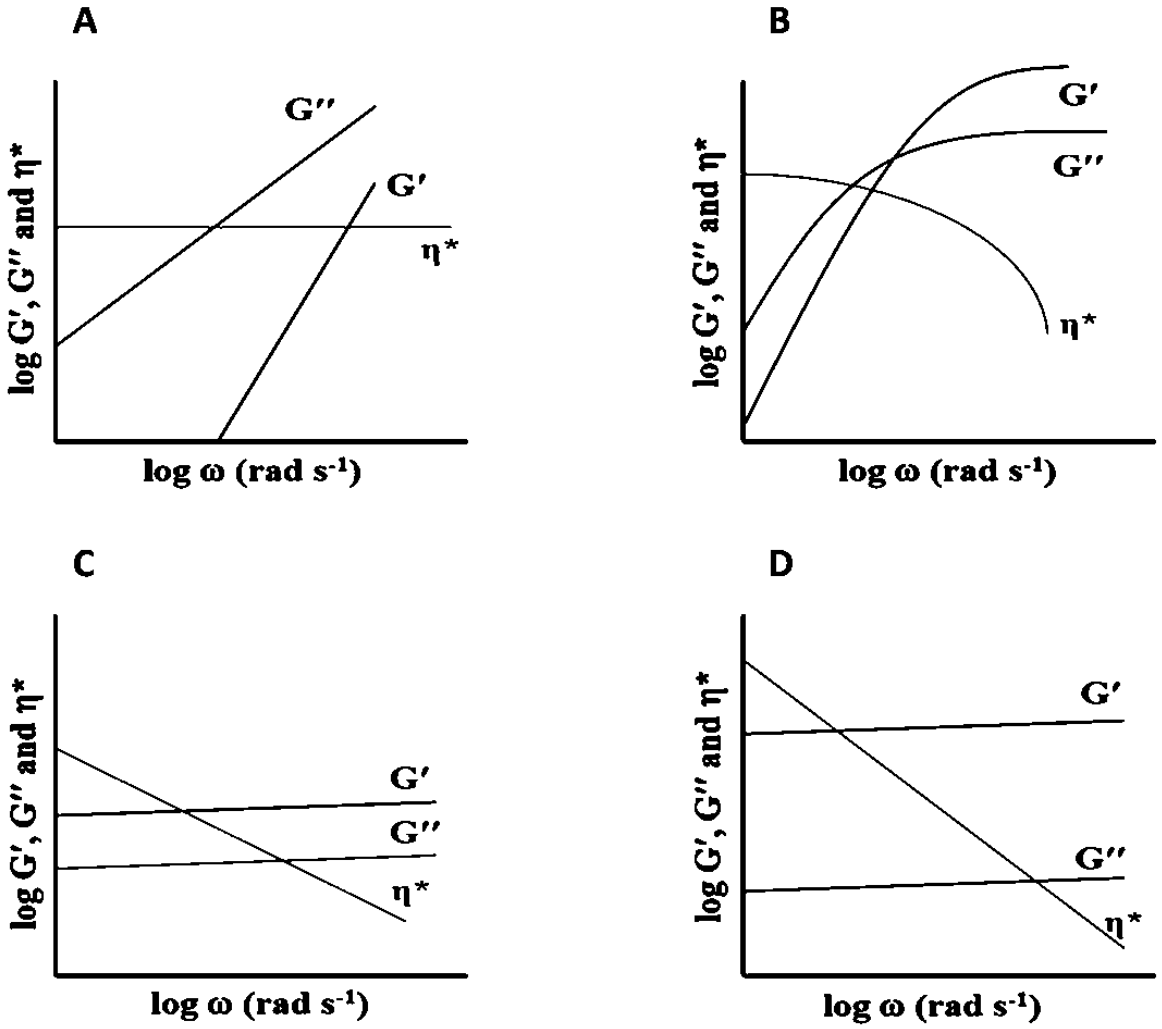

Figure 1.7: Schematic representation of frequency sweeps of four different polysaccharide samples (A) dilute polymer solution (B) concentrated polymer solution (C) weak gel (D) true gel (Morris et al., 2012).

The common feature of a structured fluid is having rigid and ordered structure of polymer molecules which are tenuously associated. The frequency sweep of weak gel is characterised by frequency dependent moduli and linear relationship between η^* and ω (Figure 2.7C). The conventional 'true' gel fractures in response to high stress where a structured fluid would flow. The other terms which are used to describe weak gels are 'pourable gel', 'fluid gel' or 'structured liquid' (Morris et al., 2012). Typical examples of structured fluids are solutions of xanthan and schizophyllan.

Frequency sweeps of true gels are characterised by higher G′ than G". The difference between two moduli is much higher than weak gel and η* decreases as ω increases (Figure 2.7D). Sometimes G′ is 5 to 10 times greater than G" (Picout and Ross-Murphy, 2003). True gels are also described as ‘self-supporting’ or ‘demouldable’ (Morris et al., 2012) and they cannot be stirred or poured.

1.6.6.3 *Temperature Sweeps*

Temperature sweeps are vital rheological experiments as many polymers undergo sol-gel (or gel-sol) transitions upon changing temperature. Samples are loaded onto a temperature controlled lower plate of a rheometer and measurements of G′ and G" are taken as a function of temperature. Analysis is performed within the LVR of the polymer and the strain and frequency are usually kept constant throughout the test. Any gelation (or melting) events are observed with changes in G′ and G" (Figure 2.8).

The examples of biopolymers that undergo sol-gel transitions upon cooling are gellan, gelatin, and κ-carrageenan (Clark and Ross-Murphy, 2009). There are some biopolymers whose gelation is triggered by heating; for example; collagen and methylcellulose.

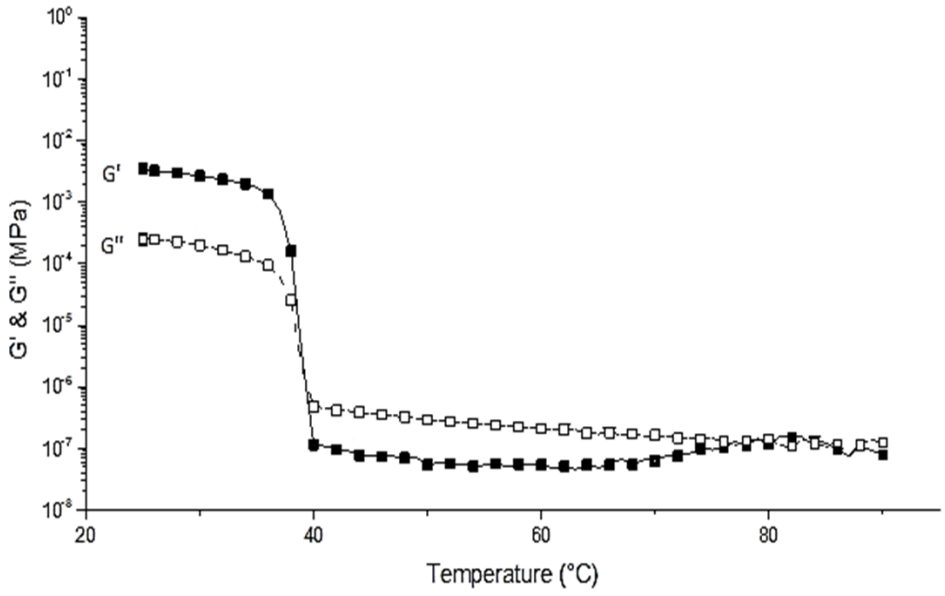

Figure 1.8: Example of temperature sweep of gellan gum showing changes in G′ and G" upon cooling (gelation temperature is around 40°C) (Ana et al., 2016)

1.7 Adaptations and Limitations of Commercial Rheometers

The gel forming polysaccharides undergo physical and chemical changes due to changes in the physiological environment. Many polysaccharides show sol-gel transition in response to changes in temperature or pH. Sometimes they undergo sol-gel transition via a cross linking reaction between polymer chains due to presence of ions in physiological fluid. Rapid gelation behaviour of a polysaccharide due to changes in temperature can easily be analysed using commercially available rheometers. However, monitoring the sol-gel transitions in real-time due to changes in pH or presence of cross linking ions is still not possible using commercially available rheometers. To understand polymer behaviour during gelation, various modifications to commercial rheometers have been developed either to stimulate an application/industrial process or from characterisation perspective.

In some of these modifications, rheological equipment is added to a spectroscopic technique such as rheo-Raman. In this technique, rheometer is combined with a quartz outer cylinder

to a Raman spectrophotometer. *In situ* monitoring of free-radical polymerization of acrylic acid has been reported using the rheo-Raman (Chevrel et al., 2012). Somani et al., (2002) investigated the nature of shear induced precursor structures of isotactic polypropylene by using the *in situ* rheo- small angle X-ray scattering or rheo-SAXS. During the experiment, isotactic polypropylene was melted at 165°C by rheo-SAXS and SAXS pattern showed the oriented structures upon the termination of shear. Recently, a new technique has been reported which couples an optical microscope and Raman spectrometer to a rotational rheometer (Kotula et al., 2016). This combined technique is advantageous where the rheological behaviour is influenced by conformational or chemical changes in molecular structure, such as gelation, crystallization or melting. A light curing lower plate is another adaptation where the lower glass plate is fitted with UV and visible light source and are particularly useful for studying light curable polymers. The gelation of chemically modified polysaccharides upon UV irradiation can also be analysed using this type of adapted rheometer (Higham et al., 2014). Some fluids change their rheological properties upon application of magnetic fields which are known as magneto rheological fluids (MRF), such as magnetisable particles (cobalt or iron) dispersed in silicone or mineral oils (Hao, 2005). To apply magnetic fields on MRF and analyse the influence of the magnetic fields, a Magneto-Rheological Device (MRD) has been developed where more than 1 Tesla of magnetic field strengths can be applied to observe the rheological changes. Electro-rheological Devices (ERD) have also been developed which allow the application of electrical fields to measure the rheological changes of materials when subjected to electric fields (Läuger, 2009). Immobilization cell is another accessory which can be coupled to a controlled stress rheometer to analyse the rheological changes of some materials (such as paints, sludge) during the process of dewatering (Ayol et al., 2010).

Although some of these modifications can measure rheological changes *in situ* (*i.e* light

curing cell, ERD and MRD), none of these however, can monitor changes when crosslinking is initiated by changes in pH or ionic concentration, as occurs when an *in situ* gelling drug delivery system is administered. Moreover, release of active ingredients from gel forming drug delivery systems can be influenced by rheological changes, which need to be analysed for successful formulation development. It would therefore, be a great advantage to the pharmaceutical industry and formulation scientists if the release of drugs could also be monitored during the process. Here, a novel method has been demonstrated which could address these current limitations by replacing the lower plate of the conventional rheometer with a 3D printed cell capable of measuring the rheological changes and drug release simultaneously.

This thesis consists of two further introductory chapters before proceeding to the result chapters. Chapter 2 demonstrates the basic concepts of *in situ* gel forming drug delivery systems. Besides showing the general mechanisms of *in situ* gelation, this chapter presents a few examples of reported *in situ* gelling systems. Current techniques used to investigate *in situ* gelation are also discussed in this chapter.

Chapter 3 provides the general background of the gel forming polysaccharides along with structure and conformation. It presents the in depth concepts of gelation of polysaccharides and different stimuli to induce gelation. Profiles of the polysaccharides used in the experiments presented in this thesis are described in detail.

Chapter 2: General Introduction of *In Situ* Gel Forming Drug Delivery Systems

2.1 Introduction to *In Situ* Gel Forming Drug Delivery Systems

Controlled drug delivery systems are one of the most progressing areas of drug delivery technology with numerous advantages compared to the conventional drug delivery systems. They can offer improved efficacy of drugs by controlling the release over an extended duration (Uhrich et al., 1999). Reduced toxicity, improved patient compliance and convenience are other advantages of these delivery systems. In particular, these systems are beneficial for the drugs that are rapidly metabolized and have a tendency to eliminate from the body after administration (Uhrich et al., 1999). Polymers have played an essential role in the advancement of controlled drug delivery technology by providing controlled release of both hydrophilic and hydrophobic drugs in consistent doses over a long period (Liechty et al., 2010). Polymeric controlled drug delivery systems can effectively be delivered to a target site which enhance the therapeutic effects of the drugs (Soppimath et al., 2001).

Among several polymeric drug delivery platforms, *in situ* gel forming drug delivery systems are particularly attractive and they can be formulated to be administered via oral, ocular, nasal, vaginal and rectal routes (Madan et al., 2009).These systems are formulated as liquid and convert to gel upon exposure to the physiological environment of the body.

2.2 General Mechanism of *In Situ* Gelation

Mucous membranes line the tracts and structures of the body which include the nose, mouth, eyelids, trachea, lung, stomach, intestine, urethra, uterus, urinary bladder, vagina and anus. Although types of cells in a mucosa vary from organ to organ, generally mucosa consists of layers of epithelial cells which are responsible for secreting mucus. Mucus is responsible primarily for protection and lubrication. It is composed primarily of water (~95%), lipids (phospholipids, cholesterol and fatty acids), proteins and mucin (Bansil and Turner, 2006). Under the epithelial cells, there are deep layers of connective tissues. The epithelium layer of mucosa consists of either simple columnar epithelium cell or stratified squamas epithelial cells (Guyton and Hall, 2005; Augustyn et al., 2018).

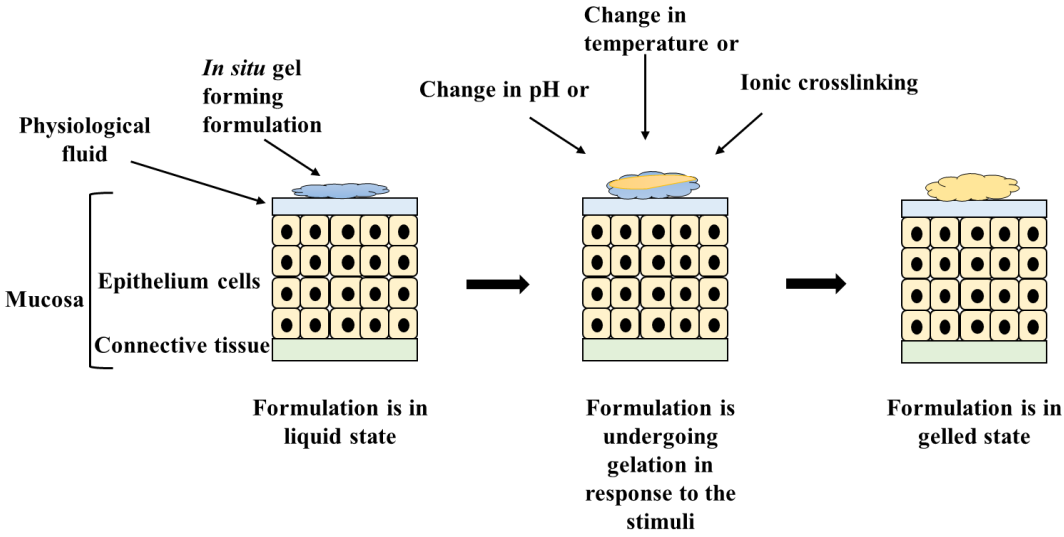

Figure 2.1: Schematic representation of *in situ* gelation in physiological environment

When an *in situ* gel forming formulation comes in contact with the mucosal layer of the body, the formulation starts to undergo gelation in response to the physiological conditions of the mucosa (Table 2.1). Gelation can be triggered *in situ* by changes in temperature, pH or ionic strength of the physiological fluid present on mucosa of different site of actions (Figure 2.1) (Ruel-Gariépy and Leroux, 2004).

Table 2.1: Physiological conditions (pH, temperature and ionic content) of different physiological sites

***In situ* Gelling Drug Delivery Systems**	**Physiological Site of Actions**	**Physiological Conditions**		
		pH	**Temperature °C**	**Ions**
Oral	Gastric fluid in GI tract	1.5 to 3.5 (fasted condition) (Marieb and Hoehn, 2010) 3 to 7 (fed condition) (Ashford, 2007)	37	H^+
	Saliva in oral cavity	5.3 to 7.8 (Gittings et al., 2015)	37	Na^+. K^+, Ca^{2+}, Mg^{2+} (Marques et al., 2011)
Nasal	Nasal mucosa	5.5 to 6.5 (England et al., 1999)	29 to 34 (Bhandwalkar and Avachat, 2012)	Na^+. K^+, Ca^{2+} (Cao et al., 2009)
Vaginal	Vaginal fluid	4.2 (Chang et al., 2002)	37.2 (Chang et al., 2002)	Na^+. K^+, Ca^{2+} (Rashad et al., 1992)
Ophthalmic	Lacrimal fluid	7.4 (Marques et al., 2011)	35 (Wei et al., 2002)	Na^+. K^+, Ca^{2+} (Marques et al., 2011)

In situ gelling systems are usually formulated with thermosensitive, pH sensitive or ion-activated polymers which are responsible for the activation of the stimuli present in the mucosa. For example, pH sensitive polymers undergo gelation in high or low pH depending on the ionisable groups present in the polymer. Such as, poly (N,N′ -diethylaminoethyl meth acrylate) is a cationic polymer and poly(acrylic acid) is anionic polymer (Qiu and Park, 2001). Most of the anionic pH sensitive *in situ* gelling polymers used in *in situ* gelling

formulations are based on poly(acrylic acid) (carbomer, Carbopol®) or its derivatives (Nirmal et al., 2010).

Srividya et al. (2001) developed a pH triggered *in situ* gelling ophthalmic formulation of fluoroquinolone, which is used in the external infections of the eye, such as keratoconjunctivitis and bacterial keratitis. Carbopol® was used as an *in situ* gelling polymer and hydroxypropylmethylcellulose (HPMC) was used as viscosity enhancing agent in the formulation. The formulation was in the liquid state at formulated pH (6.0) and underwent sol-gel transition at physiological pH (7.4). The formulation was able to provide sustained release of drug over an 8-hour period.

Thermoreversible polymers undergo sol-gel transition in response to the changes in temperature and the formed gel can change back to the solution state if the temperature change is reversed (Borchard, 1998). Pluronics®, Tetronics® (Qiu and Park, 2001), poloxomer (Nirmal et al., 2010) are the most commonly used thermoreversible polymers. Qian et al. (2010) developed thermosensitive *in situ* gelling ophthalmic drug delivery system of methazolamide to minimize intra ocular pressure using poloxamers (P407 and P188). The formulation was in free flowing liquid state at 25 ± 0.1°C and underwent sol-gel transition in the cul-de-sac in response to the physiological temperature (35 ± 0.1°C) upon administration into the eye. Methazolamide was then released in a controlled manner for over 10 hours from the *in situ* gel of poloxomer formulation.

Besides synthetic/semi-synthetic polymers, polysaccharides have been extensively used to formulate the *in situ* gelling systems. They are widely used to formulate ion induced *in situ* gelling formulations because of their ability to form gels in response to the physiological ion concentrations. Also, they have the ability to undergo sol-gel transition in response to the

changes in pH and/or temperature. Physical crosslinking methods and nontoxic nature are other advantages of using polysaccharides to formulate such delivery systems (Bae and Park, 2016). Gellan gum (Rajinikanth and Mishra, 2008; Diryak et al., 2018), pectin (Kubo et al., 2004), carrageenan (Endo et al., 2000) and alginate (Flink and Johansen, 1985) are all examples of polysaccharides that can undergo gelation by ionic crosslinking and/or change in pH and therefore of have been of interest to researchers as *in situ* gelling materials for use at various physiological target sites.

Cao et al., (2009) developed an *in situ* gel forming nasal formation of mometasone furoate which is used for the treatment of allergic rhinitis. Gellan gum was used as an *in situ* gelling polymer in the formulation. The formulation was sprayed as liquid and underwent rapid sol-gel transition on exposure to the ions (Na^+. K^+. Ca^{2+}) of artificial nasal fluid (gelation mechanisms of *in situ* gelling polysaccharides will be discussed in greater detail in chapter 3). When tested *in vivo*, this formulation was shown to be more effective in the treatment allergic rhinitis compared with a nasal suspension. However, gellan gum can also undergo gelation in response to changes in pH and/or temperature. Miyazaki et al., (1999) reported development of gellan gum based *in situ* gelling oral formulation of theophylline. The formulation turned into gel in acidic environment of the stomach (pH 1.2) and *in vitro* release of theophylline from the gel occurred over a 6-hour period.

Alginate is another example of polysaccharide which turns into a gel in response to the change in pH and has been used in pH induced *in situ* gelling drug delivery systems (Miyazaki et al., 2000; Kubo et al., 2003). Also, it crosslinks with Ca^{2+} to form gel. Liu et al., (2006) developed an *in situ* gelling ophthalmic formulation of gatifloxacin which is a broad spectrum antibacterial agent and used in the treatment of ocular infections. Alginate was used as an ion inducing *in situ* gelling polymer in this formulation. The liquid

formulation underwent gelation in response to the Ca^{2+} ions of lacrimal fluid upon instillation. The release of drug was sustained for a period of 8-hours. Gellan gum and alginate along with other polysaccharides have also been used in commercialized *in situ* gelling products (Table 2.2).

Table 2.2: Examples of commercialised *in situ* gelling formulations (Jain et al., 2016; Wu et al., 2018)

Name of the Product	Active Ingredient	Polymer	Route of Administration	Type of *In Situ* Gelling System
Timpotol LA® (Merck Sharp & Dohme, USA)	Timolol maleate	Gellan gum	Ocular	Ion induced
AzaSite® (inSite Vision, USA)	Azithromycin	Poloxamer	Ocular	Temperature triggered
Pecfent® (Archimedes Pharma, UK)	Fentanyl	Pectin	Nasal	Ion induced
Gaviscon® (Reckitt Benckiser, UK)	Sodium alginate	Sodium alginate	Oral	pH triggered
Virgan® (Laboratoires Théa, France)	Ganciclovir	Carbopol	Ocular	pH triggered

Mucin, which is responsible for gel-like properties and viscosity of mucus, plays a significant role in *in situ* gelation. Mucin is a large, extracellular glycoprotein and has tendency to form gel depending on concentrations, temperature and pH. For example, human tracheobronchial mucin undergoes gelation at temperatures below 30ºC and at a concentration above 14 mg/ml (Bromberg and Barr, 2000; Taylor et al., 2003). However, in developing *in situ* gelling formulations, mucoadhesive polymers are often used which interact with mucin and improve the residence time as well as bioavailability of the drugs by facilitating the dosage forms to adhere to the mucosal tissues. The non-covalent interactions that are formed between the polymer and the glycoprotein components of mucin

are mainly chain entanglements, hydrogen bonding and electrostatic interactions (Bansil and Turner, 2006). Gellan gum (Shastri et al., 2010), chitosan, guar gum, sodium alginate, xanthan gum, poly (acrylic acid), poly (vinyl pyrrolidone) are widely used as mucoadhesive polymers (Mythri et al., 2011) in different formulations.

In situ gel forming drug delivery systems offer numerous advantages such as ease and convenience of administration, improved patient compliance, deliverance of accurate dose, reduced frequency of administration, prolonged residence time in contact with mucosa (Nirmal et al., 2010) and improved bioavailability (Almeida et al., 2014). Despite having several advantages, formulating the *in situ* gelling systems with poorly soluble drugs is challenging. The salt forms of poorly soluble drugs can be used to increase the solubility, but may result in gelation of the formulation before administration when formulated with a gelling agent that has the tendency to crosslink with salts, such as gellan gum. To overcome this challenge, poorly soluble drugs can be added to a formulation as an inclusion complex, which will be discussed in detail in chapter 6.

2.3 Current Techniques to Investigate *In situ* Gelation

Evaluating the *in situ* gelation of an *in situ* gelling formulation is an important consideration to design a successful system. The simplest method is to shake a test tube or vial containing the *in situ* gelling formulation and observe the flow of the system. If the formulation turns into a gel, it will not flow and remain in place when inverted. This method however, does not provide any meaningful quantitative data. The most useful technique of measuring gelation properties in response to a changing environment such as a change in temperature, is to use a rheometer which consists of an upper and lower plate which can be temperature controlled. The sample is placed between the upper and lower plates and the upper plate is rotated at a controlled rate applying a shear force to the sample (Figure 2.2) allowing

viscosity and viscoelasticity to be measured.

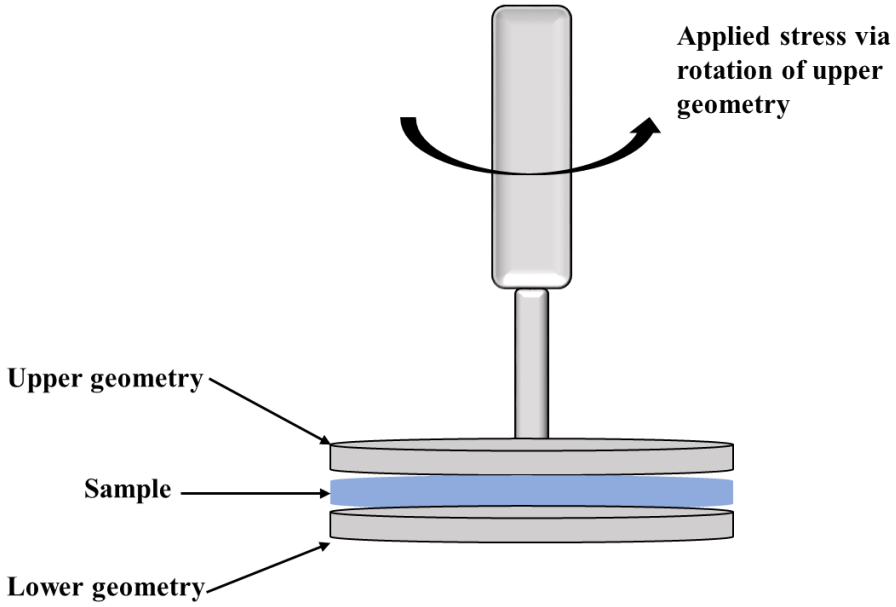

Figure 2.2: Conventional rheometer showing the sample between upper and lower geometry

By using a temperature controlled rheometer, thermal transitions of *in situ* gelling systems can be accurately measured, but when the sol-gel transitions are the result of a change in pH or ionic strength/species, measurements are considerably more challenging. When the sol-gel transition is induced by a change in pH change or ionic strength, the systems can undergo rapid gelation reactions. This is a problem, because if the pH or ionic strength of the sample is changed before loading onto a rheometer, the sol-gel transition may well have occurred (within 2/3 minutes (Mahdi et al., 2016)) before the sample can be loaded and therefore cannot be measured. Moreover, there is currently no mechanism on commercially available rheometers that can induce change of pH or ionic strength *in situ* despite many other modifications that have been applied to the conventional rheometers which have been discussed in previous chapter (chapter 01).

There are bespoke methods reported in the literature that investigate the gelation of *in situ* gelling polymers. These include loading the gelling material into dialysis tubing and then immersing it into a solution containing the required crosslinking ions/pH for various periods of time before removing and cutting the gel to an appropriate size for mechanical testing using a rheometer (Figure 2.3).

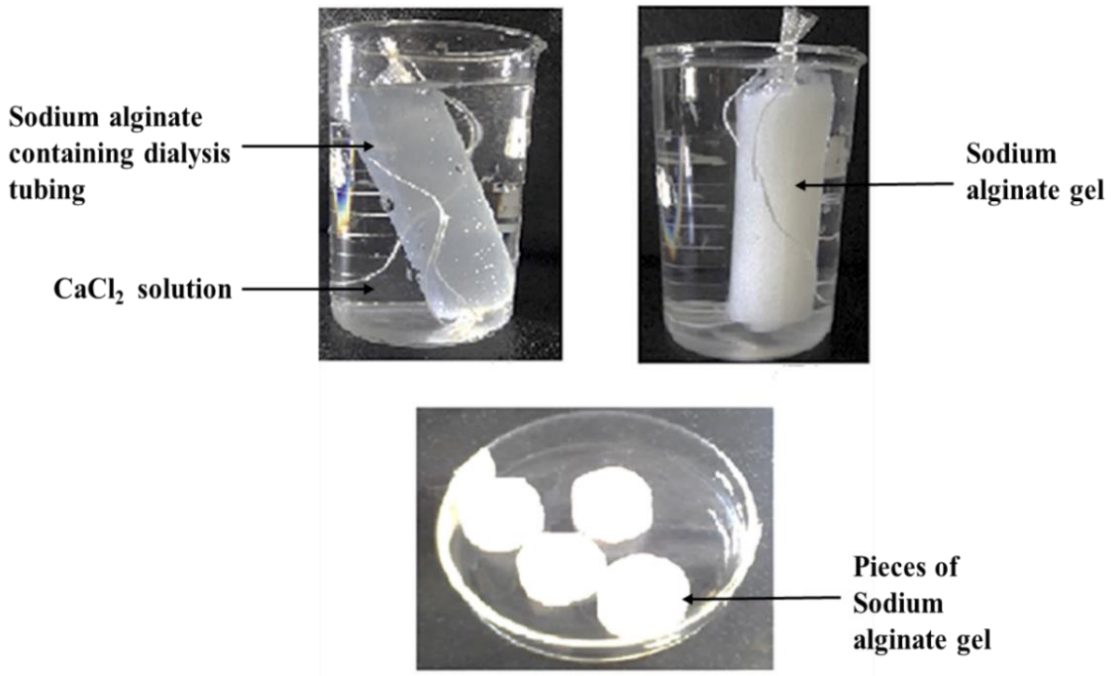

Figure 2.3: Gelation of sodium alginate in the dialysis tubing by immersing into the crosslinking ion solution (Bajpai et al., 2016)

Another method has been used where two filter papers are impregnated with soluble crosslinking ions. The *in situ* gelling polymer is poured into tissue culture plates and the filter papers are placed above and below the polymer (Figure 2.4). Then the polymer is allowed to gel for a specific time before the mechanical properties are measured (Mahdi et al., 2016).

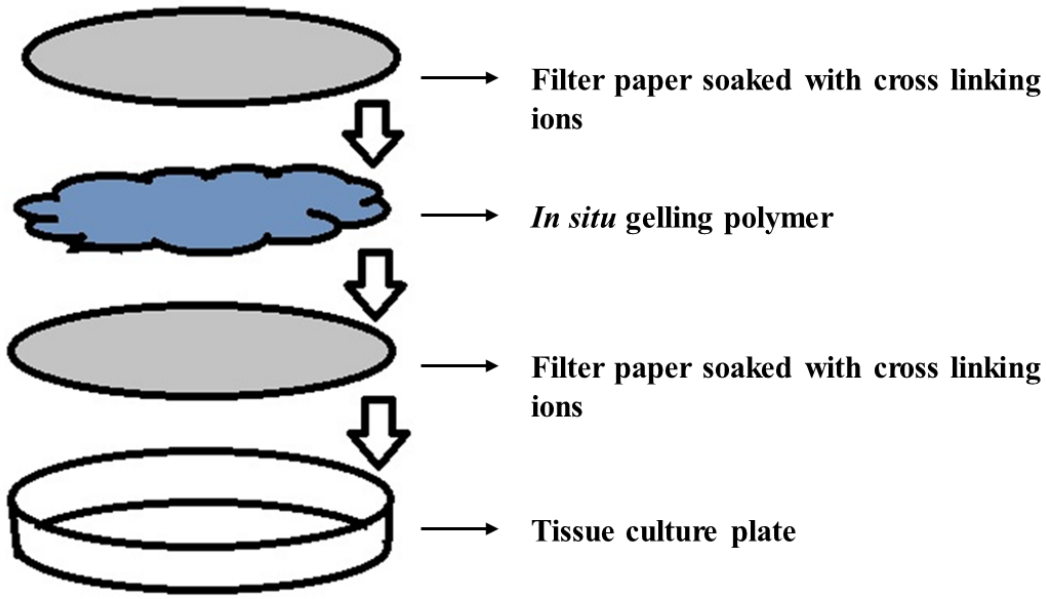

Figure 2.4: Schematic representation of the method of investigating gelation by using filter papers

To explore the real time gelation of such materials, Mahdi et al., (2016) proposed a method of using a rheometer where petri dish containing a filter paper soaked with $CaCl_2$ solution was securely attached to the lower plate of the rheometer (Figure 2.5). A hydrated dialysis membrane was placed on top of the filter paper to prevent the imbibition of the sample by the filter paper and samples of the gelling biopolymer (alginate) were loaded on the surface of the dialysis membrane. This investigation showed gel formation in alginate occurred over the first 3 min of exposure to $CaCl_2$. The increase of gel strength was proportional to the concentration of $CaCl_2$.

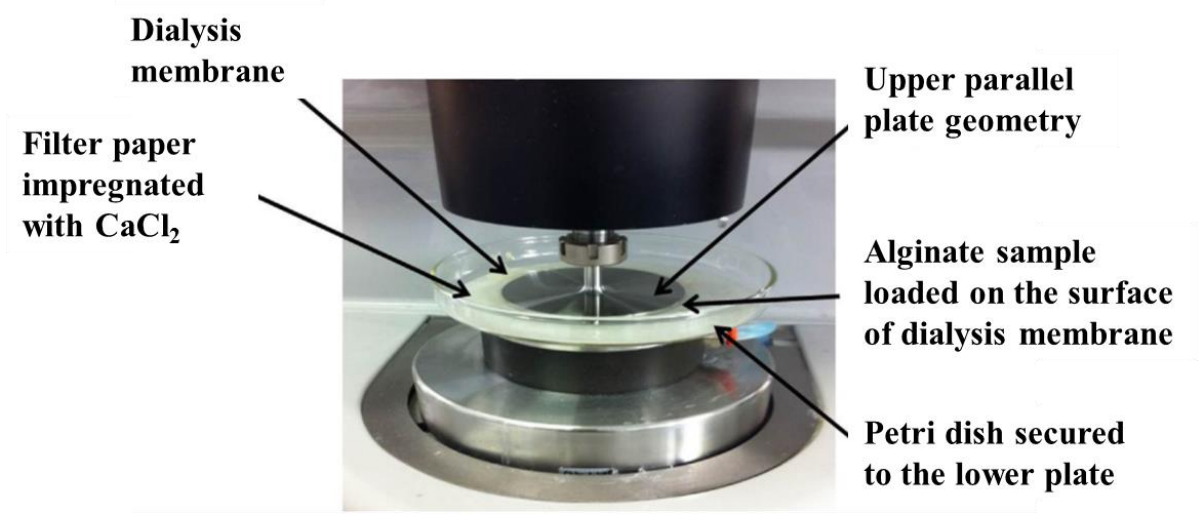

Figure 2.5: *In situ* rheological measurement of external gelation of alginate (Mahdi et al., 2016b)

Although this method showed that it was possible to monitor the rapid gelation of alginate on contact with Ca^{2+}, it does not allow ionic strength or pH to be easily changed, as a fixed filter paper is used as the crosslinking reservoir. Also, release of drugs from such systems cannot be performed during the rheological analysis. Drug release from such systems is usually measured separately following gelation using a Franz diffusion cell which does not realistically represent the real life scenario.

None of the modifications to rheometers or the external gelation methods allow the monitoring of gelation and drug release *in situ*, which is scientifically important, as the molecular interplay between the polymer molecules during gelation and the impact that has on drug diffusion and subsequent bioavailability are poorly understood. Developing an *in vitro* model (on which the thesis is based) can provide real time correlation between the rheological behaviour and drug release following administration which would facilitate designing reliable formulations of these innovative dosage forms during the early development process.

Chapter 3: Polysaccharides

3.1 Introduction to Polysaccharides

Biopolymers are polymers that are produced by nature. They are composed of repeating units of nucleic acids, saccharides or amino acids derived directly from living organisms. Also, they can be chemically synthesized from biological materials or engineered from microbial sources (Beneke et al., 2009). Because of having numerous functional and physicochemical properties, biopolymers are particularly useful in the development of pharmaceutical products. Besides, biopolymers exhibit several functional, economic and environmental benefits; for example; availability, low cost, ease of fabrication, relatively low toxicity, biocompatibility and biodegradability. This versatility has made biopolymers suitable for designing conventional and modified release drug delivery systems. They are included as excipients in drug formulations to fulfil multifunctional roles to ensure quality, safety and efficacy of pharmaceutical formulations (Beneke et al., 2009; Koo, 2011). They are frequently used to formulate nanoparticles, microparticles, matrix systems, films, implants, inhalable systems and injectables (Beneke et al., 2009; Builders and Attama, 2011). Biopolymers can be classified into polysaccharides, proteins or peptides and polynucleotides (Builders and Attama, 2011). Polysaccharides are the most abundant and diverse family of biopolymers (Perez and Kouwijzer, 1999). They are widely used as excipients to formulate pharmaceutical dosage forms.

Polysaccharides are polymeric carbohydrate composed of monosaccharides which are covalently linked to each other by a glycosidic linkage. In living organisms, polysaccharides exist as a source of energy such as starch and glycogen, and as structural polysaccharides that provide support such as cellulose and chitin (Builders and Attama, 2011). Agar,

carrageenan, alginate play key role in maintaining the plasticity of the cell wall in marine species. In animals, glycosaminoglycans play significant role in building extracellular matrix and also maintain the solution properties of physiological fluids. The examples of glycosaminoglycans are chondroitin sulphate, hyaluronate, and dermatan sulphate (Perez and Kouwijzer, 1999). Table 3.1 shows some common examples of polysaccharides from different origins.

Table 3.1: Examples of polysaccharides from different origin (Ross-murphy et al., 1998; Aravamudhan et al., 2014)

Sources of Polysaccharides	Examples
Plant polysaccharides	starch, cellulose, pectin, guar
Marine polysaccharides	carrageenan, agarose, alginate
Animal polysaccharides	hyaluronic acid, glycosaminoglycans, chitin, chitosan
Microbial polysaccharides	gellan gum, xanthan gum, bacterial cellulose

The different properties of polysaccharides allow a wide variety of uses in the food industry, tissue engineering and pharmaceutical manufacturing. In food industry, polysaccharides are frequently used as thickeners or stabilizers. They are included in a product to create reproducible flow properties during manufacturing and throughout the shelf life (Kontogiorgos, 2014; Mahdi, 2016). Native polysaccharides and their semi synthetic derivatives are widely used in drug delivery applications to regulate the drug release or as a carrier in controlled release devices (Jain et al., 2007; Builders and Attama, 2011). Tissue engineering and cell delivery are other promising fields where polysaccharides are used to make scaffolds and matrices whose structural integrity and mechanical stability closely resembles that of tissues and organs (Malafaya et al., 2007).

3.1.1 Structure of Polysaccharides

Polysaccharide chains are composed of monosaccharide units linked by O-glycosidic linkages. Differences in composition of monosaccharides, chain shapes, types and patterns of linkage and degree of polymerization cause great versatility of structural features of polysaccharides. This structural diversity plays key role in dictating the physical properties such as gelling potential, flow behaviour and solubility (Izydorczyk et al., 2005). The linkage of repeating units of polymer backbone involves condensation reaction between the OH group at C-1 of on one unit and one of the -OH groups of the adjacent unit at C-2, C-3, C-4 or C-6 position, with the removal of water (Mahdi, 2016). Figure 3.1 shows an example of glycosidic bonds between two glucose molecules to form a disaccharide (maltose).

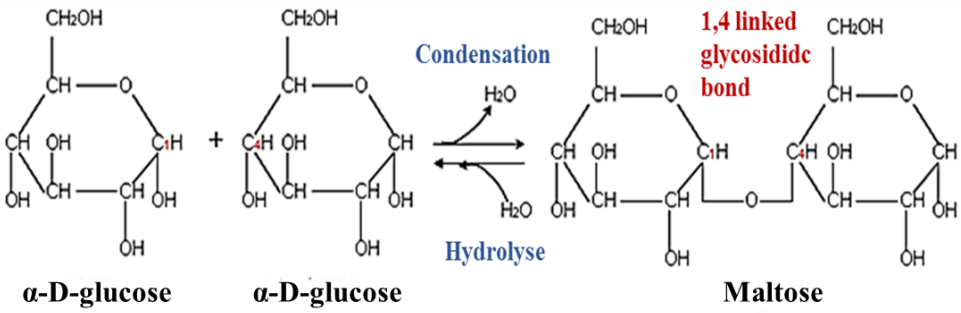

Figure 3.1: Condensation reactions to form glycosidic bonds between α-D-glucose to form maltose (Pelley, 2012)

There are many monosaccharides in nature, but the polysaccharide chains are not composed of all the monosaccharides. Common monosaccharides that are included to form the backbone of some most important polysaccharides are glucose and mannose. There are some other common sugar units which can be found in some commercially relevant polysaccharides, such as, xylose, galactose, guluronic acid, arabinose and mannuronic acid (Kontogiorgos, 2014).

Polysaccharides can be classified into homopolysaccharides and heteropolysaccharides

based on the number of sugar units on the backbone of polysaccharides. Polysaccharides that consist of single monosaccharide unit are called homopolysaccharides. Homopolysaccharides can be distinguished according to the constituent monosaccharide in the backbone. For example, homopolysaccharides that are derived from glucose are classified as glucans; such as, amylopectin, cellulose, amylose, glycogen and dextran. Polysaccharides consisting of more than one sugar units are called heteropolysaccharides. They are abundant in both animals and plants. Heteropolysaccharides usually contain a regular repeating sequence and these can be linear or branched. The examples of repeating pattern of polysaccharides that are commercially used are carrageenan, gellan, alginate, agarose (Voet et al., 2006; Mcnaught, 2008; Kontogiorgos, 2014). In both classes of polysaccharides, the monosaccharide units can be linear or branched out into complex formation (Figure 3.2) (Xie et al., 2016).

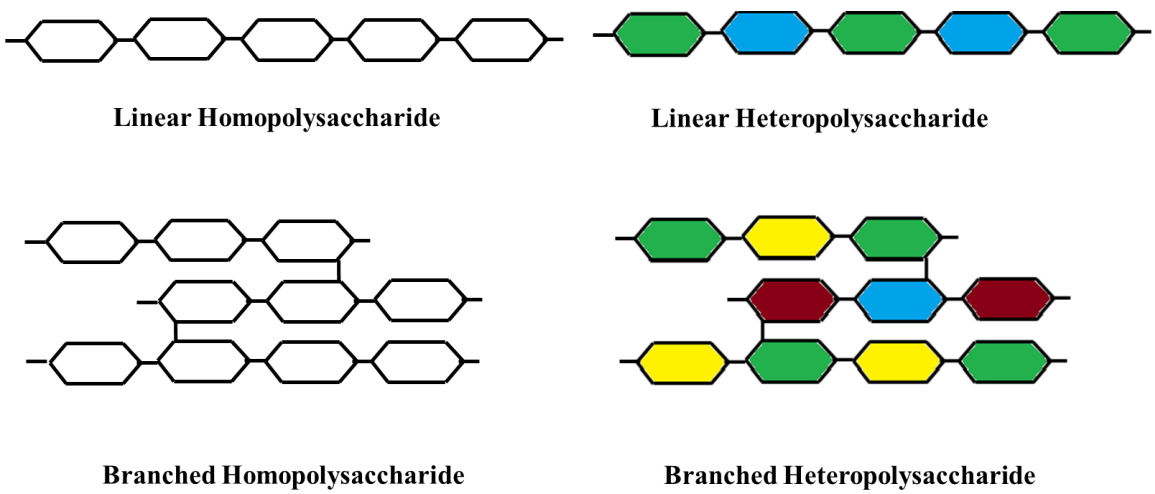

Figure 3.2: Classification of polysaccharides into homopolysaccharides and heteropolysaccharides; different colour indicates different monosaccharide units (adopted from Xie et al., 2016)

3.1.2 The Conformation of Polysaccharides

The sequence of monosaccharide units in a polysaccharide chain form a primary structure which is a prerequisite for further structural diversion. The conformation of an individual sugar unit is relatively fixed in a polysaccharide backbone. The monosaccharides linked through the glyosidic linkage have the ability to rotate around the bond with two or three torsion angels. As a result, geometrical shapes are formed which are classified as secondary structures; such as, ribbon-like, crumbled hollow-helix and loosely jointed. Ribbon-like and hollow helix types are most common types of conformation (Figure 3.3).

Ordered structure and disordered structures are two classes of conformation of polysaccharides. The values of torsion angles between the monosaccharides are fixed in ordered conformation. The disordered conformation is characterized by continuous fluctuation of local and overall chain conformation.

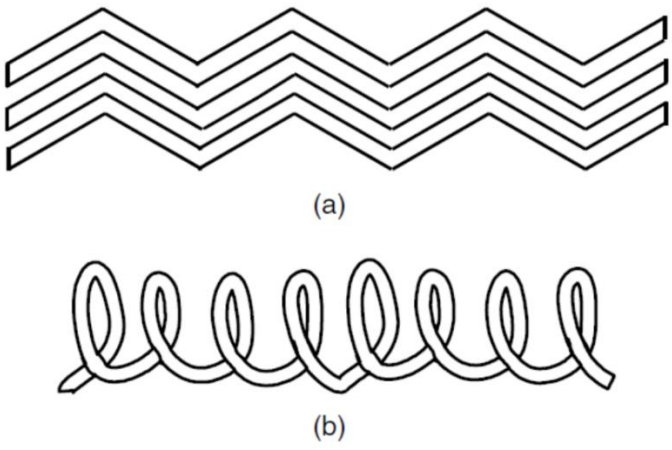

Figure 3.3: Secondary structures of polysaccharides (a) ribbon-like (b) hollow helix (Wang and Cui, 2005)

The interactions between the polysaccharide chains with well-defined secondary structures cause the formation of ordered organizations which are classified as tertiary structures. The

quaternary structures are another higher level of organizations which involve associations of ordered entities (Perez and Kouwijzer, 1999; Cui, 2005).

3.2 Application of Polysaccharides in Drug Delivery

Polysaccharides have been widely used for the development of drug delivery systems because of their functional versatility. Due to the biochemical similarity with human extracellular matrix components, polysaccharides are readily accepted by the body (Shelke et al., 2014). The non-toxic, biocompatible nature and physicochemical properties of polysaccharides have made them suitable for applications in drug delivery systems (Coviello et al., 2007). Many polysaccharides are used in the development of conventional and modified release drug delivery systems. Polysaccharides are generally used in immediate release formulations as binders, diluents, disintegrants and compaction enhancers. For example, starch derivatives (sodium starch glycolate) are used as disintegrants, diluents and binders; cellulose derivatives (ethyl cellulose, microcrystalline cellulose, hydroxymethylpropyl cellulose) are used as binders in rapid release tablets (Builders and Attama, 2011); guar gum is used as thickener, emulsion stabiliser and tablet binder (Beneke et al., 2009).

Polysaccharides are used in modified release drug delivery systems because of their ability to improve drug bioavailability by regulating the release of the drugs in the body. Polysaccharides have also shown superiority in terms of reducing dosing frequency, minimizing the side effects, maintaining continuous therapeutic levels of drug at specific target site or in the systemic circulation while used in modified release systems (Tao and Desai, 2003). Modified release drug delivery systems can be classified into four categories which are delayed release, sustained release, site specific targeting and receptor targeting.

Delayed release drug delivery systems are designed to delay the release of the drugs at a

time other than promptly after administration. Delaying the release of a drug can be controlled by time or *in vivo* environmental conditions such as pH. In oral drug delivery, this system is used to release the drugs to the specific sites within the gastrointestinal tract (GIT), for example, targeting of drug to the colon. Delayed release of drugs followed by immediate release or extended release may be beneficial to delivery of drugs to the target sites. The examples of polysaccharides that are widely used in the formulation of delayed release delivery systems are chitosan, carrageenan, dextrin, karaya gum, gellan gum, and locust bean gum (Builders and Attama, 2011).

Sustained release drug delivery systems are designed to release the drugs for extended period of time after administration. There are several advantages of this system including reducing side effects, better patient compliance, improved efficacy, and reduced dosing. Also, there is less fluctuation of plasma drug levels in sustained release delivery systems due to reduced dosing frequency. Because of having versatile functional and physiochemical properties, polysaccharides are extensively used in design and development of sustained release drug delivery systems to act locally or systemically for extended period of time (Builders and Attama, 2011). For example, cellulose derivatives have been used to formulate monothilic matrix systems, pectin has been used in matrix type transdermal patch, alginate has been used in preparation of matrices, microparticles, pellets, beads, films, nanoparticles (Beneke et al., 2009); gellan gum and alginate have been used to formulate *in situ* gelling sustained release systems because of their physical crosslinking mechanism (Nirmal et al., 2010).

Site specific targeting systems provide improved overall drug delivery to the target sites. These systems offer reduced accumulation of drugs at the non-target sites which causes less toxicity. Other advantages include increased efficacy and optimal bioavailability. Site specific drug targeting systems are used in cancer chemo-therapy. Polysaccharides are

widely used for preparation of carrier systems for cancer drugs to improve permeability and retention of the drugs at the target sites (Reubi, 2003; Kaparissides et al., 2006; Builders and Attama, 2011).

Receptor targeting systems are designed to specify the ligand-receptor interactions for diagnosis and management of drugs for certain diseases. For example, specific agents are injected to bind with receptors located on tumour cells to diagnose the tumours. Functional peptides from natural origin are usually used for receptor targeting systems (Builders and Attama, 2011).

However, intrinsic physicochemical properties of polysaccharides such as having numerous hydrogen bonding functional groups, viscoelastic properties and hydrophilicity, facilitate the mucoadhesion characteristics which have been widely utilized in the development of mucoadhesive formulations (Sworn et al., 1995; Gibson and Sanderson, 1997). The great versatility of polysaccharides and physically crosslinked gels are of great interest in drug delivery systems due to their gelation under mild conditions and without any presence of organic solvents (Coviello et al., 2007). The *in situ* gelation properties of polysaccharides have been utilized to formulate *in situ* gel forming drug delivery systems on which this thesis is based.

3.3 Polysaccharide Gels

A range of polysaccharides have the ability to self-assemble to form gels which is one of the most useful properties of polysaccharides. They can form firm gels at relatively low concentrations typically between 0.5 – 2.0 % w/w (Wüstenberg, 2014). These polysaccharides are widely used as gelling agents in food, pharmaceutical, cosmetic, photographic, paint, petroleum and chemical industries. Gels can be defined as solid, jelly-

like materials formed from polysaccharides, synthetic polymers and proteins (Clark and Ross-Murphy, 2009; Tako, 2015). There is a widely cited definition of gel by Lloyd, (Lloyd, 1926) which is 'the colloidal condition, the gel, is one which is easier to recognize than to define'. From rheological point of view, the gel can be defined as a swollen polymeric system with no steady-state flow and will rupture in response to steady shear deformation (Clark and Ross-Murphy, 2009).

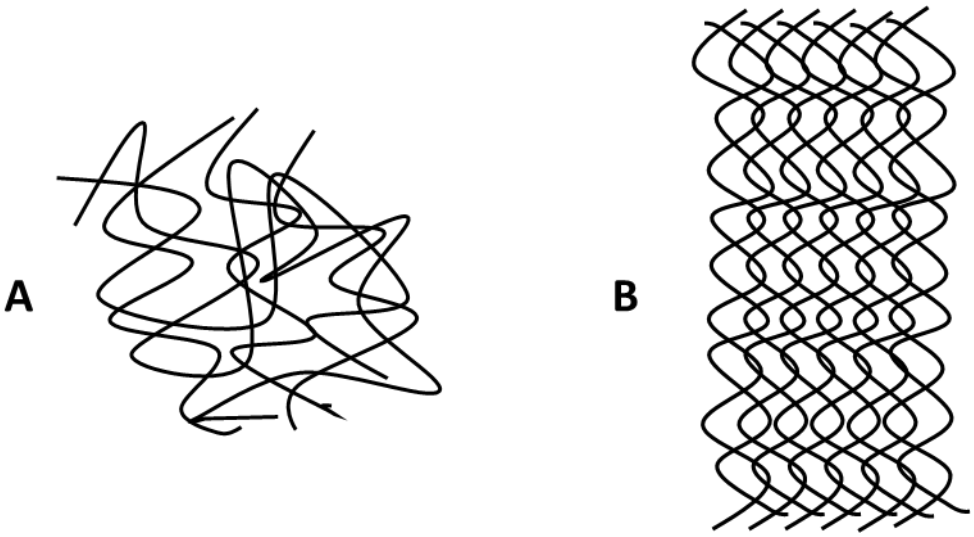

Figure 3.4: Schematic illustration of formation of (A) entanglement in viscous polymer solution (B) ordered network in gel

Commercial products, such as, shower gels and topical gels do not follow the rheological definition of gel. These commercial gel products can be described as highly viscous polymer solutions formed by entanglement of polymeric micelles (Clark, 2010). Figure 3.4 represents differences between viscous polymer solutions and ordered gel network.

Polysaccharide gels are often termed as hydrogels because of the ability to absorb and hold large amount of water (up to 500 times their weight (Gooch, 2010)) which facilitates the formation of a three dimensional network (Peppas et al., 2000). Attention has been directed towards the research on hydrogels with respect to drug delivery and tissue engineering over

the last few decades. Hydrogels can swell to high water content (>80%) which has made them attractive candidate to make 3D cell scaffolds to replace natural soft tissues (Waters et al., 2011).

3.3.1 Gelation of Polysaccharides

Gelation can be defined as a general way to convert a fluid into solid. Gelation involves formation of a network structure through association of polysaccharide chains (Hill et al., 1998; Linden and Foegeding, 2009). The gel structures formed either *in vivo* or *in vitro* are normally crosslinked by extended intermolecular 'junction zones' of conformationally ordered chains (Figure 3.5) (Morris, 1986). The structure of junction zones are different for different polysaccharides, for example, ionically crosslinked double helices in carrageenan and gellan, ribbon-ribbon association of egg box type in alginate and pectin stabilised by divalent cations, bundles of double helices in agarose (Figure 3.6) (Cui, 2005).

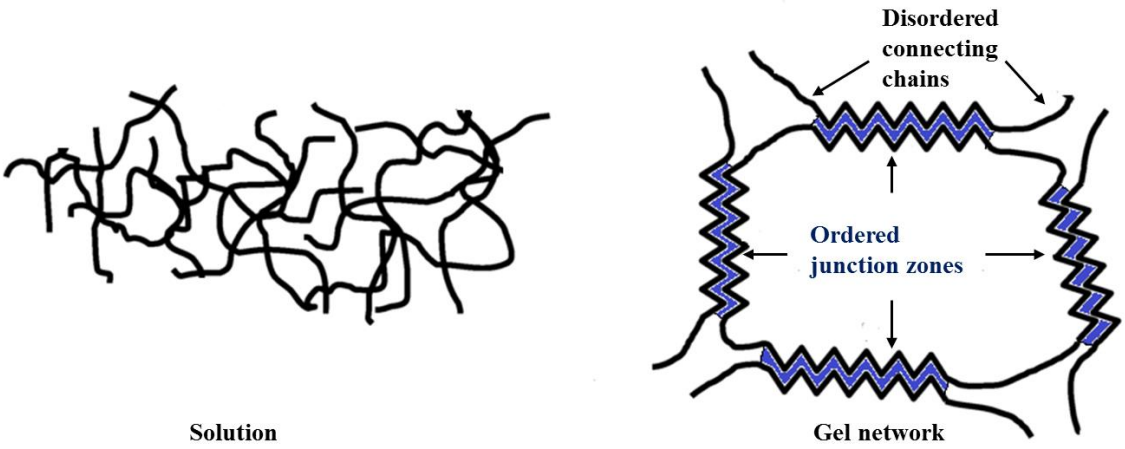

Figure 3.5: Generalised schematic representation of polysaccharide gel network formation (Posocco et al., 2015)

Large quantities of water are trapped within the gel network which causes the prevention of collapsing into a compact mass (Solari, 1994). Most polysaccharides undergo gelation as a

result of physical crosslinking in response to changes in temperature, pH or ionic strength (Hoare and Kohane, 2008). For example, in thermally driven gelation process, increasing or decreasing the solution temperature can cause changes in polysaccharide conformational state. This is often followed by an association process of polysaccharide chains which results in gelation. Such as agarose, which forms a thermo-reversible gel upon cooling a hot, aqueous solution (Ross-murphy et al., 1998; Nordqvist and Vilgis, 2011).

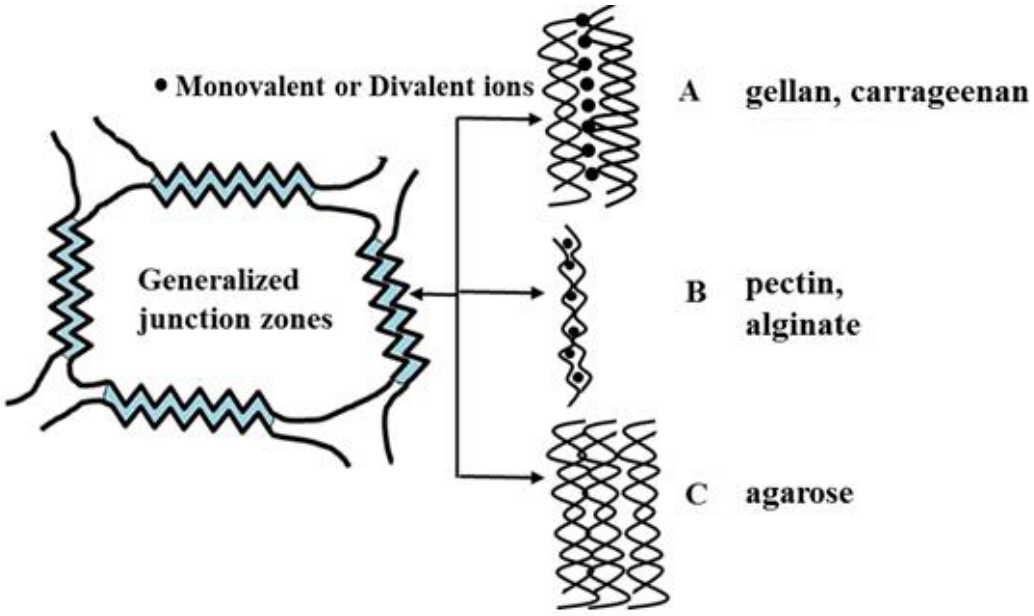

Figure 3.6: Different types of junction zones (A) crosslinked double helix in κ-carrageenan (crosslinked with K^+) or ι-carrageenan (crosslinked with Ca^{2+}) (B) ribbon-ribbon association of egg box in alginate crosslinked with Ca^{2+} (C) bundle of double helices in agarose (adapted from (Posocco et al., 2015))

The chains of charged polysaccharides can be held together by addition of appropriate concentrations of salts to the polymer solution. For example, gelation of gellan gum can be induced by adding Na^+, K^+ and Ca^{2+} (Morris et al., 2012). Gelation can also be initiated by adding acid, alkali or changing the pH of the polymer solution. Such as, alginate which undergoes gelation at acidic pH (Haug, 1961).

3.4 Gel Forming Polysaccharides

The gel forming polysaccharides that are used to prepare the formulations in this work are mainly gellan gum, alginate and agarose.

3.4.1 Gellan Gum

Gellan gum is an extracellular bacterial polysaccharide and it is produced by aerobic fermentation from *Sphingomonas elodea.* Gellan gum is an anionic polymer with a linear structure consisting of repeating tetrasaccharide units. The tertrasaccharide unit comprises of two β-D-glucose residues, one β-D-glucoronate and one α-L-rhamnose residue (Smith et al., 2007; Morris et al., 2012). Gellan gum is marketed in two forms which are high acyl and low acyl. The native polymer is high acyl gellan gum which contains O-5-acetyl and O-2-glyceryl groups on the 1-3 linked glucose residue. Low acyl gellan gum is obtained from high acyl gellan by complete deacetylation using hot alkaline solution. Both forms of gellan gum produce gels that are different, both physically and mechanically. Soft and elastic gels are produced by high acyl gellan gum whereas low acyl gellan gum forms hard and brittle gels. (Mahdi et al., 2015). Figure 3.7 represented tetrasaccharide repeating sequence of gellan gum.

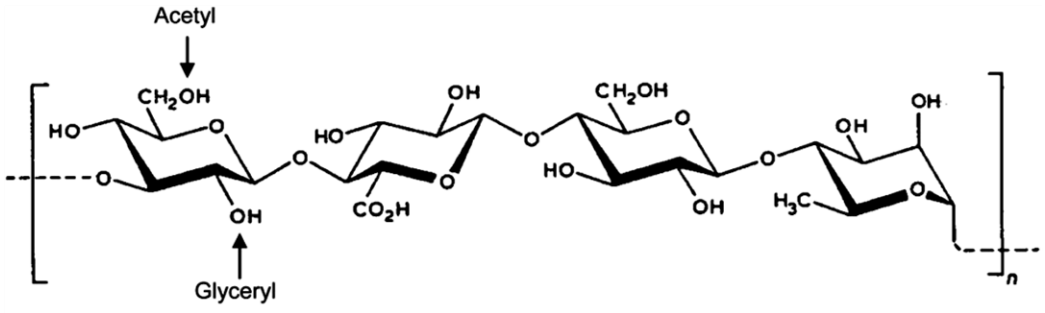

→ 3)-β-D-Glc*p*-(1 → 4)-β-D-Glc*p*A-(1 → 4)-β-D-Glc*p*-(1 → 4)-α-L-Rha*p*-(1 →

Figure 3.7: Representation of tetrasaccharide repeating sequence of gellan gum in deacylated form. Acetyl and glyceryl substituents indicates the native polymer (high acyl) (Morris et al., 2012)

3.4.1.1 *Gelation of Gellan Gum*

Gelation of gellan gum involves conversion of random coil to double helix state. Gellan gum exists as disordered coils at elevated temperature (above 80°C) and converts to helical structures upon cooling. The formation of these helical structures exhibit weak gel characteristics because of tenuous association of ridged order structure (Robinson et al., 1991). Helical structures need to be associated into stable aggregates to form true gel. Aggregation is formed by suppression of electrostatic repulsion between the gellan helices. Suppression can be initiated by either reducing the pH or adding salt to the aqueous media. By reducing the pH, glucoronate carboxyl groups lose their charges and negatively charged COO^{-} converts to uncharged COOH resulting in a gel (Morris et al., 2012). Direct addition of acid to gellan gum solutions results immediate ordering and aggregation of the gellan helices. This phenomena has been utilized to produce self-structuring formulations such as, delayed release oral formulation which takes the advantage of natural digestive process (Miyazaki et al., 1999; Bradbeer et al., 2014; Mahdi et al., 2014).

Introduction of cations in the solution of gellan gum causes further suppression of the repulsion between the helices (Figure 3.8). Monovalent cations reduce the effective negative charges of the helices by clustering around the negatively charged carboxylates of the glucuronic acid residues. The electrostatic interaction between cations and the carboxylate groups act as a trigger for the clustering. The affinity of different monovalent ions to promote aggregation and gel formation lies in order of $Li^{+} < Na^{+} < K^{+} < Cs^{+} < H^{+}$ (Grasdalen and Smidsrød, 1987). The mechanism of gelation is different for divalent cations such as Ca^{2+} and Mg^{2+}, which suppress the repulsion by forming direct bridges between the carboxylate groups on adjacent pairs of helices.

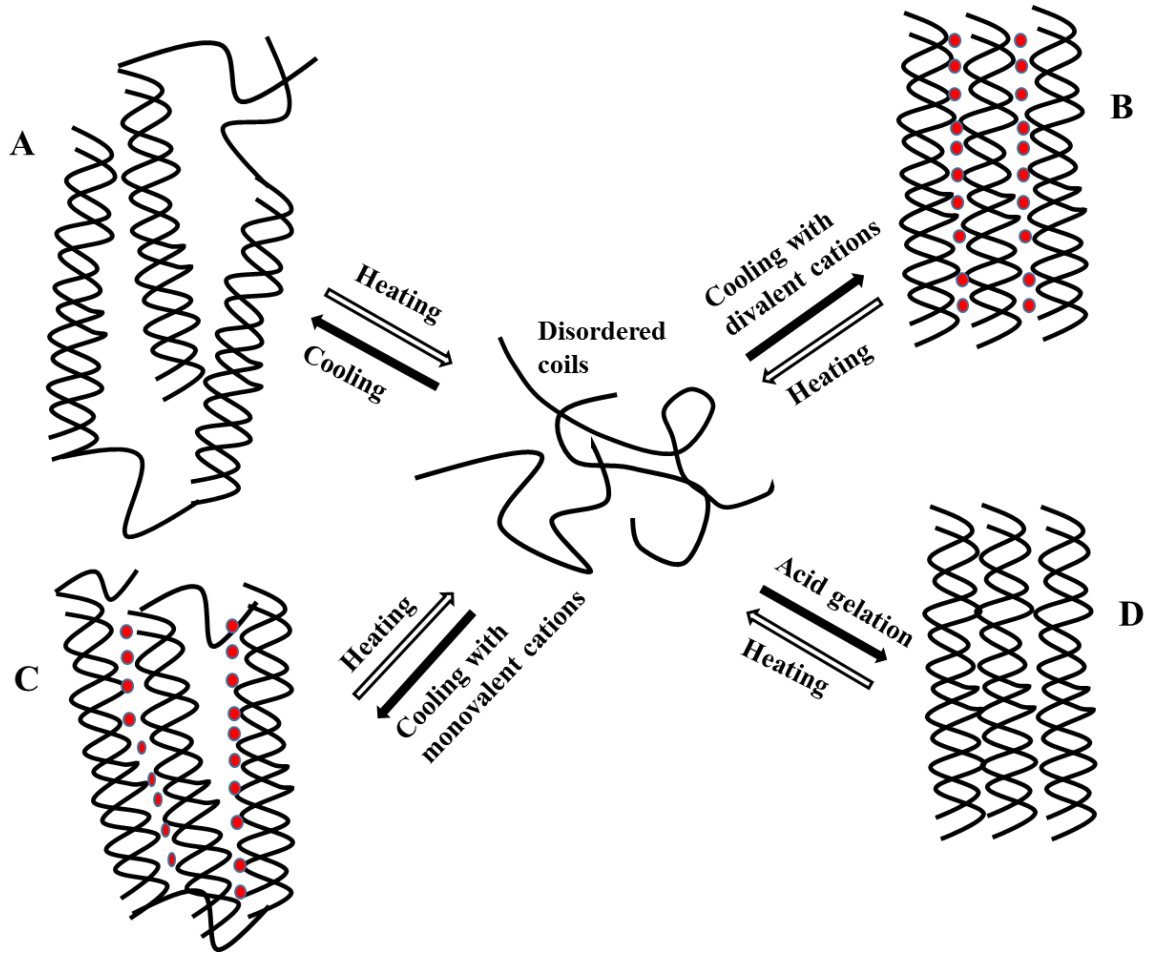

Figure 3.8: Schematic representation of gelation of gellan (A) formation of weak gel upon cooling (B) formation of strong gel in presence of divalent cations (such as Ca^{2+}, Mg^{2+}) (C) Formation of strong gel in presence of monovalent cations (such as H^{+}, Na^{+}) (D) formation strong gel in presence of acid

Therefore, it facilitates the aggregation to form strong gels. Gel strength, clarity, rate of gel formation and texture depend on concentration of gellan gum and ions. The concentration require to crosslink gellan gum is typically ≈5 mM for Ca^{2+} and Mg^{2+} whereas it is ≈100 mM for Na^{+} and K^{+} (Smith et al., 2007). The ion induced gelation of high acyl gellan gum is restricted because of the presence of acyl groups which causes steric hindrance and blocks the aggregation. As a result, more soft and elastic gels are formed. Absence of acyl groups in low acyl gellan gum allows cation mediated aggregation and forms hard gel (Morris et al., 1996). Thus low acyl gellan gum is widely used in *in situ* gel forming formulations

because of the ability to form strong gels in contact with physiological ions.

A successful commercial gellan gum based ophthalmic formulation is Timpotol LA® which is an *in situ* gel forming ophthalmic formulation and is used to reduce elevated intra ocular pressure that occurs in glaucoma. The active ingredient is timolol maleate and low acyl gellan gum is used as the gel forming agent. Once the formulation is instilled into the eye, gels are formed via rapid sol-gel transition because of the presence of Ca^{2+}, K^{+} and Na^{+} (Rismondo et al., 1989) ions in the lacrimal fluid. Following gelation, timolol maleate is released in a sustained manner (Kumar and Himmelstein, 1995; Gupta et al., 2009) from the *in situ* gel.

3.4.2 Alginate

Alginate is a natural polymer which is extracted from brown algae such as *Ascophyllum nodosum, Macro cystis pyrifera* and *Laminaria hyperborean*. It is a linear polysaccharide consisting of the residues of homopolymeric blocks of β-D-mannuronic acid (M) and α-L-guluronic acid (G). The blocks can be arranged G-G or M-M with M-G or G-M sequence (Figure 3.9). (Cohen et al., 1997; Park et al., 2009).

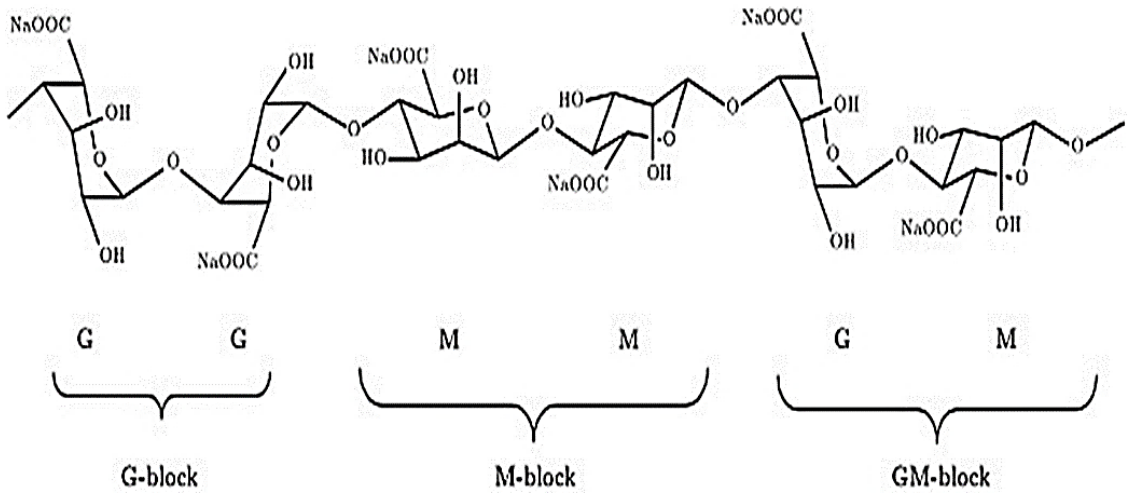

Figure 3.9: Chemical structure of sodium alginate with arrangements of G and M blocks (Moxon, 2016)

3.4.2.1 *Gelation of Alginate*

Alginate undergoes gelation in presence of ionic crosslinking agents. It has affinity for divalent cations, such as Ca^{2+} and can physically crosslinks to form gel in presence of this ion. The G blocks of alginate chains offers a high degree of coordination to the divalent cations compared to the M blocks. Therefore, the divalent cations attach to the G blocks and form junction with the G blocks of adjacent alginate chain to create an ordered gel network. This type of gel network is called egg box cross linking (Figure 3.10) (Grant et al., 1973) This type of crosslinking is mediated by interactions between the carboxylic acid groups of the G blocks and the cations. The subsequent gel strength is directly influenced by the ratios of G and M blocks in alginate. Alginate with 'high G' produces stronger gels whereas less stronger gels are produced by alginates with 'low G' (Park et al., 2009). Grasdalen et al., (1981) reported using NMR spectroscopy to determine the frequency of G and M blocks in alginate polymer chains, such as monad (G or M), diad (MM, GG, MG, GM) and triad (GGG, MMM. GMG, MGM, GMM, MMG). The average G block length can be determined using this frequency which directly influence the strength of alginate gel.

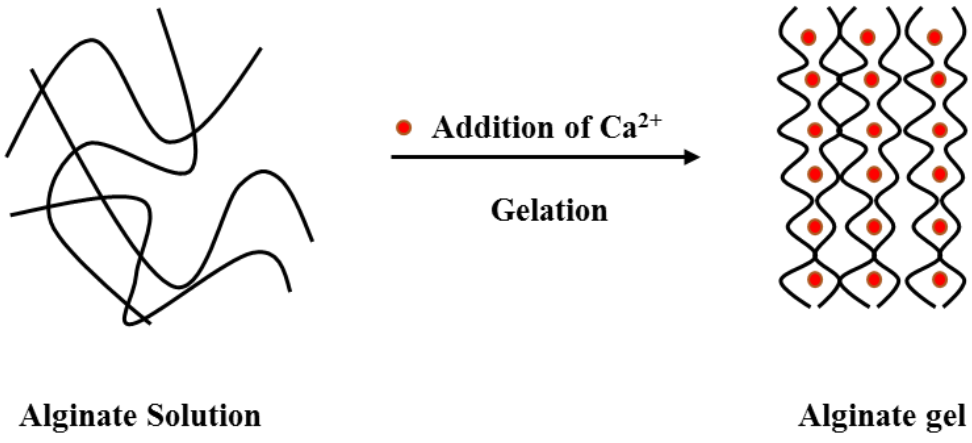

Figure 3.10: Schematic representation of ion induced gelation of alginate and formation of egg box network in presence of Ca^{2+} ion

Alginate also forms alginic acid gels at acidic pH when alginate is protonated. The mannuronic acid and the guluronic acid have the pKa of 3.38 and 3.65 respectively (Haug, 1961). So when the pH of the alginate is below the pKa of the alginate monomers, alginic acid gel is formed (Draget et al., 1994). This property of alginate has been widely used in formulation of pharmaceutical dosage forms. Successful commercial product Gaviscon® is an *in situ* gelling oral formulation which is used to treat heartburn, acid indigestion and upset stomach. The active ingredient of Gaviscon® is sodium alginate and is marketed as oral liquid and tablet. When the oral liquid formulation is swallowed, the formulation comes in contact with the stomach acid. The sodium alginate undergoes rapid so-gel transition on contact with H^+ of the stomach acid and prevent the acid reflux by forming a protective barrier (gel raft) on the surface of gastric fluid (Grover and Smith, 2009; Mahdi, 2016).

3.4.3 Agarose

Agarose is a neutral linear polysaccharide consisting of β-1,3-linked D-galactose and α-1,4-linked 3,6-anhydro-α- L-galactose (Figure 4.7). It is hydrophilic and does not have any significant net charge. It is extracted from red algae/seaweed and the main sources are *Gelidium* and *Gracilaria genera*. Agarose is used in separation techniques to characterise biomolecules such as electrophoresis or affinity chromatography, in the biotechnology applications (*e.g.* encapsulation medium, growth medium for microorganisms) and as a constituent in the food industry (Nordqvist and Vilgis, 2011; Le Goff et al., 2015)

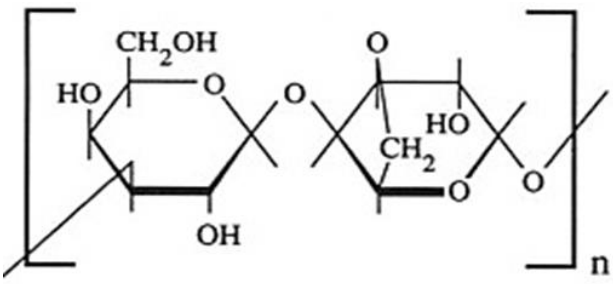

D-Galactose **3,6-Anhydro-L-Galactose**

Figure 3.11: Chemical structure of agarose (Watase and Arakawa, 1968)

After being dissolved in water above the melting temperature (95ºC), agarose molecules are in disordered state. At higher temperature, the agarose chains (in solution) exhibit a random coil which changes to a helical conformation with decreasing temperature. The gelation of agarose follows the following scheme; coil → double helix → aggregates of helices (gel) (Piculell and Nilsson, 1989; Nordqvist and Vilgis, 2011) (Figure 4.8).

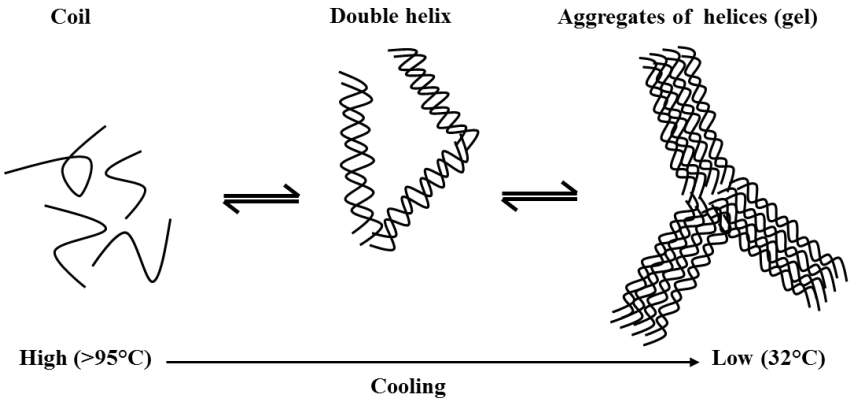

Figure 3.12: A schematic overview of the gelation process in agarose solutions

The gelling temperature of agarose is 32°C (Jessop et al., 2018) . The helices aggregate without the need of an ionic crosslinker. Agarose has a capability to undergo sol-gel transitions into ordered polymer networks at a concentration of <1% w/w which is similar to gellan (Moxon, 2016).

3.5 *In situ* Gelation of Polysaccharides

Many investigations using polysaccharides to form *in situ* gel forming drug delivery systems have been reported for their *in situ* gelation properties (Coviello et al., 2007), some examples of the different mechanisms are described in the following section.

3.5.1 Mechanisms of *In Situ* Gelation

In situ gels are usually formed through a crosslinking reaction between polymeric chains which can be triggered by one or more of the following three stimuli; changes in temperature, pH or the presence of ions (Xiong et al., 2011). These environmental triggers influence polymer-polymer and polymer-solvent interactions. There are many synthetic and natural polymers which undergo sol-gel transition in response to physiological stimuli and could potentially be used for drug delivery via multiple administration routes (Diryak et al., 2018).

3.5.1.1 *Temperature Induced In situ Gelation*

Thermally induced gelation is the most extensively studied stimuli responsive gel system because there is no physicochemical conditions or toxic chemical products involved in this crosslinking strategy (Delair, 2012). Thermosensitive polysaccharides which undergo a sol-gel transition as a result of a change in temperature are used to formulate thermally triggered *in situ* gelling systems. Thermosensitive polysaccharides feature an upper critical solution temperature (UCST) above which the polysaccharides are soluble and undergoes gelation on cooling. For example gellan gum, κ- and ι-carrageenan exist as random coil at high temperature and transform into a 3D gel network gel on cooling (Yuguchi et al., 2002; Delair, 2012). Some cellulose derivatives such as methylcellulose (MC) and hydroxypropyl methylcellulose (HPMC) exhibit the opposite characteristics. They exist as liquid at low temperature (1-10% concentrations) and transform into opaque gels upon heating (40 to

50°C for MC and 75 to 90°C for HPMC). Physical or chemical modifications can alter the phase transition temperatures of these cellulose derivatives (Ruel-Gariépy and Leroux, 2004). Several developments of thermally induced *in situ* gel forming drug delivery systems have been reported where thermosensitive polysaccharides were used to activate the systems. For example, Bain et al., (2009) reported an *in situ* gel forming ophthalmic formulation of keteorolac tromethamine where MC was used as an *in situ* gelling polymer. Fructose and sodium citrate tribasic dehydrate were added to reduce the gelation temperature of MC (1%) from 59°C to the physiological temperature (37°C). The developed formulation stayed liquid at room temperature and underwent gelation in contact with lacrimal fluid at 37°C. The *in vitro* release of drug was sustained for 9 hours from the *in situ* gel of MC. Dhaval et al., (2020) developed a microemulsion based *in situ* gelling ophthalmic formulation of sparfloxacin where poloxamer 407 was used as the *in situ* gelling agent. The formulation stayed as a liquid at 20ºC and converted to a gel at physiological temperature (37ºC). *In vitro* drug release study of the formulation showed sustained release of sparfloxacin for more than 10 hours from the *in situ* gel.

3.5.1.2 *pH Triggered In Situ Gelation*

In pH triggered *in situ* gelling systems, the gelation is induced by pH alterations. They are formulated with pH sensitive polysaccharides that contain acidic or basic groups and they accept or release protons as a result of changing pH. For example, chitosan is a cationic polysaccharide (Delair, 2012) whereas alginate and gellan are anionic (Rajinikanth and Mishra, 2007; Delair, 2012) polysaccharides. These polysaccharides are also termed as polyelectrolytes. pH triggered *in situ* gelling systems stay as liquid at formulated pH and undergo sol-gel transitions in response to the physiological pH, which can vary depending on the sites of action (for example pH 7.4 in the eye, pH 1 – pH 4.5 in the stomach) opening

up potential for different materials to be used depending on their pH sensitivity.

Several research investigations on pH triggered *in situ* gelation have been reported. For example, an *in situ* gelling system consisting of gellan gum and clarithromycin has been investigated to treat stomach ulcer which is caused by *Helicobacter pylori* (*H. Pylori*). Upon contact with simulated stomach acid, the formulation formed strong gel and increased the residence time by becoming buoyant in gastric fluid. The release of drug was sustained for over the period of 8 hours. The *in situ* gelling formulation showed better effect than conventional formulations along with reduced dosing frequency (Rajinikanth and Mishra, 2008). Patel et al., (2011) also developed oral *in situ* gelling formulation based on floating, formulated with amoxicillin and sodium alginate to treat *H. pylori*. The aqueous formulation underwent gelation in presence of simulated gastric fluid (pH 1.2) and started to float within 30 seconds. The release of drug was sustained for 10 to 12 hours. Nief et al., (2019) developed a pH triggered oral *in situ* gelling formulation of itraconazole with carbopol 934 in combination with HPMC, hyaluronic acid and xyloglucan. The formulation was in the liquid state at pH range 4.2-5.1 and converted to the gel state at the pH of the oral cavity (pH 6.2-7.6). It showed prolonged residence time in the oral cavity compared with the conventional oral gel and provided 80% release of drug over 8 hour period.

3.5.1.3 *Ion Induced In situ Gelation*

Charged polysaccharides may undergo *in situ* gelation in presence of ions. This phenomenon has been utilized in designing ion induced *in situ* gel forming formulations. Monovalent and divalent ionic species, such as; H^+, $Ca^{2+,}$ K^+, Na^+, Mg^{2+} are abundant in physiological fluids which attract the oppositely charged polymer molecules. Addition of oppositely charged ions suppress the repulsive charges of the polysaccharides resulting in three dimensional structure by formation of conformationally ordered junction zones. Thus, the solution turns

into gel in contact with physiological fluid upon administration into the body. For example, alginate undergoes gelation in presence of Ca^{2+} (Lee and Mooney, 2012), gellan gum transforms into gel in presence of Na^{+}, K^{+}, Ca^{2+} and Mg^{2+}, κ-carrageenan transforms into rigid, brittle gel in presence of K^{+} and ι-carrageenan forms elastic gel when Ca^{2+} is present. The gel strength depends on the polymer concentration and concentrations of the cations used as the crosslinker (Kara et al., 2006).

Balasubramaniam et al., (2003) reported development of an *in situ* gelling ophthalmic formulation of gellan gum and indomethacin. The formulation underwent sol-gel transition upon contact with the cations of lacrimal fluid and provided *in vitro* sustained release for over 8 hours period. The formulation showed better therapeutic efficacy compared to the standard suspension. Furthermore, Cohen et al., (1997) formulated *in situ* gel forming ophthalmic formulation of pilocarpine where sodium alginate was used as an *in situ* gelling agent. The formulation was made without any external ions and it was found that the release of pilocarpine was dependent on guluronic acid percentage of the alginate. The formulation formed a gel instantly on exposure to the simulated lacrimal fluid when the alginates had G contents of more than 65%. A relatively weak gel was formed at a slow rate when there was low G content in alginate. The release study suggested slow release of drug from the alginate gel for over 24 hours. Mahajan et al., (2019) reported an ion induced *in situ* gel forming nasal formulation of opioid analgesic tapentadol hydrochloride for nasal delivery where gellan was used as an *in situ* gelling polymer. The formulation showed sol-gel transition on exposure to the ions of nasal fluid and the formulation showed sustained release of drug.

In situ gelling formulations are also developed as multi-responsive stimuli systems. They can be formulated with one polysaccharide which is themosensitive and pH triggered /ion induced or multiple polysaccharides activated by dual physiological mechanisms of *in situ*

gelation (for example, pH and temperature). Gupta et al., (2010), developed an ion and pH activated *in situ* gel forming ophthalmic formulation of timolol maleate. In this formulation, gellan was used as an ion activated polymer and chitosan was used as a pH sensitive polymer. The *in vitro* parameters such as *in situ* gelation, gel strength, transcorneal permeation profile and retention time showed that the system can be a feasible alternative to conventional eye drops of timolol maleate. The developed formulation was also reported to be well tolerated and non-irritant.

The following chapters in this thesis will highlight the rheological evaluation and drug release studies of *in situ* gel forming ophthalmic formulations based on gellan gum. The work will also focus on exploring alginate to develop *in situ* gel forming oral formulation because of its variation in rheological behaviour in different pH environments, which also affect the release of drugs.

3.6 Aim and Objectives

The overall aim of this work was to develop a novel technique to simultaneously analyse the rheological behaviour and drug release from *in situ* gelling systems on exposure to physiological fluids. The main objectives were to:

- develop a suitable design and construct a cell to replace the lower plate of conventional rheometer that allows exposure of physiological fluid to a sample while rheological measurements are in process.
- develop *in situ* gelling formulations using different polysaccharides and then to evaluate the developed cell by simultaneously measuring the rheological changes and release of drugs from the *in situ* gelling formulations in context of different physiological fluids.

- develop an *in situ* gelling formulation using a poorly soluble drug-cyclodextrin inclusion complex and evaluation of the rheology and drug release from the formulation on exposure to physiological fluid.

Initially, an *in situ* gel forming ophthalmic formulation was prepared where low acyl gellan gum was added as an *in situ* gelling polymer. Rheological evaluation of the formulation was performed using the conventional rheometer and the release of the drug was evaluated separately. The effect of potential interaction between the anionic gellan gum and oppositely charged drug was also evaluated.

Then the lower plate of the rheometer was replaced with a 3D printed cell with the capacity to expose samples to different fluids and simultaneously measure drug release (This device will be referred to as the rheo-dissolution cell from this point forward). Changes in rheological behaviour as well as drug release from the *in situ* gel forming formulations were performed using the rheo-dissolution cell which replaced the lower plate of rheometer, loaded with physiological fluid and connected to a circulatory peristaltic pump for facilitating sampling during the experiment. This technique was explored for an ophthalmic and oral formulations on exposure to the simulated lacrimal fluid and simulated gastric fluid respectively.

Finally, the permeability of a poorly soluble drug was increased by formulating an *in situ* gelling ophthalmic formulation using drug-cyclodextrin inclusion complex. The novel method of concurrently measuring rheology and drug release was also performed to evaluate the formulation.

3.7 Thesis Structure

This thesis consists of three results chapter and a concluding chapter.

Chapter 4 is the first of the results chapters which describes the development and rheological evaluation of an *in situ* gel forming ophthalmic formulation. The chapter begins with the background of *in situ* gel forming ophthalmic formulations and the anatomy of the ocular system. It demonstrates the methodology of formulating *in situ* gelling formulations based on a commercial product and performing oscillatory rheological analysis to evaluate the formulations. Furthermore, interactions between the anionic polysaccharide gellan gum and the positively charged drug timolol maleate are investigated and the importance of considering drug-polymer interactions when designing drug delivery systems with two oppositely charged molecules are discussed. In addition, the design, development and validation of the 3D printed rheo-dissolution cell is described in this chapter.

Chapter 5 builds on the development of the rheo-dissolution cell to simultaneously measure rheological changes and drug release of *in situ* gelling systems on exposure to the physiological fluids. The experimental set up of the rheo-dissolution technique is described in depth along with the methodology of simultaneous measurement of rheological changes and drug release of *in situ* gelling systems on contact with simulated lacrimal fluid and simulated gastric fluid. It also highlights the ability of the rheo-dissolution cell to change the chemical environment (pH change) while the experiment is in progress.

As the formulations in chapter 5 use water soluble drugs, in Chapter 6 a poorly soluble drug (flurbiprofen) was investigated. Here, an *in situ* gelling ophthalmic formulation using flurbiprofen-cyclodextrin inclusion complex was developed. This chapter begins with addressing the problem of formulating an *in situ* gelling system of poorly soluble drug as a

salt form and offers a method to overcome the problem by formulating as drug-cyclodextrin inclusion complex. This chapter presents a background to cyclodextrin and discusses the detailed methodology used in developing the formulation. Besides rheo-dissolution studies, *ex-vivo* permeation studies of the formulation using porcine cornea are also discussed.

Chapter 7 provides a final conclusion with summary based on chapter 4 to 6. It also highlights the recommendations for future work.

3.8 Publications and Presentations

Conference Presentations

- **4th UK Hydrocolloids Symposium, Leeds (UK), 12th September, 2019**

Oral Presentation- Rheo-Dissolution: A new technique for the simultaneous measurement of rheology and drug release from *in situ* gelling formulations (Faria G. Senjoti, Muhammad U. Ghori, Barbara R. Conway and Alan M. Smith)

- **RSC Biomaterials Chemistry Annual Conference, Liverpool (UK), 9th to 11th January, 2019**

Oral Presentation- Rheo-dissolution: A New Technique for the Simultaneous Measurement of Rheology and Drug Release from Hydrogels (Faria G. Senjoti, Muhammad U. Ghori, Barbara R. Conway and Alan M. Smith)

- **3rd UK Hydrocolloids Symposium, Nottingham (UK), 13th September, 2017**

Poster Presentation- Rheology and Dissolution Study for *In situ* Gel Forming Ophthalmic Drug Delivery Systems (Faria G. Senjoti, Barbara R. Conway, and Alan M. Smith)

Publications

Senjoti, F.G., Ghori, M.U., Diryak R., Morris G.A., Conway B.R., and Smith, A.M. (2020) Rheo-dissolution: A New Platform for the Simultaneous Measurement of Rheology and Drug Release. Carbohydrate Polymers, 229, 115541

Senjoti, F.G., Timmins, P., Conway B.R., and Smith, A.M. Modulating the Permeability of a Poorly Soluble Drug for Ophthalmic Delivery, European Journal of Pharmaceutics and Biopharmaceutics, 2019, under review

Chapter 4: Development and Rheological Evaluation of an *In Situ* Gel Forming Ophthalmic Formulation

4.1 Introduction

Ophthalmic drug delivery is one of the most challenging areas to develop drug delivery systems because of the unique anatomy and physiology of eye (Lang, 1995). Most ocular diseases are treated with topical eye drop formulations which are convenient and relatively easy to self-administer for the patient. But the precorneal, dynamic and static barriers restrict the delivery of drugs to the targeted ocular tissues. Nasolacrimal drainage, tear turnover and reflex blinking also significantly restricts drug permeation (Bourlais et al., 1998; Patel et al., 2013). Therefore, less than 5% of the applied drug reaches the target sites (Gaudana et al., 2010). Also, the therapeutic drug levels are not maintained in the target sites for a prolonged duration (Patel et al., 2013; Wu et al., 2018). Different approaches have been investigated during the past decades to improve bioavailability at the target sites without increasing the risk of systemic side effects or damaging the ocular tissues (Gaudana et al., 2010; Rupenthal et al., 2011). Polymers have played a vital role in the advancement of ophthalmic drug delivery technology by providing controlled release of therapeutic agents in consistent doses over prolonged periods for both hydrophilic and hydrophobic drugs (Liechty et al., 2010). Poor bioavailability of ophthalmic solutions caused by dilution and drainage from the eye can be overcome by using *in situ* gel forming ophthalmic drug delivery systems prepared from polymers that exhibit reversible liquid-gel phase transition (Cohen et al., 1997).

In situ gel forming ophthalmic systems are formulated as liquid dosage forms (2.5 to 10 ml in volume) which can conveniently instil as a solution into the eye. Upon administration, the liquid dosage form undergoes transition into a gel phase due to changes in temperature, pH

or ions which are abundant in the lacrimal fluid as discussed in the previous chapter. The gel then controls the release by providing a diffusional barrier for the drug, which is subsequently released more gradually than immediate release ophthalmic formulations. By transforming into the gel phase, *in situ* gel forming ophthalmic drug delivery systems not only prolong the pre-corneal residence time of drugs but also enhances ocular bioavailability. As a result, patient compliance is also improved (Cohen et al., 1997; Edsman et al., 1998; Liu et al., 2006).

To design potential *in situ* gel forming ophthalmic drug delivery systems, anatomy of the ocular system should be considered.

4.2 Anatomy of the Ocular System

The adult human eye ball is spherical in shape and is divided into two segments; the anterior segment and the posterior segment. The largest diameter of the eye ball is 24 mm antero-posteriorly. The anterior segment includes cornea, conjunctiva, iris, pupil, ciliary body, aqueous humour and crystalline lens. The posterior portion consists of sclera, retina, choroid, vitreous humour and optic nerve (Davson, 1984; Born et al., 1997; Addo et al., 2016) (Figure 4.1).

The pupil is a part of anterior segment of the eye and acts as an aperture. It is adjusted by the surrounding iris which acts as diaphragm. The pupil and iris are both covered by the cornea (Warwick and Williams, 1973).

Cornea is the clear avascular part of the eye and consists of five major layers which are corneal epithelium, Bowman's membrane, stroma, Descemet's membrane and epithelium layer. Therapeutic drug concentration at the aqueous humour depends on the corneal permeability of the drug. The five layers of the cornea play significant role in the corneal

permeability. The exterior layer is the corneal epithelium and it is a rate limiting barrier for most hydrophilic drugs.

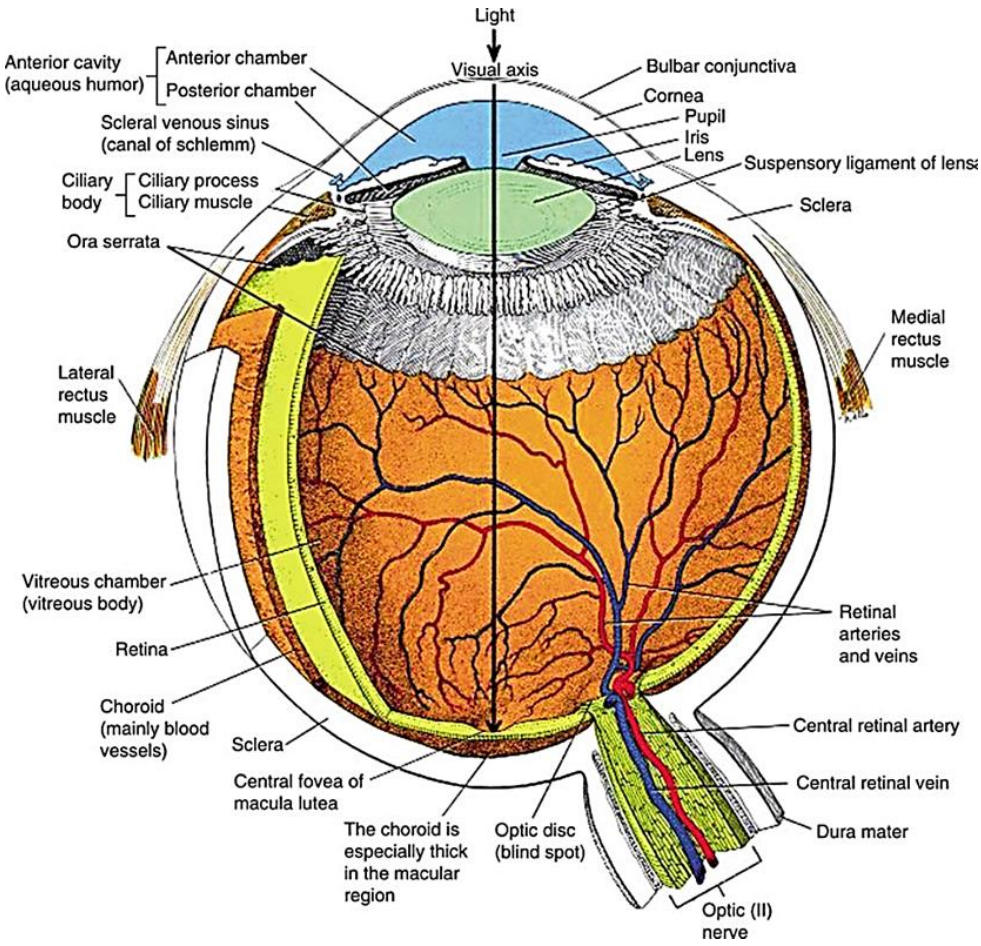

Figure 4.1: Schematic diagram of the human eye (Hickson, 1998)

The Bowman's membrane is the next layer which acts as a barrier between corneal epithelium and stroma. Stroma is hydrophilic in nature and consists of highly organized charged hydrophilic collagen. It acts as barrier for diffusion of hydrophobic drug molecules (Almeida et al., 2014; Malavade, 2016; Weng et al., 2017). Figure 4.2 shows the corneal barrier for diffusion of drugs.

Conjunctiva consists of goblet cells and stratified epithelium. It is a thin film membrane and it covers the inner eyelid surface and the sclera. It secrets mucus to protect the eyes from

microorganisms and also plays a role in lubricating the eyes. Systemic circulation of the drugs used in ophthalmic formulations are inhibited because of conjunctival blood capillaries and lymphatics. As a result, ocular bioavailability of the drug is decreased. (Addo et al., 2016; Huang et al., 2017).

The crystalline lens together with cornea, is responsible for the creation of image on the retina. Suspensory ligaments attached to the ciliary muscle hold the crystalline lens in place. The anterior chamber between the cornea and iris and the posterior chamber between iris and crystalline lens, are filled with aqueous humour. The vitreous humour is loose gel like substance and fills the cavity between crystalline lens and retina. Both aqueous and vitreous humour maintains the intraocular pressure and helps the eyeball to maintain its shape. The aqueous humour provides nutrients to the cornea. It also removes the waste from the non-vascular tissues and nourishes the lens and the cornea (Born et al., 1997; Achouri et al., 2013).

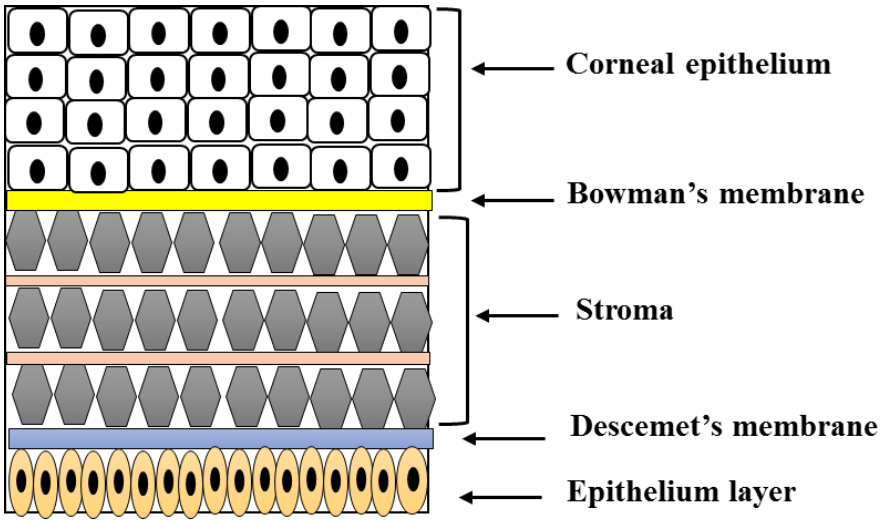

Figure 4.2: Schematic representation of the corneal barriers to the diffusion of the drugs

The retina is the multi-layered sensory tissue of the posterior segment and consists of

vascular, glial cells and nerve fibres. When light enters into the eye, it is focused onto retina to form reversed and inverted image. The retina is the major barrier of high molecular weight drug molecules (*e.g.* peptides, oligonucleotides). The external layer of the retina is the choroid which consists of a dense capillary plexus, small arteries, veins and blood vessels. Nutrients and necessary oxygen is supplied by the choroid to the posterior part of the eye. The sclera is the protective outer layer of the eye which is visible. It acts as the attachment part for the extraocular muscle and also maintains the intraocular pressure (Warwick and Williams, 1973; Almeida et al., 2014; Malavade, 2016; Huang et al., 2017).

4.2.1 Lacrimal Fluid

Lacrimal fluid is an aqueous solution and exists as a film on the surface of the eye. It plays a significant role to maintain a healthy eye environment by providing nutrients, removing waste and particulates, keeping the eye lubricated and protecting the eye from infection and injury. It also creates a smooth and transparent surface on the eye for light to pass through. It contains proteins, metabolites, electrolytes and lipids. The tear film consists of three layers which are the lower mucous layer, the middle aqueous layer and the upper oil layer. The mucous layer is hydrophilic in nature and is secreted by the goblet cells of conjunctiva. It maintains the stability of the aqueous layer of the tear film. The aqueous layer protects the eye from infection by carrying defensive proteins and antibodies. The fluid of this layer is mainly produced by the lacrimal gland. The oil layer is the thin top layer of the tear film and is spread over the aqueous layer. It maintains the stability of the tear film and prevents the evaporation. The oil of this layer is secreted from the Meibomian glands of the eyelids (Milder, 1987; Filik and Stone, 2008). The pH of lacrimal fluid is approximately 7.4 (Fischer and Wiederholt, 1982).

To effectively design an *in situ* gelling system, it is important to monitor the rheological behaviour of the gel former and release of the active molecule from the *in situ* gel. Besides rheological properties of the polymer, drug-polymer especially drug-polyelectrolyte interactions also play important roles in controlling drug release behaviour from polymeric drug delivery systems. Many drug molecules can have strong interactions with polymers used as *in situ* gel formers. Hydrophobic and electrostatic are the most common types of drug-polymer interactions although electrostatic interactions are more likely when the polymer is a polyanion or polycation. The arrangement of hydrophobic and polar segments in the chemical structures of the charged molecules plays an important role in drug-polymer interaction. Also, the surrounding medium plays a key role as it can regulate the degree of dissociation of ionisable groups depending on the pKa of the polymer and/or drug. Therefore, electrostatic interactions between two oppositely charged substituents are highly dependent on the pH of the surrounding medium which define the extent of ionisation of the charged molecules (Caram-Lelham and Sundelöf, 1996).

In the present study, an *in situ* gel forming ophthalmic formulation was prepared based on a currently marketed formulation Timoptol LA®. The formulation contained low acyl gellan gum (gellan) as the gel former and 6.8 mg/ml timolol maleate (TM) as the drug. Gellan is an anionic polyelectrolyte (Morris et al., 2012) and TM contains amino group capable of pH dependent ionization and is positively charged at pHs below its pK_a (9.21) (McKinney, 2004). So, there is a possibility that gellan and TM may undergo electrostatic interaction. Taking this into account, the present study also investigated the potential interaction between gellan and TM and their impact on drug release and rheological behaviour. The 'rheo-dissolution' cell was used as a modified dissolution apparatus to analyse the release of TM from the *in situ* gel and to validate the device as a suitable vessel to measure drug release.

4.3 Rheo-Dissolution Cell

The computer-aided design (CAD) of the rheo-dissolution cell was developed using Solidworks® (version 25, 2017). The cell was constructed from acrylonitrile butadiene styrene (ABS) using a Makerbot Replicator™ 2 3D printer (New York, USA). ABS was chosen for manufacturing due to its robust physical properties and low cost. It is considered as non-toxic and biologically inert. ABS is one of the most successful engineering thermoplastics and it is biocompatible as well as recyclable. (Adams et al., 1993; Chiang and Tzeng, 1997).

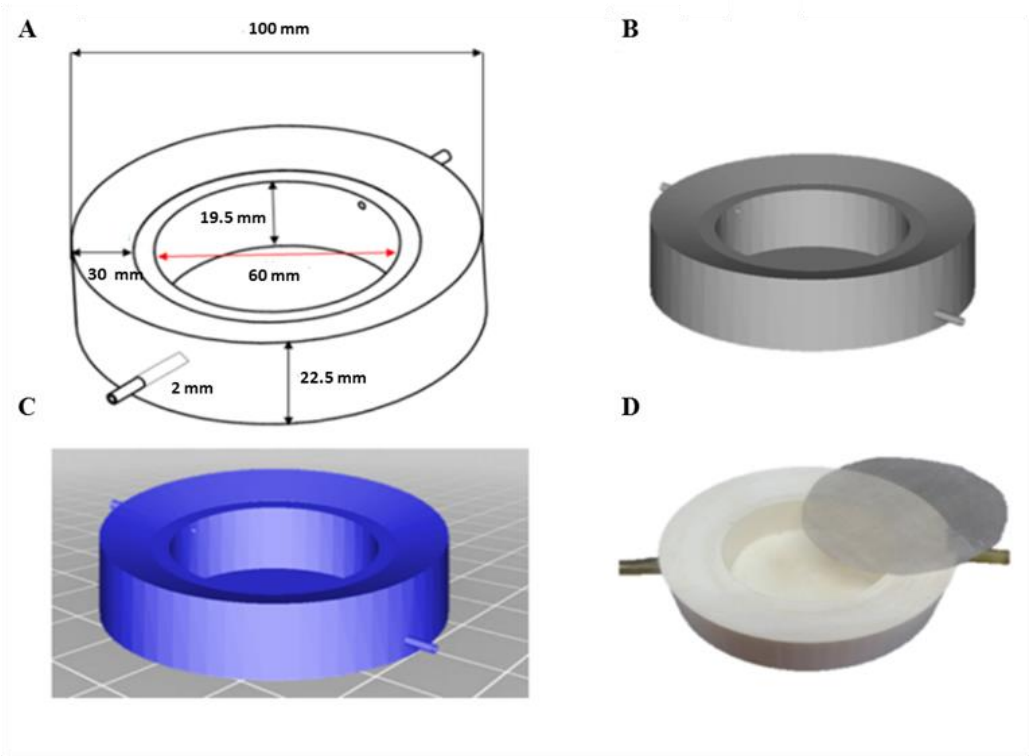

Figure 4.3: (A) Dimensions of rheo-dissolution cell (B) CAD model (C) Stl file model and (D) 3D printed rheo-dissolution cell showing removable mesh.

The cell was constructed as a circular reservoir with an opening on the top which was covered with a stainless steel mesh designed to act as a replacement for the lower plate of a rheometer. There were inlet and outlet ports (2 mm in diameter each) on the two sides of the

cell which facilitated loading and sampling the reservoir. The diameter of the reservoir was 60 mm and 19.5 mm height, enabling the cell capable of holding a 55 ml volume. Illustrations of specific dimensions of the rheo-dissolution cell with CAD and stl file models are represented in Figure 4.3A-C. A removable and interchangeable stainless steel woven wire mesh was placed on top of the reservoir where samples were loaded (Figure 4.3D). There were 80 openings per inch of the mesh (80 mesh count) with an area of 0.18 mm for each opening. For samples with low viscosity, a semipermeable membrane can be placed on the surface of the mesh to prevent sample flowing into the reservoir. By replacing the lower plate of the conventional rheometer with the rheo-dissolution cell, rheological measurements can be performed while being exposed to the physiological fluids loaded in to the reservoir. Moreover, the reservoir can be sampled in process to measure the release of active molecules from the sample while rheological measurements are being taken. These simultaneous measurements of rheology and drug release will be discussed in detail in chapter 5. In this chapter, the viscoelastic measurements (in terms of G′ and G″) and the release studies were performed separately using the rheo-dissolution cell as lower plate of rheometer and modified dissolution apparatus respectively.

4.4 Timolol Maleate

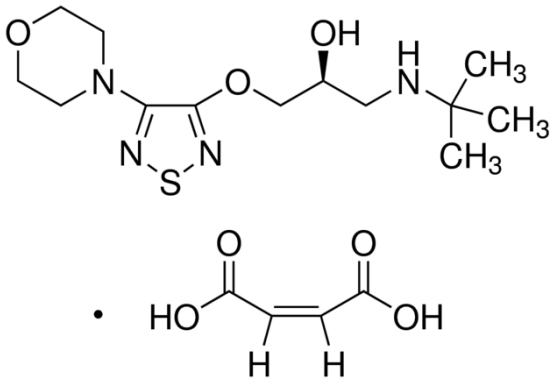

Figure 4.4: Chemical structure of timolol maleate (Joshi et al., 2009)

Timolol maleate (TM) was used as the active molecule to formulate the *in situ* gel forming ophthalmic formulation. It is a non-selective beta adrenergic antagonist. Its chemical name is (-)-1-(tert-Butylamino)-3-[(4-morpholino-1,2,5-thiadiazol-3-yl)oxy]-2-propanol maleate (1:1) (salt) (Figure 4.4). The molecular weight of TM is 432.50. It is a white, odourless, crystalline powder with a melting point 202 ± 0.5 ºC. It is soluble in methanol, water, and alcohol (Grunwald, 1986). TM is extensively used in the management of glaucoma which is a major cause of blindness in the elderly. Also, it is indicated for the management of hypertension as well as in reduction risk of reinfarction in patients who have survived the acute phase of myocardial infarction. In tonography and fluorophotometry, it was found that this adrenergic receptor blocking agent lowers the intraocular pressure through a reduction in the quantity of aqueous humour formation. In addition, it was also shown to increase the drainage of aqueous humour from the anterior chamber into the ciliary muscle, further reducing intra ocular pressure (Grunwald, 1986; Rathore et al., 2010).

4.5 Materials and Methods

4.5.1 Materials

Low acyl gellan gum (Gelrite®) (molecular weight 1,000 kg/mol) was purchased from Sigma-Aldrich (Poole, UK). TM was purchased from Tokyo Chemical Industry (Oxford, UK). Sodium bicarbonate was purchased from Fisher Scientific (Loughborough, UK). Calcium chloride dihydrate and sodium chloride were purchased from Sigma-Aldrich (Poole, UK). All chemicals were used without further purification.

4.5.2 Preparation of Simulated Lacrimal Fluid

Simulated lacrimal fluid (SLF) was used as a model physiological fluid. Table 4.1 shows the composition of SLF which was used to evaluate the *in situ* gel forming ophthalmic formulation of gellan-TM. The solution was prepared by dissolving the correct amount of

$NaHCO_3$, $CaCl_2$ and NaCl in 500 ml DI water with continuous stirring for 30 minutes. The pH of the simulated lacrimal fluid was 7.5. The use of this formulation has been previously reported by Anumolu et al., (2009) and Lin et al., (2010) to evaluate the *in vitro* release of pilocarpine from hydrogels and nanoparticles respectively. Pandit et al., (2007) reported the use of SLF formulated with same recipe to evaluate the *in vitro* release of indomethacin from a sodium alginate gel.

Table 4.1: Composition of SLF (Marques et al., 2011)

Ingredients	mM
$NaHCO_3$	23
$CaCl_2$	1 (as $CaCl_2 \cdot 2H_2O$)
NaCl	114

4.5.3 Preparation of *In situ* Gel Forming Ophthalmic Formulations

Gel forming eye drop solutions were prepared based on Timpotol LA® 0.5% w/v containing low acyl gellan as the gel former and 6.8 mg/ml TM as the drug. Four different formulations were prepared containing 0.2%, 0.3%, 0.4% and 0.5% w/v gellan and 6.8 mg/ml TM. TM was dissolved in DI water at room temperature. The solutions were heated up to 85°C while stirring with a magnetic hot plate stirrer (Starlab, Blakelands, UK) and the required amount of gellan was then added to the solutions. Once the gellan was completely hydrated, the stirring was stopped and the solutions were re-weighed. Any water lost was replaced and the formulations were transferred to airtight containers. All samples were allowed to cool to room temperature prior to further analysis.

4.5.4 Formulation Development

To analyse the gelation behaviour of the formulations prepared in section 4.5.3 on exposure to the SLF, viscoelastic measurements in terms of elastic (G′) and viscous (G″) modulus were performed. These measurements were taken to analyse and identify the similarities in gelation behaviour between the prepared formulations and Timpotol LA®. The developed rheo-dissolution cell was used to monitor the viscoelastic measurements by replacing the conventional lower plate of Kinexus rotational rheometer (controlled stress and strain) (Malvern, UK) (Figure 4.5). The cell was filled with 55 ml SLF and covered with a stainless steel mesh (mesh count 80). The mesh was securely attached to the cell to avoid any disturbance of the sample during the experiment. Inlet and outlet ports were closed using 10 ml syringes to prevent leaking. A serrated 40 mm parallel plate (pp) geometry was used and the gap was zeroed before samples were loaded.

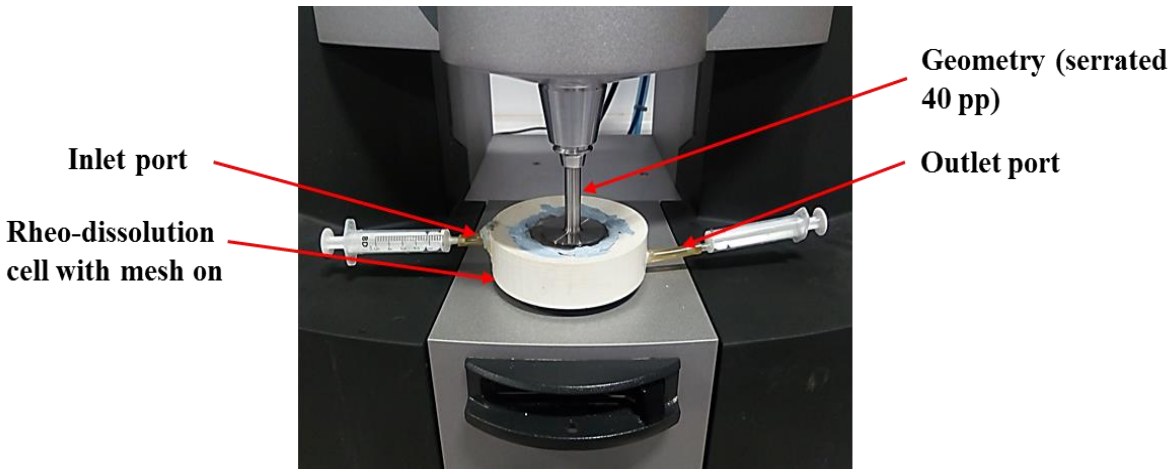

Figure 4.5: Experimental set up using rheo-dissolution cell to perform the viscoelastic measurements comparing gelation behaviour of *in situ* gelling ophthalmic formulations and Timpotol LA® on exposure to SLF

The gap was fixed at 0.8 mm and sample was loaded onto the mesh. The volume of the sample was determined according to the fixed gap. Measurement of G′ and G″ was performed at 0.5% strain (within LVR of gellan) and frequency of 1 rad/s. The tests for all

the samples were run for 30 min. The moduli (G′ and G″) of the Timpotol LA® were compared with the moduli of the formulations to select a concentration of gellan for the final formulation. All experiments were performed at 25ºC.

4.5.5 Preparation of Gellan Solutions and Gellan-TM formulations for Rheological Evaluation

Four different formulations of gellan and TM were prepared to evaluate the rheological analysis of gellan (Table 4.2). To prepare gellan alone, required amount of gellan (selected based on 4.5.4) was added into DI water while heated up to 85°C with continuous stirring. The stirring was stopped once gellan was fully dissolved and re-weighed. Any water loss through evaporation was replaced.

Table 4.2: List of the formulations of gellan used in the oscillatory rheological measurements (strain sweep, frequency sweep and temperature sweep)

Formulations	Preparation
Gellan alone	gellan in DI water
Gellan in SLF	gellan in freshly prepared SLF
Gellan-TM in DI	gellan and 6.8 mg/ml TM in DI
Gellan-TM in SLF	gellan and 6.8 mg/ml TM in freshly prepared SLF

In the preparation of gellan in SLF, DI water was replaced with freshly prepared SLF. Besides, gellan-TM in DI was prepared according to the method described in 4.5.3 with selected concentration of gellan and 6.8 mg/ml TM. The pH of the formulation was 4.5. Gellan -TM in SLF was prepared using the same methods.

4.5.6 Rheological Analysis

Rheological measurements of gellan alone and gellan in SLF were investigated to determine the impact of ions on the gelation behaviour of gellan. In addition, gellan-TM in DI and gellan-TM in SLF were also analysed to observe the effect of TM on gelation of gellan. Rheological measurements as a function of strain, frequency and temperature were performed using a Bohlin Gemini HR Nano Rheometer (Malvern Panalytical, UK) using serrated PP 25 geometry with the gap fixed at 1 mm. Silicone oil was added on the periphery of the samples to prevent evaporation during the measurement. All rheological experiments were performed at 25ºC.

4.5.6.1 *Strain Sweeps*

Strain sweeps measurements were conducted to determine the maximum LVR of the sample. The measurements were performed within 0.001 to 100 strain and the frequency was 10 rad/s.

4.5.6.2 *Frequency Sweeps*

The moduli of all the formulations were measured in response to increasing oscillatory frequency. The angular frequency increased from 1 to 628 rad/s with constant strain of 0.5% (0.005). The chosen strain was within the linear viscoelastic region.

4.5.6.3 *Temperature Sweeps*

Temperature sweeps of the formulations were conducted to determine the gelation point of gellan in presence and absence of ions and TM. Freshly prepared formulations (heated up to 90ºC) were loaded onto the similarly heated (90°C) lower plate of the rheometer and temperature sweeps were performed by cooling at a rate of 2 °C/min from 90°C to 20 °C at an angular frequency of 1 rad/s and 0.5% strain. No strain sweeps were required at 90ºC as

the gellan is in the disordered form as a solution, and the linear viscoelastic strain of biopolymer solutions extends out to approximately 100% strain (Clark and Ross-Murphy 2009).

4.5.6.4 *Gellan -TM Interaction*

TM contains an amino group which has a capability of pH dependent ionization. Therefore, to observe the potential interaction between positively charged TM and negatively charged gellan, pH of gellan-TM formulation was increased to 10, (which is above the pK_a (9.21) of the amino group) using 0.1M NaOH and oscillatory rheological analysis as a function of temperature was performed using the same method described in 4.5.6.3.

4.5.7 *In Vitro* Release Studies

In vitro drug release studies of TM from the *in situ* gel forming formulations were performed using the rheo-dissolution apparatus containing 55 ml of freshly prepared SLF. The cell was covered with a stainless steel mesh (mesh count 80) and the release media (SLF) was magnetically stirred at a speed of 100 RPM. The mesh was securely attached to the cell to avoid any disturbance of the sample during the experiments. Two 10 ml syringes were attached to the inlet and outlet of the cell to prevent the SLF leaking. The release media was maintained at a temperature of 37°C throughout the experiment (Figure 4.6). The formulation (1 ml) was placed on the top of the mesh and covered with a solvent trap to avoid any evaporation. The release medium in the reservoir was filled until it came in contact with the mesh which facilitated the gelation of the formulation when applied to the surface of the mesh.

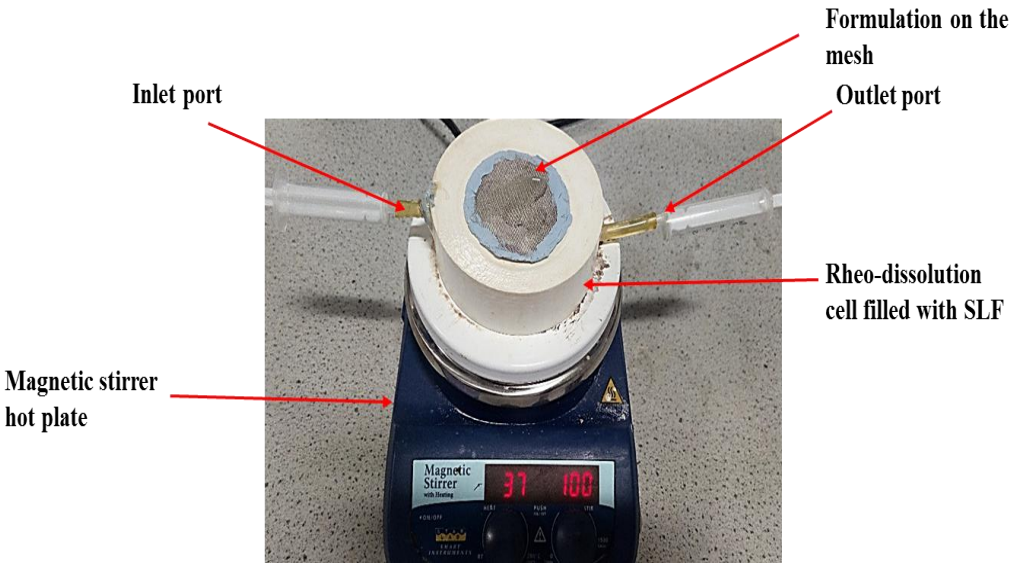

Figure 4.6: *In vitro* release study of gellan -TM formulation using the rheo-dissolution cell performed at a temperature of 37°C and 100 RPM

Samples of SLF (0.5 ml) were withdrawn at 2, 4, 6, 8, 10, 30, 60, 90, 120, 150, 180, 240 and 300 min from outlet port and replaced with same volume of freshly prepared SLF via the inlet port. The collected samples were diluted 10 fold and were analysed using reverse phase high performance liquid chromatography (HPLC). Drug release studies were performed for formulations prepared at both pH 4.5 and pH 10. All the experiments were done in triplicate.

4.5.7.1 *Determination of TM Using HPLC*

Reversed-phase high performance liquid chromatography (HPLC) method was used for the determination of TM in the collected samples. The experiments were performed on a Shimadzu System equipped with a SPD-20 AV Prominence UV/VIS detector, a LC 20 AT pump, and SIL-20A Prominence auto sampler.

4.5.7.2 *Chromatographic Conditions and Optimization of Experimental Parameters*

The mobile phase composition for the analysis of TM was optimized using various organic solvents including triethylamine, methanol, acetonitrile and water in different compositions. The mobile phase composition that resulted in the best resolution and shorter analysis time

of the studied compound was selected as the mobile phase for the drug release analysis. The selected mobile phase comprised of methanol: 0.2% triethylamine dissolved in HPLC grade water (60:40 v/v), pH 2.75 adjusted with 85% phosphoric acid. A flow rate of 1 ml/min was used throughout the experiments and the run time was 5 min. C18 HPLC column (Phenomenex) was used in the analysis and UV detector sat at a wavelength of 295 nm was used to detect TM (Nasir et al., 2011). The sample (20 µl) was injected onto the column and the data was acquired using LC Solution software (Shimadzu system). All the solvents used in the experiments were HPLC grade and the reagents were analytical grade. Methanol was purchased from Fisher Scientific, Loughborough, UK; triethylamine and phosphoric acid were purchased from Sigma-Aldrich, Poole, UK.

4.5.7.3 *Calibration Curve Preparation*

The linearity of the proposed method was determined from the calibration curves constructed at five concentration levels. Stock solutions of TM were prepared by dissolving 100 mg in 100 ml of SLF. The concentrations of the standard solutions were between 10 µg/ml and 50µg/ml and were analysed by HPLC using the experimental parameters described above. All the solutions were analysed in triplicate. Calibration curves were constructed by plotting the area under the curve (AUC) with respect to their respective concentrations using linear regression analysis. The slope (m), intercept (b), and correlation coefficient (r) were calculated from the regression equation. The linearity was assessed by linear regression (R^2 of 0.999). The limit of detection (LOD) and limit of quantification (LOQ) for the analytes were also quantified. LOD and LOQ are important parameters which are used to describe the smallest concentrations of a sample that can be reliably measured by an analytical procedure. LOD is defined as minimal concentration of analyte that can be detected with a certain degree of confidence and LOQ is defined as the minimal

concentration that can be measured with acceptable accuracy (Mahdi, 2016). LOD and LOQ are quantified by using Equations 4.1 and 4.2 respectively:

$$LOD=3.3\ \sigma/S \qquad \textbf{Equation. 4.1}$$

$$LOQ=10\ \sigma/S \qquad \textbf{Equation. 4.2}$$

Where σ is the standard deviation of Y-intercept and S is the slope of the calibration curve.

4.5.8 Fourier Transform Infrared Spectroscopy (FTIR)

Fourier transform infrared spectroscopy (FTIR) is one of the widely used spectroscopic techniques which analyses the sample by measuring the absorption of different infrared (IR) frequencies by that sample. In traditional FTIR analyses, the sample is positioned in the path of an IR beam and a spectrum is generated depending on the absorbance of the radiation at different wavenumbers (Bertrand, 1997). This spectrum represents the molecular fingerprint of a sample. In this work, FTIR analysis was performed in transmittance mode for samples using a Thermo Nicolet 380 FTIR across a wavelength range of 4000 to 400 cm^{-1} at 2 cm^{-1} resolution averaging 100 scans. FTIR spectra were taken for seven different samples (Table 4.3).

Table 4.3: List of samples and their preparation for FTIR analysis

Samples	Sample Preparation
Gellan dry powder	Gellan dry powder without further purification
TM dry powder	TM dry powder without further purification
Dry mix	Mixture of gellan and TM dry powder
Gel at 0 hour (pH 4.5)	*In situ* gel of gellan-TM formulation of pH 4.5 collected prior to the release study
Gel at 5 hour (pH 4.5)	*In situ* gel of gellan-TM formulation of pH 4.5 collected after 5 hours of release study
Gel at 0 hour (pH 10)	*In situ* gel of gellan-TM formulation of pH 10 collected prior to the release study
Gel at 5 hour (pH 10)	*In situ* gel of gellan-TM formulation of pH 10 collected after 5 hours of release study

The collected gel samples placed in 5 ml vials and stored in a freezer at -20ºC for 12 h. The frozen samples were then dried using a (Christ Alpha 2-4 L Dplus) freeze drier. The drying procedure was performed for 24 hours at -84.6ºC with the vacuum set at 0.001 mbar. The collected freeze dried samples along with powder standards (gellan, TM and dry mix) were then analysed using FTIR.

4.5.9 Replacing Gellan with Non Ionic Polysaccharide

To investigate the hypothesis that electrostatic interactions between gellan and TM could potentially impact on release of TM, gellan was substituted with a non-ionic polysaccharide and *in vitro* release studies were performed. Agarose was chosen as a non-ionic polysaccharide because it is experimentally well studied and undergoes a rapid sol-gel

transition upon cooling, following a similar gelation mechanism to gellan producing gels that are relatively stable (Nordqvist and Vilgis, 2011).

4.5.9.1 *Preparation of the Formulation*

To prepare the formulation, TM (6.8 mg/ml) was dissolved in DI water at room temperature. 0.4% w/v agarose was added to the solution under mechanical stirring at a temperature at 95ºC. The stirring was stopped once agarose was fully dissolved and the solutions were allowed to cool to room temperature to form gel.

4.5.9.2 *In Vitro Release Studies*

In vitro release studies were conducted according to the experimental set up described in 4.5.7 using the rheo-dissolution cell. The reservoir filled with 55 ml of SLF allowing contact with the mesh and 1 g of the gel was loaded on the top surface of the mesh and covered to avoid evaporation. Samples of SLF (0.5 ml) were withdrawn at 4, 6, 8, 10, 60, 120, 180, 240, 300 min and replaced with same volume of fresh SLF. The experiments were performed in triplicate. The collected samples were analysed using HPLC according to 4.5.7.2.

4.5.10 Statistical Analysis

Student's t test was applied to compare the data obtained from the *in vitro* release studies and $p < 0.05$ was considered as statistical significant level. IBM® SPSS Statistics software, version 24 was used for statistical analysis.

4.6 Results

4.6.1 Comparison of Gelation

To analyse the gelation behaviour of gellan, viscoelastic measurements of the prepared formulations (gellan and 6.8 mg/ml TM) and Timpotol LA® were performed in presence of SLF using the rheo-dissolution cell. The moduli (G' and G") showed low and similar values (~0.6 pa) for first few seconds which indicated an entangled polymer solution. Rapid increase of the moduli was observed over first 2 min on exposure to SLF and gelation continued for the remainder of the test.

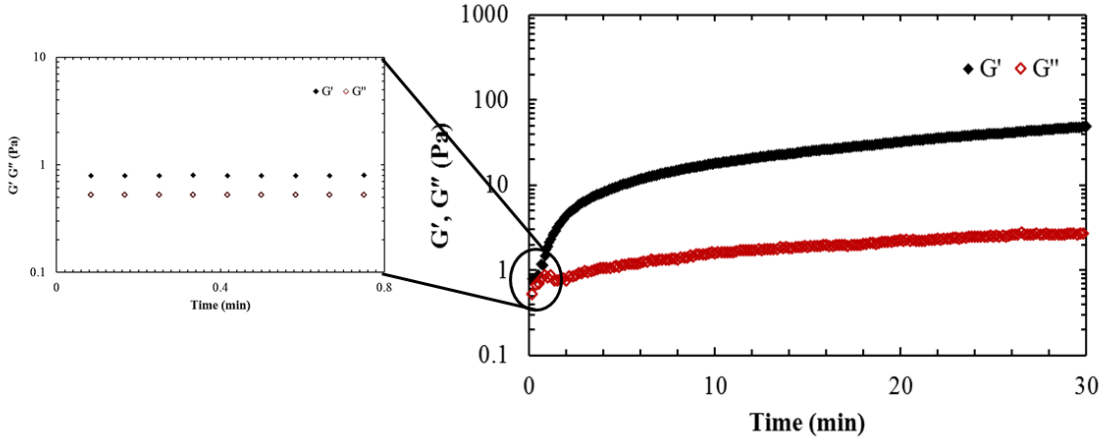

Figure 4.7: Measurement of elastic modulus (G′) and viscous modulus (G″) (Pa) of Timoptol LA® on exposure to SLF performed in the rheo-dissolution cell at 25ºC. Moduli values over first few seconds are shown in the zoomed in section on the left side

The G′ value reached at 48.85 Pa at the end of 30 min and G′ was higher than G″ throughout (Figure 4.9). Low gel strength was observed for the formulations containing 0.2% (Figure 4.10A) and 0.3% (Figure 4.10B) gellan. Onset of gelation was rapid for all the formulations but gels were stronger as the concentration was increased to 0.4% (Figure 4.10C) and 0.5% (Figure 4.10D). Table 4.4 shows comparison among the values of the moduli of the formulations and Timoptol LA®.

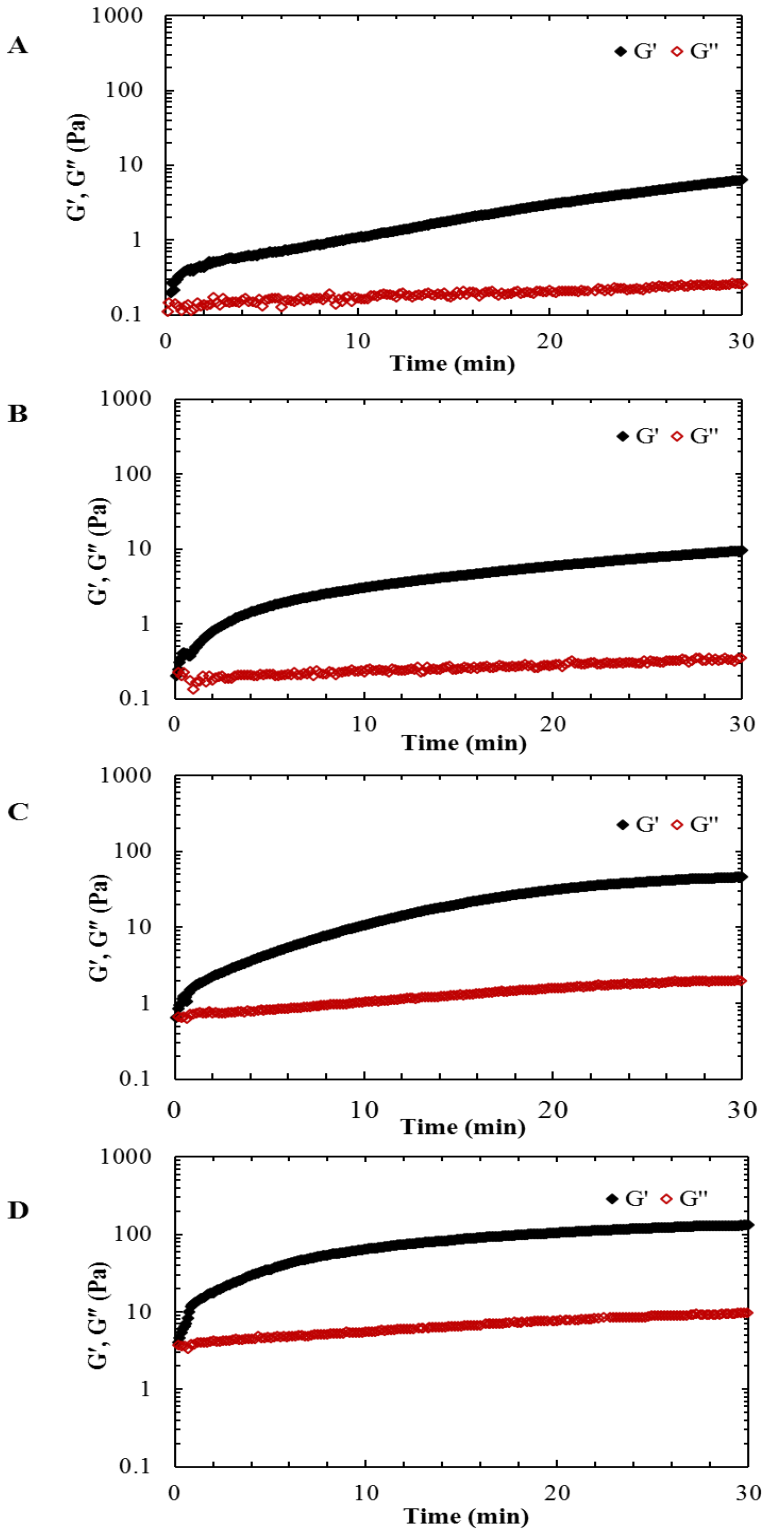

Figure 4.8: Measurements of G′ and G″ of formulation containing (A) 0.2% (B) 0.3% (C) 0.4% (D) 0.5% gellan and 6.8 mg/ml TM on exposure to SLF, performed in rheo-dissolution cell at 25°C.

Table 4.4: Comparison of the final values of moduli (G′ and G″) among Timpotol LA® and other formulations containing 0.2%, 0.3%, 0.4%, 0.5% gellan and 6.8 mg/ml TM. Values represent mean ± SD (n=3)

Formulation	G′ (Pa)	G″ (Pa)
Timoptol LA®	48.82 ± 2.47	2.70 ± 0.51
0.2% gellan and TM (6.8mg/ml)	6.35 ± 0.24	0.25 ± 0.02
0.3% gellan and TM (6.8mg/ml)	9.53 ± 0.69	0.35 ± 0.07
0.4% gellan and TM (6.8mg/ml)	46.27 ± 2.75	2.01 ± 0.38
0.5% gellan and TM (6.8mg/ml)	132.30 ± 2.11	9.67 ± 0.58

It is clear from the data that the values of the moduli of the formulation containing 0.4% were similar to the values of Timoptol LA®. Z score was used to compare the data obtained from viscoelastic measurements of Timoptol LA® and formulation containing 0.4% gellan and 6.8 mg/ml TM. 95% was considered as confidence level and was calculated using the following equation.

$$M \pm Z(s_M) \qquad \textbf{\textit{Equation 4.3}}$$

Where M is mean, Z is the chosen Z value (1.96 for 95% confidence level) and s_M was calculated from the following equation.

$$\sqrt{\frac{s^2}{n}} \qquad \textbf{\textit{Equation 4.4}}$$

Where S is the standard deviation and n is sample size.

The calculation showed that it is 95% confident that mean of G' (of both formulations) falls between 45.35 and 49.71; and the mean of G" falls between 2.08 and 2.68. So, 0.4% concentration of gellan was selected as a concentration for the final formulation.

4.6.2 Oscillatory Rheological Analysis

4.6.2.1 *Strain Sweeps*

Strain sweeps were performed to determine the critical strain required to break down the gellan networks. All gellan samples were composed of 0.4% w/w. Gellan in DI suggested larger linear region and displayed a higher critical strain (1.6) (Figure 4.11A). Addition of TM to gellan (gellan-TM in DI) showed increased moduli (Figure 4.11B) which required 0.2 strain to break. Gellan in SLF showed increased moduli (G′ ~20000 Pa and G″ ~2000 Pa) and it required less strain (0.08) to break the gel (Figure 4.11C). Formulation of gellan -TM in SLF did not change the values of the moduli but reduced the strain further (0.06) for the deformation of gel network (Figure 4.11D).

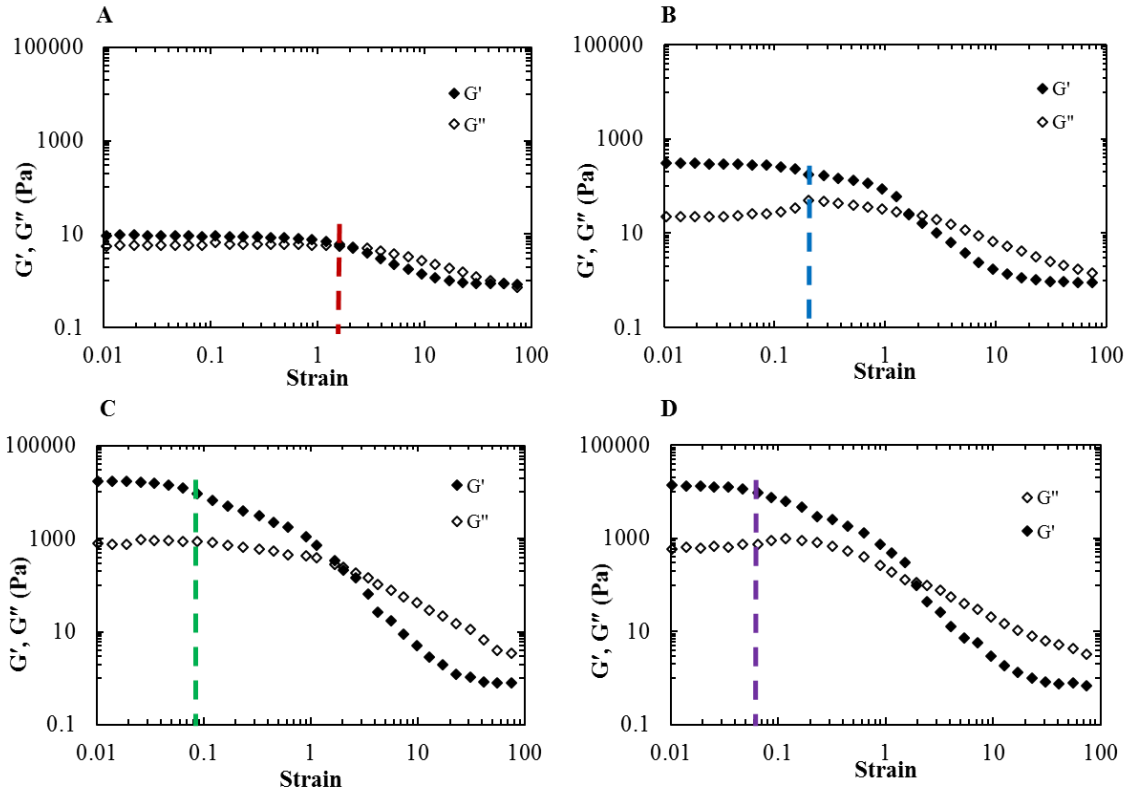

Figure 4.9: Strain sweeps of (A) gellan in DI (B) gellan-TM in DI (C) gellan in SLF (D) gellan-TM in SLF, performed within 0.001 to 100 strain, at 10 rad/s frequency and at 25°C. The lines indicate critical strain to breakdown the gel

4.6.2.2 *Frequency Sweeps*

Frequency sweeps of gellan in DI exhibited an increase in G′ in response to increased oscillatory frequencies. At an angular frequency of 1 rad/s, the sample had a G′ of 0.50 Pa which increased to 7630 at 620 rad/s (Figure 4.12A) and indicated an entangled system. Addition of TM (gellan-TM in DI) showed increased G′ (266.3 Pa) at 1 rad/s and maintained a similar trend of gel strength until the end of the experiment (Figure 4.12B). In presence of SLF (Figure 4.12C) and in case of the formulation of gellan-TM in SLF (Figure 4.12D); G′ increased to the values of 16120 and 20420 Pa respectively. Lack of frequency dependence indicated the formation of a strong gel.

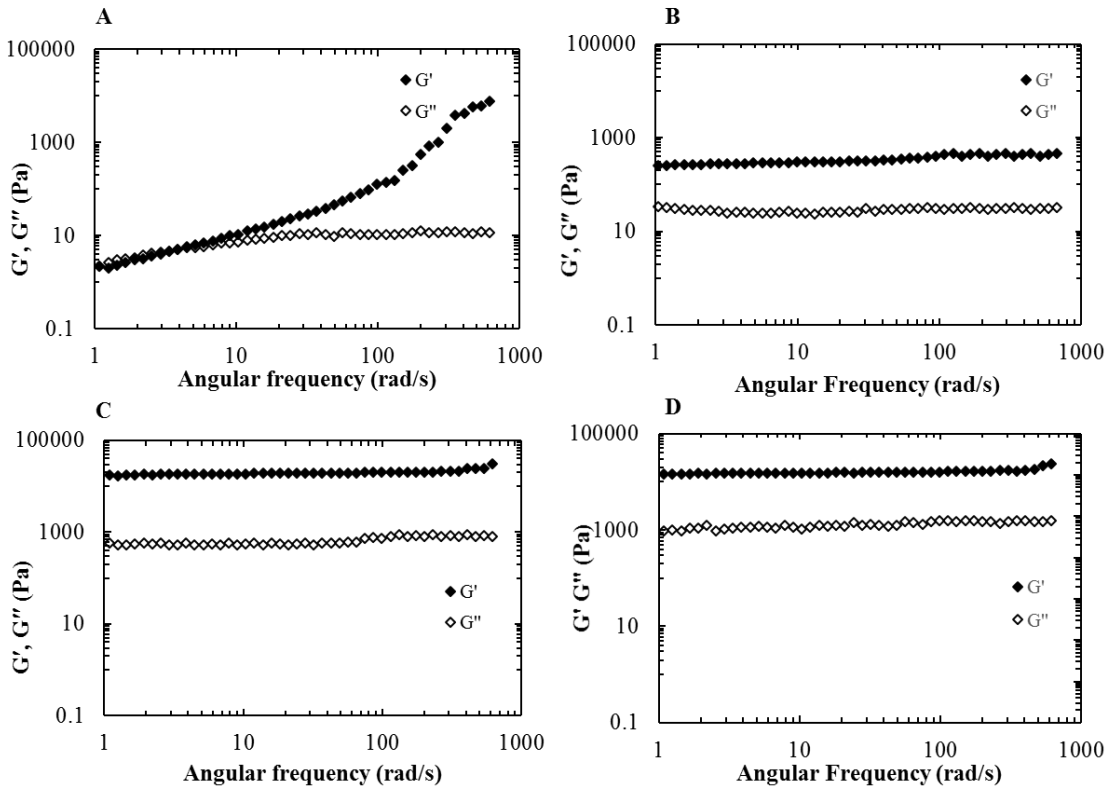

Figure 4.10: frequency sweeps (A) gellan in DI (B) gellam-TM in DI (C) gellan in SLF (D) gellan-TM in SLF at angular frequency increased from 1 to 628 rad/s with constant strain of 0.5%, performed at 25°C.

4.6.2.3 *Temperature Sweeps*

To evaluate the gelation properties of 0.4% gellan in presence of SLF and TM, viscoelasticity measurements were carried out on cooling from 90°C to 20°C. The gelation of gellan (in DI) occurred at ~30°C however this produced a relatively weak gel with an average G′ value of ~10 Pa at 20°C (Figure 4.13A). When prepared in SLF, the onset of gelation occurred at ~55°C resulting in a dramatic increase in G′ and G″ values as the gel was cooled further, plateauing at ~45 °C with a large difference between the values of G′ and G″ (G′ > G″) which represented the behaviour of a strong gel (Figure 4.13B). The effect of adding TM to gellan in the presence of SLF resulted in a gel of similar strength (Figure 4.13C) with G′ and G″ plateauing at a similar temperature as occurred without the TM.

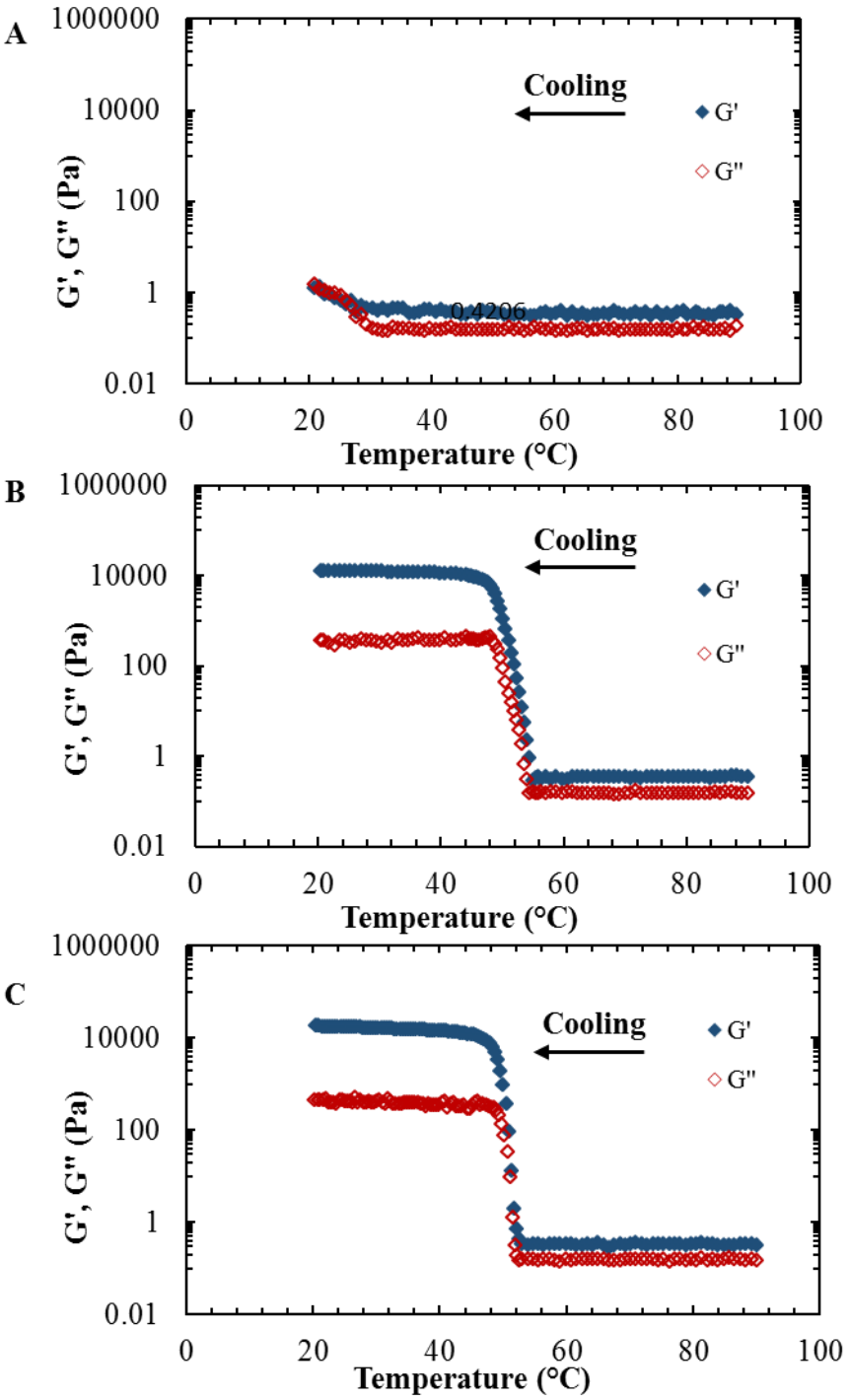

Figure 4.11: Oscillatory cooling scan at 2°C/min from 90°C to 20°C showing G′ and G" of (A) gellan in DI (B) gellan in SLF (C) gellan-TM in SLF performed at an angular frequency of 1 rad/s, 0.5% strain and at 25ºC.

4.6.2.4 *Effect of pH*

To investigate the potential interaction between two oppositely charged molecules of TM and gellan, formulations of two different pH (4.5 and 10) were analysed rhelogically. The positively charged amino group of TM was fully ionized at pH 4.5 whereas it was partially ionized at pH 10.

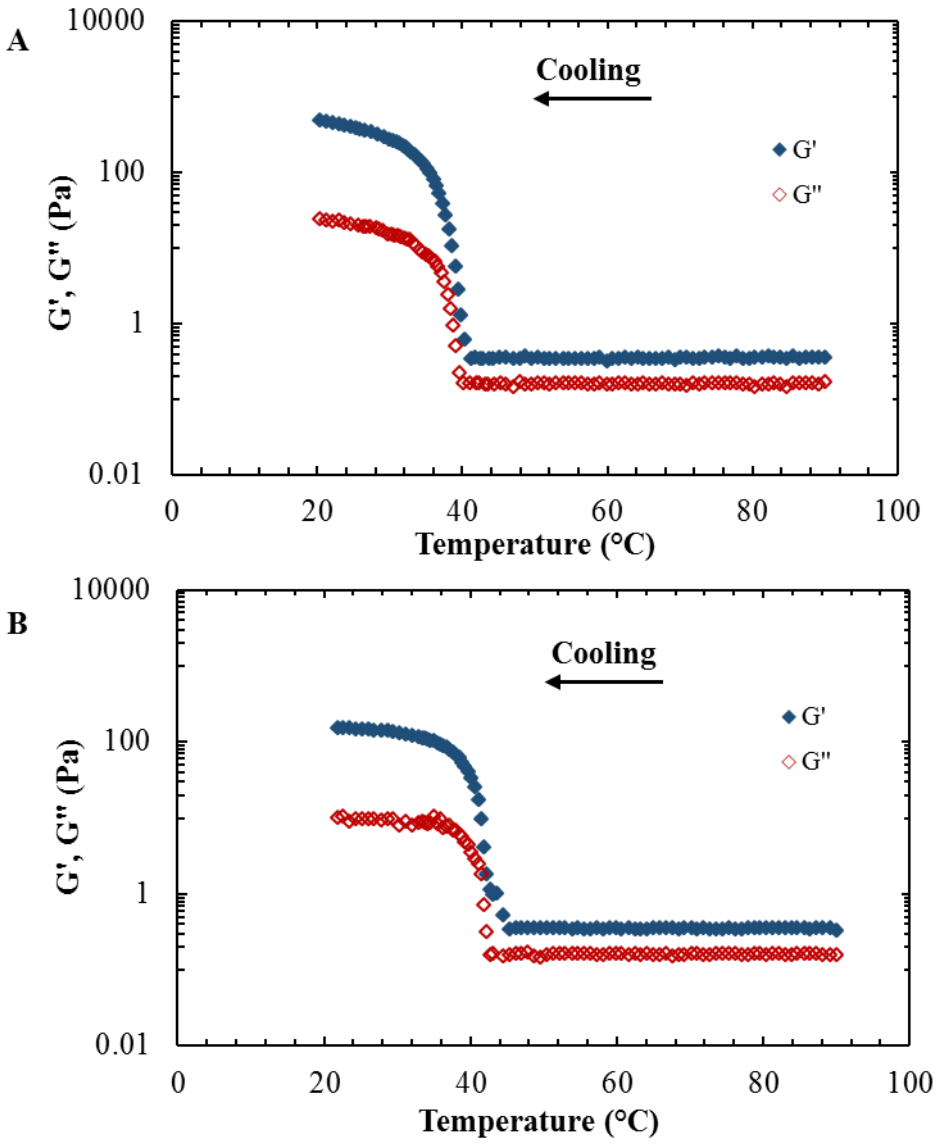

Figure 4.12: Oscillatory cooling scan at 2°C/min from 90°C to 20°C showing G′ and G" of the formulation containing 0.4% gellan and 6.8 mg/ml TM at (A) pH 4.5 (B) pH 10 in SLF performed at an angular frequency of 1 rad/s, 0.5% strain and at 25°C

The formulation of gellan-TM showed an increase in moduli at ~40°C (Figure 4.14A and B) at both pH (4.5 and 10). However, there was a distinct difference in the resultant gel strength. The gelation of gellan -TM at pH 4.5 produced a strong gel with an average G′ value of ~1000 pa. At pH 10, a relatively weak gel was produced with an average G′ value of ~100 pa.

4.6.3 Development of HPLC Method for the Determination of TM

For the determination of TM in *in situ* gel forming ophthalmic formulation of gellan -TM, a reversed phase HPLC method was developed using UV detection at 295 nm. Sample chromatogram of TM at 295 nm with retention time 3.1 min is shown in Figure 4.15.

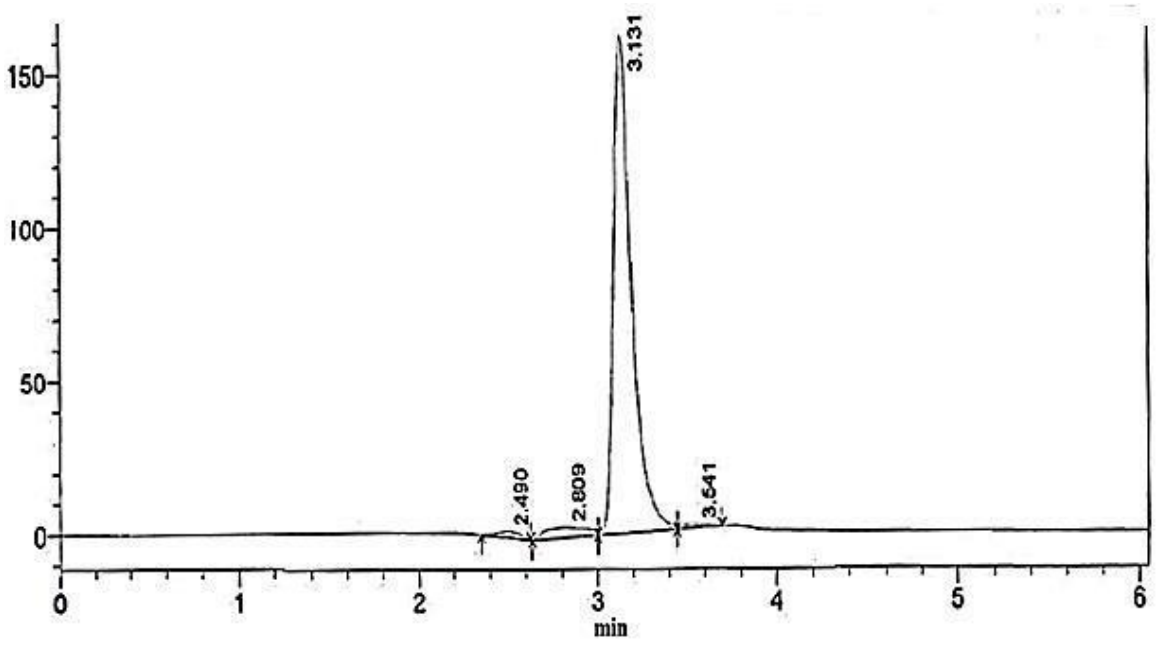

Figure 4.13: Chromatogram of TM detected at 295

The linearity of the proposed method was established by the least square regression analysis of the calibration curve (Figure 4.16). The constructed calibration curve was linear over the concentration range of 10-50 μg/ml (R^2 = 0.998). HPLC method validation is presented in Table 4.5.

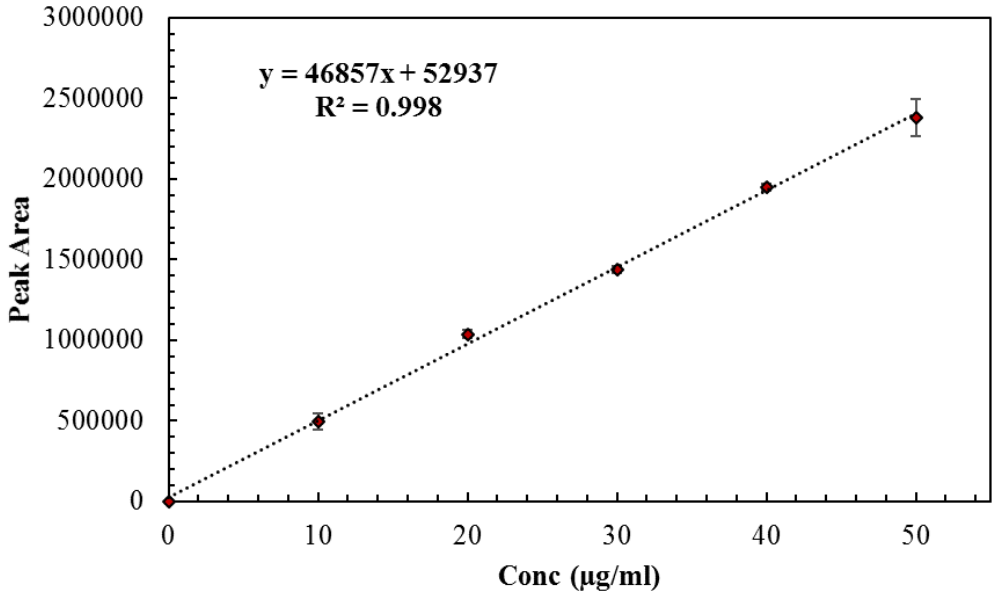

Figure 4.14: Calibration curve of TM at 295 nm by RP-HPLC Method; Values represent mean ± SD (n=3).

Table 4.5: HPLC method validation for the determination of TM

Range (µg/ml)	**0 to 50**
Regression equation	y = 46857x+52937
Correlation Coefficient	0.998
Retention time (min)	3.10
LOD(µg/ml)	3.22
LOQ(µg/ml)	10.73

4.6.4 Drug Release

The drug release profile of the formulation at pH 4.5 showed an initial average release of 4.45 (± 2.64) % of the drug at 2 minutes following which release continued to rise gradually (Figure 4.17). Average drug release was 47.56 % (± 5.51) at the end of 150 min and remained plateaued until the end of the test. A drug release study was also performed for the formulation at pH 10 (Figure 4.17) which showed initial burst release of 10.33 % (± 1.08) and showed significantly higher release ($p < 0.05$) than the formulation of pH 4.5. Moreover,

the plateau was reached at 180 min (30 min later that at pH 4.5) and drug release was 57 % (± 2.71) at the end of the test.

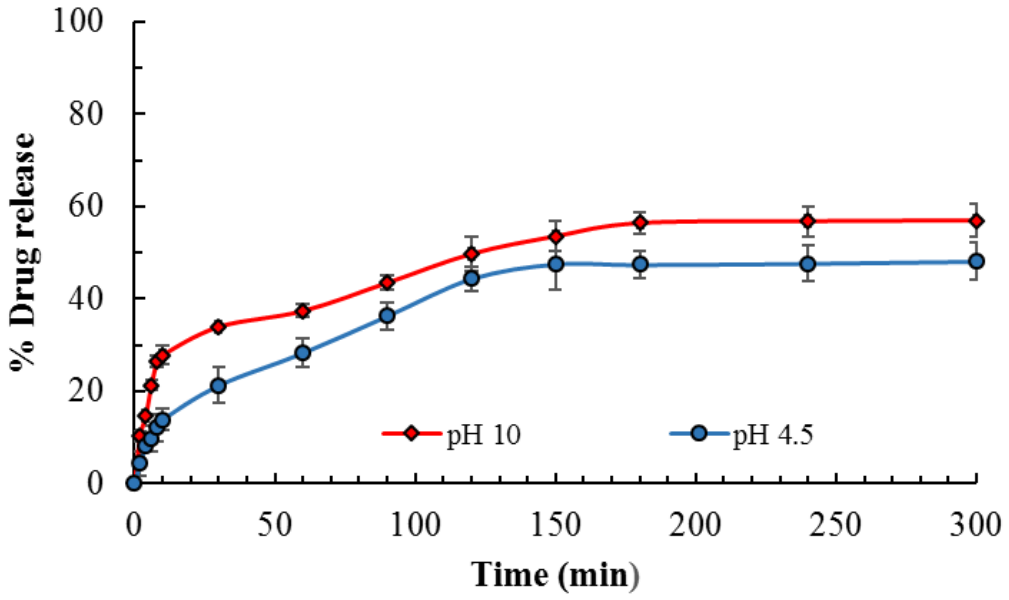

Figure 4.15: Release profile of TM from *in situ* gel forming ophthalmic formulation of gellan -TM at pH 4.5 and pH 10, performed in the rheo-dissolution cell containing SLF stirred at 100 RPM at a temperature of 37ºC. Values represent mean ± SD (n=3)

4.6.5 FTIR

To investigate the possible chemical interaction between gellan and TM, freeze dried samples of the gel at 0 and 5 hours (pH 4.5 and 10), dry powder of gellan and TM, dry mix of gellan and TM were analysed using FTIR. In the gellan dry powder (Figure 4.18A), a broad peak appeared at 3329 cm^{-1} due to O-H stretching. The bands at 2914 cm^{-1}, 1610 cm^{-1}, 1406 cm^{-1} and 1020 cm^{-1} were due to C-H, asymmetric COO- stretching, symmetric COO- stretching and C-O stretching respectively. In case of TM dry powder (Figure 4.18B), a broad band appeared at 3273 cm^{-1} due to O–H/N–H stretching vibrations. The band at 2964 cm^{-1} was due to aliphatic C–H stretching vibrations. A band at 1695 cm^{-1} was due to the acid carbonyl group of maleic acid. The band at 862 cm^{-1} and 1119 cm^{-1} was due to C-O stretching and C-N stretching respectively (Agnihotri et al., 2006; Joshi et al., 2009). The

dry mix of gellan and TM (Figure 4.18C) was not different from the individual FTIR spectra of gellan (Figure 4.18A) and TM (Figure 4.18B) dry powder. The bands of O-H stretching, C-H, asymmetric COO- stretching, symmetric COO- stretching and C-O stretching of gellan remained same for all gel samples. The band at 1695 cm^{-1} due to acid carbonyl group of maleic acid disappeared at gel at 5 hours (pH 4.5) (Figure 4.18E) and pH 10 (Figure 4.18G). But the samples of pH 10 showed an intense peak at 833 cm^{-1} which was present in the gel at both 0 and 5 hours (Figure 4.18F and G). The peak at 833 cm^{-1} however, is assigned to NH wagging which increased in intensity at pH 10 when the amino group was protonated and would not occur in the deprotonated state.

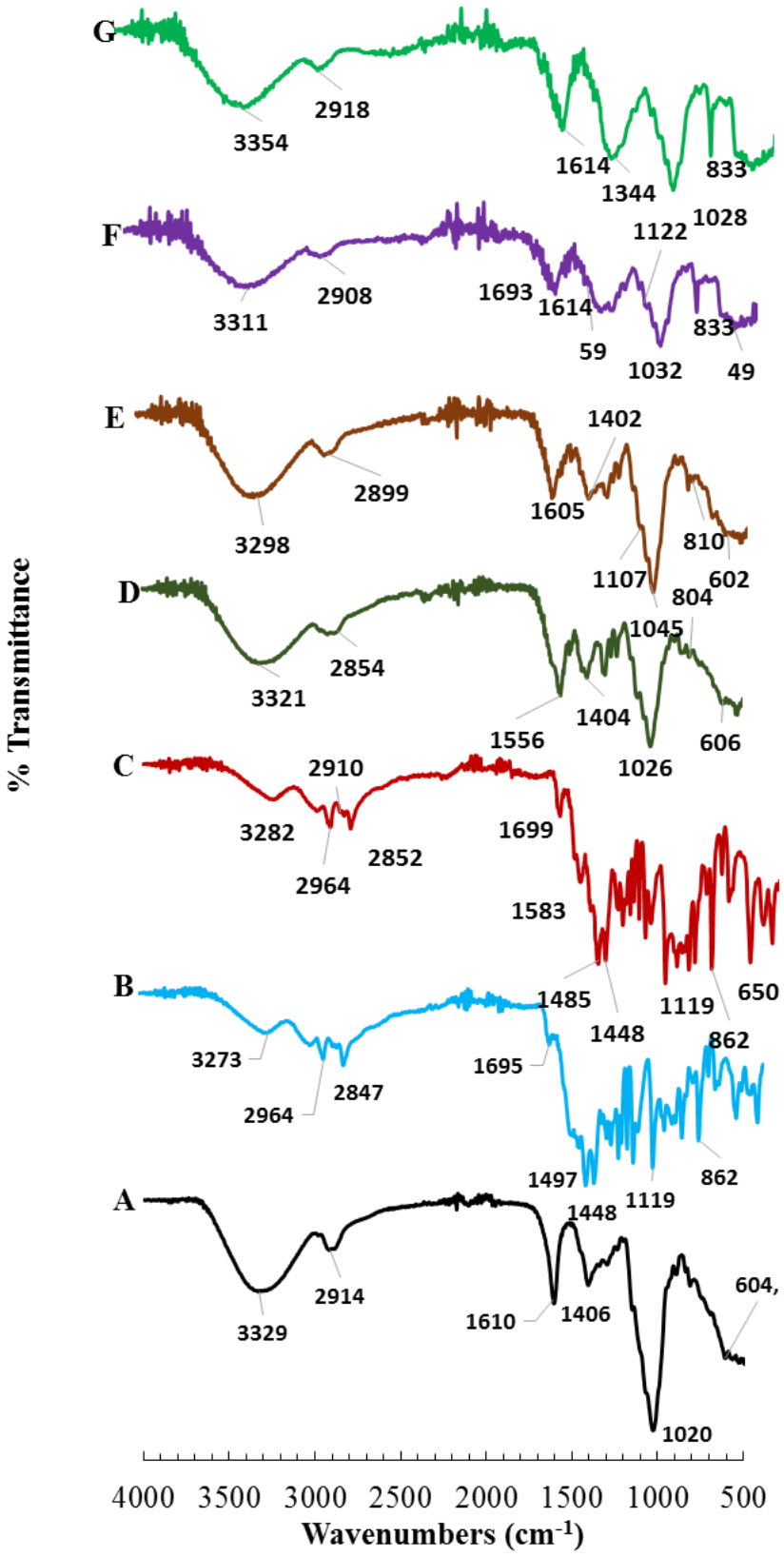

Figure 4.16: FTIR spectra of (A) gellan (B) TM (C) dry mix of gellan-TM (D) gel at 0 hour pH 4.5 (E) gel at 5 hour pH 4.5 (F) gel at 0 hour pH 10 (G) gel at 5 hour pH 10

4.6.6 Release of TM from Agarose

To observe the potential impact of gellan -TM interaction on TM release, gellan was replaced with 0.4% agarose and drug release study was performed (Figure 4.19). Initial burst release was observed at 5 min (9.30 ± 6.38 %) which increased gradually to 35.87 % (± 8.25) after 1 hour.

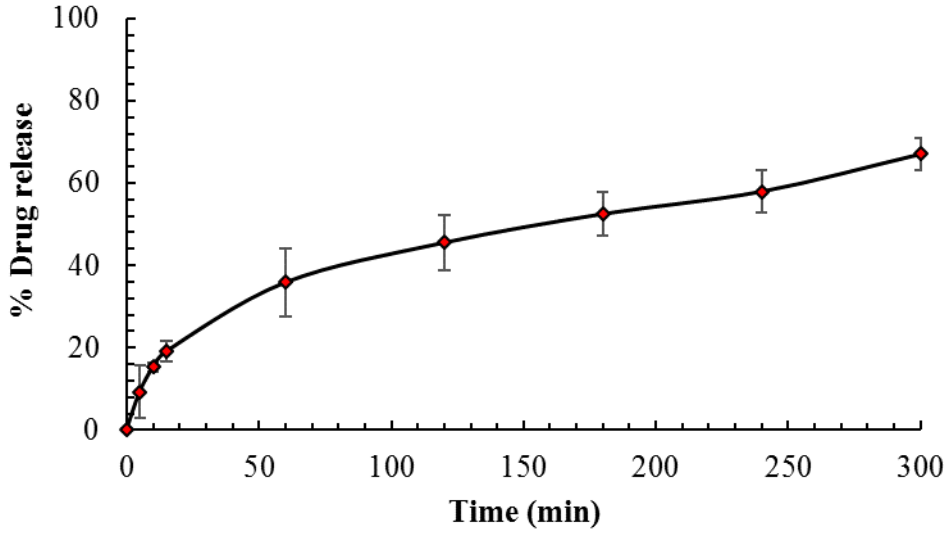

Figure 4.17: Release profile of TM from *in situ* gel forming ophthalmic formulation of agarose (0.4%) and TM (6.8 mg/ml) performed in the rheo-dissolution cell containing SLF (pH 7.5) stirred at 100 RPM at a temperature of 37ºC. Values represent mean ± SD (n=3)

The drug continued to be released from the gel until the end of the test when 67.02 % (± 4.03) of the drug was released at 5 hours (300 min). In comparison to the release from the gellan formulation (pH 4.5) (Figure 4.17), release of TM from the agarose formulation was significantly higher ($p < 0.05$) and no plateau was observed in the data.

4.7 Discussion

Rheological properties of the formulation directly influence the ocular residence time of *in situ* gel forming ophthalmic drug delivery systems. The rate of *in situ* gelation is important because a solution or a weak gel can be easily eroded by the fluid mechanics of the eye before a strong gel is formed (Carlfors et al., 1998). Sufficient gel strength not only inhibits the gel draining away but also preserves the integrity to facilitate sustained release of drug. Here we have shown rheological behaviour of gellan as a gel former in an *in situ* gel forming ophthalmic drug delivery systems. Different concentration of gellan (0.2%, 0.3%, 0.4%, and 0.5%) were used to make the formulations with 6.8 mg/ml of TM. A rheo-dissolution cell was used to evaluate the gelation of these formulations by facilitating their exposure to the ions in SLF. Timoptol LA® showed rapid *in situ* gelation in presence of SLF and elastic modulus (G′) was dominant over viscous modulus (G″) across the test (Figure 4.9). The gelation behaviour of the formulations (Figure 4.10) showed increased gel strength with increased concentrations. The formulation containing 0.4% gellan showed a similarity in gel strength when compared to Timoptol LA® (Figure 4.9). The resemblance of the values of moduli between two formulations confirmed (95% confidence level) the concentration of gellan in the marketed product (0.4% w/v) based on which the final formulation was prepared. So the *in situ* gelling ophthalmic formulation taken forward for the release studies contained 0.4% w/v gellan and 6.8 mg/ml TM.

The gelation of 0.4% gellan was investigated in presence and absence of electrolytes for better understanding regarding the rate of the sol/gel transition occurring in the eye. Strain sweeps provide an indication of gel stiffness (Farrés and Norton, 2015) and can quantify the deformation of polymeric gel networks. The strain sweep of gellan in DI presented low moduli values indicative of a weak gel (Figure 4.11A) which was more elastic within

relatively longer LVR. It was interesting to observe that addition of TM (in DI) produced relatively firm gel which required less strain to break the gel (Figure 4.11B). This behaviour was considered as an indication of gellan -TM interaction. In presence of cations (gellan in SLF), gellan became a firmer gel ($G' > G''$) because of the aggregation of helical domains and the critical deformation occurred at lower strain than in the weaker gels (Figure 4.11C) which could be due to the brittleness of the gel. Addition of TM (gellan-TM in SLF) did not change the firm but brittle gel behaviour (Figure 4.11D) when compared to the strain sweep of gellan in presence of cations (Figure 4.11C).

Frequency sweeps were conducted to assess the changes in modulus with increased angular frequency. According to the frequency sweep of gellan (Figure 4.12A), G' was slightly greater then G" which is a characteristic of weak gel (Ikeda and Nishinari, 2001). With the addition of TM, the gel strength increased with $G' > G''$ across the frequency range tested (Figure 4.12B). The predominance of elastic behaviour of gellan over its viscous behaviour and the mechanical rigidity indicated the formation of stronger gel in SLF (Figure 4.12C). Again, the presence of TM strengthened the gel and G' became more dominant over G" with increased angular frequency. It was also considered as an indication of gellan -TM interaction which was further confirmed by the cooling scan performed in elevated pH (pH 10).

The temperature sweeps perfumed on cooling, illustrated that the addition of ions caused early onset of gelation and strong gel formation (Figure 4.13B). Addition of TM increased the gel strength further (Figure 4.13C). Even the cooling scan of TM and gellan (pH 4.5) without any ions indicated higher gel strength with increased onset of gelation temperature (Figure 4.14A). The presence of the amino group in the structure of TM is likely to be responsible for the changes of the rheological behaviour of gellan. To investigate this, pH

of the gellan -TM solutions were elevated from 4.5 to 10 to protonate the amino group of the TM, thus removing its charge. The amino group of TM is capable of ionizing depending upon the environmental pH. At the pH below its pK_a (9.21), the amino group is positively charged however at pH above the pK_a the charge is removed (Figure 4.21) (McKinney, 2004). At pH 10, the onset of gelation (Figure 4.14B) was similar to the solution at pH 4.5 (Figure 4.14A) but the values of the moduli were significantly reduced and indicated the formation of a much weaker gel when the amino group of TM was positively charged.

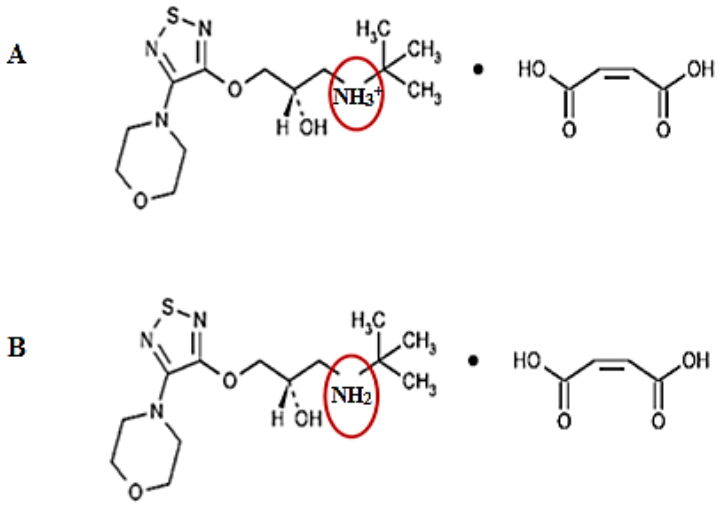

Figure 4.18: Structure of TM showing pH dependent ionization at (A) pH 4.5 (B) pH 10

It is thought that strong gels were formed at pH 4.5 due to suppression of the repulsion of negatively charged gellan by the positively charged amino groups of the TM. At pH 10, amino group was almost unionized (98%) (Aronson, 1983). It is predicted from the Henderson–Hasselbalch equation (Equation 4.3) that a weakly acidic drug is almost completely unionized when the pH is two units away from the pK_a (Aulton, 2007). But in the current scenario, pH was not completely two units away which helps to assume that there was still some charges left at pH 10. So, it was found that the ratio of ionized and unionized

drug at pH 10 was 6.165:1 whereas it was $1.95x10^{-5}$:1 at pH 4.5. Therefore, the electrostatic repulsion of the gellan was not fully suppressed by the TM resulting in the formation of relatively weak gel at pH 10.

$$p^H = pK_a + log_{10}\frac{[H^-]}{[HA]} \qquad \textit{Equation 4.4}$$

In the release study, the maximum release of TM from the *in situ* gel was approximately 48% after 5 hours at pH 4.5 (Figure 4.17). The release increased at pH 10 to approximately 57%. This was also probably due to electrostatic interaction between anionic gellan and positively charged TM for which significant amount drug was retained in the formulation. This was further supported by FTIR (Figure 4.18). The presence of band at 833 cm^{-1} was assigned to NH wagging; which indicated the existence of TM in the gel at 5 hours even at pH 10 (Figure 4.18G). Therefore, the presence of TM in unionized state and the incomplete release of TM shown in Figure 4.17, indicated that interactions other than electrostatic may occurring between gellan and TM.

Logarithm of partition coefficient (P) or log P of a drug plays role in the hydrophilicity or hydrophobicity of that drug. Negative Log P value indicates high hydrophilicity of the compound whereas value of 0 indicates equal ratios hydrophilicity and hydrophobicity. The compounds having log P value of 1 show hydrophilicity and hydrophobicity at a ratio of 10:1 (Bhal, 2007) and as hydrophobicity increases, the log P value also increases. The log P value of TM according to the literature is 1.83 (Hansch et al., 1995) and therefore, indicates the presence of hydrophobicity in the compound which increases the possibility of occurring hydrophobic interactions between gellan and TM. Indeed, Li et al., (1995) investigated the interaction between polyelectrolytes and oppositely charged surfactants and revealed that hydrophobic interactions also played a role besides electrostatic interactions between the two oppositely charged molecules. Moreover, there are also possibilities for hydrogen

bonding between the TM and the gellan. The many hydroxyl groups on the gellan chains are potential hydrogen bond donors which could interact with the hydrogen bond acceptors on the TM (Andrews et al., 2009; Marsac et al., 2009). Duxfield et al., (2016), developed polymeric nanoparticles of gatifloxacin where cationic Eudragit was used as the polymer. Slow release of gatifloxacin was observed, which was thought to be due to hydrophobic interactions between drug and polymer. Also, electrostatic interactions between the quarternary ammonium groups of Eudragit and the carboxyl group of gatifloxacin further prevented the release of drug.

However, the electrostatic interactions between the protonated amino group of TM and anionic materials have been previously reported. Joshi et al., (2009) reported incomplete release of TM from a formulation where montmorillonite was used as a drug delivery system. Electrostatic interactions between the protonated amino groups of the TM and the anionic charges at surface of montmorillonite led to partial drug release (43-48%). Bonferoni et al., (2004) utilized the interaction between anionic polymer carrageenan and cationic drug TM to control the drug release. Rozier et al., (1989) reported incomplete release of TM following 6 hours submerged 650 ml of SLF from an ophthalmic vehicle of gellan. When gellan was replaced with non-ionic polysaccharide agarose, increased release of TM was observed (Figure 4.20). This is thought to be due to the absence of interaction between agarose and TM. As agarose is a non-ionic polysaccharide, no electrostatic interaction occurred between the positively charged amino group of TM and uncharged agarose, however, as the release was slow and also incomplete following 5 hours further supports potential hydrophobic interactions occurring between the TM and the polymer.

The drug-polymer interactions therefore, can directly influence the characteristics of drug delivery systems including the release behaviour. So, the drug-polymer interactions are of

great importance in designing a drug delivery system in particular when using charged polysaccharides and oppositely charged drugs.

4.8 Conclusion

This study has demonstrated the gelation behaviour of gellan (as the gel former) on contact with SLF which is a key to the successful formulation of *in situ* gel forming ophthalmic drug delivery systems. This study has shown the development of rheo-dissolution cell which can replace the conventional lower plate of a rheometer to perform rheological measurement of *in situ* gelling systems on exposure to physiological fluid. Also, this can be used as a modified dissolution apparatus to study drug release. However, the impact of TM on gelation behaviour of gellan has been demonstrated here which showed the existence of interactions between TM and gellan. The release data supported the finding by showing incomplete release of TM from the *in situ* gel which is thought to have occurred as a result of electrostatic interactions between the negatively charged gellan and positively charged TM. Therefore, drug polymer interactions should be an important consideration when designing *in situ* gelling formulations especially when using charged polymers with oppositely charged drugs.

Chapter 5: Development of a Model for Simultaneous Measurement of Rheology and Dissolution for *In situ* Gel Forming Drug Delivery Systems

5.1 Introduction

In the previous chapter, a 3D printed rheo-dissolution cell was developed and tested for the ability to work as a lower plate of a conventional rheometer. Also, it was tested separately as a reservoir to perform drug release measurements. In this chapter, the methods of measuring rheological changes and release of drug have been tested simultaneously (rheo-dissolution) with an *in situ* gel forming ophthalmic formulation of gellan-TM that was developed in chapter 4. Also, to highlight the versatility of the rheo-dissolution method, an *in situ* gelling oral formulation was tested. Sol-gel transitions triggered by changes in pH or ionic strength tend to occur rapidly and are therefore considerably more challenging to measure as discussed in chapter 1 to 3. Besides, the conventional methods of measuring drug release from *in situ* gelling systems are always performed without observing the impact of gelation on drug release. This is despite the fact that release of drugs from *in situ* gelling systems is generally governed by drug diffusion through the polymeric material and/or by erosion/dissolution of the gel. The rate of drug release therefore, is strongly related to the gel properties such as, gelation kinetics, gel strength and gel dissolution (Sako et al., 1996; Roshdy et al., 2001). So, by designing a method of analysing rheological changes while measuring the release of active molecules *in situ* can be beneficial when designing *in situ* gelling systems.

In this work, rheo-dissolution experiments of *in situ* gelling formulations were conducted on exposure to two different physiological fluids. Experiments using the ophthalmic

formulation of gellan-TM (developed in chapter 4) were conducted on exposure to simulated lacrimal fluid whereas studies on the oral formulation were performed on exposure to simulated gastric fluid. It is important to understand the concept of anatomy of the physiological system on which the drug delivery is based. The concepts of *in situ* gel forming ophthalmic formulations and anatomy of the ocular system have been discussed in chapter 4. The concepts of *in situ* gel forming oral formulation and anatomy of the gastrointestinal system will be discussed in this chapter before proceeding to the experimental parts.

5.2 *In Situ* Gel Forming Oral Drug Delivery Systems

Oral drug delivery is the most convenient and preferred route of drug administration due to flexibility in the dosage form design, ease of production, cost effectiveness, high patient compliance and flexible dosing schedule. Orally administered drugs are exposed to variable pH of the gastrointestinal tract (GIT) where the pH varies from highly acidic in stomach (pH 1 to 3) to neutral or slightly alkaline in the small intestine (pH 6 to 7.5) (Liu et al., 2017). Exposure of drugs to these pHs may result in oxidation, hydrolysis or deamidation of drugs (for example protein drugs). To achieve adequate bioavailability is another challenge of orally administered drugs (Sood and Panchagnula, 2001; Choonara et al., 2014). To overcome these barriers, pH responsive polymeric systems are widely used and have been proven to increase the stability of drugs in the stomach along with release of drugs in a sustained manner (Liu et al., 2017). pH triggered *in situ* gelling oral drug delivery systems have been major research focus which use pH responsive polymer as *in situ* gelling agents. Alginate has been considered as an attractive material to formulate such delivery systems because of its ability to undergo gelation at acidic pH and break into a soluble viscous layer at intestinal pH (Kulkarni et al., 2001).

In this work, the oral *in situ* gelling formulation was formulated using metronidazole (200 mg/5 ml) and 2% alginate as an *in situ* gelling polymer. It was apparent on visual observation that 2% alginate had sufficient viscosity and was easily pourable. Also, the use of the same concentration of alginate has been reported in several published papers (Patel et al., 2011; El Maghraby et al., 2012; Szekalska et al., 2018). Rheo-dissolution study of this formulation was investigated over two different pHs (acidic and alkaline) to evaluate the impact of variations in gastric pH on rheology and drug release behaviour. However, to design an *in situ* gel forming oral drug delivery system successfully, it is important to consider gastrointestinal anatomy.

5.2.1 Gastrointestinal Anatomy and Physiology

GIT, also called the alimentary canal, consists of the digestive system structures and the accessory organs. The system is approximately 10 meters long and can be divided into two parts; the upper GIT and the lower GIT (Peate, 2018). The contents of GIT vary widely in volume, viscosity, composition and pH (Schanker, 1960) which affect the absorption of drugs from the GIT.

The upper GIT is composed of oral cavity, salivary glands, oesophagus, stomach and small intestine (duodenum, jejunum and ileum) (Figure 5.1). The key functions of upper GIT are to transport the swallowed food, enzymatic digestion of the food and absorption of nutrients. The upper GIT also plays a role in protective barrier function against the external environment. The oral cavity is the first portion of upper GIT and the process of digestion begins here. Salivary glands produce saliva from the clusters of cells and it flows from the salivary glands into the collecting ducts. Saliva contains approximately 99% water and a variety of electrolytes which are potassium (19.5 mmol/L), calcium (1.32 mmol/L), sodium

(5.76 mmol/L), magnesium (0.2 mmol/L), phosphate (5.7 mmol/L), bicarbonate (5.5 mmol/L) and chloride (16.40 mmol/L) (Whelton, 1996). It also contains enzymes, mucosal glycoproteins, polypeptides, oligopeptides and traces of albumin (De Almeida et al., 2008). The normal pH of saliva is 6 to 7 (Humphrey and Williamson, 2001).

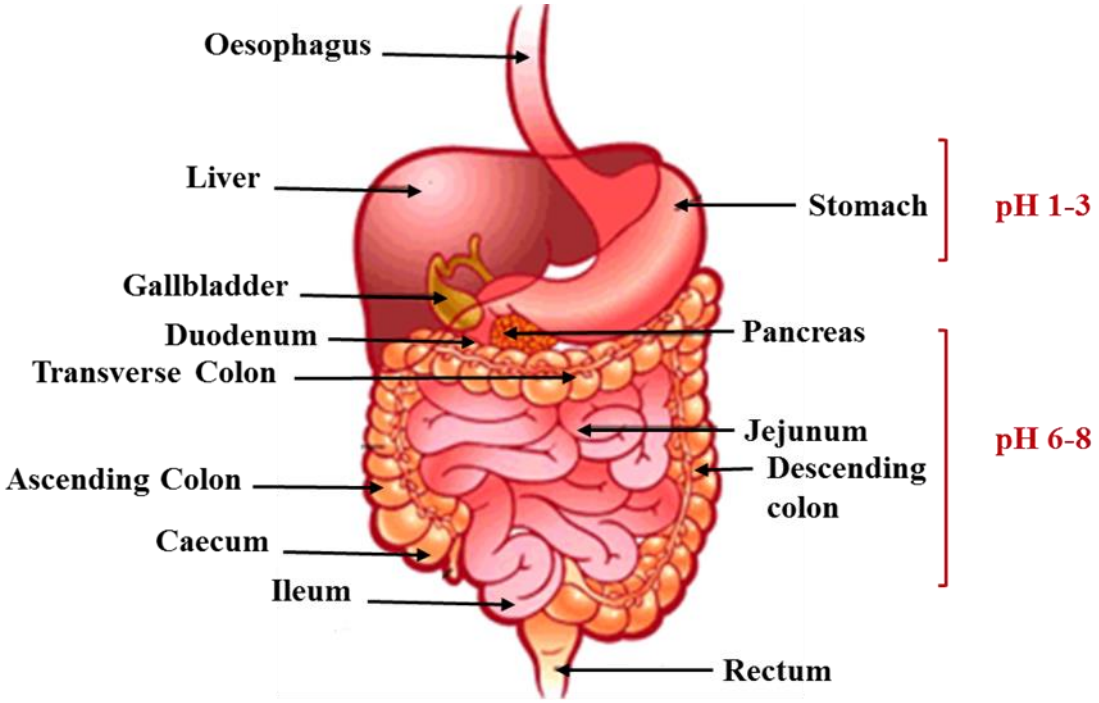

Figure 5.1: Schematic diagram of anatomy of human GIT with varying pH

5.2.1.1 *Oesophagus*

Oesophagus extends from laryngopharynx to the stomach and is approximately 25 cm in length and 2 cm in diameter. It is a thick-walled structure composed of multiple layers and organized as a muscular tube surrounding a hollow central lumen. It transports the masticated and swallowed material (also called bolus) from the pharynx to the stomach. The pH of oesophagus lumen ranges from 5 to 6 (Patti et al., 1997; Ashford, 2007).

5.2.1.2 *Stomach*

The stomach is the dilated portion of the GIT and is located on the left side of the upper abdomen. The main responsibility of stomach is to store and process the food into chime and deliver to the duodenum (Treuting et al., 2017; Peate, 2018). It is approximately 0.2 m in length with a surface area of 0.2 m^2 (Minami and Mccallum, 1984). The stomach is divided into four anatomic regions which are cardia, fundus, body and antrum. The fundus and the body of the stomach cause compaction of the stomach contents by contracting the muscle walls (Hoichman et al., 2004). Gastric acid is a digestive fluid that is formed in stomach and plays significant role in digestion. The main constituent of the gastric fluid is hydrochloric acid (~ 0.1M) which is produced by the parietal cells of the gastric glands. Other constituents are pepsin (secreted in the form of pepsinogen), gastrin, mucus and gastric lipase. The pH of the gastric fluids ranges from 1 to 3 (Ashford, 2007; Liu et al., 2017) Approximately 1.5 Litres of gastric acid is secreted daily by a typical adult human (Dworken, 2016). The pH of the stomach depends on the amount of HCl secreted and on the fed or fasted state of the person. The pH is usually between 1 and 3 under fasted conditions. Under fed conditions, the gastric fluid is less acidic with the pH ranging between 3 and 7. It takes approximately 2 to 3 hours to return the fed state gastric fluid pH to fasted state pH (Ashford, 2007; Bowles et al., 2010; Batchelor et al., 2013).

The pyloric sphincter plays a key role in releasing the stomach contents into the small intestine through relaxation. Migrating motor complex (MMC) and digestive motility pattern control the gastric transition. MMC is cyclic waves of electrical activity which triggers the recurring motility pattern of peristalsis occurring in stomach and small intestine. MMC can be divided into 4 phases starting from phase I which is also called basal phase. It lasts for 45 min to an hour and phase II lasts for 40 to 60 min (Minami and Mccallum, 1984).

Low mechanical activity of stomach is observed in these two phases whereas phase III (burst phase) consists of intense regular contraction but it lasts for only 4 to 6 min. Phase III helps to empty the stomach contents into the small intestine. Phase IV lasts for maximum 5 min due to declining the stomach activity between phase III and I. It takes approximately 90 to 120 min to complete a cycle (Soppimath et al., 2001; Pawar et al., 2011).

Gastric emptying of pharmaceutical dosage forms depends on the active cycle of the stomach at the time of administration with emptying times ranging from 5 to 120 min (Ashford, 2007). Delayed gastric emptying is useful for the drugs that are absorbed mainly from the stomach. Solids and larger particles are emptied from the stomach more slowly whereas liquids and small particles are easily transferred into the small intestine (Conway, 2005). When *in situ* gelling formulations are administered orally, they undergo acid gelation in the stomach and are transformed into solid gel which is emptied from the stomach more slowly. Therefore, *in situ* gelling in the stomach can be a useful strategy to increase retention time and therapeutic effects of the drugs.

5.2.1.3 *Small Intestine*

The small intestine starts from the pyloric sphincter of the stomach and ends at the ileocecal junction where it attaches to the large intestine. The length of small intestine is approximately 4 to 5 m (Ashford, 2007). The duodenum is the first section of small intestine and is about 25 cm long. It is responsible for the breakdown of food with the use of enzymes. The duodenum controls the rate of emptying of stomach and proceeds to the jejunum and ileum. The jejunum has a thicker wall and is about 0.9 meters long. It runs from duodenum to ileum (Young et al., 2013). The duodenum and jejunum are responsible for the absorption of most carbohydrates and proteins. The longest segment of the small intestine is ileum and

is about 1.8 meters long. It has more mucosal folds than the jejunum. It is responsible for the absorption of bile salts, fat soluble vitamins and vitamin B12. The absorption of most fluids and electrolytes take place in the ileum and the large intestine. (Jeejeebhoy, 2002; Young et al., 2013). The intragastric pH rapidly changes from highly acidic to approximately pH 6 in the duodenum (Fallingborg, 1999) and it continues to rise gradually to about 7 to 8 in the terminal ileum. The small intestine is the main site of drug uptake from orally administered dosage forms and the transit time of small intestine has an impact on drug bioavailability especially in controlled release systems (Ashford, 2007). The intestinal transit time is usually quite consistent and unaffected by the presence of food in stomach, gastric emptying and size or physical states of the dosage forms. The transit time is usually 3-4 hours in most of the people (Davis et al., 1986).

5.2.1.4 *Large Intestine*

The lower GIT consist of large intestine (caecum, colon, rectum and anus). The large intestine is approximately 1.5 meters in length and has a smooth inner wall. The food residue containing very low nutrients enters to the caecum. The large intestine turns the food residue into semi solid faeces by absorbing water (Peate, 2018). Mucus is secreted from the large intestinal mucosa to ease the passages of faeces and protects the colonic walls. The transit time of drugs depend on the type of dosage forms, disease state, frequency of defecation and eating habits; it usually varies between 2 to 48 hours (Ashford, 2007). The pH drops to 5.7 in the caecum and increases to 6.7 in the rectum (Fallingborg, 1999).

5.2.2 Metronidazole

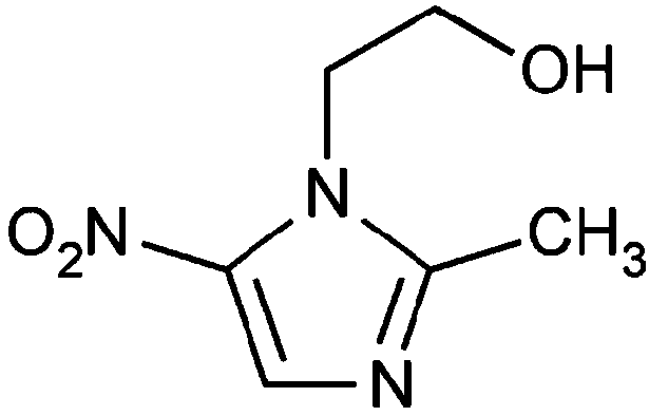

Figure 5.2: Chemical structure of metronidazole (Diós, 2015)

Metronidazole (MNZ) was used as the drug in this work to formulate an *in situ* gel forming oral drug delivery system. It is a synthetic derivative of nitroimidazole with antibacterial and antiprotozoal activities. The chemical name is 2-(2-methyl-5-nitroimidazol-1-yl) ethanol (Figure 5.2). The molecular weight is 171.156 g/mol. It is a crystalline powder that is white to pale yellow in colour. The pKa of metronidazole is 2.38. Obligate anaerobic organisms take the unionized MNZ which is then reduced by specific proteins and turns into an active, intermediate product. Reduced MNZ inhibit the bacterial cell growth by breaking the DNA strand. It is primarily used in the treatment of *H. pylori* infection (Salcedo and Al-Kawas, 1998). Besides, it is used to treat trichomonas infection and vaginitis. It is also highly effective in the treatment of periodontal disease (Slots and Rams, 1990) and intestinal amoebiasis (Krishnaiah et al., 2002).

MNZ is usually absorbed 80-90% by oral route and the oral bioavailability is above 90% (Turgut and Özyazici, 2004). It reaches a plasma concentration of approximately 10 µg/ml in about 1 hour after administration of a single dose of 500 mg (Lau et al., 1992). For oral administration, MNZ is usually marketed as tablets with a potency of 250, 400 and 500 mg

or capsule of 375 mg. It is also available as of 200 mg/5 ml oral suspension. But low therapeutic activity due to short gastric residence time and poor accessibility of MNZ at the site of actions are the obstacles to treat the disease (for example; *H. pylori* infection). Several sustained release formulations such as, beads (Ishak et al., 2007; Adebisi and Conway, 2014), *in situ* gelling raft systems (Youssef et al., 2015), *in situ* gelling floating formulations (Thomas, 2014) of MNZ have been reported in combination with alginate to improve the efficacy with sustained release of MNZ in the stomach in the treatment of *H. pylori* infection. So, in this study, MNZ was selected as a drug because of its ability to eradicate *H. pylori* in the stomach while using a formulation that contained alginate. Also, an *in situ* gel of alginate formed in the stomach could potentially increase the residence time of MNZ in the stomach enhancing therapeutic activity.

5.3 Materials and Methods

5.3.1 Materials

Sodium alginate and was purchased from Sigma-Aldrich, (Poole, UK). The M:G ratio of sodium alginate was 0.39:0.61 and molecular weight was 120,000-190,000 g/mol. Sodium bicarbonate was purchased from Fisher Scientific (Loughborough, UK). Low acyl gellan (Gelrite®), calcium chloride, sodium chloride, sodium hydroxide, hydrochloric acid (37.5%) and metronidazole were purchased from Sigma-Aldrich (Poole, UK). Timolol Maleate was purchased from Tokyo Chemical Industry (Oxford, UK). All chemicals and drugs were used without further purification.

5.3.2 Preparation of *In situ* Gel Forming Ophthalmic Formulation

A 0.5% gel forming eye drop solution was prepared based on marketed formulation (Timoptol LA®) which contained 6.8 mg/ml TM and 0.4% gellan. TM was dissolved in the

DI water at room temperature and heated up to 85°C while stirring in hot plate stirrer. 0.4% gellan was added to the solution and stirring was continued until the gellan was fully dissolved. The solutions were allowed to cool to room temperature prior to further analysis and the pH of the formulation was 4.5.

5.3.3 Preparation of *In situ* Gel Forming Oral Formulation

In situ gelling oral formulation was prepared containing metronidazole (MNZ) (200 mg/5 ml) and 2% sodium alginate. Sodium alginate (2%) was dissolved in DI water at room temperature and stirred until it was fully dissolved. MNZ (200 mg/5 ml) was then added to the alginate solution and stirring was continued for an hour until a uniform dispersion was formed. The prepared suspension was then stored at room temperature for 2 hours prior to further analysis.

5.3.4 Preparation of Simulated Physiological Fluids

Simulated lacrimal fluid (SLF) (pH 7.5) was prepared according to the formulation described in section 4.5.2. 0.1 M HCl was used as simulated gastric fluid (SGF) without any pepsin as it does not have any effects on polysaccharides. To prepare 0.1M HCl, 8.17 ml of 37.5% HCl was added to 1 L of DI water. The pH of SGF was 1.2.

5.3.5 Comparison of Rheological Measurements Using a Standard Parallel Plate Geometry and the Rheo-Dissolution Cell

Rheological measurements of *in situ* gelling ophthalmic and oral formulations were performed using Kinexus rotational rheometer (Malvern Panalytical, UK). A 40 mm serrated parallel plate geometry was used to measure elastic modulus (G′) and viscous modulus (G″) and the gap was fixed at 0.3 mm. Freshly prepared sample solutions were loaded onto the rheometer at 25ºC and measurements performed within the LVR (0.5% strain and a

frequency of 1 rad/s). All the experiments were performed at 25ºC. Silicone oil was added on the periphery of the samples to prevent evaporation during the measurements.

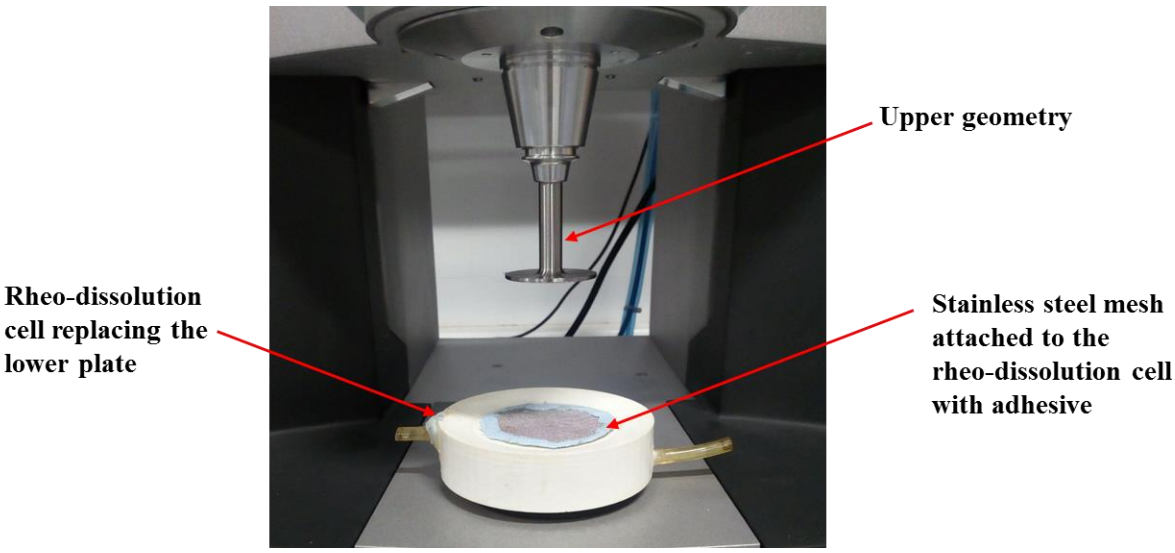

Figure 5.3: Rheological measurements using rheo-dissolution cell replacing the lower plate of rheometer performed at 0.5% strain, 1 rad/s frequency and 25ºC

Rheological measurements were also conducted replacing the lower plate of the rheometer with the rheo-dissolution cell to compare the performance of the system with the standard geometry. A stainless steel woven wire mesh (mesh count 80) was placed on top of the reservoir and attached securely to the surface of the cell (Figure 5.3). After attaching 40 mm parallel plate geometry, the samples were loaded on to the mesh. The gap was fixed at 0.8 mm and the volume of the sample was determined by the set gap. The gap size was relatively high in this experimental setting to compensate for slight undulations in the stainless steel mesh. The parameters used during the rheological measurements were adjusted according to the set gap. Oscillatory measurements of the moduli (G′ and G″) were measured using 0.5% strain 1 rad/s frequency. As the viscosity of the alginate formulation was very low, a dialysis membrane of 14000 mwco was used during the measurement of the *in situ* gelling oral formulation to prevent the passing of the formulation through the mesh. The membrane

had been soaked in DI water and was placed on the surface of the mash where samples were loaded.

5.3.6 Rheo-Dissolution Measurements for *In situ* Gel Forming Ophthalmic Formulation

Rheo-dissolution experiments were performed using Kinexus rotational rheometer where the rheo-dissolution cell replaced the lower plate of the rheometer. Two pieces of silicone tubing was attached to the inlet and outlet of the rheo-dissolution cell and was connected to a circulating peristaltic pump with a flow rate of 1ml/min. The pump was used to enable continuous flow of SLF in the reservoir and the flow rate was sufficient to maintain sink conditions (presence of sufficient dissolution media in the reservoir to ensure unimpaired dissolution of drug). It also facilitated sampling during the experiments. A 3-way sampling port was used to collect and replace the samples and was attached to the tubes. The circulatory system consisted of the cylindrical reservoir (55 ml) and the silicone tubing (45 ml) was capable of holding 100 ml volume. A stainless steel woven wire mesh (mesh count 80) with an aperture of 180 µm was securely attached to the top of the reservoir. The selected aperture was sufficient to prevent any sample passing through the mesh. The secure attachment of the mesh to the cell prevented any disturbance of the sample during the experiments. Figure 5.4 shows the cartoon representation of the experimental set up of the rheo-dissolution cell with the circulating pump and sampling port.

To begin the experiment, 90 ml of SLF was added to the circulatory system. The level of fluid was below the mesh and allowed space to accumulate a further 10 ml more fluid before it would come in contact with the mesh. Once the circulatory system had settled, a 40 mm serrated parallel plate geometry was attached to the rheometer.

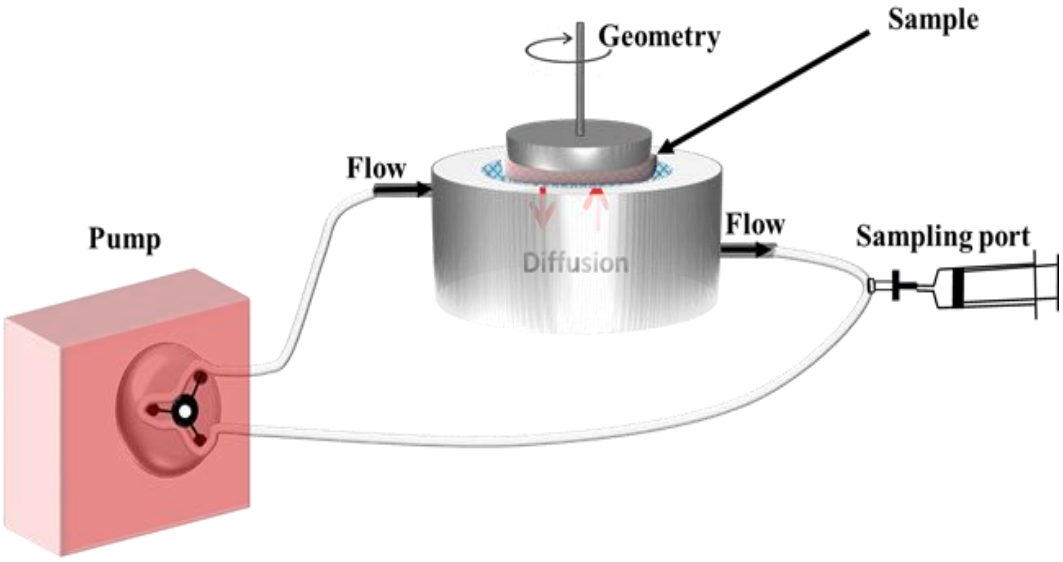

Figure 5.4: Cartoon representation showing the experimental set up for the measurement rheo-dissolution

The gap was fixed at 0.8 mm and sample of *in situ* gelling ophthalmic formulation of gellan-TM was placed on the top of the mesh. The volume of the sample was determined by the set gap. The test was started immediately to measure G′ and G″ as a function of time at 0.5% strain 1 rad/s frequency. After the test had started, 10 ml of SLF was injected through the sampling port immediately to initiate the gelling process by enabling the contact of SLF with the formulation on the mesh. A solvent trap was used to prevent any evaporation of the sample during the experiment. Figure 5.5 shows the experimental setup for the rheo-dissolution.

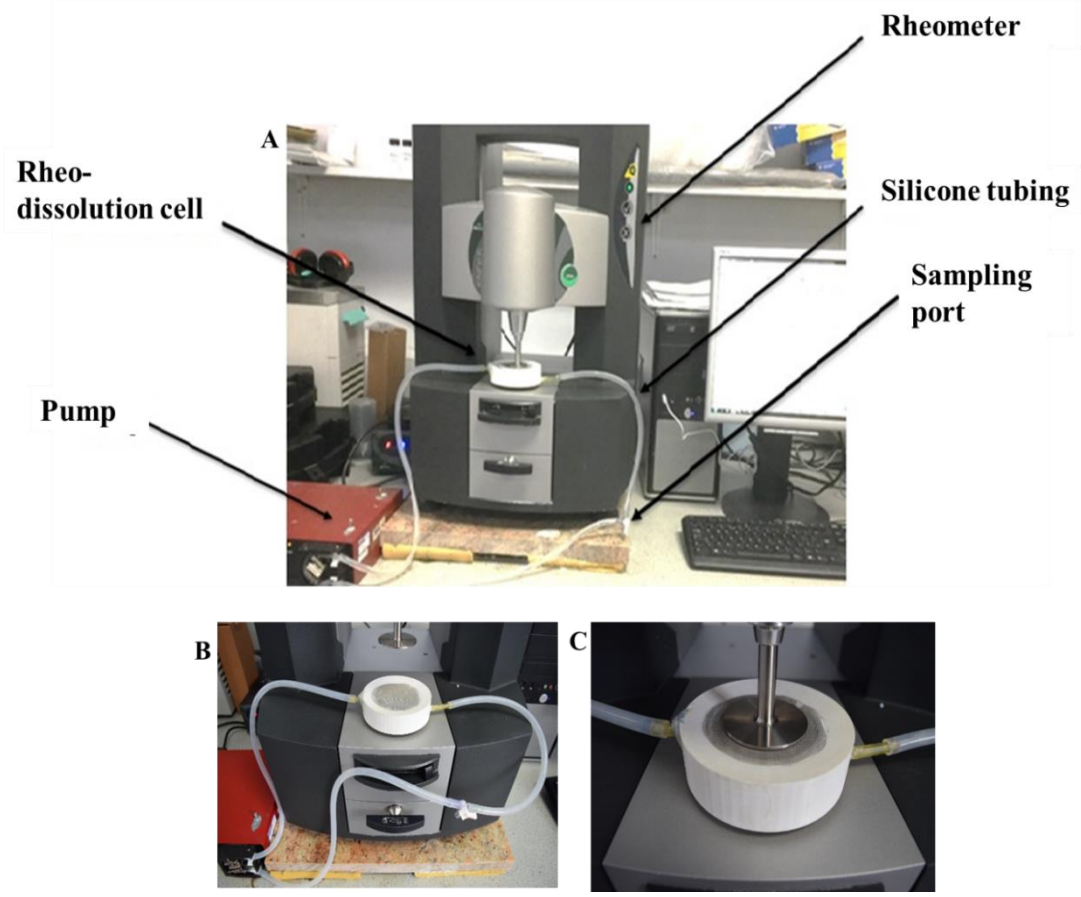

Figure 5.5: (A) Schematic demonstrating of the experimental set up of rheo-dissolution cell with the conventional rheometer in the laboratory (B) rheo-dissolution cell attached to the lower plate of rheometer prior to loading sample and (C) rheo-dissolution experiments in process

0.5 ml of samples were collected through the sampling port at regular time intervals (2, 4, 6, 8, 10, 30, 60, 90, 120, 150, 180 min) and were replaced with same volume of fresh SLF. To ensure the continuous contact of SLF with the sample, the volume of SLF was maintained 100 ml throughout the system. All the experiments were performed in room temperature and were done in triplicate. Collected samples were then analysed for the drug released from the gels using HPLC according to the method described in 4.5.7.2.

To validate the rheo-dissolution method against the conventional dissolution testing, release studies were performed using a dissolution bath containing 100 ml of SLF. The solution was

magnetically stirred at a speed of 100 RPM and a temperature of 37°C was maintained throughout the experiment. The same sampling regime was applied as used in the rheo-dissolution experiments.

5.3.7 Effect of Gellan Concentrations on Rheology and Drug Release

Rheological properties of a gel depends on the polymer concentration (Farahnaky et al., 2010) which also plays significant role in drug diffusion. An investigation was performed to analyse the effect of concentration of gellan on the rheological behaviour and diffusion of TM from the gel. Rheo-dissolution experiments were conducted for three formulations containing three different concentrations of gellan and 6.8 mg/ml TM.

5.3.7.1 *Preparation of the Formulations*

Three *in situ* gelling formulations of gellan-TM were prepared using three different concentrations of gellan (0.3%, 0.6% and 0.8%). TM (6.8 mg/ml) was dissolved in the DI water at room temperature. Required amounts of gellan was added at 85°C while stirring the solution in magnetic hot plate stirrer. The stirring was stopped when gellan was completely dissolved. The formulations were allowed to cool to room temperature prior to further analysis.

5.3.7.2 *Rheo-Dissolution Measurements*

Rheo-dissolution experiments of three formulations were performed using the experimental setup described in 5.3.6. The experiments were performed in triplicate for each formulation and the collected samples were analysed using HPLC according to the method described in 4.5.7.2.

5.3.8 Rheo-Dissolution Measurements for *In situ* Gel Forming Oral Formulation

Rheo-dissolution experiments were performed to monitor release of drug during gelation and subsequent dissolution of the alginate gel that occurs at acidic and alkaline pH respectively. The experimental setup described in 5.3.6 was used to perform the tests which was adapted by the addition of a dialysis membrane (14000 mwco) on the surface of the mesh. The membrane had been soaked in DI water prior to the experiments. This adaptation facilitated pre-gelation state measurements due to the extremely rapid gelation kinetics of alginate that occur on contact with acid. Moreover, this adaptation prevented the flow of alginate solution through the mesh prior to the rheological measurements.

At the beginning of the test, the flow through system contained 90 ml of SGF (pH 1.2) and the liquid level was below the mesh to prevent any contact with sample. The geometry was zeroed and the gap was fixed at 0.8 mm. The required volume of *in situ* gelling oral formulation of alginate-MNZ was placed on the top of the dialysis membrane. Oscillatory measurements of G′ and G″ was started immediately as a function of time (0.5% strain, 1 rad/s frequency). Before inducing gelation, measurements of the moduli in the pre-gel state was performed for 10 min. Addition of 10 ml SGF (pH 1.2) to the circulatory system (that already contained 90 ml of SGF) allowed the formulation to come in contact with SGF and enabled the system to capture measurements for the whole gelation event. The experiment was continued for 7 hours and the samples of SGF (0.5ml) were withdrawn at 4, 8, 12, 16, 20, 30, 60, 90, 120, 150, 180, 210, 240, 270, 300, 330, 360, 390 and 420 min. The same volume of fresh SGF (pH 1.2) was used to replace the volume at each time point.

As discussed in chapter 3 (3.4.2.1 Gelation of alginate) alginate gels are stable in acidic pH in stomach because of the lower pH value than the pK_a of the uronic acids which causes the

removal of the negative charge and formation of gel by intermolecular hydrogen bonding. At alkaline pH of the intestine, the acidic groups become charged which causes electrostatic repulsion and breaks down the alginate gels (Pawar and Edgar, 2012; Rasel and Hasan, 2012; Francis et al., 2013). So, a further rheo-dissolution experiment was conducted to monitor MNZ release during the dissolution of alginate gel at alkaline pH. Here, the experiment performed at pH 1.2 was allowed to proceed for 120 min. Then the pH of the gastric media was converted to alkaline media (pH 8.0) by replacing 9 ml of SGF with same volume of 1M NaOH. The rheo-dissolution study was continued at pH 8.0 until the *in situ* gel was broken down. The dissolution of the gel was identified by the reduction in moduli. The samples (0.5 ml) were withdrawn every 30 min and replaced with same volume of fresh media (pH 8.0). All experiments were performed in room temperature. UV spectrophotometry (Agilent technology, Cary 60) was used to analyse the collected samples. The percentage of MNZ released from the *in situ* gel was determined from the linear regression equation obtained from the UV standard calibration curve (Figure 5.11). All experiments were done in triplicate. The MNZ release data during the rheo-dissolution experiments were curve fitted to the zero order model using equation 5.1.

$$\boldsymbol{Q = Q_o + K_o t} \qquad \textit{Equation 5.1}$$

Where Q is the amount of drug released at time t, Q_o is the initial amount of drug and K_0 is the zero order release constant.

5.3.9 Determination of MNZ by UV Spectroscopy

A stock solution of MNZ was prepared by dissolving 2.5 mg of MNZ in 25 ml of 0.1 M HCl (pH 1.2). The final concentration of the stock solution was 100 µg/ml. The stock solution was diluted and scanned (400 nm to 200 nm) using Cary 60 (Agilent technology) UV

spectroscopy to obtain the maximum wavelength (λ_{max}) of MNZ. The maximum absorbance was found at a wavelength of 277 nm. Five different standards (2 to 10 µg/ml) were prepared from the stock solution of MNZ. All the standard solutions of MNZ were measured at 277 nm and the absorbance was plotted against the respective concentration to obtain a calibration curve. All the measurements were done in triplicate and the linear regression equation was calculated from the calibration curve. LOD and LOQ was calculated using the Equation 4.1 and 4.2. Accuracy and precision studies were performed for this method. Accuracy is one of the important aspects of the validation a method and it shows the extent of agreement between the reference and experimental values. Precision demonstrates the reproducibility and repeatability of the method (Moosavi and Ghassabian, 2018). Accuracy studies were performed at three concentration levels (50%, 100% and 150%). Precision studies were evaluated through analysis of the sample on three different days with intra-day and inter-day repeatability. Accuracy and precision studies were done in triplicate.

5.3.10 Solubility Profile of MNZ at pH 1.2 and 8

To determine the solubility of MNZ, saturated solutions were prepared by adding excess amounts of MNZ to 0.1M HCl of pH 1.2 and 8 at room temperature (22 ± 1°C). The solutions were stirred overnight to attain equilibrium. The solutions were then filtered and diluted as necessary to analyse the MNZ content spectrophotometrically at 277 nm (Wu and Fassihi, 2005; Adebisi, 2014). The experiments were done in triplicate.

5.3.11 Statistical Analysis

Student's t test was applied to compare the data obtained from the dissolution experiments of both (ophthalmic and oral) formulations. One-way Analysis of Variance (ANOVA) was applied for comparing the dissolution data from the formulations containing four different concentrations of gellan. Statistical significant level was considered as $p < 0.05$. IBM® SPSS Statistics software version 24, was used for the statistical analysis.

5.4 Results

5.4.1 Comparison of Rheological Measurements Using a Standard Parallel Plate Geometry and the Rheo-Dissolution Cell

Measurements of viscoelastic properties (G′ and G″) of *in situ* gel forming ophthalmic and oral formulations were performed using Kinexus rheometer fitted with serrated parallel plate geometry. The experiments were also conducted with the rheo-dissolution cell (covered with mesh) which replaced the lower serrated parallel plate. In the case of the ophthalmic formulation, the modulus (G′ and G″) were in steady state and maintained almost similar values throughout the tests in both experimental settings (Figure 5.6). G′ was dominant over G″ across the tests.

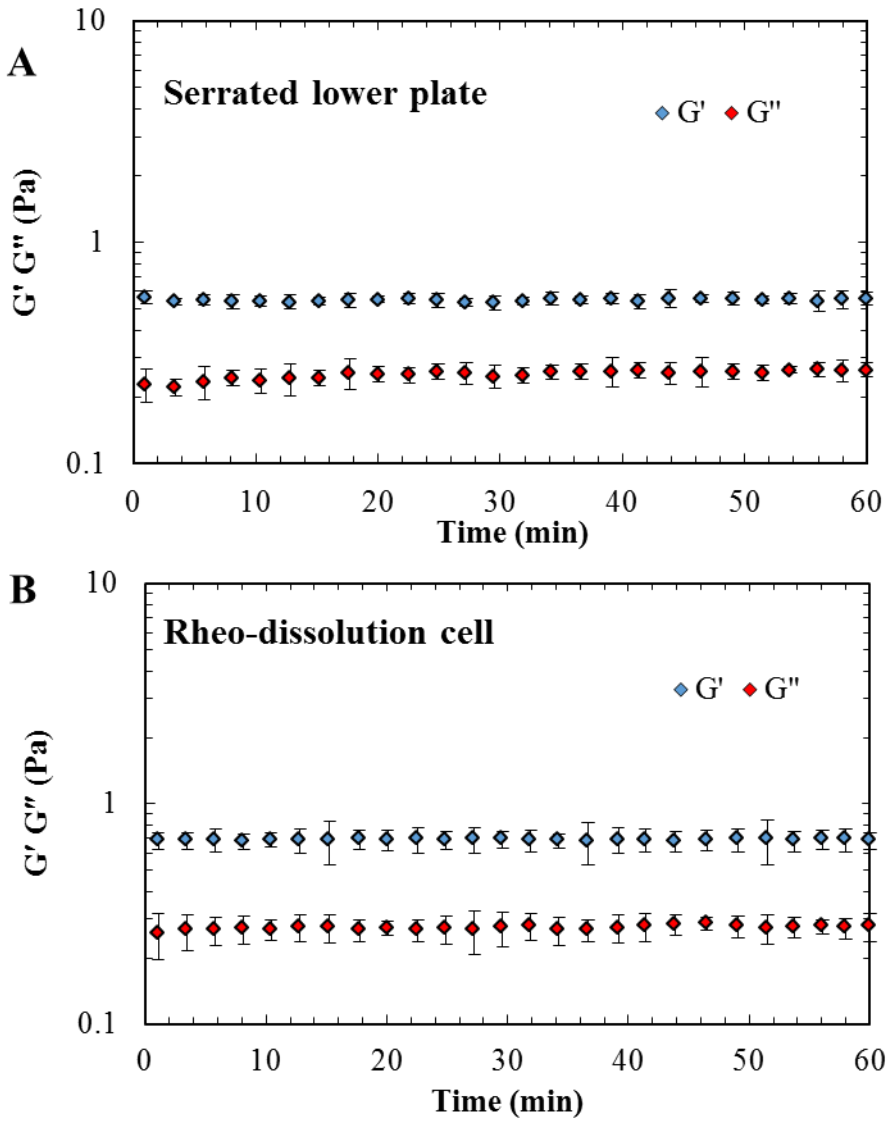

Figure 5.6: Viscoelastic measurements of G′ and G″ (Pa) against time for *in situ* gelling ophthalmic formulation of gellan-TM performed with (A) serrated parallel plate (B) rheo-dissolution cell replacing the lower plate (0.5% strain, 1 rad/s frequency and 25ºC). All data represent mean ± SD (n=3)

Similarly, viscoelastic measurements were performed for *in situ* gelling oral formulation of alginate-MNZ (Figure 5.7). Again the moduli maintained almost similar values for both experimental settings over the period of the test. Comparison of initial and final values of G′ and G″ (Pa) for both formulations in the two experimental settings are listed in Table 5.1.

No significant difference ($p > 0.05$) was observed while compared the values of moduli of both experimental settings.

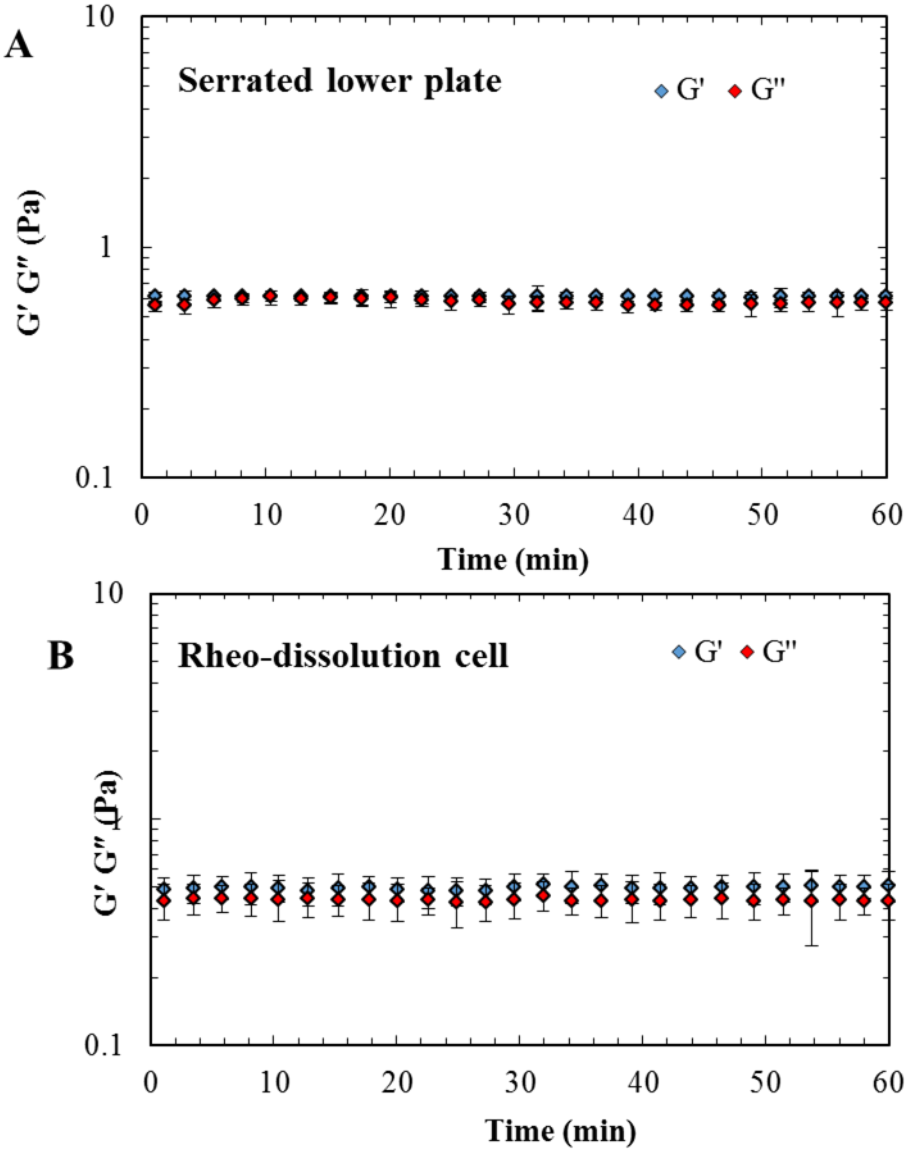

Figure 5.7: Viscoelastic measurements of G′ and G″ (Pa) against time for *in situ* gelling oral formulation of alginate-MNZ performed with (A) serrated parallel plate (B) rheo-dissolution cell replacing the lower plate (0.5% strain, 1 rad/s frequency and 25°C). All data represent mean ± SD (n=3)

Table 5.1: Comparison of viscoelastic measurements (G′ and G″) for *in situ* gelling ophthalmic (gellan-TM) and oral formulation (alginate-MNZ) performed with serrated parallel plate and rheo-dissolution cell replacing the lower plate (0.5% strain and a frequency of 1 rad/s). Values represent mean ± SD (n=3)

Formulation	Conventional rheometer with serrated lower plate				Rheo-dissolution cell replacing the lower plate of rheometer			
	G′ (Pa)		G″ (Pa)		G′ (Pa)		G″ (Pa)	
	Initial	Final	Initial	Final	Initial	Final	Initial	Final
Gellan-TM	0.56 ± 0.04	0.56 ± 0.04	0.26 ± 0.04	0.27 ± 0.02	0.68 ± 0.06	0.68 ± 0.08	0.26 ± 0.06	0.27 ± 0.04
Alginate-MNZ	0.61 ± 0.04	0.61 ± 0.03	0.55 ± 0.02	0.57 ± 0.03	0.49 ± 0.06	0.49 ± 0.08	0.43 ± 0.06	0.43 ± 0.09

5.4.2 Rheo-Dissolution Measurements for *In Situ* Gel Forming Ophthalmic Formulation

The simultaneous measurements of rheological changes and drug release were performed for an *in situ* gelling ophthalmic formulation containing 0.4% gellan and 6.8 mg/ml TM (Figure 5.8). A rapid increase in moduli was observed over the first 20 min of exposure to the SLF. After the formulation gelled, G′ and G″ reached values of 1248 Pa and 134.6 Pa respectively. The modulus plateaued for the rest of the test. The gelation reaction was allowed to proceed for 180 min while sampling the SLF from the reservoir and analysing for release of TM. The release curve showed an initial burst release of 12.54 (± 2.97) % TM in the first 10 min as the formulation began to gel. This was followed by a period of sustained TM release until 120 min (42.91 ± 1.82%). After this time point, the release slowed and by 180 minutes 45.97 (± 1.52) % of drug was released while approximately 54% of drug remained in the formulation.

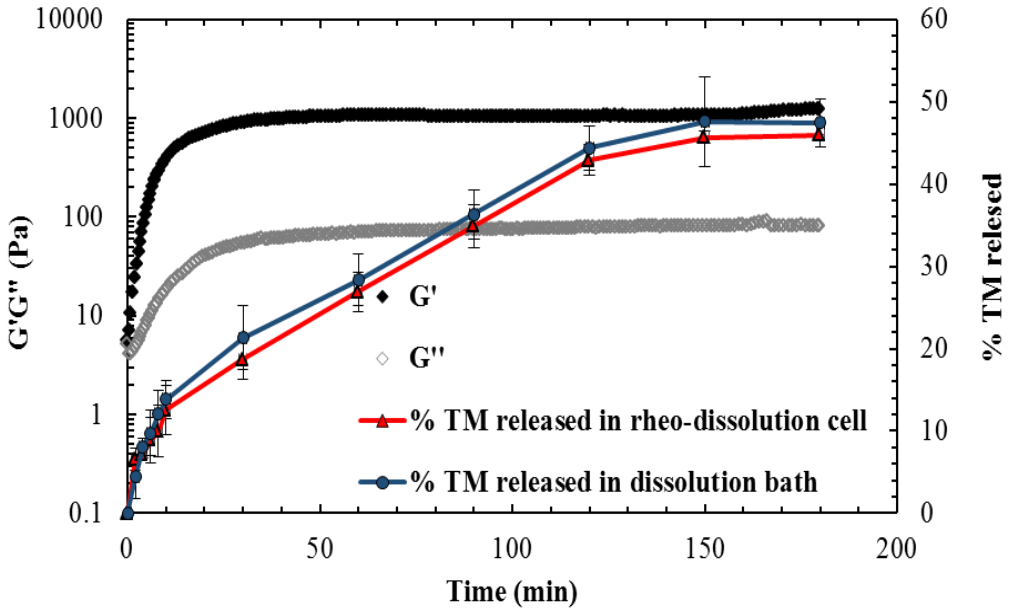

Figure 5.8: Rheo-dissolution experiments showing the progression of the moduli (G' and G") and comparison between the TM release performed in rheo-dissolution cell (0.5% strain, 1 rad/s frequency); and in dissolution bath at 37ºC (100 RPM)

To validate the rheo-dissolution method against conventional dissolution testing, release studies were performed using a dissolution bath using the same sampling regime (Figure 5.8).Initial release of 12.07 (± 2.85) % TM was observed in 10 min which increased gradually to 44.39 ± 2.72 % at 120 min after which the release slowed and 47.42 (± 2.96) % TM was released at 180 min. Release of TM from dissolution bath showed no significance difference ($p > 0.05$) when compared to the release data obtained from rheo-dissolution experiment (Figure 5.8).

5.4.3 Effect of Gellan Concentrations on Rheology and Dissolution of the Drug

The simultaneous measurements of rheological changes and drug release were also performed for 3 other different concentrations of gellan to investigate the impact of increasing gel strength on drug release. The formulation containing 0.3% gellan (Figure

5.9A) showed rapid increase of the modulus over first 30 min of the exposure to the SLF as gelation occurred. G′ reached to 313.8 Pa and G″ to 47.5 Pa once the formulation was fully gelled. The moduli reached a plateau after the gelation and maintained the same trend for remainder of the test. Initial burst release (23.22 ± 3.27) % was observed in the first 10 min of the test while the gel was undergoing gelation. The release slowed for the remainder of the test with the total release of 48.67 (± 3.55) % at 180 min with little change in G′ and G″ over this period. The onset of gelation became more rapid as the concentration of gellan increased to 0.6% (Figure 5.9B). G′ and G″ reached to the values of 2275 Pa and 346.3 Pa after complete gelation of the formulation. Here, there was no evidence of an initial burst release as TM was released steadily until 60 min reaching 21.29 (± 5.13) % TM at this time point and only 36.59 (± 3.68) % of TM was released at the end of the test (180 min). Further increase to the gellan concentration (0.8%) caused the formation of strong gel (G′>>G″) at the onset of the test which continued throughout the experiment (Figure 5.9C). The release of TM from this formulation was only 23.63 (± 2.1) % at the end of the experiment which was less than half of the release achieved from the 0.3% gellan formulation (Figure 5.9A).

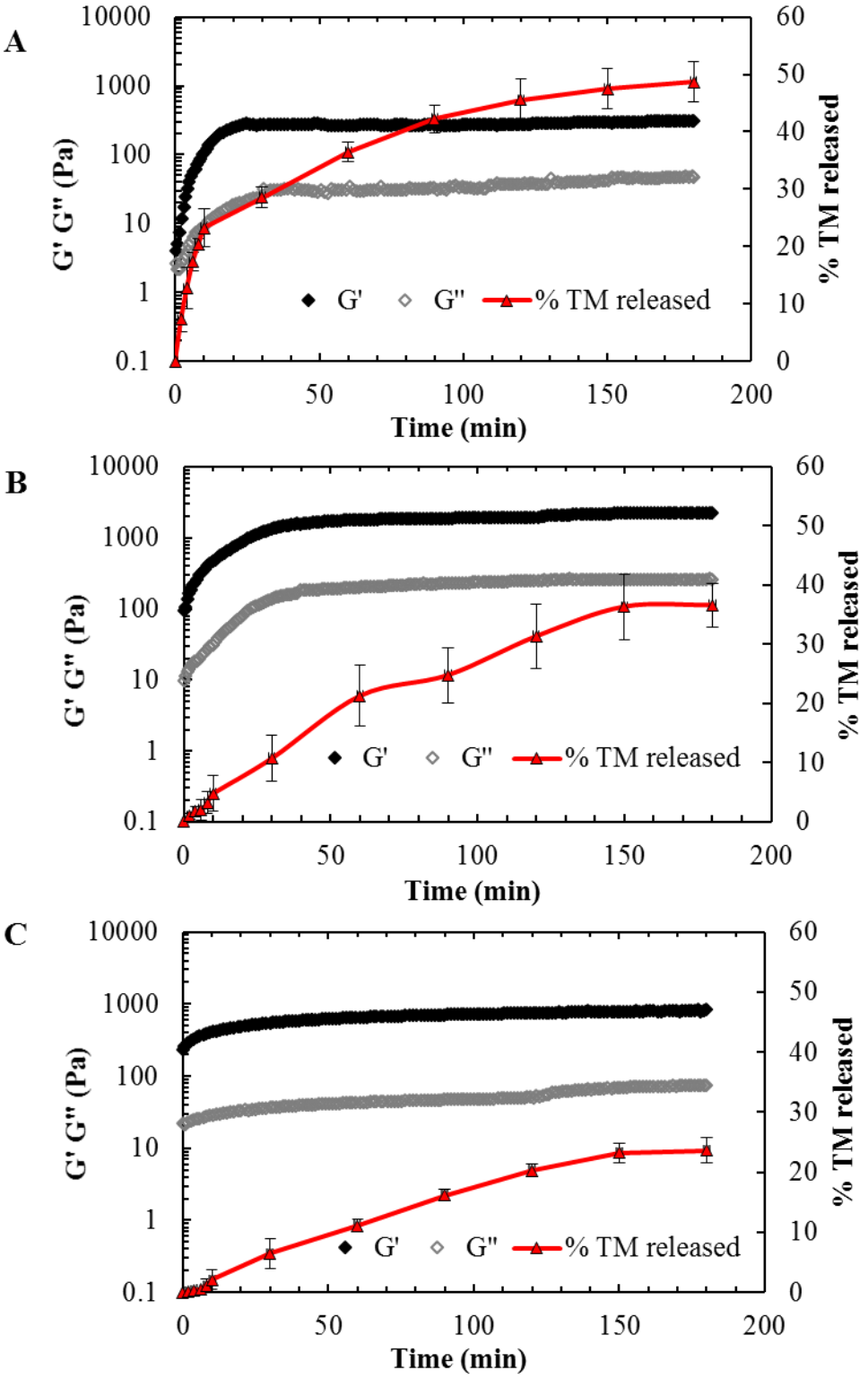

Figure 5.9: Rheo-dissolution experiments of *in situ* gel forming ophthalmic formulations containing 6.8mg/ml TM and (A) 0.3% (B) 0.6% (C) 0.8% gellan

5.4.4 Development of UV-Vis Spectrophotometric Method for the Estimation of MNZ

The absorbance of MNZ standards were measured at a wavelength of 277 nm to generate a calibration curve (Figure 5.10) which was used to determine the concentration of MNZ in the collected samples. The linearity of this analytical procedure was determined by the correlation coefficient (R^2). It is the ability of the analytical procedure within a given range to attain the test results which are directly proportional to the amount of analyte used for the test (Mahdi, 2016). The constructed calibration curve was linear over the concentration range of 2-10 µg/ml (R^2 = 0.999). For accuracy and precision, the RSD for all samples were within the satisfactory range. The method validation data of the MNZ assay are presented in Table 5.2.

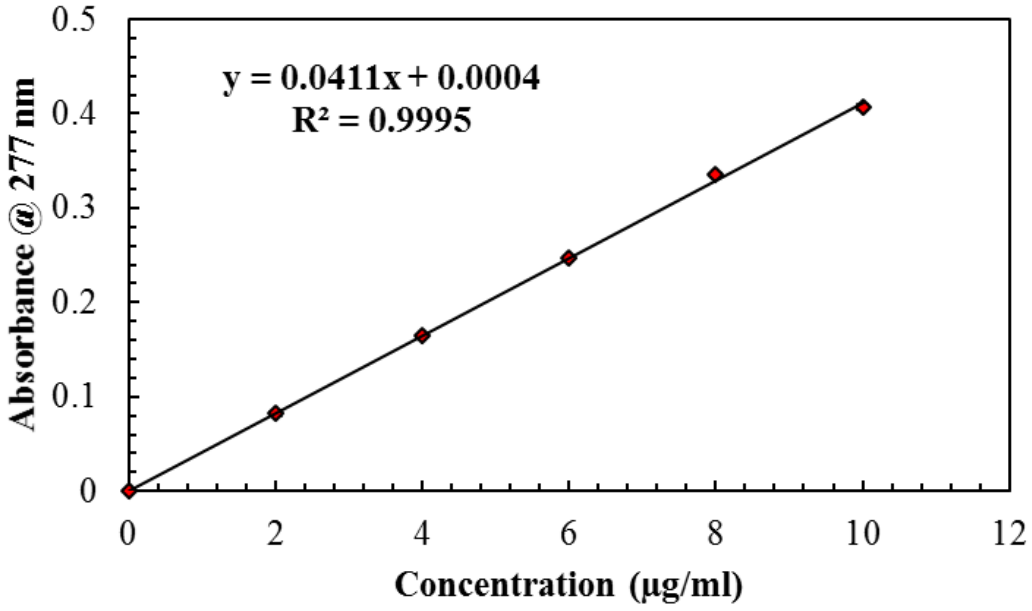

Figure 5.10: Mean calibration curve of MNZ measured at 277 nm. All data represent mean ± SD (n=3)

Table 5.2: Evaluation data of UV spectroscopic method of MNZ

Range (µg/ml)	2 to 10
Regression equation	y= 0.0411x+0.0004
Correlation Coefficient	0.9995
LOD (µg/ml)	0.23
LOQ (µg/ml)	0.59
Accuracy	RSD < 2%
Precision	RSD < 3%

5.4.5 Rheo-Dissolution Measurements of *In Situ* Gel Forming Oral Formulations

Rheo-dissolution experiment of an *in situ* gelling oral formulation consisting of MNZ (200 mg/ 5 ml) and alginate (2%) was performed at pH 1.2 and 8.0. Oscillatory rheological measurements of the sample were performed prior to the exposure to the gastric fluid to ascertain the behaviour of the formulation that would be apparent prior to administration. Low values of the modulus (~0.6 Pa) at this stage indicated an entangled polymer solution (figure 5.12). Upon exposure to the acidic media (pH 1.2), G′ increased rapidly to almost 3 orders of magnitude and both moduli continued to increase steadily after the initial rapid gelation. At the end of the test, G′ and G″ reached to the values of 1286 and 210 Pa respectively (Figure 5.11A). During the first 30 min of the test while the gelation process was occurring, 11.95 (±1.84) % MNZ was released. In the following 3.5 hours, when the alginate had formed a strong gel, 49.54 ± 1.71 % MNZ was released (at 210 min) and plateaued for the remainder of the experiment with a release of 53.34 ± 2.84 % at 420 min. The pH of the gastric media was raised to from 1.2 to 8 at 120 min in a second experiment with same experimental setup to demonstrate the feasibility of changing dissolution media during the experiment (Figure 5.11B).

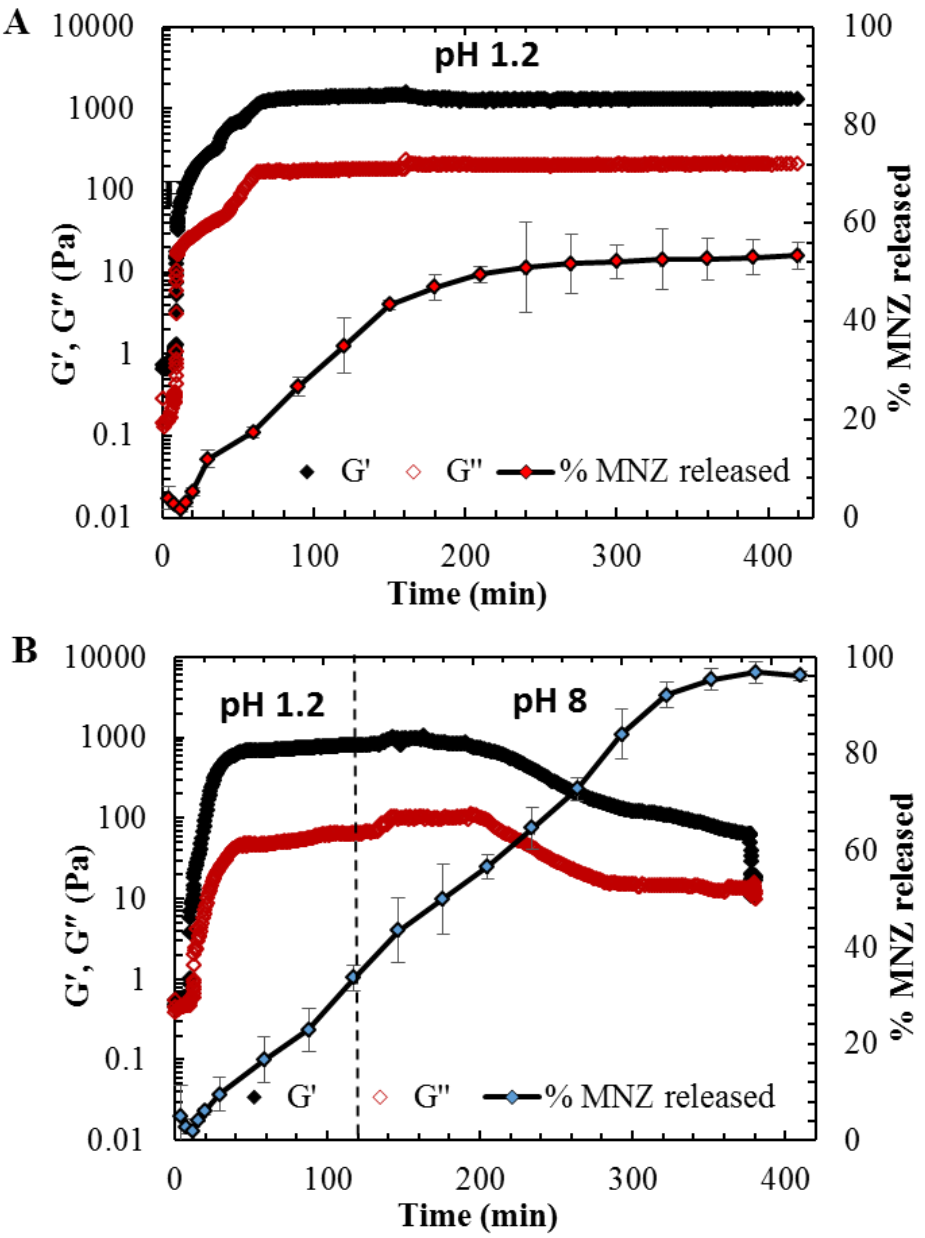

Figure 5.11: Rheo-dissolution experiment of *in situ* gel forming oral formulation containing MNZ (200mg/5ml) and 0.2 % sodium alginate at (A) pH 1.2 (B) pH 1.2 and 8.0 (0.5% strain, 1 rad/s frequency and 25ºC)

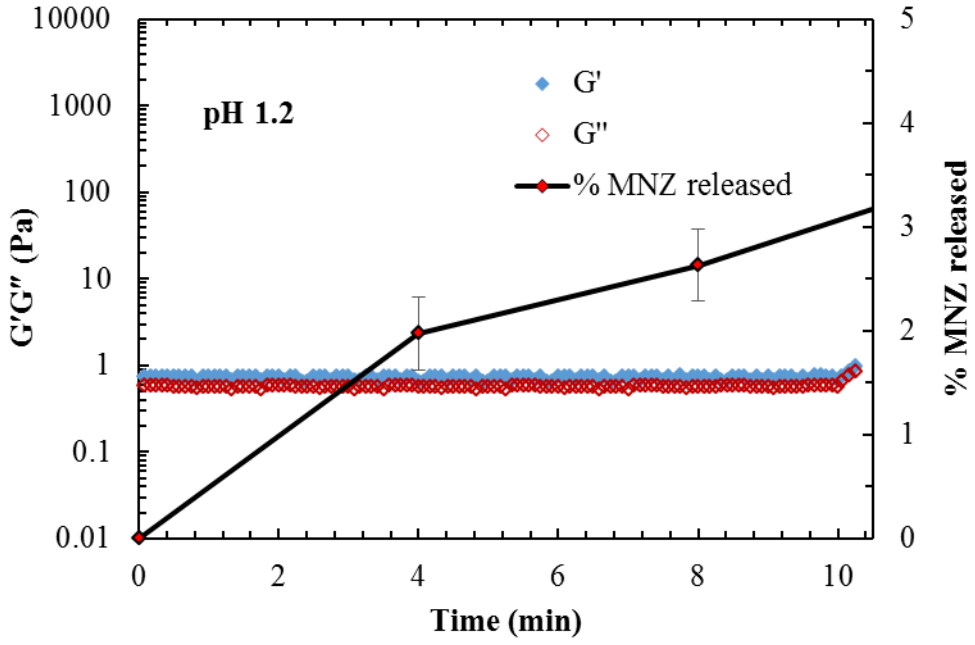

Figure 5.12: Progression of the modulus (G' and G") and release of MNZ at the earlier time points (0 to 10 min) before exposure to the acidic media (pH 1.2)

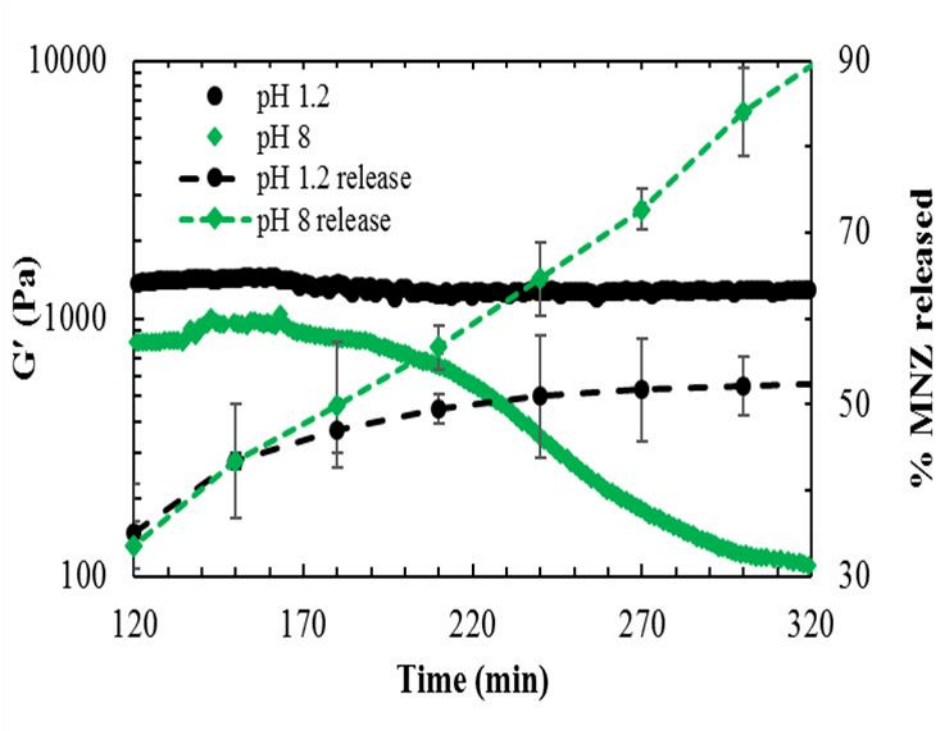

Figure 5.13: Comparison of G′ and release of MNZ following 120 min when maintaining pH 1.2 or adjusting pH 8.0

Also, this was performed to examine the release behaviour of MNZ when the sol-gel reaction was reversed. Similar release behaviour as Figure 5.11A was observed over the first 2 hours of the experiment when the formulation was exposed to the acidic media (pH 1.2) with 33.6 % (± 2.7) MNZ released at 120 min before changing the dissolution media to pH 8.0.

Upon changing the pH, however, no significant difference ($p > 0.05$) was observed in release data compared to the rheo-dissolution experiment performed at pH 1.2 (Figure 5.11A) until 120 min which is clearly detectable in Figure 5.13. At pH 8.0, a rapid reduction of gel strength was observed by a fall in G′ at 190 min from ~801 Pa to ~28.64 Pa at 370 min. The reduction in the modulus indicated breakdown of gel and rheological measurements were stopped at this point. Rapid reduction of gel strength in alkaline media coincided with rapid increase in MNZ release with ~50% MNZ was released in 180 min. The release curve continued to show zero order release and ~96% of MNZ was released at the end of the test while the alginate gel was broken down (Figure 5.11B).

When the media was changed to pH 8.0, negligible variations of release constant (K_0) was maintained across the entire profile, which was revealed by zero order kinetic modelling of the release data (Figure 5.14). The release curve did not follow zero order kinetic model when the experiment was performed in pH 1.2 (Figure 5.14A). But, the release curve fitted well to the zero order model while the experiment was performed in both pH (1.2 and 8.0) (Figure 5.14B). When pH 1.2 was maintained in first 120 min in both experiments (Figure 5.14C and D), the release curves followed the model, but upon changing the dissolution media to pH 8.0, the release curve sharply deviated from the zero order model (Figure 5.14D). Zero order release kinetic parameters are summarized in Table 5.3.

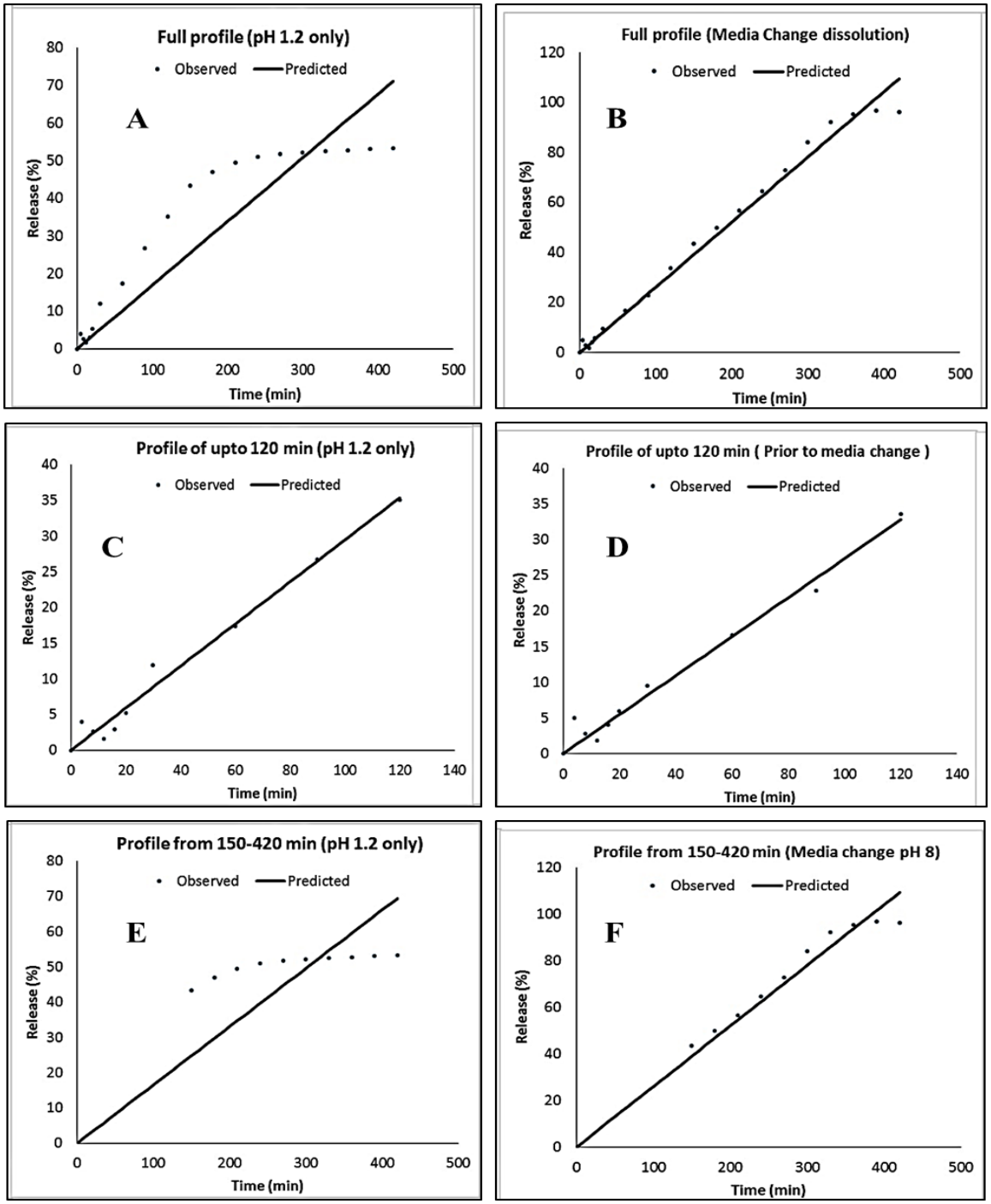

Figure 5.14: Zero order kinetic modelling of the release data obtained from rheo-dissolution experiments performed at (A) pH 1.2 (B) pH 1.2 and 8 (C) pH 1.2 (up to 120 min) (D) pH 1.2 and 8 (up to 120 min; before changing the media to pH 8) (E) pH 1.2 (150 to 420 min) (F) pH 1.2 and 8 (150 to 420 min; after changing the media to pH 8).

Table 5.3: Summary of zero order drug release kinetic parameters

Media Maintained at pH 1.2	K_0	R^2	Media changed to pH 8.0	K_0	R^2
Full release profile	0.169	0.79	Full release profile	0.261	0.98
0-120 min (pH 1.2)	0.295	0.98	0-120 min (pH 1.2)	0.273	0.98
120-420 min (pH 1.2)	0.165	0.77	120-420 min (pH 8.0)	0.260	0.92

5.4.6 Solubility Profile of MNZ at pH 1.2 and 8.0

Weakly basic drugs show decreased solubility as pH increases along the gastrointestinal tract, which also has an impact on the dissolution of the drug (Streubel et al., 2000). Decreased release of drug is observed with increased pH (Chen and Rodríguez-Hornedo, 2018). MNZ is weak base (pKa 2.62), which is highly soluble at pH $\leq$ 2.0 and solubility of MNZ decreases as pH increases. Solubility test of MNZ was performed at pH 1.2 and 8.0 and it was found that the solubility of MNZ was 65.31 mg/ml at pH 1.2 and 16.24 mg/ml at pH 8.0 (Figure 5.15). However, in the rheo-dissolution experiment, high release of MNZ (~96%) was observed at high pH (pH 8.0) when the alginate gel was broken down (Figure 5.11B) which contradicts the above statement regarding pH dependent drug release and therefore highlights the influence of gel degradation on the release behaviour of MNZ. Therefore, lower solubility at pH 8.0 indicates that the increased release of MNZ at pH 8.0 was more likely a result of degradation of the gel rather than increased solubility.

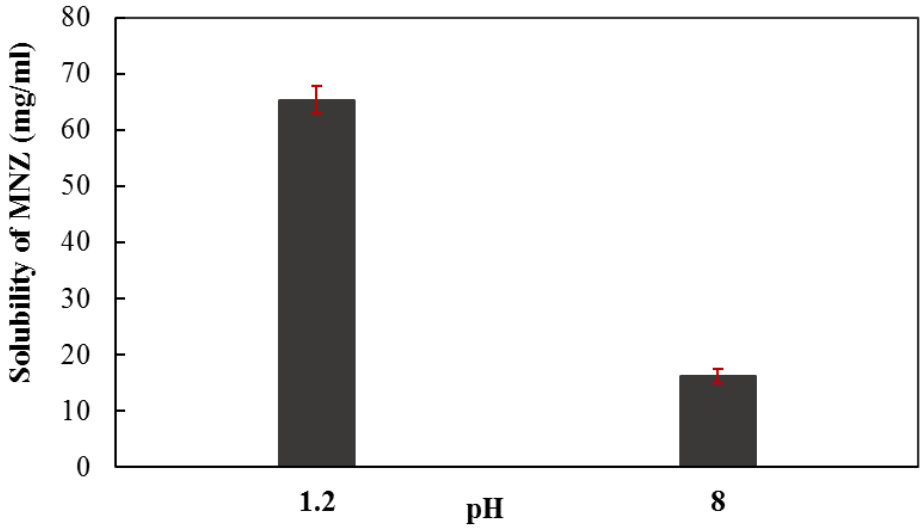

Figure 5.15: pH solubility of MNZ at pH 1.2 and 8.0 (n=3)

5.5 Discussion

The gelation behaviour of the gel former is an important consideration in designing an *in situ* gel forming drug delivery system. Besides measuring gelation behaviour, sampling of drug from the system to analyse release could be beneficial for successful *in situ* gelling formulation development. Here, a novel method has been demonstrated using a rheo-dissolution cell replacing the lower plate of a conventional rheometer to analyse gelation and drug release simultaneously (rheo-dissolution) of *in situ* gelling formulations. *In situ* gel forming ophthalmic (gellan-TM) and oral (alginate-MNZ) formulations were used to demonstrate this method. Before conducting rheo-dissolution experiments, viscoelastic measurements in terms of G′ and G″ were performed with conventional lower plate and rheo-dissolution cell to compare the performances (Figure 5.6 and 5.7). No significant differences ($p > 0.05$) were observed between the moduli of both formulations for both experimental settings (Table 5.1) which ensured the feasibility of using the cell as the lower plate of rheometer to perform rheo-dissolution analysis.

In situ gel forming ophthalmic formulations were prepared according to the marketed formulation Timoptol LA® where 0.4% gellan was used as an *in situ* gelling polymer. Besides, three other concentrations (0.3%, 0.6% and 0.8%) of gellan were used to prepare the formulation and rheo-dissolution experiments were conducted to observe the effect of concentration on rheo-dissolution. Rapid increase of the moduli (G′ and G″) were observed when the formulations containing 0.3% (Figure 5.10A) and 0.4% (Figure 5.8) were exposed to the crosslinking ion solution as gelation occurred. But as concentration increased to 0.6% (Figure 5.10B) gelation occurred much more rapidly and a strong gel (G′ >> G″) was already formed before the first measurements were taken when 0.8% gellan was used (Figure 5.10C). It was interesting to observe in real time that when gel strength was weak (during first 10 min of exposed to SLF) TM was released more rapidly from the samples. Initial burst release disappeared with increasing the concentration of gellan and final release also slowed down to 23.63 ± 2.1 % at 180 min for the formulation containing 0.8% gellan when G′>>G″ was observed throughout the experiment (Figure 5.10C). Linear reduction in TM release was observed with increased concentration when the releases of 180 min were plotted against the concentrations of gellan (0.3%, 0.4%, 0.6% and 0.8%) (Figure 5.16).

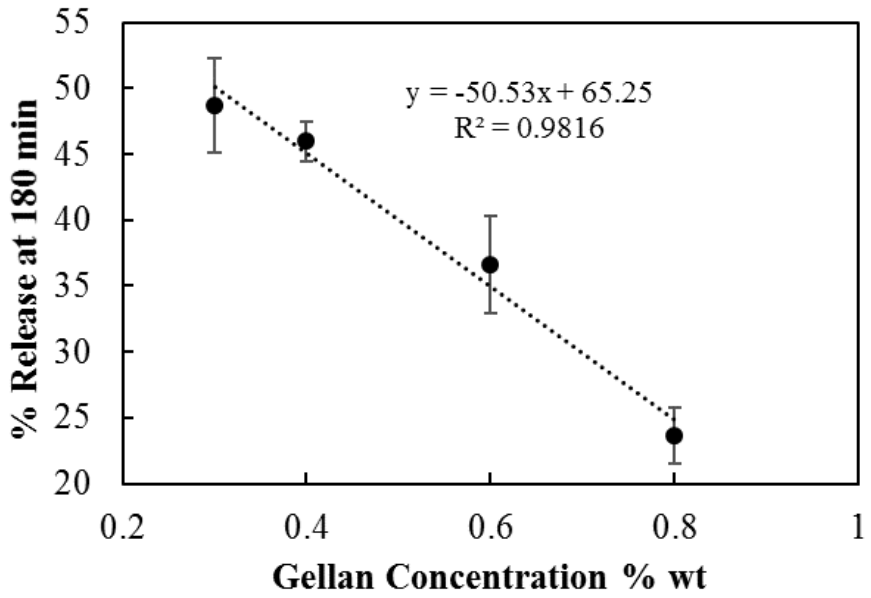

Figure 5.16: Release of TM at 180 min with increasing gellan concentrations from 0.3% to 0.8%

Although the gel strength significantly ($p < 0.05$) affect the release of TM from the *in situ* gelling formulations of gellan-TM, but it may not be a critical factor to control TM release as potential electrostatic interaction could occur between positively charged TM and negatively charged gellan which has been described previously in 4.7. The release study of TM from the formulation containing 0.4% gellan performed in dissolution bath (Figure 5.9) also showed incomplete release and was comparable with Figure 5.8. The molecular interplay between the polymer molecules during sol-gel transition has an impact on the release of drug and subsequent bioavailability. It is poorly understood especially in ophthalmic formulations. However, utilizing this *in vitro* technique can provide real time correlation between rheological behaviour and release of drug from *in situ* gelling ophthalmic formulation upon exposure to SLF.

In situ gelling oral formulations were investigated to demonstrate a similar approach where alginate was used as the *in situ* gelling polymer because of the rapid gelation behaviour on exposure to the stomach acid. This attractive and well-known property of alginate has been utilized in oral liquid formulations previously to control drug release and to enhance the gastric retention time (Miyazaki et al., 2000, 2001; Kubo et al., 2003). The fasted and fed state of stomach also plays a role on the gelation behaviour of alginate. The low pH (1-3) in the fasted state initiates the gelation of alginate. But if the formulation is administered in fed state (pH 3-7), pH triggered gelation of alginate is less likely to happen. Therefore, the development of alginate solutions have been reported where free calcium ions are prepared as complex with sodium citrate in the solutions which delay the gelation of alginate solutions until the solutions reaches to the acidic environment of the stomach and calcium ions are released. The presence of optimum quantities of sodium citrate and calcium chloride maintain the fluidity of the solutions before administration.(Miyazaki et al., 2000, 2001). There are also some reports of development of alginate solutions without calcium ions where *in situ* gelation is induced by oral administration of calcium salt solutions immediately following the alginate solution (Zatz and Woodford, 1987; Katayama et al., 1999). However, in this experiment the alginate-MNZ formulation was prepared without any calcium ions and the rheo-dissolution experiments of alginate-MNZ were conducted in two different pH (1.2 and 8.0) to observe the rheological behaviour in varying pH and its impact on drug release.

Low modulus (G′) was observed (Figure 5.12A and B) before the exposure of the formulation to acidic media which turned into almost instantaneous increase upon exposure, which has been previously reported by Diryak *et al.,* (2018). The alginate continued to develop its gel structure and both moduli continued to increase steadily following the initial

rapid gelation. The formulation was exposed to the acidic media for 420 min and gradually increased in strength (Figure 5.12A) as the gel stiffness of an alginic acid gel depends on the duration of the exposure to acidic pH (Bradbeer et al., 2014). It is clear from the graph that the moduli maintained steady state when the formulation was in acidic media and the release followed zero order kinetic model over the 120 min test (Figure 5.14C). The pH of the media was then increased to 8.0 at 120 min which demonstrated that it was feasible to change the dissolution media during the course of an experiment. Reduction in G′ was witnessed from 190 min which indicated the initiation gel dissolution. An apparent lag time was observed between the time of changing pH and observing the reduction (Figure 5.13) in the moduli which can be explained by the time required for diffusion of release media into the gel. Besides, the lower surface of the sample which was in contact with the media began to dissolve first resulting in an anisotropic gel for the diffusion of the media. It allowed continuous release of drug from the gel, at the surface in contact with the release media. The diffusion of the media into the gel progressed resulting in significantly ($p < 0.05$) higher release (~96%) and G′ value of ~28.64 pa at the end of the test. The high solubility of MNZ (65.31 mg/ml) at pH 1.2 and low solubility (16.24 mg/ml) at pH 8.0 (Figure 5.15) confirmed that continuous release of MNZ at pH 8.0 was a result of degradation of the gel and not a solubility effect. Similar solubility (64.80 mg/ml) of MNZ at pH 1.2 has been reported by Wu and Fassihi, (2005).

5.6 Conclusion

A novel method was demonstrated in this study which has the potential to analyse real time *in situ* gelation on exposure to the cross linking medium, with a facility of sampling to analyse the release of drugs at the same time. Also, this method allows the operator to change the pH during the experiment, which could be used to correlate the changes in gelation

behaviour in various physiological environments and assess the subsequent impact on drug release. This technique could be utilised in early stages of the development process to design more efficient *in situ* gelling formulations and can be modified to target to different physiological sites on exposure to different physiological fluids (such as saliva, lung fluid, nasal fluid). Moreover, this technique could be utilised in any systems, beyond that of pharmaceutical formulations, where polymers undergo rapid or slow gelation in presence of metal ions, changes in pH or by small molecule cross linkers and release an entrapped compound.

Chapter 6: Formulating an *In Situ* Gelling System of Poorly Soluble Drug for Optimizing Ophthalmic Delivery

6.1 Introduction

Poor bioavailability is an obstacle for drugs to reach a therapeutic concentration level at the target site. When the target site is intra ocular, the challenge is greater because of the distinctive anatomy and physiology of the eye (Lang, 1995). Pre corneal clearance via blinking and nasolacrimal drainage can cause poor bioavailability of ophthalmic solutions in the eye (Cohen et al., 1997). Over the past few decades, *in situ* gel forming ophthalmic drug delivery systems have been a major research focus for offering improved bioavailability of the active ingredients at the surface of the eye. These formulations undergo sol-gel transition in response to the changes in pH, temperature or ions present in lacrimal fluid which has been described in the previous chapters.

Poor water solubility of drugs and subsequent low bioavailability, has been attributed to the majority of the failures in new drug development. Approximately 90% of current pipeline drugs and 40% drugs with market approval are poorly water-soluble (Kalepu and Nekkanti, 2015). However, poorly soluble drugs, despite of potential useful therapeutic effects, are not suitable to incorporate in *in situ* gelling systems because of the aqueous based gelling formulations and low volumes administered. The administered drugs must exhibit sufficient solubility to diffuse into the eye in order to make such formulation successful (Loftsson and Stefánsson, 2017). The salt form of poorly soluble drugs can improve the solubility but can subsequently interact with the ionotropic gel formers such as gellan resulting in gelation before administration or increasing the viscosity of the formulation. For example,

Flurbiprofen (FBP) is an arylpropionic nonsteroidal anti-inflammatory drug (NSAID) and considered as Class II drug with low water solubility and high permeability according to Biopharmaceutic Classification System (BCS) (Cirri et al., 2005). In commercialized anti-inflammatory eye drop Ocufen®, sodium salt of FBP is used to enhance the solubility of FBP which is difficult to formulate as an *in situ* gelling formulation using gellan because of the tendency of gellan to undergo gelation by crosslinking with sodium ions.

To increase the solubility of poorly soluble drugs, a number of other strategies have been employed such as, formulating as nanogels to increase the residence time of drug on the target site, using solubilizing systems such as microemulsions and liposomes to enhance the solubility (Loftsson and Stefánsson, 1997) and using drug-cyclodextrin complexes to increase the bioavailability, stability and solubility of the ophthalmic drugs (Loftssona and Järvinen, 1999; Felton et al., 2014). In recent years, cyclodextrin (CD) complexes have been employed successfully to improve solubility and rate of dissolution (Cirri et al., 2005). CDs are cyclic oligosaccharides having hydrophilic outer surface and hydrophobic/lipophilic internal cavity. The hydrophobic inner cavity forms inclusion complex with poorly soluble drugs by allowing the drug molecules to enter into the cavity (Loftsson and Brewster, 2010; Felton et al., 2014).

In the present study, FBP was investigated as a poorly soluble drug and CD was used to create a drug-CD inclusion complex to increase the solubility of FBP. Gellan was added as a gel former in the solution of the complex to formulate an *in situ* gelling ophthalmic formulation. Simultaneous measurements of rheology and drug release were performed using the rheo-dissolution method described in chapter 5 and an *ex-vivo* permeation study was performed using a porcine corneal model.

6.2 Cyclodextrins

Cyclodextrins (CDs) are natural cyclic oligosaccharides consisting of (α-1, 4)-linked D-glucopyranose units (Jansook et al., 2018) (Figure 6.1A). They are formed by bacterial digestion of starch. The most common CDs which are used in pharmaceutical products are αCD, βCD and γCD. They consist of different numbers of D-glucopyranose units, for example, αCDs have 6, βCDs have 7 and γCDs consist of 8 D-glucopyranose units. CD molecules are described as doughnut shaped molecules and exhibit a lipophilic central cavity with a hydrophilic outer surface. In CDs molecules, the secondary hydroxyl groups extend from the wider edge of doughnut shape and primary groups extend from the narrow edge causing the outer surface to be hydrophilic (Figure 6.1B).

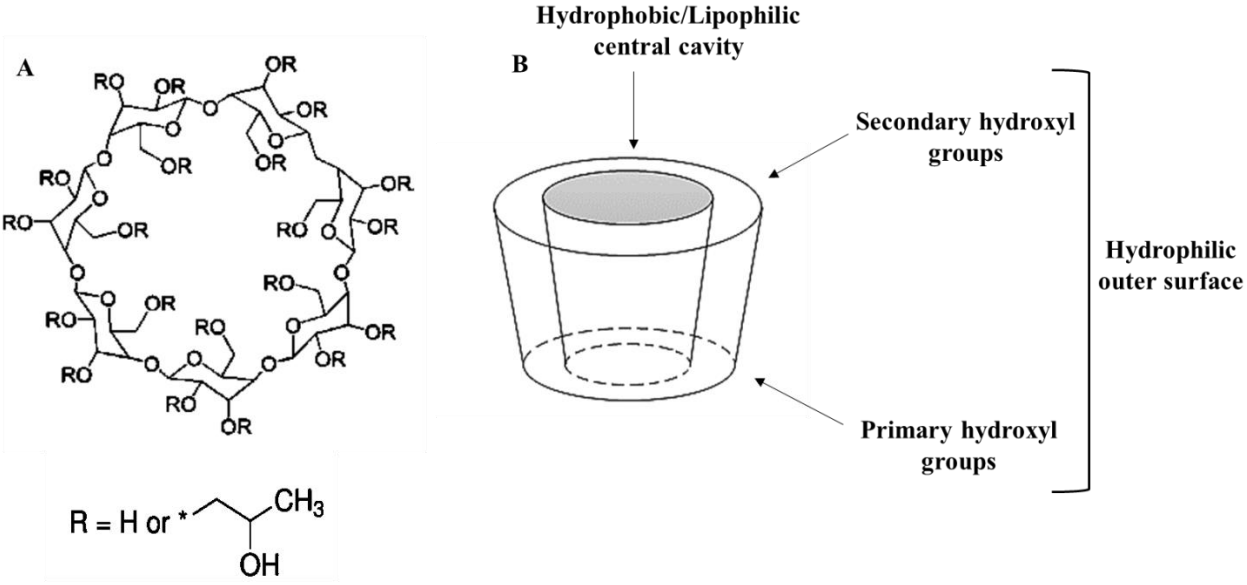

Figure 6.1: (A) Chemical structure of CD (B) Doughnut structure of CD molecule showing lipophilic inner cavity and hydrophilic outer surface (adapted from Loftsson & Stefánsson, 2017)

CDs have the ability to form water soluble inclusion complexes by taking poorly soluble lipophilic drugs into their central cavity. Even though having hydrophilic nature, CDs exhibit limited aqueous solubility because of the orientation of hydroxyl groups in CD

molecules. β CDs are less soluble in water compared with α and γ CDs (table 6.1). In β CD, the orientation of the hydroxyl groups of the adjacent glucopyranosyl units causes maximum interaction with each other resulting in less availability to be hydrated. In α CDs, the hydroxyl groups are further apart and are able to interact more with water. In γ CD, the hydroxyl groups interact more with water and less with each other resulting greater water solubility (Hedges, 2009). Random hydroxyl group substitution with hydroxypropyl groups increases the solubility of CDs and their complexes, for example hydroxypropyl β CD. Natural CDs convert from crystalline solid to physically stable, amorphous mixtures of isomer upon random substitutions. The complexation capabilities and aqueous solubility of CD molecules depend on the structure, location and number of appended substituents per CD molecule (Loftsson and Brewster, 2010; Jansook et al., 2018). The height of the CD cavity is same for three commonly used CD (α, β and γ) but the internal diameter and volume vary depending on the number of the glucose units. Based on the dimensions, α-CDs form inclusion complexes with compounds having aliphatic side chains or low molecular weight, β-CDs form complexes with aromatic and heterocyclic compounds, and larger molecules (such as steroids) form inclusion complexes with γ CDs (Valle, 2004). Besides enhancing the solubility of highly insoluble molecules, inclusion formation exerts some other beneficial modification to the temporarily locked guest molecule such as, stabilisation against degradative effects of oxidation, controlling the sublimation and volatility, taste modification, chromatographic separation. Table 6.1 represents general properties of three commonly used CDs.

Table 6.1 General properties of commonly used CDs (Valle, 2004)

Property	α-CD	β-CD	γ-CD
Number of glucopyranose units	6	7	8
Molecular weight (g/mol)	972	1135	1297
Outer diameter (Å)	14.6	15.4	17.5
Cavity diameter (Å)	4.7-5.3	6.0-6.5	7.5-8.3
Cavity volume ($Å^3$)	174	262	417
Solubility in water at 25°C (%, w/v)	14.5	1.85	23.2

6.2.1 Drug-CD Complex Formation

The hydrophobic central cavity of CD molecule allows hydrophobic drug molecules to enter and form water-soluble inclusion complexes. During the formation of drug-CD inclusion complexes, no covalent bonds are formed or broken (Loftsson and Brewster, 2010). Water is typically the solvent of choice for complex formation. The complexes can be formed in the crystalline state or in solution (Valle, 2004). To form the inclusion complexes in the crystalline state, CDs are dissolved in DI water at room temperature and the guest molecules are added to the aqueous solutions of CDs while the solutions are continuously stirred. The solutions become turbid and white precipitates are formed. The resulting white suspensions are stirred at room temperature for 24 h and filtered. The collected precipitates are dried for 24 h in oven and formation of inclusion crystals are confirmed by X-ray diffraction (Uyar et al., 2006).

Inclusion complex formation of CD with a drug molecule depends on certain functional groups within the drug and relative size of the CD to the size of the drug molecule. Thermodynamic interactions between the components of the system (CD, solvent and drug molecule) is another key factor for the inclusion complex formation. A favourable net energetic driving force must be present for the drug molecule to enter into the CD cavity.

The slightly nonpolar CD cavity is occupied by water molecules in an aqueous solution and are replaced by the guest drug molecule to form the complex (Figure 6.2). Here, the release of enthalpy-rich water molecules from the hydrophobic central cavity acts as the driving force for the formation of the inclusion complex.

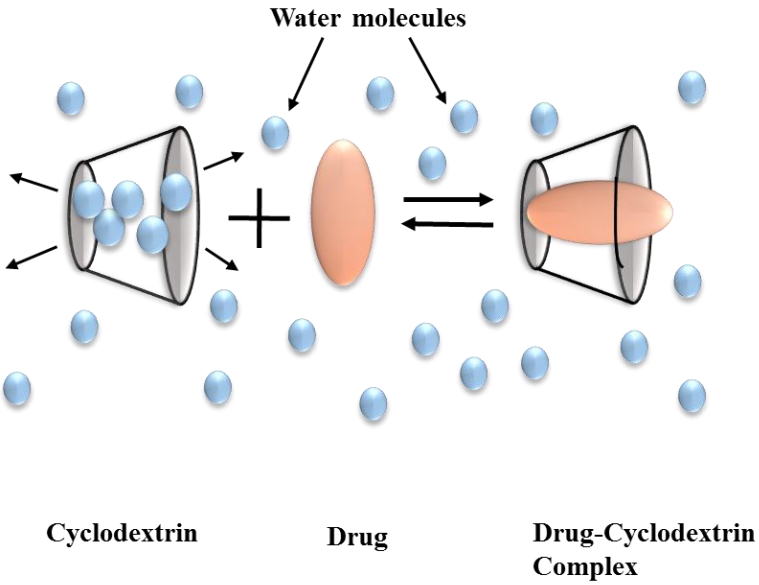

Figure 6.2: Schematic representation of formation of drug-CD complex in aqueous solution, here the water molecules are replaced by the drug inside the cavity

In the most simple and frequent cases, 1:1 of CD:drug ratio exist however, 2:1, 2:2 or 1:2 or higher associations can also exist (Szejtli, 1998; Valle, 2004). An equilibrium is established between the dissociated and associated species upon dissolving the complexes and this is expressed by complex stability constant (K).

$$CD + D \rightleftharpoons CD.D \qquad \textit{Equation 6.1}$$

$$K_{1:1} = \frac{[CD.D]}{[CD][D]} \qquad \textit{Equation 6.2}$$

The stability constant determines the affinity of a drug for the given CD and can be calculated from the method of titrating changes of the drug molecule within the CD before

analysing the concentration dependencies (Loftsson and Brewster, 2010). Complexation of CD and drug is a dynamic process and drug molecules continuously associate and dissociate from the CD. Values of association and dissociation rate constants range from 10^7 to 10^8 M^{-1} s^{-1} and 10^5 s^{-1} respectively (Stella et al., 1999). The initial equilibrium to form the complex is very rapid and takes place within minutes. The shifting of the initial equilibrium to the completed formation of the inclusion complex takes longer time to attain because it involves energetically favourable interactions such as displacement of the polar water molecules from the CD cavity, increased hydrogen bonds as a result of returning back of the water molecules to the aqueous environment, reduction of repulsive interactions between the water molecules and drug, and an increase in the hydrophobic interactions due to the drug entering into the nonpolar CD cavity. Once inside the CD, the drug molecule makes conformational adjustments utilizing existing weak van der Walls forces within the cavity to optimise inclusion complexation (Valle, 2004).

A variety of techniques can be used to form the inclusion complex. The techniques depend on several factors such as, properties of the active ingredient and other formulation ingredients, the equilibrium kinetics, formulation process and desired final dosage forms. The common techniques include mixing in solutions and suspensions followed by suitable separation, simple dry mixing, preparation of pastes and other thermo-mechanical techniques (Valle, 2004). Simple dilution is the major driving force to release the drug from drug-CD complexes. There are some other mechanisms which also contribute to release the drug rapidly from the complexes such as, drug-protein binding, competitive binding and direct drug partition from the complex to the tissues (Loftsson and Brewster, 2010)

6.2.2 CDs in Ophthalmic Drug Delivery

Incorporation of CDs into ophthalmic preparations has gained considerable attention recently and has been shown to be useful additives in ophthalmic formulations to increase the aqueous solubility and stability of poorly soluble drugs. Besides, addition of CDs improves drug absorption and reduces local irritation inside the eye. Complexation of CDs with poorly soluble drugs have also been shown to enhance the bioavailability of drugs (Loftssona and Järvinen, 1999). Several reports of using CDs in ophthalmic formulations have been published which showed increased solubility, bioavailability, permeability and reduced irritation of lipophilic drugs. Davies et al., (1997) reported the development of a formulation of poorly soluble steroidal drug hydrocortisone with 2-hydroxypropyl-β-cyclodextrin (HβCD) to increase the solubility of the drug. The solubility of the drug was increased approximately two-fold with the addition of CD in the solution. Chemical stability of the drug was also increased and the decomposition was reduced as a result of complexation formation. Kristinsson et al., (1996) reported development of dexamethasone-HβCD complex as an aqueous eye drop solution which showed enhanced permeability and higher concentration of dexamethasone in aqueous humour compared to the conventional formulation. Moreover, HβCD has been reported to significantly increase the aqueous solubility and chemical stability of poorly soluble anandamides in the preparation of eye drop formulations (Pate et al., 1995, 1996, 1997). The antihistamine drug cetirizine showed strong irritation upon ocular administration but it has been reported that addition of CDs (α, β and γ) to a solution of cetirizine eliminated the irritation. Although slight decrease in the efficacy of the applied dose was reported (Ikejiri et al., 1995). Some of the other reports of using CDs in ophthalmic formulations are summarized in Table 6.2.

Table 6.2: Examples of reports of using CDs in ophthalmic drug delivery systems

Cyclodextrin	Drug	Reference
HβCD, Randomly methylated-β-CD	Diclofenac sodium	Reer et al., 1994
HβCD	Enalapril Maleate	Loftsson et al., 2010
HβCD	Ketoconazole	Zhang et al., 2008
αCD, βCD	Riboflavin	Morrison et al., 2013
HβCD	Rufloxacin	Cappello et al., 2002
HβCD	Enoxacin	Liu et al., 2005
γCD	Amphotericin B	Serrano et al., 2012

6.2.2.1 *Mechanism of Permeation of Drug into the Cornea*

The ocular bioavailability of ophthalmic formulations is less than 5% in general (Loftssona and Järvinen, 1999). Lipophilic (hydrophobic) membranes (Cornea, conjunctiva and sclera) are the main barriers for drug permeation into the eye. There is aqueous tear fluid and a hydrophilic mucin layer at the outside of the lipophilic membranes. To permeate this exterior eye surface and penetrate the ocular barrier, the drug molecule must be hydrophobic (*i.e.* lipophilic) and hydrophilic at the same time (Loftsson and Stefánsson, 1997). High drug concentration at the membrane surface acts as a driving force for passive drug permeation through the ocular barrier. Through drug-CD complexation, solubility of poorly soluble drugs (lipophilic) can be enhanced without altering the molecular structure and permeation abilities of the drug molecules. The process of releasing drug from drug-CD complex into the cornea can be explained by the mechanism proposed by Loftssona and Järvinen, (1999) (Figure 6.3).

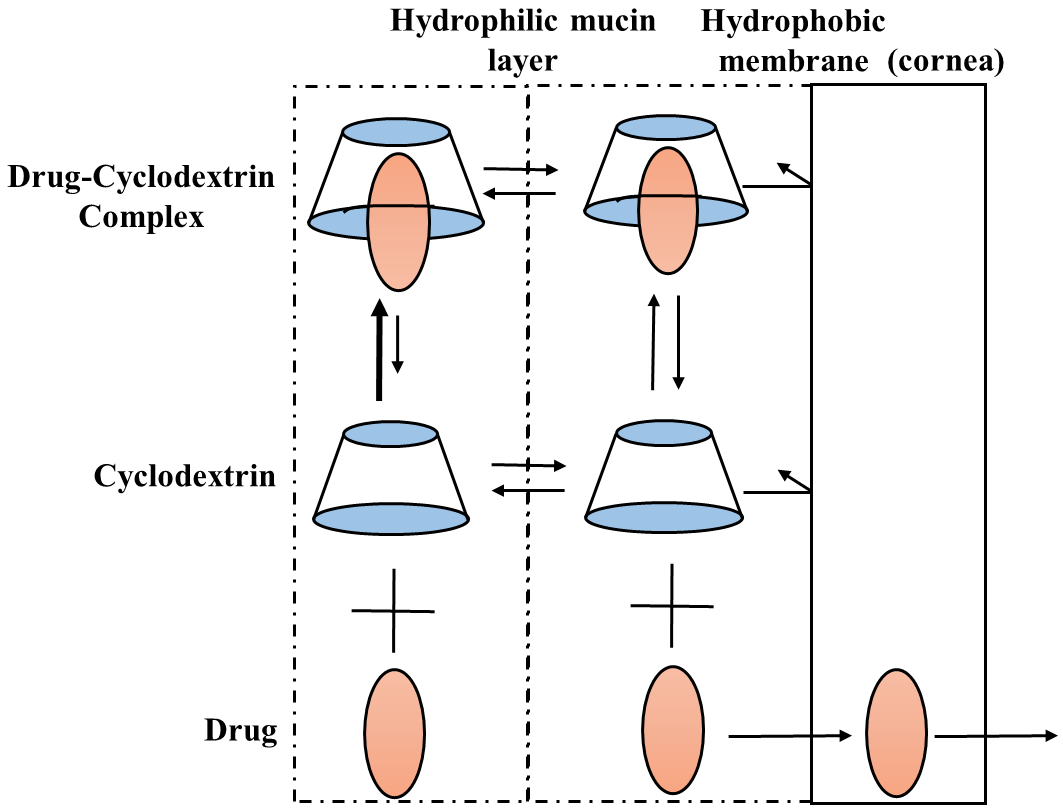

Figure 6.3 Schematic diagram representing the proposed mechanism of permeation of drug to the cornea from drug-CD complex by Loftssona & Järvinen, 1999.

According to this mechanism, CDs act as carriers by keeping the hydrophobic poorly soluble drug inside the cavity. CD delivers the drug molecule through the hydrophilic mucin layer to the surface of the ocular barrier consisting of hydrophobic membranes (i.e. Cornea). Delivery of the drug through the hydrophilic mucin layer is controlled by diffusion, and delivery through the hydrophobic membranes is membrane controlled. As the drug-CD complex continuously associate and dissociate, they diffuse through the hydrophilic mucin layer to the hydrophobic membrane both as a complex and free CD. The complex delivers the drug to the surface of hydrophobic membrane and the poorly soluble drug easily passes the barrier while the free CD remains in the surface. When there are excess drug molecules and low CD concentrations, the donor phase is saturated with the drugs and thermodynamic activity of the drugs is at its maximum. The permeability co-efficient increases with

increasing CD concentrations which results in an increasing amount of dissolved drugs. Therefore, more drugs (as drug-CD complexes) diffuse to the surface of the barrier. When there is excess CD present, drug activity at the donor phase decreases which results decreased permeability coefficient.

6.2.3 Toxicological Considerations

According to toxicity studies, CDs are practically non-toxic when administered orally due to lack of absorption from the gastrointestinal tract (GIT) (Irie and Uekama, 1997). When CD containing eye drop solutions are administered topically, CD is washed away rapidly from the eye surface to the GIT via nasolacrimal drainage. If pure isotonic CD solution (20 to 25% w/v) is administered to each eye (two drops three times a day), total CD would be 1.7 mg/kg/day which is less than $1/10^{th}$ of normal daily usage. So the local or systemic toxicity in the GIT can be excluded (Loftssona and Järvinen, 1999). There are some concerns that methylated β-CD can cause some irritation in the eye after administration (Jansen et al., 1990) although these are based on limited experimental data. *In vivo* studies have shown that CDs can damage the ocular membrane only at relatively high concentration (isotonic drops contains >25% w/v CD) (Loftssona and Järvinen, 1999).

Several studies however, have shown that HβCD in ocular formulations is well tolerated in animals and humans even when the concentration is as high as 45% w/v. It is therefore, the most commonly used CD in eye drop formulations (Loftsson and Stefánsson, 2017). It also can be used for oral, dermal, rectal and formulation (Stella et al., 1999; Malanga et al., 2016). Table 6.3 represents commercialized ophthalmic formulations containing CDs.

Table 6.3: Marketed eye drop solution containing CDs (Loftsson and Brewster, 2010)

Drug	Cyclodextrin	Trade name	Company
Indomethacin	2-Hydroxypropyl-β-cyclodextrin	Indocid	Chauvin (France)
Chloramphenicol	Randomly methylated β-cyclodextrin	Clorocil	Oftalder (Portugal)
Diclofenac sodium salt	2-Hydroxypropyl-γ-cyclodextrin	Voltaren Optha	Novartis (France)

In the present study, 2-hydroxypropyl-beta-cyclodextrin (HβCD) has been used to make the drug-CD inclusion complex.

6.3 Flurbiprofen

Flurbiprofen (FBP) is a poorly soluble NSAID. It exhibits analgesic, anti-inflammatory and antipyretic properties. It is a weak acid (pKa 4.22) and contains a biphenyl group with a fluorine atom in the ortho position (Xu and Madden, 2010) (Figure 6.4). It is cyclooxygenase (COX) inhibitor which converts arachidonic acid to prostaglandins. Prostaglandins regulate pain, fever and inflammation. So by inhibiting the activity of COX, prostaglandin synthesis is inhibited, therefore, pain and inflammation are also inhibited. FBP reduces the production of aqueous humour by decreasing bicarbonate ion concentrations which causes lowering intraocular pressure. Currently FBP sodium is marketed as Ocufen® (0.03% FBP sodium). Ocufen® is used to inhibit intraoperative miosis and treat postoperative ocular inflammation.

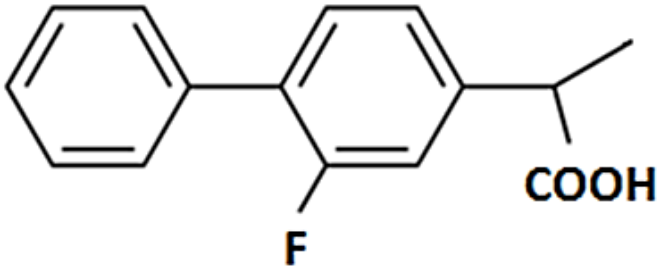

Figure 6.4 Chemical structure of FBP (Duarte et al., 2004)

6.4 Martials and Methods

6.4.1 Materials

FBP, low acyl gellan gum (Gelrite®), HβCD, hydrochloric acid, phenol, sulphuric acid, calcium chloride dehydrate and sodium chloride were purchased from Sigma Aldrich (Poole, UK). Sodium bicarbonate was purchased from Fisher Scientific (Loughborough, UK). All materials were used as received. Fresh porcine cornea was purchased from a local abattoir.

6.4.2 Determination of FBP Content by UV Spectroscopy

A stock solution of FBP was prepared by dissolving 5 mg of FBP in 25 ml of SLF (pH 7.5) containing 10% HβCD to get a final concentration of 200 µg/ml. The stock was diluted and scanned (400 nm to 200 nm) using UV spectroscopy (Agilent Cary 60 UV-Vis) to obtain the maximum absorbance wavelength (λ_{max}). The maximum absorbance was found at a wavelength of 247 nm. Five different FBP standards were prepared from the stock solution at a concentration ranging from 0.05 to 0.5 µg/ml. SLF with 10% HβCD was used as a blank. The standards were measured at 247 nm to produce a calibration curve. All the experiments were done in triplicate. The absorbances were plotted against the concentrations of standards and a linear regression equation was obtained. LOD and LOQ were determined using

equation 4.1 and 4.2. Three different concentration levels (50%, 100% and 150%) were used to perform accuracy studies. Precision studies were performed by analysing the samples with inter-day and intra-day repeatability.

6.4.3 Phase Solubility Studies

Stoichiometry is an important characteristic of drug-CD complex and a phase-solubility diagram is used to obtain the stoichiometry of drug-CD complexes. In this diagram, drug solubility is monitored as a function of total CD added to the complexation medium. Here the concentrations of dissolved drugs are plotted against the concentrations of CD. This technique shows how CD influences the solubility of a drug (Loftsson and Brewster, 2010).

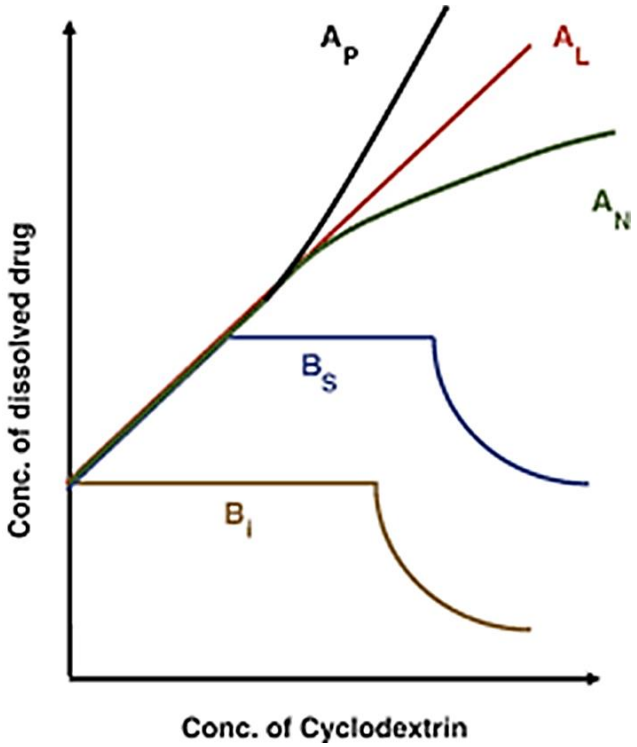

Figure 6.5: Types of phase solubility diagrams according to Higuchi and Connors, (1965) where concentrations of CDs are plotted against the concentrations of dissolved drug. The resultant diagrams are A_L: linear, A_P: positive deviation from linearity; A_N: negative deviation from linearity; B_S: limited solubility of complex or B_I: insoluble (Brewster and Loftsson, 2007; Saokham et al., 2018)

Several types of behaviours can be identified based on the shapes obtained from the phase solubility relationships. Higuchi and Connors, (1965) have classified the phase solubility diagrams into two different plots based on their shapes, which are type A and B (Figure 6.5). In system A, the solubility of drug increases as a function of CD concentration and this system can be classified into three subtypes which are A_L, A_P and A_N. A_L diagram indicates linear increase in solubility of drug as a function of CD. A_P diagram indicates that the curve is deviated from linearity in a positive direction, *i.e.* when CD is more effective at higher concentrations. A_N shows negative deviation from linearity and it can happen when CD is less effective at higher concentrations. These diagrams are observed in complexation media containing water soluble CDs. B type solubility profiles indicates limited water solubility of drug-CD complex which are usually associated with natural CDs with limited solubility, such as β CD. B type diagrams can be further classified into B_S and B_I subtypes. When concentration of CD is increased in a system, a soluble drug-CD complex is formed which enhances total solubility of poorly soluble drugs and can be identified by the ascending portion of B_S type isotherm (Figure 6.5). Maximum solubility of the drug is attained at a particular point of the solubilisation process (plateau segment of Bs type diagram in Figure 6.5). Additional complexes are formed by additional CDs which precipitate and all solid drugs are consumed at some point. Further addition of CDs causes formation of additional insoluble complexes which precipitate and can be identified by the descending portion of the B_S type solubility profile. B_I type profile indicates similar system to the B_S type except that the formed complexes are insoluble and therefore no ascending portion is observed at the beginning of the isotherm (Brewster and Loftsson, 2007).

Phase solubility studies are performed by saturating the drug in aqueous media to form high order complex aggregates (Loftsson and Brewster, 2010; Saokham et al., 2018). To perform

phase solubility studies, excess amount of FBP were added to 10 ml SLF (pH 7.5) in sealed glass containers to obtain 0.5, 1, 2, 5, 10 and 20% (3.4, 6.8, 13.7, 34.2, 68.5 and 137 mM) of HβCD. A constant temperature (25°C) was used for mixing the solutions for 24 hours using electromagnetic stirrer (200 rpm). 0.45 µm pore sized filter paper was used to filter the solutions. After dilution, the solutions were analysed spectrophotometrically (λmax 247 nm) to determine the drug concentrations. The concentrations of total dissolved drugs were plotted against the concentration of HβCD to create the phase solubility diagram.

6.4.4 Interaction Studies between HβCD and Gellan

Oscillatory rheological analysis was performed on the solutions containing HβCD and gellan to observe any interference in gelation of gellan caused by HβCD. HβCD solutions were prepared by adding precise amounts of HβCD in DI water at room temperature to prepare 0.5%, 1%, 2%, 5% and 10% w/v final concentration. The solutions containing HβCD were heated up to 85°C with continuous stirring and 0.4% gellan was added to the solutions. The concentration of gellan was selected according to the commercial Timoptol LA® eye drop formulation (discussed in chapter 4). Once gellan was completely dissolved, stirring was stopped and the solutions were allowed to cool to room temperature prior to further analysis. Oscillatory measurements G′ and G″ (Pa) were measured as a function of time (0.5% strain and 1 rad/s frequency) according to the experimental set up described in 5.3.6. All experiments were performed at 25ºC.

6.4.5 Preparation of *In Situ* Gel Forming Ophthalmic Formulation of FBP with HβCD and Gellan

In the present study, the concentration of HβCD was selected based on the results of phase solubility studies which was 10%. To prepare the formulation, required amount of HβCD was added to the DI water at room temperature to obtain the concentration 10% w/v and precise amount of FBP was added to the solution to obtain final concentration of 0.029% w/v (without salt form). The concentration of FBP was selected based on the marketed product Ocufen® which contains 0.03% w/v FBP sodium. The solution of FBP-HβCD was heated up to 85°C and 0.4% gellan was added. The solution was stirred until the gellan was completely dissolved. The prepared formulation was cooled down to room temperature and pH was measured using Jenway 3510 pH meter. A formulation was also prepared using 20% HβCD according to the same procedure to compare the rheo-dissolution properties with the formulation containing 10% HβCD. The pH of the formulations ranged between 4.30 to 4.32.

6.4.6 Confirmation of Complexation

Differential Scanning Calorimetry (DSC) was performed to confirm the complexation between drug and HβCD (Mettler Toledo, DSC 1, STARe system). DSC is a thermal analysis technique to measure the heat energy uptake within a controlled increase or decrease in temperature. Energy is introduced and raised similarly over time to the sample of known mass and reference. The difference in heat input between the sample and the reference is measured as detection of transition such as melting and glass transition. The heat flux (ΔH/dt) is plotted against the average sample temperature or time (Adebisi, 2014).

To perform thermal analysis, formulations containing FBP-HβCD and FBP-HβCD with gellan were prepared for freeze drying. The formulations were stored in a freezer at -20ºC

overnight. The frozen samples were then dried using a (Christ Alpha 2-4 L Dplus) freeze drier. The drying procedure was performed for 24 hours at -84.6ºC with the vacuum set at 0.001 mbar. All the samples (FBP, gellan, HβCD, physical mix and freeze dried samples) were accurately weighed (Mettler AT201) and heated in crimp sealed aluminium pans at 10°C per min between 50 to 150°C. The nitrogen gas flow was 200 ml/min. Thermograms of FBP, HβCD, gellan, alone and as physical mixtures of all components were compared with the freeze dried samples.

6.4.7 Simultaneous Determination of Rheology and Dissolution of the Drug (Rheo-Dissolution Study)

Rheo-dissolution experiments were conducted according to the experimental set up described previously (5.3.6). The samples were allowed to form gels *in situ* in the presence of SLF and measurements of G′ and G″ were performed to determine gelation behaviour. Aliquots of SLF were withdrawn (0.5 ml) at pre-determined time intervals (60, 120, 180, 240 and 300 min) from the circulatory system while measuring the rheological changes. An equal amount of fresh SLF was replaced at each time point. All samples were diluted and analysed using a UV spectrophotometer at 247 nm. The contents of FBP in the withdrawn samples were determined from the linear regression equation of the calibration curve. Rheo-dissolution experiments were performed on the formulations containing 10% and 20% HβCD at room temperature and in triplicate.

6.4.8 Carbohydrate Analysis by Phenol-Sulphuric Acid Method

Phenol-sulphuric acid (PSA) method is the most reliable, easiest and rapid colorimetric method to measure the total carbohydrates present in a sample (Masuko et al., 2005). This method is widely used to determine the concentrations of sugars and their methyl derivatives, polysaccharides and oligosaccharides (Dubois et al., 1956). The method

requires 5% phenol solution and concentrated sulphuric acid. Addition of concentrated H_2SO_4 breaks down any polysaccharides to monosaccharides and the 6 carbon compounds (hexoses) dehydrate to hydroxymethyl furfural while 5 carbon compounds (pentoses) dehydrate to furfural. Addition of phenol to these solutions causes a reaction which produces yellow-gold colour. The amount of carbohydrates present in the sample can be determined from linear regression equation obtained from standard calibration curve. D-glucose is commonly used to prepare the calibration curve at 490 nm (Nielsen, 2010). In this experiment, amount of dissolved HβCD and gellan were determined in the withdrawn samples using PSA method.

6.4.8.1 *Preparation of 5% Phenol Solution*

5g of phenol was dissolved in 100 ml of DI water to produce 5% phenol solution. This mixture formed a clear liquid and was ready to use (Dubois et al., 1956).

6.4.8.2 *Determination of Sugar Content by UV Spectroscopy*

A stock solution of D-glucose was prepared by adding 25 mg of D-glucose in 25 ml of SLF to produce concentration of 1 mg/ml. Six different standard solutions were prepared from the stock solution ranging from 10 to 100 µg/ml (10, 20, 40, 60, 80 and 100 µg/ml). 1 ml of 0.5% phenol solution was added to the filtered standards (1 ml) followed by adding 5 ml of concentrated H_2SO_4. The solutions were mixed for 10 min and placed in a water bath for 20 min. The temperature of the water bath was maintained between 25-30 °C. The absorbance of the resultant yellow-gold coloured solutions were measured using a UV spectrophotometer at wavelength of 490 nm (Ghori et al., 2014). The absorbance was then plotted against concentration of the standards and a linear regression equation was obtained.

6.4.8.3 *HβCD Dissolution Studies*

Rheo-dissolution experiments were performed for the formulations containing 10% and 20% HβCD and same sample regime was applied as used in 6.4.7. Content of HβCD in the withdrawn samples were measured using PSA method. 1 ml of 5% phenol was added to the filtered samples (1 ml) followed by 5 ml of concentrated H_2SO_4. After mixing vigorously for 10 min the resultant solutions were placed in a water bath (25-30 °C for 20 min). The solutions were analysed at 490 using UV spectrophotometer and HβCD concentration in the samples was determined from the prepared calibration curve.

6.4.8.4 *Gellan Dissolution Studies*

Rheo-dissolution experiments were conducted for a control sample consisting of 0.4% gellan solution without HβCD and FBP. To prepare the solution, precise amounts of gellan (0.4%) was dissolved in DI water at 85°C while stirring the solution. Stirring was stopped once gellan was dissolved completely. The solution was allowed to cool before performing the rheo-dissolution experiment according to 5.3.6. While analysing rheological changes, samples (0.5 ml) were collected at 60, 120. 180, 240 and 300 min. The same volume of freshly prepared SLF was used to replace the withdrawn sample. The collected samples were subjected to PSA assay according to the procedure described in 6.4.7.3 and gellan concentration in the samples were calculated from the prepared calibration curve.

6.4.9 *Ex-vivo* Permeation Studies Using Porcine Cornea

Permeation studies were performed for the formulation containing 10% HβCD and marketed Ocufen® eye drop (pH 6.68).

6.4.9.1 *Preparation of Cornea for Permeation Study*

Porcine corneas used in permeation studies were obtained from fresh porcine eye balls which were purchased from a local abattoir. The collected eye balls were used within few hours of enucleation. The fat and muscles around the eye balls were trimmed and an incision was performed between optic nerve and cornea. The sclera was cut all the way round and vitreous humour, lens and ciliary body were removed (Figure 6.6). The cornea was removed and care was taken to avoid any distortion (method adopted from Fathalla et al., 2016).

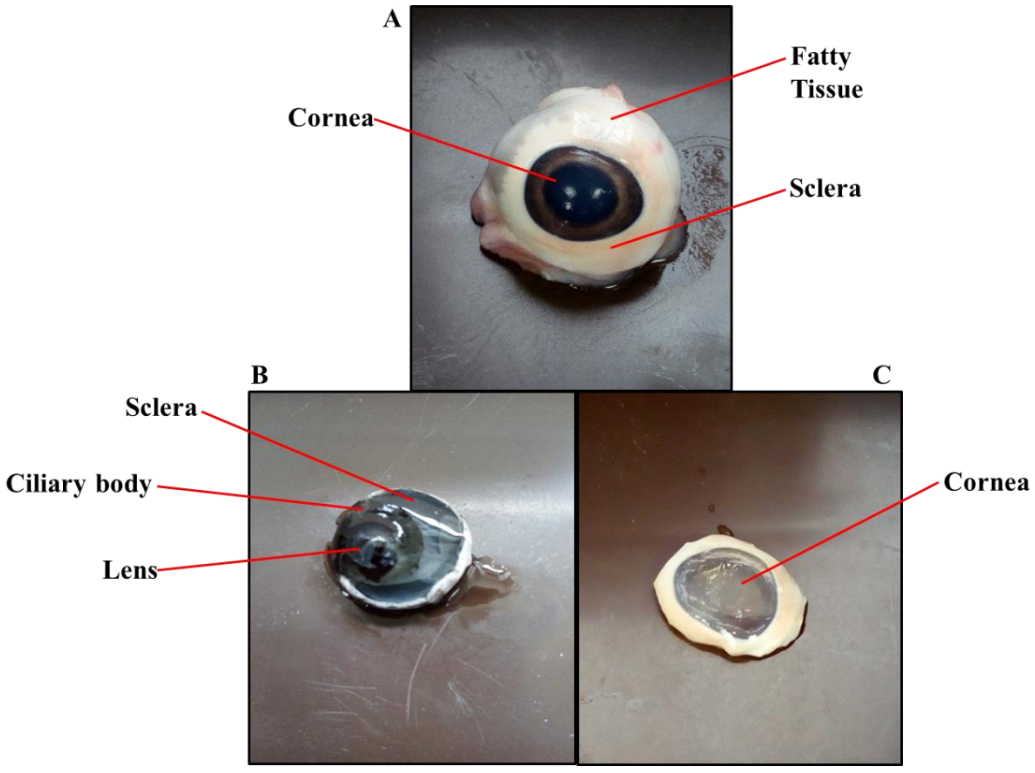

Figure 6.6: (A) Pig eyeball before dissecting (B) Back view of anterior half of the pig eye (C) removed cornea

6.4.9.2 *Ex vivo Permeation Studies*

Permeability of FBP through the porcine cornea was performed using a Franz diffusion cell. A Franz diffusion cell is constructed with two compartments, the upper part is the donor compartment where test samples are loaded and the lower part is receptor compartment, which contains receptor fluid that is analysed for permeated drugs. The two compartments are held in place by a horseshoe clamp and the tissue is placed in between the compartments. The receptor compartment can be jacketed and connected to water source to control the temperature throughout the experiment (Pineau et al., 2012). The receptor compartment contains a sampling port to collect and replace the sample.

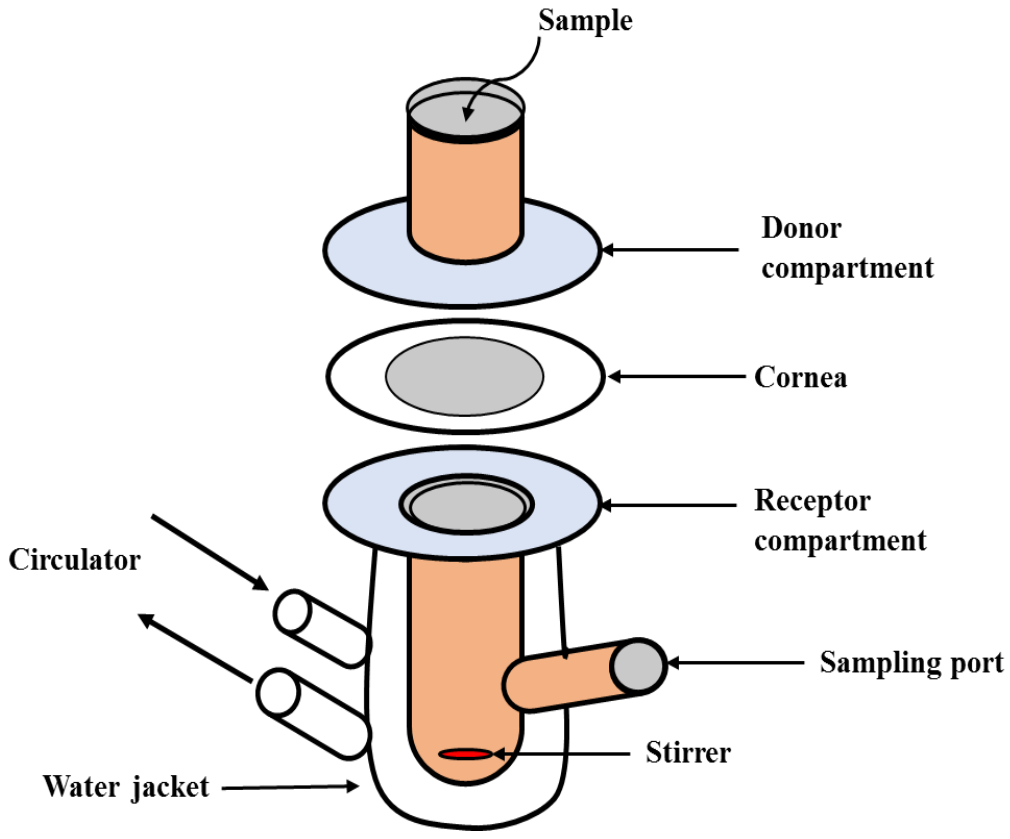

Figure 6.7 Schematic diagram of a Franz diffusion cell

In this study, permeation studies were performed using a Franz diffusion cell (Figure 6.7) with a 4 ml fixed volume receptor compartment with a sampling port. The diffusion surface of the cell was 1.76 cm^2. The cornea was placed between the donor and receiver compartments and horseshoe clamp was used to hold the two compartments. The endothelial side of the cornea faced the receptor compartment. The surface of the cornea was placed on the diffusion surface area. The receptor compartment was filled with SLF (pH 7.5) and 35°C was maintained throughout the experiment with a magnetic stirrer bar used to ensure an isothermal temperature was maintained throughout the receiver fluid. Test samples were placed directly on the cornea in the donor compartment and the compartment was under occlusion with Parafilm® to avoid any evaporation (Pineau et al., 2012). Samples (0.5 ml) of the receiver fluids were withdrawn at different time intervals (60, 120, 180, 240 and 300 min) from the sampling port and were replaced with same volume of fresh SLF. The amount of FBP and FBP sodium permeated across the cornea was determined by the UV spectroscopy. Three corneas (n=3) were used for each of the formulations.

6.4.10 Statistical Analysis

Student's t test was applied to compare the data obtained from the dissolution experiments, PSA assays and permeation studies. ANOVA was applied for comparing the dissolution data of HβCD and gellan obtained from PSA assays. Statistical significant level was considered as $p < 0.05$. IBM® SPSS Statistics software, version 24 was used for the statistical analysis.

6.5 Results

6.5.1 Development of UV-Vis Spectrophotometric Method for the Estimation of FBP

Scanning a diluted stock solution of FBP showed maximum absorbance at 247 nm. The absorbance of FBP standards were therefore measured at 247 nm and were plotted against the correspondent concentrations to produce a calibration curve (Figure 6.8). Correlation

coefficient (R^2) was used to determine the linearity of the analytical procedure. The method validation and represented data are presented in Table 6.4.

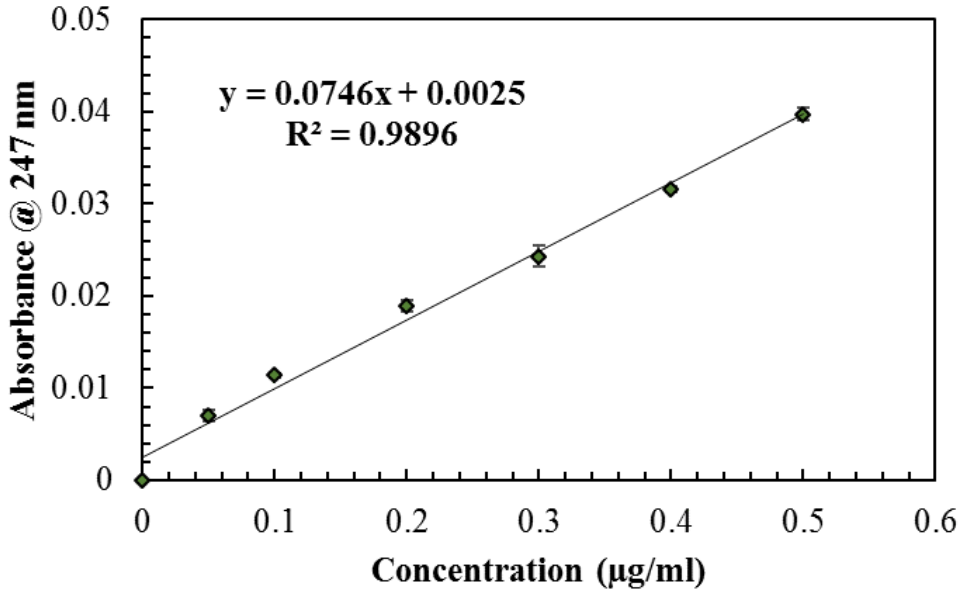

Figure 6.8: Calibration curve of FBP prepared in SLF (pH 7.5) and measured at 247 nm. Values represent mean ± SD (n=3)

Table 6.4: Evaluation and method validation data of UV spectroscopic method of FBP

Range(µg/ml)	0.05 to 0.5
Regression equation	y= 0.0746x+0.0025
Correlation Coefficient	0.9896
LOD (µg/ml)	0.027
LOQ (µg/ml)	0.08
Accuracy	RSD < 8%
Precision	RSD < 9%

6.5.2 Phase Solubility Studies

To initially determine how HβCD influenced the solubility of FBP, phase solubility studies were performed. These experiments revealed that the solubility of FBP increased linearly with increased amount of HβCD (Figure 6.9). The solubility of FBP was 48.53 mM at maximum concentration of HβCD (137 mM or 20%) which was in good agreement with the reported solubility of FBP in phosphate buffer system (pH 7.4) by Felton et al., (2014). According to Higuchi and Connors, (1965), the graph was type A which indicated the formation of a soluble complex. The linear portion of the graph (R^2=0.993) indicated A_L type and allowed the assumption that a 1:1 inclusion complex of FBP-HβCD was present in the media. Based on Ocufen® (0.03% FBP sodium), 0.029% FBP was selected as the concentration used in the test formulations. Although it was apparent that any concentration of HβCD ranging from 3.4 (0.5%) to 137 mM (20%) was able to solubilize 1.23 mM of FBP, the time taken for this to occur varied considerably. At concentrations above 34.2 mM (5%) HβCD, solubilisation took approximately 30 minutes whereas at concentrations less than 34.2 mM required stirring overnight to fully solubilise the FBP. Therefore, further experiments were performed using 68.5 mM (10%) and 137 mM (20%) of HβCD.

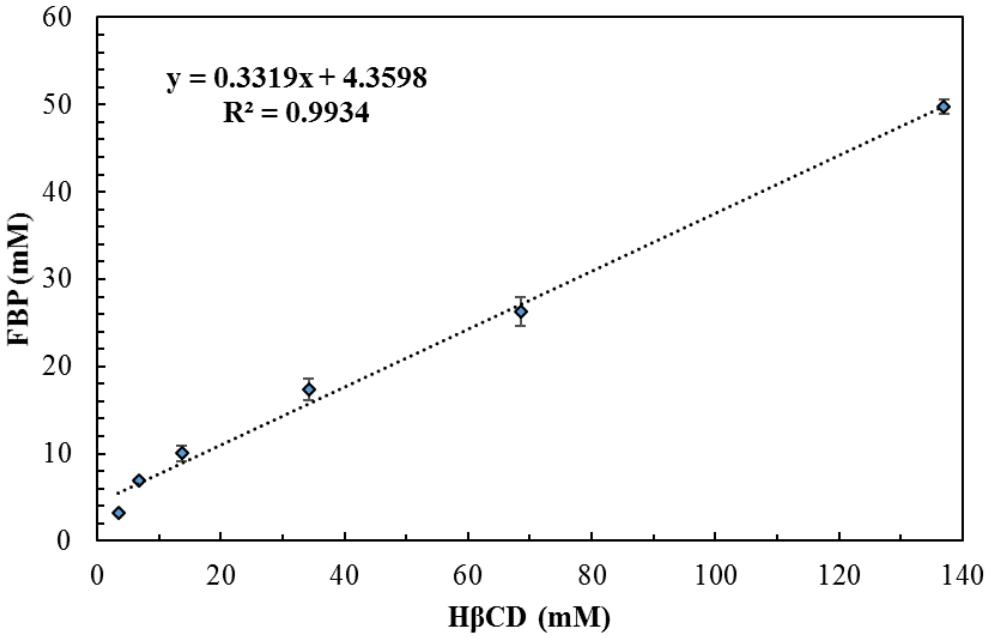

Figure 6.9: FBP solubility as a function of HβCD

6.5.3 Interaction Studies between HβCD and Gellan

Oscillatory rheological analysis was performed to evaluate the *in situ* gelling behaviour of gellan in contact with SLF and in presence of different concentration (0.5%, 1%, 2%, 5% and 10%) of HβCD (Figure 6.9). A sample of 0.4% gellan (w/v) was used as a control and G′ and G″ was measured as a function of time using the rheo-dissolution cell according to the experimental setup in 5.3.6. On exposure to SLF, 0.4% gellan showed rapid onset of gelation within first 2 min (Figure 6.10A). The G′ value at the end of the test (after 30 min) was ~ 320 Pa and G′ was significantly dominant over G″ throughout the test. Addition of increasing concentration of HβCD (0.5, 1, 2, 5 and 10%) to the gellan solution did not alter the rheological characteristics of gellan in terms of onset of gelation and average final gel strength of 312 Pa ± 56.89 indicated an absence of physical interactions between gellan and HβCD.

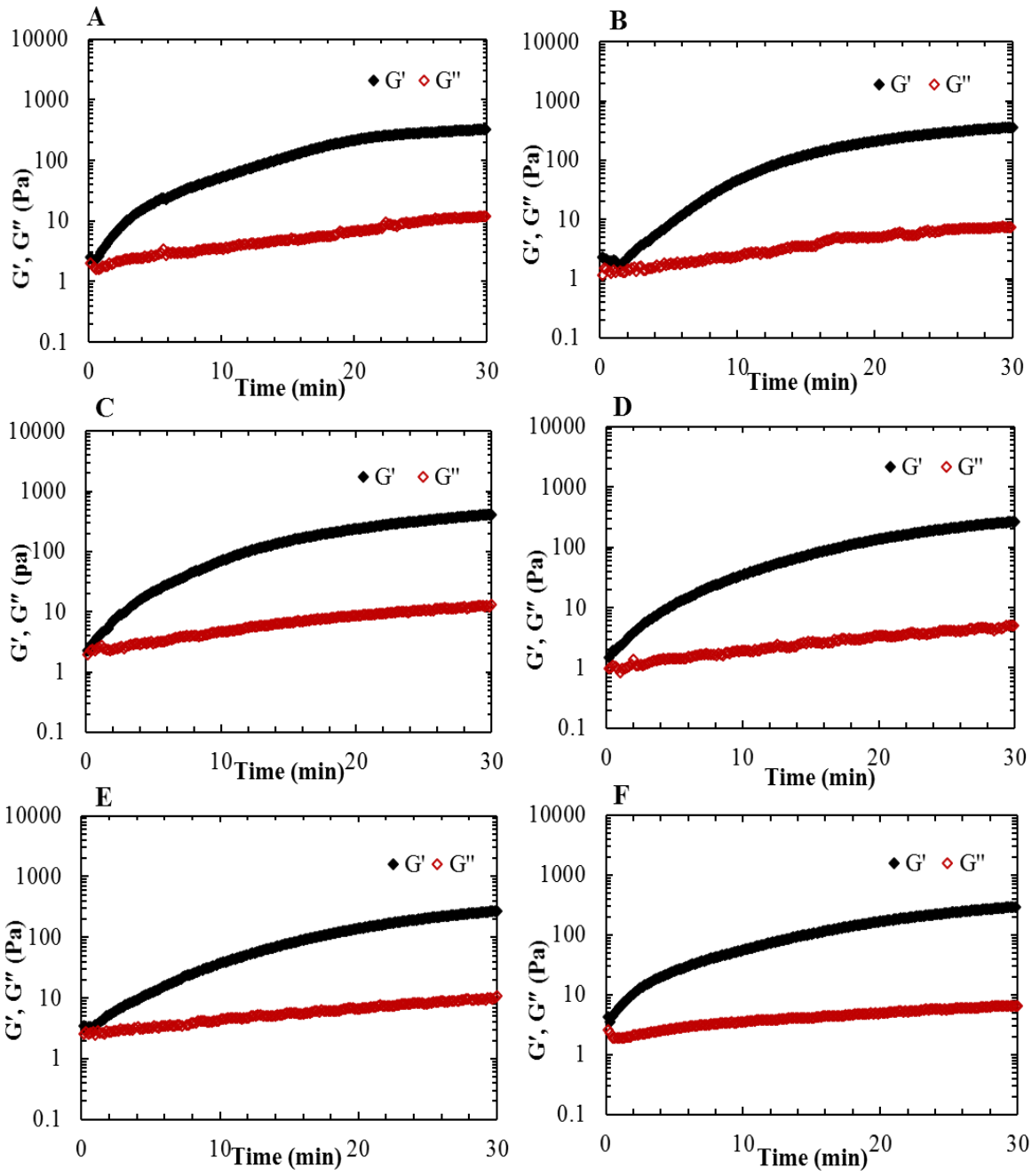

Figure 6.10: ***In situ*** **gelation of 0.4% gellan showing G′ and G" on exposure to SLF (A) 0.4% gellan only and in presence of (B) 0.5% (C) 1% (D) 2 % (E) 5% and (F) 10% HβCD performed at 0.5% strain, 1 rad/s frequency and 25ºC**

6.5.4 Confirmation of Complexation by DSC

Thermal analysis was conducted to confirm the complexation of FBP- HβCD with gellan (Figure 6.11). Pure FBP showed a single and sharp endothermic peak at 117.28°C (figure 6.11A) (enthalpy 48.21j/g) and no melting transitions were observed for gellan (Figure 6.11C) and HβCD (Figure 6.11B) as expected. The well recognized melting transition of FBP appeared in the physical blends of FBP- HβCD (Figure 6.11D) and FBP- HβCD with gellan (Figure 6.11E).

Melting endotherms were absent in the freeze-dried samples (Figure 6.11F and G). It has been reported that pure FBP is crystalline in nature (Abdel-Aziz et al., 2012) as shown in figure 6.11A and there is no evidence of any crystallisable material in the complex. However, absence of any glass transition exothermic peaks in the freeze dried samples (Figure 6.11F and G) confirms that the absence of melting transition of FBP is due to the formation of an inclusion complex and not due to transforming into the amorphous solid after freeze drying.

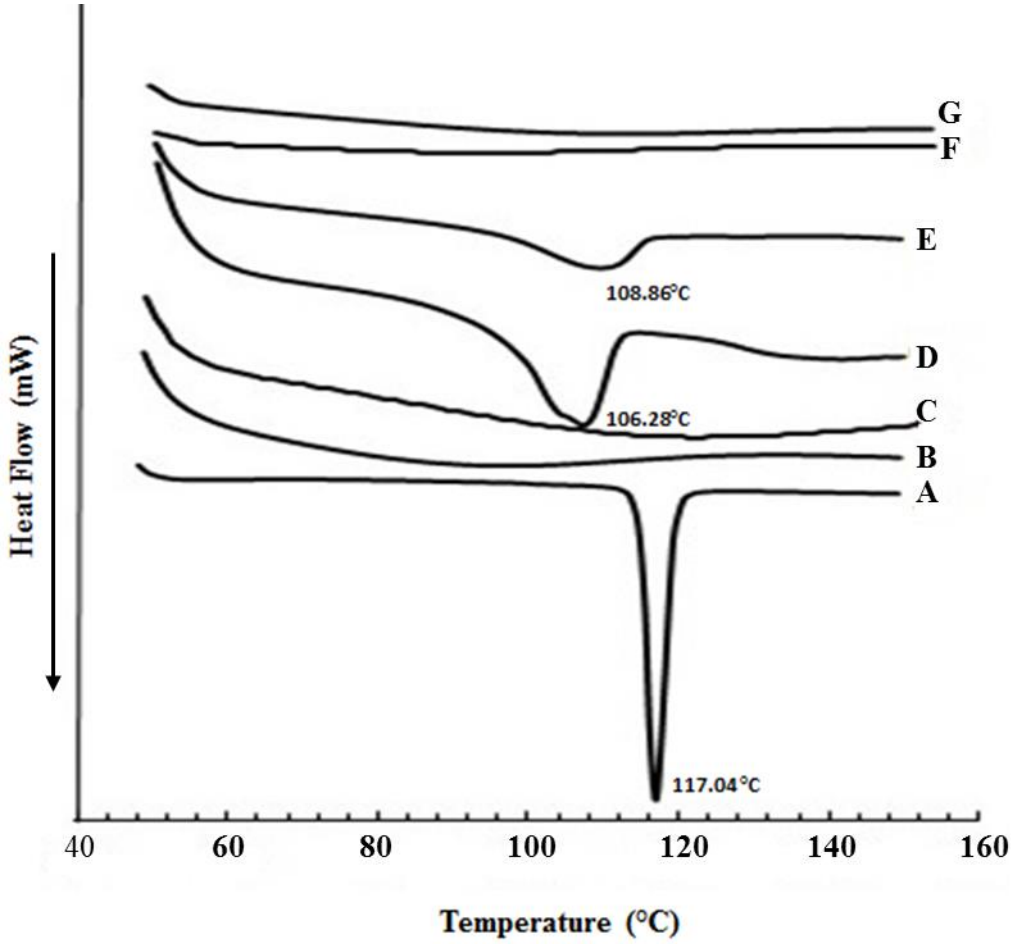

Figure 6.11: DSC thermogram of (A) FBP (B) HßCD (C) gellan (D) physical mix of FBP and HßCD (E) physical mix of FBP, HßCD and gellan (F) freeze dried formulation of FBP and HßCD (G) freeze fried formulation of FBP, HßCD and gellan

6.5.5 Simultaneous Determination of Rheology and Dissolution of the Drug (Rheo-Dissolution Study)

Once the formulations of FBP-HβCD and gellan were exposed to SLF, gelation occurred. A rapid increase of G′ and G″ was observed over first 10 min of the exposure. The modulus reached a steady state once gelation was complete and G′ remained higher than G″ throughout the remainder of test in both formulations (Figure 6.12A and B). The release data for FBP indicated initial release with 26% (± 5.64) FBP released over the first 60 min for the formulation containing 10% HβCD.

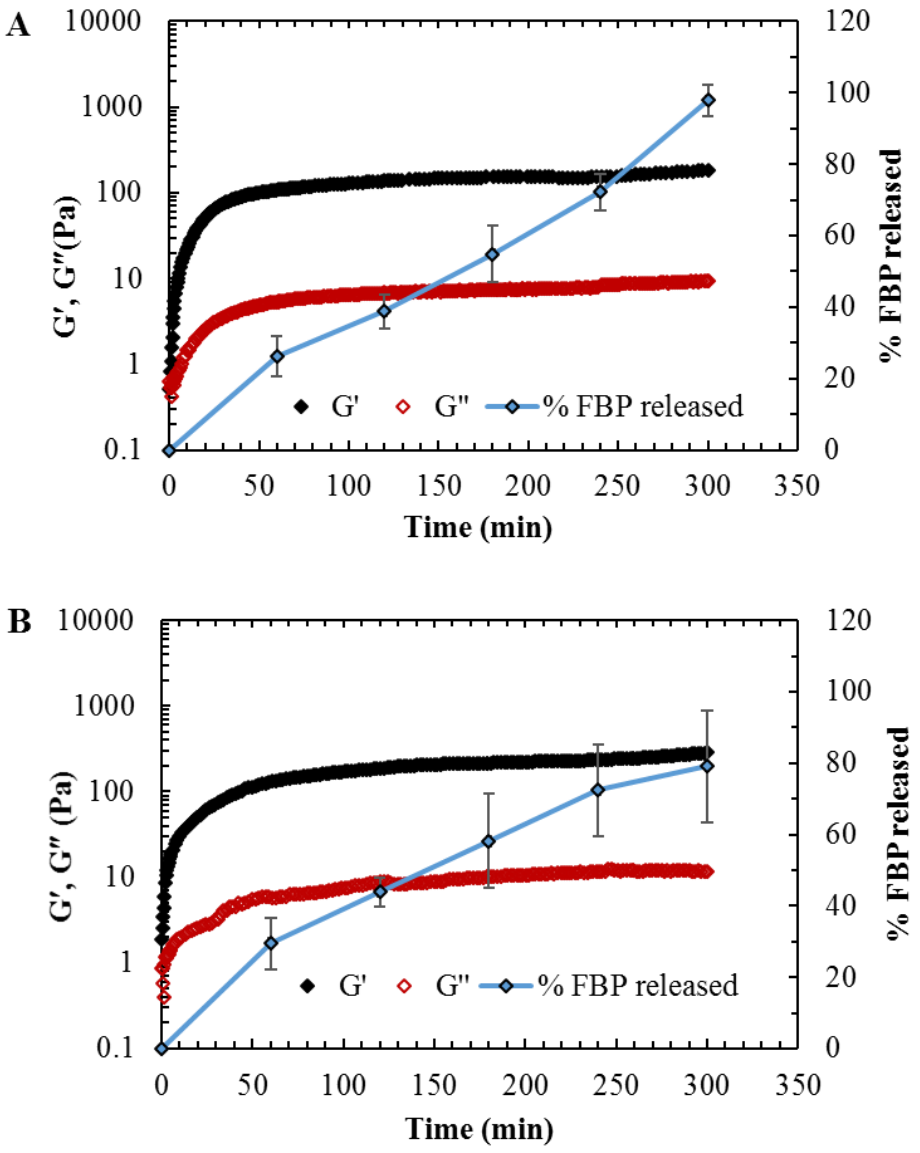

Figure 6.12: Simultaneous determination of rheological changes (G′ and G") and drug release study of the formulations containing 0.029% FBP, 0.4% gellan and (A) 10% HβCD (B) 20% HβCD performed at 0.5% strain, 1 rad/s frequency and 25ºC

The release of FBP followed a similar trend even after complete gelation and 97 % (± 4.52) FBP was released at 300 min (Figure 6.12A). In comparison, the release from the 20% HβCD formulation released much less at 300 min (79.11 ± 15.75%) (Figure 6.12B) although the initial release was almost similar (29.51 ± 7.22%) to the formulation containing 10% HβCD (26.00 ± 5.64%) (Figure 6.12A).

6.5.6 Development of Phenol-Sulphuric Acid (PSA) Method for Carbohydrate Analysis

A calibration curve was generated for the PSA assay to determine total carbohydrate in the sample. Five different standards were prepared from the stock solution ranging from 10 to 100 µg/ml and were measure spectrophotometrically at 490 nm wavelength. The required amount of 5% phenol solution and concentrated sulphuric acid were added to the standards before the measurement.

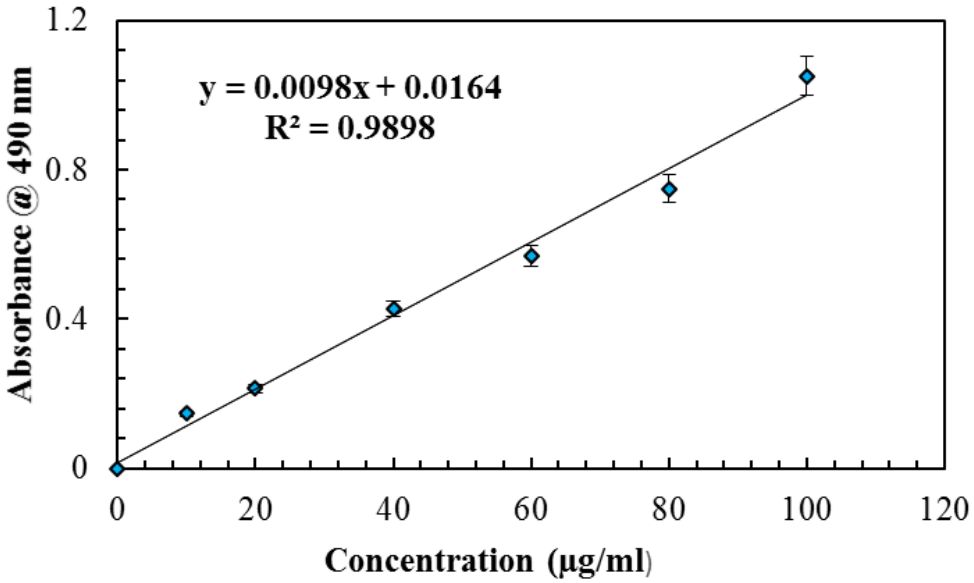

Figure 6.13: Calibration curve of D-glucose measured at 490 nm. All data represent mean ± SD (n=3)

All the absorbance measurements were taken in triplicate. The mean absorbances of the standards were then plotted against the respective concentration to generate a calibration curve (Figure 6.13). Table 6.5 shows the evaluation data of UV spectroscopic method for the determination of carbohydrate measured at a wavelength of 490 nm.

Table 6.5: Evaluation data of UV spectroscopic method for PSA assay

Range(µg/ml)	10 to 100
Regression equation	y= 0.0098x+0.0164
Correlation Coefficient	0.99
LOD (µg/ml)	1.05
LOQ (µg/ml)	3.29
Accuracy and Precision	RSD < 2%

6.5.7 HβCD Dissolution Studies

Release of HβCD from the *in situ* gel forming formulation containing varying concentration of HβCD (10% and 20%) was quantified using PSA assay method (Figure 6.14). Rheological analysis showed a sharp increase of the moduli values on exposure to SLF. After complete gelation, both moduli reached a steady state and remained same until the end of the experiments. G′ was visibly dominant over G″ for both formulations throughout the experiments (Figure 6.14A and B). The initial release of HβCD from the formulation containing 10% HβCD was 430.32 mg/ml (± 27.38) which increased gradually and reached 859.04 (± 27.19) mg/ml by the end of the test (300 min) (Figure 6.14A).

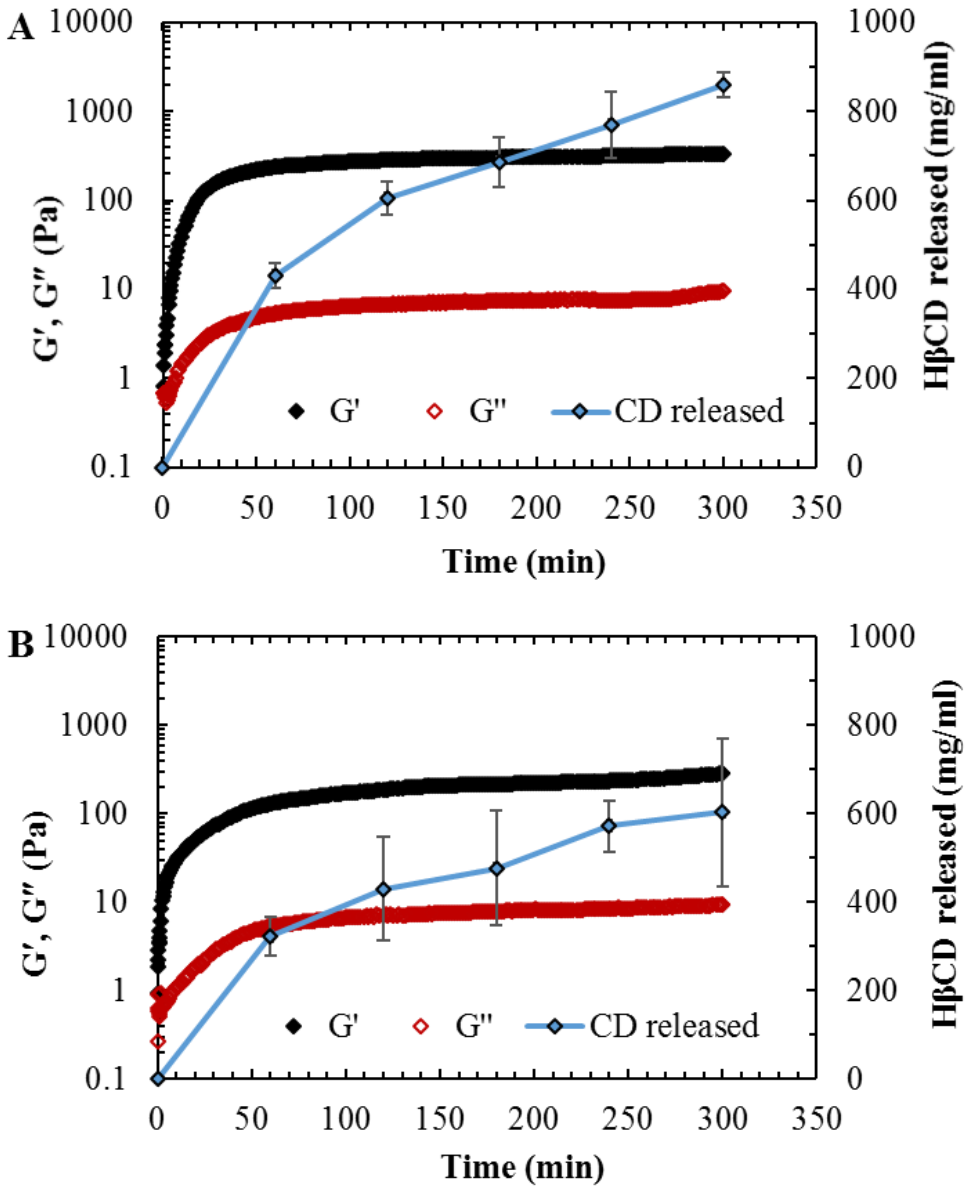

Figure 6.14: Simultaneous determination of rheological changes (G′ and G") and HβCD release study of the formulations containing 0.029% FBP, 0.4% gellan and (A) 10% HβCD (B) 20% HβCD performed at 0.5% strain, 1 rad/s frequency and 25ºC

The release of HβCD from the formulation containing 20% HβCD (Figure 6.14B) showed initial burst release (322.73 mg/ml ± 44.90) at 60 min which increased to 603.18 mg/ml (± 166.63) HβCD release at the end of the test (300 min).

6.5.8 Gellan Dissolution Studies

A blank rheo-dissolution analysis was also performed with 0.4% gellan. The samples were analysed using PSA assay to examine the presence of gellan in the withdrawn sample (Figure 6.15). This experiment was conducted to evaluate potential interference of gellan in the HβCD release data.

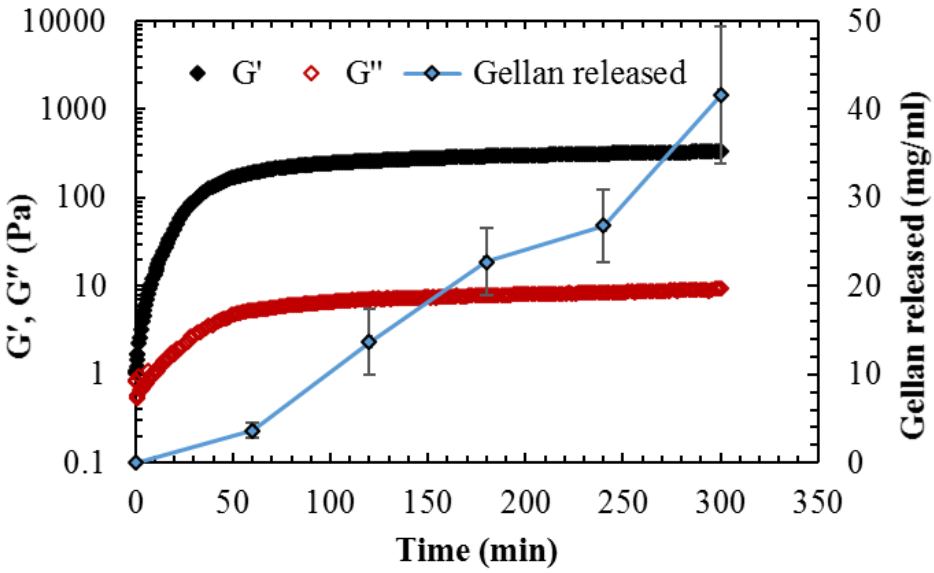

Figure 6.15: Simultaneous determination of rheological changes (G′ and G") and gellan release from the formulation containing 0.4% gellan performed at 0.5% strain, 1 rad/s frequency and 25ºC

The modulus raised rapidly upon exposure to SLF as expected and maintained a steady state after complete gelation. The release of gellan from the formulation was low throughout the experiment. Only 3.64 mg/ml (±0.88) of gellan was detected at 60 min which increased to only 41.61 ± 7.73 mg/ml at 300 min.

6.5.9 *Ex-vivo* Permeation Studies Using Porcine Cornea

The *ex-vivo* permeation studies of the formulation containing 10% HβCD and Ocufen® highlighted significantly ($p < 0.05$) higher percentage of permeation of FBP from the formulation containing 10% HβCD and 0.4% gellan compared to FBP sodium of Ocufen®. Permeation of FBP was 17.57% (± 4.93) at 60 min while 11.60% (± 1.17) of FBP sodium permeated through the porcine cornea in the same time. Permeation of FBP and FBP sodium increased gradually and at 300 min, 55.94 ± 7.85 % of FBP permeated whereas permeation of FBP sodium was only 37.35 ± 4.15 %.

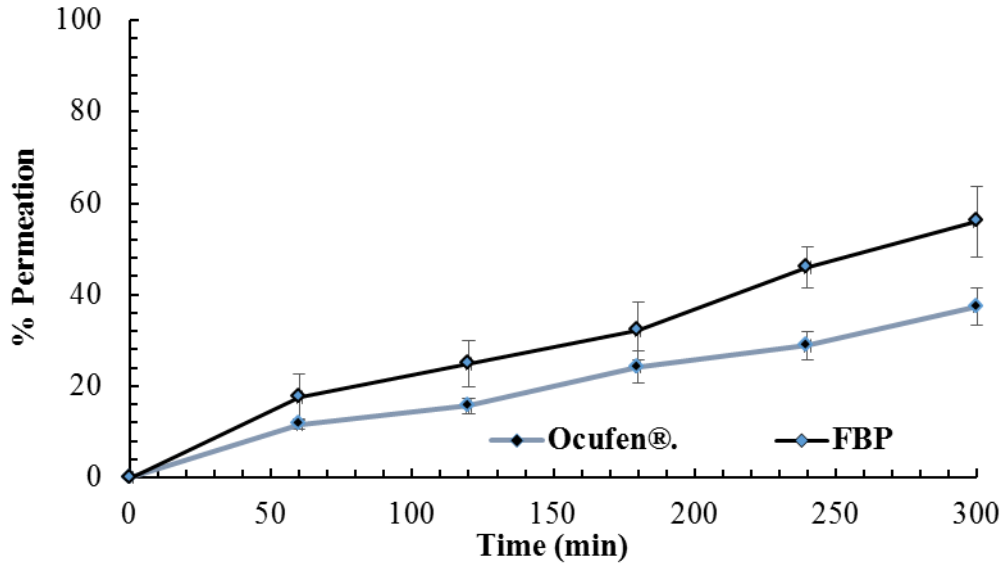

Figure 6.16: Percentage of FBP permeated from the formulations containing 0.029% FBP with 10% HβCD and 0.4% gellan compared with the commercial product Ocufen® containing 0.03% FBP sodium (n=3)

6.6 Discussion

The concentration of CD used is 10% to 30% in the majority of CD based commercialized eye drops and eye drop formulations which have been used for clinical evaluation (Kearse et al., 2001; Okamoto et al., 2010; Tanito et al., 2011; Loftsson et al., 2012; Mohamed-Ahmed et al., 2017). In the present study, 10% and 20% HβCD were selected as

concentrations to be used in the *in situ* gelling formulations of FBP and gellan. Although the phase solubility studies confirmed the solubilisation of 0.029% w/v of FBP by the addition of 0.5% to 20% HβCD (Figure 6.9), 10% and 20% were selected based on the time required for the solubilisation to take place.

Rheological behaviour of *in situ* gelling polymers is an important factor when designing a successful *in situ* gel forming drug delivery systems. Gellan was chosen as an *in situ* gelling polymer because of its ability to form strong and clear gels on exposure to physiological ion concentrations. (Robinson et al., 1991; Hägerström, 2003). Rheological analysis of 0.4% gellan alone and with HβCD was performed to observe any changes in gelation behaviour of gellan influenced by HβCD. It was clear from the data that addition of increasing concentration of HβCD (0.5, 1, 2, 5 and 10%) did not alter the rheological characteristics of gellan in terms of onset of gelation and final gel strength (Figure 6.10).

When the formulations were subjected to thermal analysis, the well-recognized melting transition of FBP in the physical blends (without freeze drying) indicated incomplete complexation by HβCD (Figure 6.11). Melting endotherms however, were completely absent from the freeze dried samples and it has been discussed previously (6.5.4) that FBP is crystalline in nature, so there was less possibility that melting transitions were absent due to the state of the drug (amorphous). However, the absence of these peaks indicated complete inclusion complexation of FBP-HβCD (Felton et al., 2014). The appearance of the melting endotherm of FBP in the physical mix with HβCD and gellan; and the absence of the melting endotherm in the freeze dried complex containing gellan indicated that gellan did not interfere with the complex formation.

Simultaneous determination of rheology and drug dissolution was conducted for the formulations containing 10% and 20% HβCD (Figure 6.12). Both formulations exhibited

similar rheological behaviour upon exposure to SLF. Release of FBP from the *in situ* gel is thought to be controlled by two parallel mechanisms. FBP- HβCD complex diffused through the gellan gel and then FBP dissociated from the complex to dissolve into the medium (Figure 6.17). The amount of drug dissolved depends on the concentration of HβCD. The percentage of dissolved FBP was greater on the terminal point when there was 10% HβCD, which was due to increased amount of free drug in the formulation.

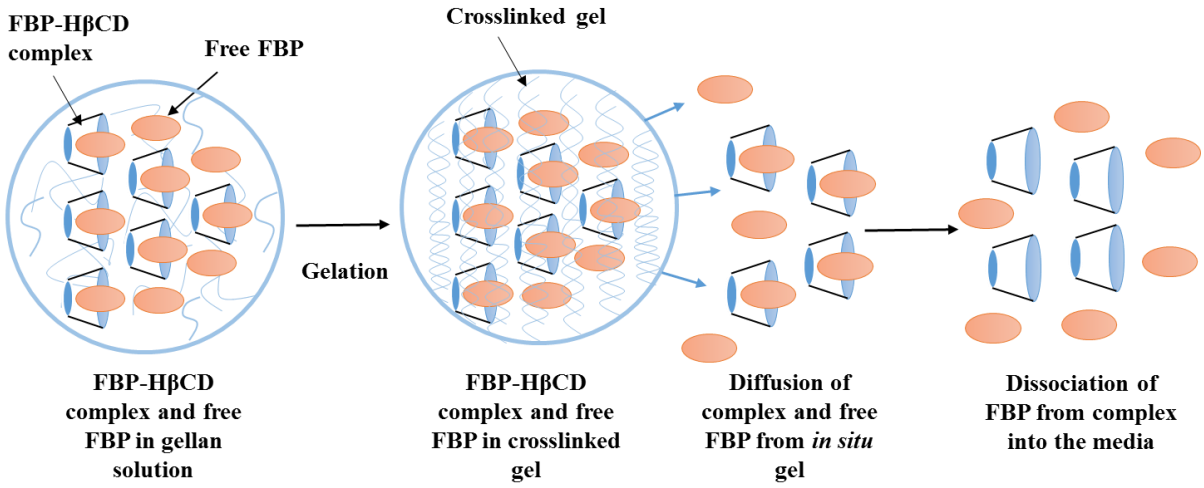

Figure 6.17: Schematic representation of diffusion of FBP- HβCD complex through the gel and dissociation of FBP from the complex

It is thought that the surface of the gel was saturated with drug and there was an equilibrium between free drug and bound drug. The unbound FBP diffused through the gel along with the complex. So the free FBP and the dissociated FBP resulted in 97% release in 300 min. The release of FBP from the formulations containing 10% and 20% HβCD was not significantly different ($p > 0.05$). However, the lower release (~79%) observed at 300 min for the formulation containing 20% HβCD compared with the formulation containing 10% HβCD (~97%) was probably due to saturation of excess HβCD at the surface of the gel and absence of unbound FBP.

The PSA analysis showed significantly ($p < 0.05$) higher release of HβCD from the formulation containing 10% (Figure 6.14A) compared to the formulation containing 20% HβCD (Figure 6.14B). This can be explained by the tendency of CDs and their complexes to self-associate and form aggregates in aqueous solutions. CDs self-assemble and form small clusters that aggregate again and form larger clusters (Figure 6.18). The aggregates usually have a diameters between 20 to 200 nm and the size of the aggregates increase with increasing the concentrations of CDs (Loftsson et al., 2004). It has been reported that formation of the largest aggregates can reach up to several micrometres in diameter and are observed in βCDs (Messner et al., 2010). Intermolecular hydrogen bonding between the OH groups of CDs and surrounding water molecules is the driving force for assembly and further aggregation of the molecules. However, there is a possibility that larger CD aggregates formed at high concentration of HβCD (20%) obstructed diffusion through the gellan and resulted in reduced HβCD release into the medium. A blank rheo-dissolution analysis performed with 0.4% gellan (Figure 6.15) suggested a negligible amount of gellan release (41.61 ± 7.73 mg/ml) into the medium which can be an indication of gellan not interfering the HβCD release data.

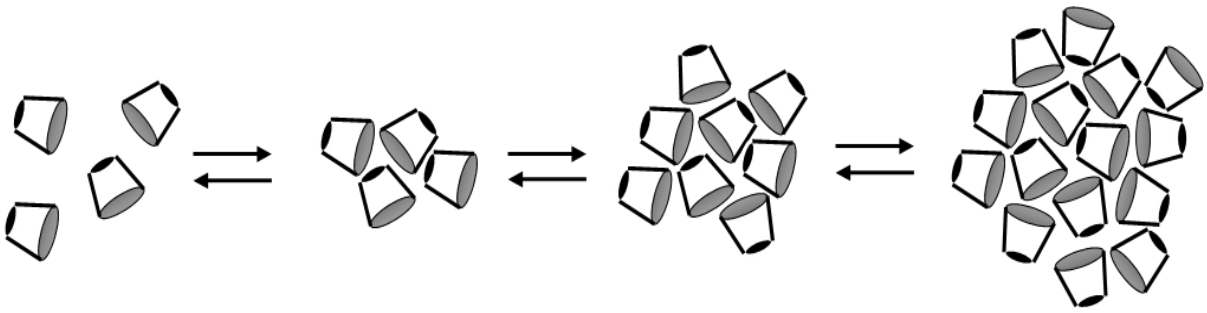

Figure 6.18: Schematic presentation of self-assembling of CD molecules to form small clusters that associate to create larger aggregates

The permeation study (Figure 6.16) highlighted that the percentage of FBP permeated through the porcine cornea was significantly ($p < 0.05$) higher in the case of the formulation containing HβCD and gellan compared with that of Ocufen®. This can be explained by the unique ability of CDs' to enhance drug permeability through biological membranes. They act as true carriers by keeping the poorly soluble hydrophobic drug molecule inside their cavity and delivering them to the surface of biological membranes (Loftsson, 1998). The FBP- HβCD inclusion complex diffused through the *in situ* gel to the surface of the cornea and FBP dissociated from the complex to permeate through the cornea.

It is well known that free acid drug can permeate faster than the equivalent salt forms (Minghetti et al., 2007) which can be explained by changing the degree of ionization. When drug and solution has the same pKa, 50% of the drug exists ionized. The state of ionization changes as the pH of the solution changes. As the pH of the solution containing FBP sodium (Ocufen®) was 6.68, which was higher than pKa of FBP (4.22), more than 99% FBP was expected to be ionized as it is an acidic drug. Therefore, the compounds became less able to pass through the membrane due to being less lipophilic compared with the unionized compounds when the pH was close to the pKa (Hale and Abbey, 2017). Furthermore, the buffering action of lacrimal fluid *in vivo* depends on its chemical buffering capacity which is 16.61 mEq/pH/L. So it can be assumed that 25-30 µl (approximate instillation into the eye) formulation of pH 4.32 will not interfere with the physiological pH of 30 µl (maximum volume of tear fluid in cul-de-sac) lacrimal fluid and the *in situ* gelling formulation of FBP-HβCD inclusion complex will not cause any irritation in the eye surface due to any pH disturbance.

6.7 Conclusion

This study has demonstrated a method of developing an *in situ* gel forming ophthalmic formulation of a poorly soluble drug (FBP) by forming inclusion complex with HβCD. Formation of the inclusion complex enhanced the solubility of FBP and allowed addition of gellan in order to form *in situ* gelling delivery system. Data obtained using rheo-dissolution revealed that the formulation containing 10% HβCD released 97% FBP in 5 hours. Comparative permeation studies indicated improved permeation of FBP as a complex compared with the sodium salt of FBP. All the data obtained indicated that gellan did not interfere with the complex formation and the complex diffused successfully through the *in situ* gel. Thus, this particular poorly soluble drug can be included without the salt form in the *in situ* gelling system by forming an inclusion complex with HβCD whilst also increasing corneal permeation.

Chapter 7: Conclusions and Future Recommendations

The purpose of this research was to develop a novel technique to simultaneously analyse the rheological changes and dissolution of drug from *in situ* gelling formulations on exposure to the physiological fluids and gain a better understanding of *in situ* gelling drug delivery systems. A rheo-dissolution cell was developed to replace the lower plate of conventional rheometer that would enable *in situ* gelling formulations to be exposed to physiological fluids during rheological measurements. This cell was connected to a peristaltic pump to allow the physiological fluid to flow beneath the gelling sample and contained a sampling port so that samples of the fluid could be analysed during rheological measurements.

An *in situ* gel forming ophthalmic formulation of gellan and TM was used to evaluate the rheo-dissolution cell where SLF was used as crosslinking ion solution. The technique was also investigated for an oral formulation of alginate and MNZ to assess the ability of the cell to perform rheo-dissolution when changing the chemical environment (changed pH). Finally, an *in situ* gelling ophthalmic formulation of a poorly soluble drug was prepared by CD complex formation with a focus on permeability enhancement following assessment using rheo-dissolution.

The following sections provide a summary of each experimental study.

7.1 Development and Rheological Evaluation of an *In Situ* Gel Forming Ophthalmic Formulation

Chapter 4 highlighted the development and rheological analysis of an *in situ* gelling ophthalmic formulation which was prepared based on the marketed product Timoptol LA®. Oscillatory rheological analysis of gellan (0.4%) alone and gellan in SLF (pH 7.5) were

performed to evaluate the impact of ions on the gelation property (in terms of G′ and G″) of gellan. Strain sweeps, frequency sweeps and temperature sweeps showed the evidence of strong gel (G′ > G″) formation. Oscillatory rheological analysis was also performed for the formulation of gellan-TM (pH 4.5) which highlighted an interaction between gellan and TM by increasing the firmness of gel even without the presence of ions. This could be explained by the positively charged amino group of TM which interacted electrostatically with anionic gellan to form strong gel. In addition, a drug release study was performed using the rheo-dissolution cell which acted as a modified dissolution apparatus. The release study revealed that only 48 % TM was released from the formulation after 5 hours and the release curve had reached a plateau. This further supported the explanation of electrostatic interactions between the gellan and the TM at pH (4.5). Rheological measurements and a release study was also performed at pH 10 (when the amino group was unionized) which confirmed the interaction further by forming a relatively weak gel and releasing increased amount of TM (57 % at 5 hour). In this case, there was some evidence of gelation occurring, probably due to the fact that at pH 10 the TM still retains a small amount of charge. Replacing gellan with non-ionic polysaccharide agarose provided additional support to the results by releasing 67 % TM in 5 hours. Previous reports on incomplete release of charged drugs in presence of oppositely charged molecules also supported the finding of the existence of electrostatic interaction. However, there are also potential hydrophobic interactions and hydrogen bonding between gellan and TM which could play further roles in the incomplete release of TM. So, besides revealing the rheological behaviour of gellan in presence of ions and release of drug from the *in situ* gelling formulation of gellan, the study also showed the importance of considering drug-polymer interaction when designing a formulation with charged polysaccharides and oppositely charged drug.

7.2 Development of a Model for Simultaneous Measurement of Rheology and Dissolution for *In Situ* Gel Forming Drug Delivery Systems

Chapter 5 focussed on developing an *in vitro* model using the rheo-dissolution cell which allowed rheological measurements during gelation and sampling of release media at the same time to enable the analysis of drug release. The *in vitro* model was developed using an experimental setup where the rheo-dissolution cell filled with crosslinking ion solutions acted as the lower plate of a rheometer and was attached to a circulating peristaltic pump to facilitate sampling. Ophthalmic (gellan and TM) and oral (sodium alginate and MNZ) *in situ* gelling formulations were used to demonstrate the power of this novel technique. Rheo-dissolution experiments of *in situ* gel forming ophthalmic formulations on exposure to the SLF (pH 7.5) showed rapid release of TM at early structuring phase of gelation and release slowed down when gel was completely structured. This phenomenon was observed in the formulations containing low concentrations (0.3% and 0.4%) of gellan, whereas in the formulations containing higher gellan concentrations (0.6% and 0.8%), the release was slow even at the beginning of the test especially when 0.8% gellan was used in the formulation. This can be explained by formation of strong gel at the onset of test because of high gellan concentration. However, beside gel strength, the electrostatic interaction between gellan and TM was thought to be another factor to control the release of TM from *in situ* gel.

Rheo-dissolution studies were also performed for *in situ* gelling oral formulations of sodium alginate and MNZ where the dissolution media was SGF. The alginate formed a strong gel once exposed to SGF (pH 1.2) and slow release (53 % in 7 hour) of MNZ was observed when the moduli plateaued. To demonstrate the feasibility of changing the chemical environment during the course of an experiment, the pH of the media was raised to 8 which caused the dissolution of the alginate gel indicated by falling moduli which interestingly coincided with a dramatic increase of MNZ release (96 % released in 7 hour). Solubility

tests of MNZ performed at pH 1.2 and 8 confirmed that the rapid release of MNZ was a result of gel degradation rather than a solubility effect.

7.3 Formulating an *In Situ* Gelling System of a Poorly Soluble Drug for Optimizing Ophthalmic Delivery

This chapter focused on increasing the permeability of a poorly soluble drug by preparing a drug-CD inclusion complex and incorporating it into an *in situ* gelling polymer solution. This work highlighted the difficulties of adding a salt form of a poorly soluble drug in an *in situ* gelling formulation when ionotropically gelling polymers such as gellan are used. FBP was used as a poorly soluble drug in this work, which is commercially available as the sodium salt form in Ocufen® eye drops (0.03% FBP sodium). To avoid gelation in the presence of salt before administration and to increase the solubility of the FBP (0.029%), FBP-HβCD inclusion complex was prepared by adding the drug to 10% and 20% HβCD solutions. These solutions were then added to a gellan (0.4%) solution to formulate an *in situ* gelling ophthalmic formulations (pH 4.30-4.32). Thermal analysis confirmed the FBP-HβCD complexation formation by showing the disappearance of melting transition of FBP in freeze-dried formulations. Rheo-dissolution experiments showed rapid onset of gelation followed by strong gel formation when exposed to SLF. The release of FBP was higher (97 % at 300 min) for the formulation containing 10% HBCD compared to the formulation containing 20% HBCD (79 % at 300 min). Diffusion of the FBP-HβCD complex through the *in situ* gel and dissociation of FBP from the complex to release into the medium were thought to be the parallel mechanisms of FBP release. Reduced release of FBP from the formulation containing 20% HβCD could be a result of absence of any unbound FBP and saturation caused by excess HβCD concentration. The PSA assay revealed a decreased release of HβCD from the formulation containing 20% HβCD (603 mg/ml) compared with

the amount released from the formulation containing 10% HβCD (859 mg/ml) which can be explained by the tendency of HβCD to aggregate at high concentration (20%) disrupting HβCD release. The permeation study showed the ability of CDs' to increase the permeability through a corneal model, with 56 % of FBP permeated at 300 min when the formulation contained CD, while only 37 % of FBP sodium permeated in the same amount of time. This can be explained by the salt form of FBP having less ability to pass through a lipophilic membrane compared with the free acid (Hale and Abbey, 2017). The pH (6.68) of the solution containing FBP sodium was higher than the pK_a of FBP (4.22) which caused more than 99% of FBP to become ionized and ionized compounds are less lipophilic to pass through the membrane.

7.4 Future Work

This work has demonstrated a novel technique to simultaneously measure rheology and drug release of polymeric *in situ* gelling systems on exposure to different physiological fluids. There are several potential areas in this work where future works could be extended. An interesting area of this thesis is the electrostatic interaction between negatively charged gellan and positively charged TM which had impact on release of TM. However, there could be also presence of hydrogen bonding and hydrophobic interactions, which further influenced the incomplete release behaviour of TM. To explore this further, future work could be performed on analysing the interaction in depth by using calorimetric studies, which will show the melting transition of gellan in presence and absence of TM in both the ionized and unionized states of the amino group of TM. The gellan and TM interactions could also be explored using pulsed-gradient spin-echo NMR where a stimulated echo sequence is used to analyse the self-diffusion of TM in presence and absence of gellan (Pygall et al., 2011). Furthermore, different charged polysaccharides (for example, sodium

alginate, κ and ι-carrageenan) could be investigated with TM to evaluate how the drug polymer interaction influences the rheological behaviour and release performance.

This work also showed the potential of the novel technique to measure gelation and drug release simultaneously on exposure to different physiological fluids. This technique allows the user to change the chemical environment during the course of an experiment and has the ability to perform rheo-dissolution in the changed environment. Changing of the chemical environment during experiments will no doubt add a new dimension for many industrial applications where there is a need to understand or develop gels that form or degrade in response to changing chemical environments. For future work, it would be interesting to investigate other physiological fluids as crosslinking media (for example; lung fluid, saliva) to perform rheo-dissolution studies with a range of *in situ* gelling formulations. Also, the design of the rheo-dissolution cell could be modified in a few ways, such as attaching the mesh with a magnetic wire to the surface of the cell to make the mesh more secure, connecting to a water jacket heater to control the temperature during the experiment. This system could be developed further by connecting to a UV spectrophotometer in a similar manner to commercially available semi-automated dissolution testing apparatus.

This work has also demonstrated a method of increasing the corneal permeability of a poorly soluble drug by formulating an *in situ* gelling ophthalmic formulation of drug-CD complex. This work could be expanded to investigate other poorly soluble drug-CD complexes (such as, ketoprofen, naproxen and ibuprofen) to develop other *in situ* gelling ophthalmic formulations. Additionally, another challenging and interesting work could be done by attaching the porcine cornea to the surface of the mesh of the rheo-dissolution cell so that the formulation could be added on the top of cornea before starting the rheological measurement. This would allow monitoring real time gelation of the formulations on contact with a cornea and sampling of the permeated drug into the media during rheological analysis.

This would give a more realistic insight into the behaviour of *in situ* gelling ophthalmic formulations and provide an additional tool for utilization in the development of new *in situ* gelling delivery systems. Furthermore, this technique could be used beyond pharmaceutical industries, wherever there is a need for understanding permeability through biological tissues, for example in biomedical sciences and diagnostics.

References

Abdel-Aziz, A., Al-Badr, A. and Hafez, G. (2012) '89- Flurbiprofen, Comprehensive Profile.' *In Profiles of drug substances, excipients, and related methodology*. Elsevier, pp. 81–113.

Achouri, D., Alhanout, K., Piccerelle, P. and Andrieu, V. (2013) 'Recent advances in ocular drug delivery.' *Drug Development and Industrial Pharmacy* pp. 1599–1617.

Adams, M. E., Buckley, D. J. and Colborn, R. E. (1993) *Acrylonitrile-butadiene-styrene Polymers*. Shropshire.

Addo, E., Bamiro, O. A. and Siwale, R. (2016) 'Anatomy of the eye and common diseases affecting the eye.' *In Ocular Drug Delivery: Advances, Challenges and Applications*, pp. 11–25.

Adebisi, A. O. (2014) *Design of gastro-retentive systems for the eradication of helicobacter-pylori infections in the treatment of peptic ulcer*. University of Huddersfield.

Adebisi, A. O. and Conway, B. R. (2014) 'Preparation and characterisation of gastroretentive alginate beads for targeting H. pylori.' *Journal of Microencapsulation*, 31(1) pp. 58–67.

Agnihotri, S. A., Jawalkar, S. S. and Aminabhavi, T. M. (2006) 'Controlled release of cephalexin through gellan gum beads: Effect of formulation parameters on entrapment efficiency, size, and drug release.' *European Journal of Pharmaceutics and Biopharmaceutics*, 63(3) pp. 249–261.

Al-Fariss, T. F. and Al-Zahranl, S. M. (1993) 'Rheological Behaviour of Some Dilute Polymer Solutions.' *Eng. Sci*, 5 pp. 95–109.

Almeida, H., Amaral, M. H., Lobão, P. and Lobo, J. M. S. (2014) 'In situ gelling systems: A strategy to improve the bioavailability of ophthalmic pharmaceutical formulations.' *Drug Discovery Today* pp. 400–412.

De Almeida, P. D. V., Grégio, A. M. T., Machado, M. Â. N., De Lima, A. A. S. and Azevedo, L. R. (2008) 'Saliva composition and functions: A comprehensive review.' *Journal of Contemporary Dental Practice* pp. 72–80.

Ana, G., Natasa, D., Rok, K., Sasa, N. and Gregor, M. (2016) 'Gellan gum soft construct for possible applications in skin tissue engineering.' *Frontiers in Bioengineering and Biotechnology*, 4.

Andrews, G. P., Laverty, T. P. and Jones, D. S. (2009) 'Mucoadhesive polymeric platforms for controlled drug delivery.' *European Journal of Pharmaceutics and Biopharmaceutics* pp. 505–518.

Anumolu, S. N. S., Singh, Y., Gao, D., Stein, S. and Sinko, P. J. (2009) 'Design and evaluation of novel fast forming pilocarpine-loaded ocular hydrogels for sustained pharmacological response.' *Journal of Controlled Release*, 137(2) pp. 152–159.

Aravamudhan, A., Ramos, D. M., Nada, A. A. and Kumbar, S. G. (2014) 'Polysaccharides and Their Derivatives. Chapter 4: Natural Polymers: Polysaccharides and Their Derivatives for Biomedical Applications.' *Natural and Synthetic Biomedical Polymers* pp. 67–89.

Aronson, J. N. (1983) 'The Henderson-Hasselbalch equation revisited.' *Biochemical Education*, 11(2) p. 68.

Ashford, M. (2007) 'Gastrointestinal tract: physiology and drug absorption.' *In* Aulton, M. E. (ed.) *Pharmaceutics: The Design and Manufacture of Medicines*. 3rd ed., New York: Edinburgh Churchill Livingstone, pp. 270–286.

Augustyn, A., Bauer, P., Duignan, B., Eldridge, A., Gregersen, E., Luebering, J. E., McKenna, A., Petruzzello, M., Rafferty, J. P., Ray, M., Rogers, K., Tikkanen, A., Wallenfeldt, J., Zeidan, A. and Zelazko, A. (2018) 'Mucous membrane.' *Encyclopædia Britannica*.

Aulton, M. (ed.) (2007) *Aulton's Pharmaceutics: The Design and Manufacture of Medicines*. *Pharmaceutics: The science of dosage form design*. 3rd ed., Elsvier.

Ayol, A., Dentel, S. K. and Filibeli, A. (2010) 'Rheological Characterization of Sludges during Belt Filtration Dewatering Using an Immobilization Cell.' *Journal of Environmental Engineering*, 136(9) pp. 992–999.

Bae, J. W. and Park, K. D. (2016) 'In Situ Crosslinked Hydrogels for Drug Delivery.' *In* Kang, L. and Majd, S. (eds) *Gels Handbook; Volume 3: Application of Hydrogels in Drug Delivery and Biosensing*. Singapore: World Scientific Publishing Co. Pte. Ltd., pp. 61–72.

Bain, M. K., Bhowmik, M., Ghosh, S. N. and Chattopadhyay, D. (2009) 'In situ fast gelling formulation of methyl cellulose for in vitro ophthalmic controlled delivery of ketorolac tromethamine.' *Journal of Applied Polymer Science*, 113(2) pp. 1241–1246.

Bajpai, M., Shukla, P. and Bajpai, S. K. (2016) 'Ca(II)+Ba(II) ions crosslinked alginate gels prepared by a novel diffusion through dialysis tube (DTDT) approach and preliminary BSA release study.' *Polymer Degradation and Stability*, 134 pp. 22–29.

Balasubramaniam, J., Kant, S. and Pandit, J. K. (2003) 'In vitro and in vivo evaluation of the Gelrite gellan gum-based ocular delivery system for indomethacin.' *Acta pharmaceutica (Zagreb, Croatia)*, 53(4) pp. 251–261.

Bansil, R. and Turner, B. S. (2006) 'Mucin structure, aggregation, physiological functions and biomedical applications.' *Current Opinion in Colloid and Interface Science* pp. 164–170.

Barnes, H. A. (2000) *A Handbook of Elementary Rheology*. 1st ed., Aberystwyth: Cambrian Printers.

Barnes, H. A., Hutton, J. E. and Walters, F. R. S. K. (1989) *An Introduction to Rheology*. Walters, K. (ed.). first, Amsterdam: Elsvier Science Publishers B.V.

Batchelor, H. K., Kendall, R., Desset-Brethes, S., Alex, R. and Ernest, T. B. (2013) 'Application of in vitro biopharmaceutical methods in development of immediate release oral dosage forms intended for paediatric patients.' *European Journal of Pharmaceutics and Biopharmaceutics* pp. 833–842.

Beneke, C. E., Viljoen, A. M. and Hamman, J. H. (2009) 'Polymeric plant-derived excipients in drug delivery.' *Molecules*, 14(7) pp. 2602–2620.

Bertrand, M. J. (1997) *Handbook of Instrumental Techniques for Analytical Chemistry*. Settle, F. A. (ed.). Prentice Hall: Upper Saddle River.

Bhal, S. (2007) *Log P — Making Sense of the Value*. Advanced Chemistry Development.

Bhandwalkar, M. J. and Avachat, A. M. (2012) 'Thermoreversible Nasal In situ Gel of Venlafaxine Hydrochloride: Formulation, Characterization, and Pharmacodynamic Evaluation.' *AAPS PharmSciTech*, 14(1) pp. 101–110.

Bonferoni, M. C., Chetoni, P., Giunchedi, P., Rossi, S., Ferrari, F., Burgalassi, S. and Caramella, C. (2004) 'Carrageenan-gelatin mucoadhesive systems for ion-exchange based ophthalmic delivery: In vitro and preliminary in vivo studies.' *European Journal of Pharmaceutics and Biopharmaceutics*, 57(3) pp. 465–472.

Borchard, W. (1998) 'Properties of thermoreversible gels.' *Beri. Bunsenges. Physi. Chem.*, 102(11) pp. 1580–1588.

Born, A. ., Tripathi, R. . and Tripathi, B. . (1997) *Wolff 's Anatomy of the Eye and Orbit*. 8th ed., London: Chapman & Hall Medical.

Bourlais, C. L., Acar, L., Zia, H., Sado, P. A., Needham, T. and Leverge, R. (1998) 'Ophthalmic drug delivery systems—Recent advances.' *Progress in Retinal and Eye Research*, 17(1) pp. 33–58.

Bowles, A., Keane, J., Ernest, T., Clapham, D. and Tuleu, C. (2010) 'Specific aspects of gastro-intestinal transit in children for drug delivery design.' *International Journal of Pharmaceutics* pp. 37–43.

Bradbeer, J. F., Hancocks, R., Spyropoulos, F. and Norton, I. T. (2014) 'Self-structuring foods based on acid-sensitive low and high acyl mixed gellan systems to impact on satiety.' *Food Hydrocolloids*, 35 pp. 522–530.

Brewster, M. E. and Loftsson, T. (2007) 'Cyclodextrins as pharmaceutical solubilizers.' *Advanced Drug Delivery Reviews* pp. 645–666.

Bromberg, L. E. and Barr, D. P. (2000) 'Self-association of mucin.' *Biomacromolecules*, 1(3) pp. 325–334.

Builders, P. F. and Attama, A. A. (2011) 'Functional Properties of Biopolymers fror Drug Delivery Applications.' *In* Johnson, B. M. and Berkel, Z. E. (eds) *Biodegradable Materials*. Nova Science Publishers, Inc.

Cao, S. lei, Ren, X. wei, Zhang, Q. zhi, Chen, E., Xu, F., Chen, J., Liu, L. C. and Jiang, X. guo (2009) 'In situ gel based on gellan gum as new carrier for nasal administration of mometasone furoate.' *International Journal of Pharmaceutics*, 365(1–2) pp. 109–115.

Cappello, B., Iervolino, M., Miro, A., Chetoni, P., Burgalassi, S. and Saettone, M. F. (2002) 'Formulation and preliminary in vivo testing of rufloxacin-cyclodextrin ophthalmic solutions.' *In Journal of Inclusion Phenomena*, pp. 173–176.

Caram-Lelham, N. and Sundelöf, L. O. (1996) 'The effect of hydrophobic character of drugs and 2 helix-coil transition of κ-carrageenan on the polyelectrolyte-drug interaction.' *Pharmaceutical Research*, 13(6) pp. 920–925.

Carlfors, J., Edsman, K., Petersson, R. and Jörnving, K. (1998) 'Rheological evaluation of Gelrite® in situ gels for ophthalmic use.' *European Journal of Pharmaceutical Sciences*, 6(2) pp. 113–119.

Chang, J. Y., Oh, Y. K., Choi, H. gon, Kim, Y. B. and Kim, C. K. (2002) 'Rheological evaluation of thermosensitive and mucoadhesive vaginal gels in physiological conditions.' *International Journal of Pharmaceutics*, 241(1) pp. 155–163.

Chen, Y. M. and Rodríguez-Hornedo, N. (2018) 'Cocrystals Mitigate Negative Effects of High pH on Solubility and Dissolution of a Basic Drug.' *Crystal Growth and Design*, 18(3) pp. 1358–1366.

Chevrel, M. C., Hoppe, S., Falk, L., Nadeìge, B., Chapron, D., Bourson, P. and Durand, A. (2012) 'Rheo-raman: A promising technique for in situ monitoring of polymerization reactions in solution.' *Industrial and Engineering Chemistry Research*, 51(49) pp. 16151–16156.

Chiang, W. and Tzeng, G. (1997) 'Effect of the compatibilizers on flame-retardant polycarbonate (PC)/acrylonitrile-butadiene-styrene (ABS) alloy.' *Journal of Applied Polymer Science*, 65 pp. 795–805.

Choonara, B. F., Choonara, Y. E., Kumar, P., Bijukumar, D., du Toit, L. C. and Pillay, V. (2014) 'A review of advanced oral drug delivery technologies facilitating the protection and absorption of protein and peptide molecules.' *Biotechnology Advances* pp. 1269–1282.

Cirri, M., Rangoni, C., Maestrelli, F., Corti, G. and Mura, P. (2005) 'Development of fast-dissolving tablets of flurbiprofen-cyclodextrin complexes.' *Drug Development and Industrial Pharmacy*, 31(7) pp. 697–707.

Clark, A. H. (2010) 'Structural and Mechanical Properties of Biopolymer Gels.' *In Food Polymers, Gels and Colloids*. Springer, Berlin, Heidelberg, pp. 322–338.

Clark, A. H. and Ross-Murphy, S. B. (2009) 'Biopolymer Network Assembly: Measurement and Theory.' *In* Kasapis, S., Norton, I. T., and Johan B. Ubbink (eds) *Modern Biopolymer Science; Bridging The Divide Between Fundamental Treatise And Industrial Application*. 1st ed., pp. 1–28.

Cohen, S., Lobel, E., Trevgoda, A. and Peled, Y. (1997) 'A novel *in situ*-forming ophthalmic drug delivery system from alginates undergoing gelation in the eye.' *Journal of Controlled Release*, 44(2–3) pp. 201–208.

Conway, B. R. (2005) 'Drug delivery strategies for the treatment of Helicobacter pylori infections.' *Current Pharmaceutical Design*, 11(6) pp. 775–790.

Coviello, T., Matricardi, P., Marianecci, C. and Alhaique, F. (2007) 'Polysaccharide hydrogels for modified release formulations.' *Journal of Controlled Release* pp. 5–24.

Cui, S. W. (2005) *Food Carbohydrates; Chemistry, Physical Properies and Applications*. *Food Carbohydrates*. Taylor & francis, FL.

Davies, N. M., Wang, G. and Tucker, I. G. (1997) 'Evaluation of a hydrocortisone/hydroxypropyl-β-cyclodextrin solution for ocular drug delivery.' *International Journal of Pharmaceutics*, 156(2) pp. 201–209.

Davis, S. S., Hardy, J. G. and Fara, J. W. (1986) 'Transit of pharmaceutical dosage forms through the small intestine.' *Gut*, 27(8) pp. 886–892.

Davson, H. (1984) *The Eye, Vol 1a*. 3rd ed., Orlando: Academic Press.

Delair, T. (2012) 'In situ forming polysaccharide-based 3D-hydrogels for cell delivery in regenerative medicine.' *Carbohydrate Polymers* pp. 1013–1019.

Dhaval, M., Devani, J., Parmar, R., Soniwala, M. M. and Chavda, J. (2020) 'Formulation, and optimization of microemulsion based sparfloxacin in-situ gel for ocular delivery: In vitro and ex vivo characterization.' *Journal of Drug Delivery Science and Technology*, 55 p. 101373.

Diós, P. (2015) *Preformulation studies and optimization of floating drug delivery systems based on pharmaceutical technological and biopharmaceutical parameters*. University of Pécs.

Diryak, R., Kontogiorgos, V., Ghori, M. U., Bills, P., Tawfik, A., Morris, G. A. and Smith, A. M. (2018) 'Behavior of In Situ Cross-Linked Hydrogels with Rapid Gelation Kinetics on Contact with Physiological Fluids.' *Macromolecular Chemistry and Physics*, 219(8).

Draget, K. I., Skjåk Bræk, G. and Smidsrød, O. (1994) 'Alginic acid gels: the effect of alginate chemical composition and molecular weight.' *Carbohydrate Polymers*, 25(1) pp. 31–38.

Duarte, A. R. C., Coimbra, P., De Sousa, H. C. and Duarte, C. M. M. (2004) 'Solubility of flurbiprofen in supercritical carbon dioxide.' *Journal of Chemical and Engineering Data*, 49(3) pp. 449–452.

Dubois, M., Gilles, K., Hamilton, J., Rebers, P. and Smith, F. (1956) 'Colorimetric method for determination of sugars and related substances.' *Analytical Chemistry*, 28(3) pp. 350–356.

Duxfield, L., Sultana, R., Wang, R., Englebretsen, V., Deo, S., Swift, S., Rupenthal, I. and Al-Kassas, R. (2016) 'Development of gatifloxacin-loaded cationic polymeric nanoparticles for ocular drug delivery.' *Pharmaceutical Development and Technology*, 21(2) pp. 172–179.

Dworken, H. J. (2016) 'Human digestive system: gastric secretion.' *Encyclopaedia Britannica*.

Edsman, K., Carlfors, J. and Petersson, R. (1998) 'Rheological evaluation of poloxamer as an in situ gel for ophthalmic use.' *European Journal of Pharmaceutical Sciences*, 6(2) pp. 105–112.

Endo, H., Watanabe, Y., Matsumoto, M. and Shirotake, S. (2000) 'Preparation and evaluation of heat-sensitive melting gel–acetaminophen gel.' *Jpn. J. Hosp. Pharm*, 26 pp. 250–258.

England, R. J. A., Homer, J. J., Knight, L. C. and Ell, S. R. (1999) 'Nasal pH measurement: A reliable and repeatable parameter.' *Clinical Otolaryngology and Allied Sciences*, 24(1) pp. 67–68.

Fallingborg, J. (1999) 'Intraluminal pH of the human gastrointestinal tract.' *Danish medical bulletin* pp. 183–196.

Farahnaky, A., Askari, H., Majzoobi, M. and Mesbahi, G. (2010) 'The impact of concentration, temperature and pH on dynamic rheology of psyllium gels.' *Journal of Food Engineering*. Elsevier Ltd, 100(2) pp. 294–301.

Farrés, I. F. and Norton, I. T. (2015) 'The influence of co-solutes on tribology of agar fluid gels.' *Food Hydrocolloids*, 45 pp. 186–195.

Fathalla, Z. M. A., Khaled, K. A., Hussein, A. K., Alany, R. G. and Vangala, A. (2016) 'Formulation and corneal permeation of ketorolac tromethamine-loaded chitosan nanoparticles.' *Drug Development and Industrial Pharmacy*, 42(4) pp. 514–524.

Felton, L. A., Popescu, C., Wiley, C., Esposito, E. X., Lefevre, P. and Hopfinger, A. J. (2014) 'Experimental and Computational Studies of Physicochemical Properties Influence NSAID-Cyclodextrin Complexation.' *AAPS PharmSciTech*, 15(4) pp. 872–881.

Filik, J. and Stone, N. (2008) 'Analysis of human tear fluid by Raman spectroscopy.' *Analytica Chimica Acta*, 616(2) pp. 177–184.

Fischer, F. H. and Wiederholt, M. (1982) ‘Human precorneal tear film pH measured by microelectrodes.’ *Graefe’s Archive for Clinical and Experimental Ophthalmology*, 218(3) pp. 168–170.

Flink, J. M. and Johansen, A. (1985) ‘A novel method for immobilization of yeast cells in alginate gels of various shapes by internal liberation of Ca-ions.’ *Biotechnology Letters*, 7(10) pp. 765–768.

Francis, N. L., Hunger, P. M., Donius, A. E., Riblett, B. W., Zavaliangos, A., Wegst, U. G. K. and Wheatley, M. A. (2013) ‘An ice-templated, linearly aligned chitosan-alginate scaffold for neural tissue engineering.’ *Journal of Biomedical Materials Research - Part A*, 101(12) pp. 3493–3503.

Gaudana, R., Ananthula, H. K., Parenky, A. and Mitra, A. K. (2010) ‘Ocular Drug Delivery.’ *The AAPS Jounal*, 12(3) pp. 348–360.

Ghori, M. U., Ginting, G., Smith, A. M. and Conway, B. R. (2014) ‘Simultaneous quantification of drug release and erosion from hypromellose hydrophilic matrices.’ *International Journal of Pharmaceutics*. Elsevier B.V., 465(1–2) pp. 406–412.

Gibson, W. and Sanderson, G. R. (1997) ‘Gellan gum.’ *In Thickening and Gelling Agents for Food*, pp. 119–143.

Gittings, S., Turnbull, N., Henry, B., Roberts, C. J. and Gershkovich, P. (2015) ‘Characterisation of human saliva as a platform for oral dissolution medium development.’ *European Journal of Pharmaceutics and Biopharmaceutics*, 91 pp. 16–24.

Le Goff, K. J., Gaillard, C., Helbert, W., Garnier, C. and Aubry, T. (2015) ‘Rheological study of reinforcement of agarose hydrogels by cellulose nanowhiskers.’ *Carbohydrate Polymers*. Elsevier Ltd., 116 pp. 117–123.

Gooch, J. W. (2010) *Biocompatible Polymeric Materials and Tourniquets for Wounds*. Springer-Verlag New York.

Graessley, W. W. (1974) ‘The entanglement concept in polymer rheology.’ *Advances in Polymer Science*, 16 pp. 1–179.

Grant, G. T., Morris, E. R., Rees, D. A., Smith, P. J. C. and Thom, D. (1973) ‘Biological interactions between polysaccharides and divalent cations: The egg-box model.’ *FEBS Letters*, 32(1) pp. 195–198.

Grasdalen, H., Larsen, B. and Smisrod, O. (1981) ‘13C-n.m.r. studies of monomeric composition and sequence in alginate.’ *Carbohydrate Research*, 89(2) pp. 179–191.

Grasdalen, H. and Smidsrød, O. (1987) ‘Gelation of gellan gum.’ *Carbohydrate Polymers*, 7(5) pp. 371–393.

Grover, L. M. and Smith, A. M. (2009) ‘Hydrocolloid and Medicinal Chemistry Applications.’ *In* Kaspas, S., Norton, I. T., and Ubbink, J. B. (eds) *Modern Biopolymer*

Science; Bridging The Divide Between Fundamental Treatise And Industrial Application. 1st ed., London, Burlington, San Diego: Elsvier, pp. 595–619.

Grunwald, J. E. (1986) 'Effect of Topical Timolol on the Human Retinal Circulation.' *INVESTIGATIVE OPHTHALMOLOGY G VISUAL SCIENCE*, 27 pp. 1713–1719.

Gupta, H., Aqil, M., Khar, R. K., Ali, A., Bhatnagar, A., Mittal, G. and Jain, S. (2009) 'Development and characterization of 99mTc-timolol maleate for evaluating efficacy of in situ ocular drug delivery system.' *AAPS PharmSciTech*, 10(2) pp. 540–546.

Gupta, H., Velpandian, T. and Jain, S. (2010) 'Ion-and pH-activated novel in-situ gel system for sustained ocular drug delivery.' *Journal of Drug Targeting*, 18(7) pp. 499–505.

Guyton, A. C. and Hall, J. E. (2005) *Textbook of medical physiology*. 11th ed., Philadelphia: W.B. Saunders.

Hägerström, H. (2003) *Polymer gels as pharmaceutical dosage forms*. *Acta Universitatis Upsaliensis*. Upsala University.

Hale, T. and Abbey, J. (2017) 'Drug Transfer During Breast-Feeding.' *Fetal and Neonatal Physiology*, 1(5) pp. 239–248.

Hansch, C., Leo, A. and Hoekman, D. H. (1995) *Exploring QSAR : hydrophobic, electronic, and steric constants*. Washington, DC: American Chemical Society.

Hao, T. (2005) 'The positive, negative, photo-ER, and electromagnetorheological (EMR) effects.' *In* Hao, T. (ed.) *Studies in Interface Science*. Elsevier, pp. 83–113.

Harnett, M. (1989) *The Rheology of Butter*. Massey University.

Haug, A. (1961) 'Dissociation of alginic acid.' *Acta Chem. Scand*, 15(4) pp. 950–952.

Hedges, A. (2009) 'Cyclodextrins: Properties and Applications.' *Starch*. Academic Press, January, pp. 833–851.

Hickson, I. (1998) *Ian Hickson's Description of the Eye*. [Online] http://academia.hixie.ch/%0Abath/eye/home.html.

Higham, A. K., Bonino, C. A., Raghavan, S. R. and Khan, S. A. (2014) 'Photo-activated ionic gelation of alginate hydrogel: Real-time rheological monitoring of the two-step crosslinking mechanism.' *Soft Matter*, 10(27) pp. 4990–5002.

Higuchi, T. and Connors, K. (1965) 'Phase-solubility techniques.' *In* Reilley, C. (ed.) *Advances in analytical chemistry and instrumentation*. New York: John Wiley & Sons, Inc, pp. 117–212.

Hill, S. E., Ledward, D. A. and Mitchell, J. R. (1998) *Functional Properties of Food Macromolecules*. 2nd ed., Maryland: Aspen Publishers,Inc.

Hoare, T. R. and Kohane, D. S. (2008) 'Hydrogels in drug delivery: Progress and challenges.' *Polymer* pp. 1993–2007.

Hoichman, D., Gromova, L. I. and Sela, J. (2004) ‘Gastroretentive controlled-release drugs.’ *Pharmaceutical Chemistry Journal*, 38(11) pp. 621–624.

Hooke, R. (1678) *De Potentia Restitutiva, or of Spring Explaining the Power of Springing Bodies*. *Spring Explaining the Power of Springing Bodies*. Sixth Cutler Lecture.

Huang, D., Chen, Y.-S. and Rupenthal, I. D. (2017) ‘Overcoming ocular drug delivery barriers through the use of physical forces.’ *Advanced Drug Delivery Reviews*.

Humphrey, S. P. and Williamson, R. T. (2001) ‘A review of saliva: Normal composition, flow, and function.’ *Journal of Prosthetic Dentistry*, 85(2) pp. 162–169.

Ibarz, A., Castell-Perez, E. and Barbosa-Canovas, G. V. (2002) ‘Newtonian and Non-Newtonian Flow.’ *In* Ibarz, A. and Barbosa-Canovas, G. V. (eds) *Unit Operations in Food Engineering*. CRC Press.

Ikeda, S. and Nishinari, K. (2001) ‘“Weak gel”- type rheological properties of aqueous dispersions of nonaggregated k-carrageenan helices.’ *Journal of Agricultural and Food Chemistry*, 49 pp. 4436–4441.

Ikejiri, Y., Tokomochi, F., Sameshima, S. and Kimura, M. (1995) ‘Antiallergic Composition for Ophthalmic or Nasal Use.’ Japan.

Irie, T. and Uekama, K. (1997) ‘Pharmaceutical applications of cyclodextrins. III. Toxicological issues and safety evaluation.’ *Journal of Pharmaceutical Sciences* pp. 147–162.

Ishak, R. A. H., Awad, G. A. S., Mortada, N. D. and Nour, S. A. K. (2007) ‘Preparation, in vitro and in vivo evaluation of stomach-specific metronidazole-loaded alginate beads as local anti-Helicobacter pylori therapy.’ *Journal of Controlled Release*, 119(2) pp. 207–214.

Izydorczyk, M., Cui, S. W. and Wang, Q. (2005) ‘Polysaccharide Gums: Structures, Functional Properties, and Applications.’ *In* Cui, S. W. (ed.) *Food Carbohydrates: Chemistry, Physical Properties, and Applications*. Taylor and Francis.

Jain, A., Gupta, Y. and Jain, S. K. (2007) ‘Perspectives of biodegradable natural polysaccharides for site-specific drug delivery to the colon.’ *Journal of Pharmacy and Pharmaceutical Sciences*, 10(1) pp. 86–128.

Jain, D., Kumar, V., Singh, S., Mullertz, A. and Shalom, D. B. (2016) ‘Newer Trends in In Situ Gelling Systems for Controlled Ocular Drug Delivery.’ *Journal of Analytical & Pharmaceutical Research*, 2(3).

Jansen, T., Xhonneux, B., Mesens, J. and Borgers, M. (1990) ‘Beta-cyclodextrins as vehicles in eye-drop formulations: An evaluation of their effects on rabbit corneal epithelium.’ *In Lens and Eye Toxicity Research*, pp. 459–468.

Jansook, P., Ogawa, N. and Loftsson, T. (2018) ‘Cyclodextrins: structure, physicochemical properties and pharmaceutical applications.’ *International Journal of Pharmaceutics*. Elsevier, 535(1–2) pp. 272–284.

Jeejeebhoy, K. N. (2002) ‘Short bowel syndrome: A nutritional and medical approach.’ *CMAJ*, 166(10) pp. 1297–1302.

Jessop, Z. M., Gao, N., Manivannan, S., Al-Sabah, A. and Whitaker, I. S. (2018) ‘3D bioprinting cartilage.’ *3D Bioprinting for Reconstructive Surgery*. Woodhead Publishing, January, pp. 277–304.

Joshi, G. V., Kevadiya, B. D., Patel, H. A., Bajaj, H. C. and Jasra, R. V. (2009) ‘Montmorillonite as a drug delivery system: Intercalation and in vitro release of timolol maleate.’ *International Journal of Pharmaceutics*, 374(1–2) pp. 53–57.

Kalepu, S. and Nekkanti, V. (2015) ‘Insoluble drug delivery strategies: Review of recent advances and business prospects.’ *Acta Pharmaceutica Sinica B* pp. 442–453.

Kang, L. and Majd, S. (2016) *Gels Handbook; Fundamentals, Properties and Application*. Singapore: World Scientific Publishing Co. Pte. Ltd.

Kaparissides, C., Alexandridou, S., Kotti, K. and Chaitidou, S. (2006) ‘Recent advances in novel drug delivery systems.’ *J. Nanotechynol. Online*, 2(3) pp. 1–11.

Kara, S., Arda, E., Kavzak, B. and Pekcan, Ö.¨(2006) ‘Phase transitions of κ-carrageenan gels in various types of salts.’ *Journal of Applied Polymer Science*, 102(3) pp. 3008–3016.

Katayama, H., Nishimura, T., Ochi, S., Tsuruta, Y., Yamazaki, Y., Shibata, K. and Yoshitomi, H. (1999) ‘Sustained Release Liquid Preparation Using Sodium Alginate for Eradication of Helicobacter pyroli.’ *Biological & Pharmaceutical Bulletin*, 22(1) pp. 55–60.

Kearse, E. C., Mcintyre, O. L., Johnson, M. H., Phillips, C. I., Lathe, R., Adams, W. and Green, K. (2001) ‘Influence of dehydroepiandrosterone on rabbit intraocular pressure.’ *Ophthalmic Research*, 33(1) pp. 42–47.

Koliandris, A., Lee, A., Ferry, A. L., Hill, S. and Mitchell, J. (2008) ‘Relationship between structure of hydrocolloid gels and solutions and flavour release.’ *Food Hydrocolloids*, 22(4) pp. 623–630.

Kontogiorgos, V. (2014) ‘Polysaccharide Nanostructures.’ *In* Marangoni, A. . . and Pink, D. (eds) *Edible Nanostructures*. 1st ed., The Royal Society of Chemistry,Cambridge, pp. 41–69.

Koo, O. M. Y. (2011) ‘Application challenges and examples of new excipients in advanced drug delivery systems.’ *In American Pharmaceutical Review*, pp. 60–68.

Kotula, A. P., Meyer, M. W., De Vito, F., Plog, J., Hight Walker, A. R. and Migler, K. B. (2016) ‘The rheo-Raman microscope: Simultaneous chemical, conformational,

mechanical, and microstructural measures of soft materials.' *Review of Scientific Instruments*, 87(10).

Krishnaiah, Y. S. R., Bhaskar Reddy, P. R., Satyanarayana, V. and Karthikeyan, R. S. (2002) 'Studies on the development of oral colon targeted drug delivery systems for metronidazole in the treatment of amoebiasis.' *International Journal of Pharmaceutics*, 236(1–2) pp. 43–55.

Krishnaiah, Y. S. R., Xu, X., Rahman, Z., Yang, Y., Katragadda, U., Lionberger, R., Peters, J. R., Uhl, K. and Khan, M. A. (2014) 'Development of performance matrix for generic product equivalence of acyclovir topical creams.' *International Journal of Pharmaceutics*. Elsevier B.V., 475(1–2) pp. 110–122.

Kristinsson, J. K., Fridriksdóttir, H., Thórisdóttir, S., Sigurdardóttir, A. M., Stefánsson, E. and Loftsson, T. (1996) 'Dexamethasone-cyclodextrin-polymer co-complexes in aqueous eye drops: Aqueous humor pharmacokinetics in humans.' *Investigative Ophthalmology and Visual Science*, 37(6) pp. 1199–1203.

Kubo, W., Konno, Y., Miyazaki, S. and Attwood, D. (2004) 'In situ gelling pectin formulations for oral sustained delivery of paracetamol.' *Drug Development and Industrial Pharmacy*, 30(6) pp. 593–599.

Kubo, W., Miyazaki, S. and Attwood, D. (2003) 'Oral sustained delivery of paracetamol from in situ-gelling gellan and sodium alginate formulations.' *International Journal of Pharmaceutics*, 258(1–2) pp. 55–64.

Kulkarni, A. R., Soppimath, K. S., Aminabhavi, T. M. and Rudzinski, W. E. (2001) 'In-vitro release kinetics of cefadroxil-loaded sodium alginate interpenetrating network beads.' *European Journal of Pharmaceutics and Biopharmaceutics*, 51(2) pp. 127–133.

Kumar, S. and Himmelstein, K. J. (1995) 'Modification of in situ gelling behavior of carbopol solutions by hydroxypropyl methylcellulose.' *Journal of Pharmaceutical Sciences*, 84(3) pp. 344–348.

Lang, J. C. (1995) 'Ocular drug delivery conventional ocular formulations.' *Advanced Drug Delivery Reviews*, 16(1) pp. 39–43.

Lau, A. H., Lam, N. P., Piscitelli, S. C., Wilkes, L. and Danziger, L. H. (1992) 'Clinical Pharmacokinetics of Metronidazole and Other Nitroimidazole Anti-Infectives.' *Clinical Pharmacokinetics* pp. 328–364.

Läuger, J. (2009) 'Combined Rheological Methods: From Rheo-Optics to Magneto-Rheology and Beyond.' *ANNUAL TRANSACTIONS OF THE NORDIC RHEOLOGY SOCIETY*, 17.

Lee, J. and Tripathi, A. (2005) 'Intrinsic viscosity of polymers and biopolymers measured by microchip.' *Analytical Chemistry*, 77(22) pp. 7137–7147.

Lee, K. Y. and Mooney, D. J. (2012) 'Alginate : properties and biomedical applications.' *Progress in Polymer Science (Oxford)*, 37(1) pp. 106–126.

Lewis, M. J. (1996) ‘Viscosity.’ *In* Lewis, M. J. (ed.) *Physical Properties of Foods and Food Processing Systems*. Woodhead Publishing, pp. 108–136.

Li, Y., Dubin, P. L., Havel, H. A., Edwards, S. L. and Dautzenberg, H. (1995) ‘Electrophoretic Light Scattering, Dynamic Light Scattering, and Turbidimetry Studies of the Effect of Polymer Concentration on Complex Formation between Polyelectrolyte and Oppositely Charged Mixed Micelles.’ *Macromolecules*, 28(9) pp. 3098–3102.

Liechty, W. B., Kryscio, D. R., Slaughter, B. V. and Peppas, N. A. (2010) ‘Polymers for Drug Delivery Systems.’ *Annual Review of Chemical and Biomolecular Engineering*, 1(1) pp. 149–173.

Lin, H., Yu, S., Lin, Y. and Wang, T. (2010) ‘High pH tolerance of a chitosan-PAA nanosuspension for ophthalmic delivery of pilocarpine.’ *J Biomater Sci Polym Ed.*, 21(2) pp. 141–157.

Linden, E. van der and Foegeding, E. A. (2009) ‘Gelation: Principles, Models and application to Proteins.’ *In* Kasapis, S., Norton, I. T., and Ubbink, J. B. (eds) *Modern Biopolymer Science; Bridging The Divide Between Fundamental Treatise And Industrial Application*. 1st ed., Elsvier, London, Burlington, San Diego, pp. 29–92.

Liu, L., Yao, W. D., Rao, Y. F., Lu, X. Y. and Gao, J. Q. (2017) ‘pH-responsive carriers for oral drug delivery: Challenges and opportunities of current platforms.’ *Drug Delivery* pp. 569–581.

Liu, Z., Li, J., Nie, S., Liu, H., Ding, P. and Pan, W. (2006) ‘Study of an alginate/HPMC-based in situ gelling ophthalmic delivery system for gatifloxacin.’ *International Journal of Pharmaceutics*, 315(1–2) pp. 12–17.

Liu, Z., Pan, W., Nie, S., Zhang, L., Yang, X. and Li, J. (2005) ‘Preparation and evaluation of sustained ophthalmic gel of enoxacin.’ *Drug Development and Industrial Pharmacy*, 31(10) pp. 969–975.

Lloyd, D. . (1926) ‘The problem of gel structure.’ *In* J., A. (ed.) *Colloid Chemistry*. Chemical Catalog, New York, pp. 767–782.

Loftsson, T. (1998) ‘Increasing the cyclodextrin complexation of drugs and drug biovailability through addition of water-soluble polymers.’ *Pharmazie*, 53(11) pp. 733–740.

Loftsson, T. and Brewster, M. E. (2010) ‘Pharmaceutical applications of cyclodextrins: Basic science and product development.’ *Journal of Pharmacy and Pharmacology*, 62(11) pp. 1607–1621.

Loftsson, T., Jansook, P. and Stefánsson, E. (2012) ‘Topical drug delivery to the eye: Dorzolamide.’ *Acta Ophthalmologica* pp. 603–608.

Loftsson, T., Másson, M. and Brewster, M. E. (2004) ‘Self-Association of Cyclodextrins and Cyclodextrin Complexes.’ *Journal of Pharmaceutical Sciences* pp. 1091–1099.

Loftsson, T. and Stefánsson, E. (1997) ‘Effect of cyclodextrins on topical drug delivery to the eye.’ *Drug Development and Industrial Pharmacy* pp. 473–481.

Loftsson, T. and Stefánsson, E. (2017) ‘Cyclodextrins and topical drug delivery to the anterior and posterior segments of the eye.’ *International Journal of Pharmaceutics*. Elsevier B.V., 531(2) pp. 413–423.

Loftsson, T., Thorisdóttir, S., Fridriksdóttir, H. and Stefánsson, E. (2010) ‘Enalaprilat and enalapril maleate eyedrops lower intraocular pressure in rabbits.’ *Acta Ophthalmologica*, 88(3) pp. 337–341.

Loftssona, T. and Järvinen, T. (1999) ‘Cyclodextrins in ophthalmic drug delivery.’ *Advanced Drug Delivery Reviews*, 36(1) pp. 59–79.

Lu, Y., An, L. and Wang, Z. G. (2013) ‘Intrinsic viscosity of polymers: General theory based on a partially permeable sphere model.’ *Macromolecules*, 46(14) pp. 5731–5740.

Madan, M., Bajaj, A., Lewis, S., Udupa, N. and Baig, J. (2009) ‘*In situ* forming polymeric drug delivery systems.’ *Indian Journal of Pharmaceutical Sciences*, 71(3) p. 242.

El Maghraby, G. M., Elzayat, E. M. and Alanazi, F. K. (2012) ‘Development of modified in situ gelling oral liquid sustained release formulation of dextromethorphan.’ *Drug Development and Industrial Pharmacy*, 38(8) pp. 971–978.

Mahajan, N., Shende, S., Dumore, N. and Nasare, L. (2019) ‘Development and evaluation of ion induced in situ gelling system of opoid analgesic for nose to brain delivery.’ *Research Journal of Pharmacy and Technology*, 12(10) pp. 4741–4746.

Mahdi, M. H. (2016) *Development of Gellan Gum Fluid Gel As Modified Release Drug Delivery Systems*. University of Huddersfield.

Mahdi, M. H., Conway, B. R. and Smith, A. M. (2014) ‘Evaluation of gellan gum fluid gels as modified release oral liquids.’ *International Journal of Pharmaceutics*. Elsevier B.V., 475(1) pp. 335–343.

Mahdi, M. H., Conway, B. R. and Smith, A. M. (2015) ‘Development of mucoadhesive sprayable gellan gum fluid gels.’ *International Journal of Pharmaceutics*. Elsevier B.V., 488(1–2) pp. 12–19.

Mahdi, M. H., Diryak, R., Kontogiorgos, V., Morris, G. A. and Smith, A. M. (2016a) ‘In situ rheological measurements of the external gelation of alginate.’ *Food Hydrocolloids*. Elsevier Ltd, 55 pp. 77–80.

Mahdi, M. H., Diryak, R., Kontogiorgos, V., Morris, G. A. and Smith, A. M. (2016b) ‘In situ rheological measurements of the external gelation of alginate.’ *Food Hydrocolloids*, 55 pp. 77–80.

Malafaya, P. B., Silva, G. A. and Reis, R. L. (2007) ‘Natural-origin polymers as carriers and scaffolds for biomolecules and cell delivery in tissue engineering applications.’ *Advanced Drug Delivery Reviews*, 59(4–5) pp. 207–233.

Malanga, M., Szemán, J., Fenyvesi, É., Puskás, I., Csabai, K., Gyémánt, G., Fenyvesi, F. and Szente, L. (2016) '"Back to the Future": A New Look at Hydroxypropyl Beta-Cyclodextrins.' *Journal of Pharmaceutical Sciences*, 105(9) pp. 2921–2931.

Malavade, S. (2016) 'Overview of the Ophthalmic System.' *In* Y., P., V., S., and A., H. (eds) *Nano-Biomaterials For Ophthalmic Drug Delivery*. Springer, Cham, pp. 9–36.

Marieb, E. N. and Hoehn, K. (2010) *Human Anatomy & Physiology*. 8th ed., San Francisco : Benjamin Cummings.

Marques, M. R. C., Loebenberg, R. and Almukainzi, M. (2011) 'Simulated biological fluids with possible application in dissolution testing.' *Dissolution Technologies*, 18(3) pp. 15–28.

Marriott, C. (2007) 'Rheology.' *In* Aulton, M. E. (ed.) *Pharmaceutics: The Design and Manufacture of Medicines*. 3rd ed., New York: Edinburgh Churchill Livingstone, pp. 42–59.

Marsac, P. J., Li, T. and Taylor, L. S. (2009) 'Estimation of drug-polymer miscibility and solubility in amorphous solid dispersions using experimentally determined interaction parameters.' *Pharmaceutical Research*, 26(1) pp. 139–151.

Masuko, T., Minami, A., Iwasaki, N., Majima, T., Nishimura, S. I. and Lee, Y. C. (2005) 'Carbohydrate analysis by a phenol-sulfuric acid method in microplate format.' *Analytical Biochemistry*, 339(1) pp. 69–72.

McKinney, R. E. (2004) *Environmental Pollution Control Microbiology: A Fifty-Year Perspective*. New York: Marcel Dekker, Inc.

Mcnaught, A. D. (2008) 'International Union of Pure International Union of Biochemistry Joint Commission on Biochemical Nomenclature.' *Pure and Applied Chemistry*, 68(10) pp. 1919–2008.

Mendoza, J. A. (1998) *A study of the rheological properties of some of the gels commonly used in the pharmaceutical, food and cosmetic industries and their influence on microbial growth*. University of Rhode Island.

Messner, M., Kurkov, S. V., Jansook, P. and Loftsson, T. (2010) 'Self-assembled cyclodextrin aggregates and nanoparticles.' *International Journal of Pharmaceutics* pp. 199–208.

Mezger, T. . (2006) 'Flow behaviour and viscosity.' *In The rheology handbook: for users of rotational and oscillatory rheometers*. 2nd ed., Vincentz Network GmbH & Co KG, pp. 19–29.

Milder, B. (1987) 'The lacrimal apparatus.' *In* Moses, R. A. and Hart, W. M. (eds) *Adler's Physiology of the Eye*. 8th ed., Mosby, St. Louis, p. 15.

Minami, H. and Mccallum, R. W. (1984) 'The Physiology and Pathophysiology of Gastric Emptying in Humans.' *Gastroenterology*, 86(6) pp. 1592–1610.

Minghetti, P., Cilurzo, F., Casiraghi, A., Montanari, L. and Fini, A. (2007) 'Ex vivo study of transdermal permeation of four diclofenac salts from different vehicles.' *Journal of Pharmaceutical Sciences*, 96(4) pp. 814–823.

Miyazaki, S., Aoyama, H., Kawasaki, N., Kubo, W. and Attwood, D. (1999) 'In situ-gelling gellan formulations as vehicles for oral drug delivery.' *Journal of Controlled Release*, 60(2–3) pp. 287–295.

Miyazaki, S., Kawasaki, N., Kubo, W., Endo, K. and Attwood, D. (2001) 'Comparison of in situ gelling formulations for the oral delivery of cimetidine.' *International journal of pharmaceutics*, 220(1–2) pp. 161–8.

Miyazaki, S., Kubo, W. and Attwood, D. (2000) 'Oral sustained delivery of theophylline using in-situ gelation of sodium alginate.' *Journal of Controlled Release*, 67(2–3) pp. 275–280.

Mohamed-Ahmed, A. H. A., Lockwood, A., Li, H., Bailly, M., Khaw, P. T. and Brocchini, S. (2017) 'An ilomastat-CD eye drop formulation to treat ocular scarring.' *Investigative Ophthalmology and Visual Science*, 58(9) pp. 3425–3431.

Moosavi, S. M. and Ghassabian, S. (2018) 'Linearity of Calibration Curves for Analytical Methods: A Review of Criteria for Assessment of Method Reliability.' *In Calibration and Validation of Analytical Methods - A Sampling of Current Approaches*.

Morris, E. R. (1986) 'MOLECULAR INTERACTIONS IN POLYSACCHARIDE GELATION.' *British Polymer Journal*, 18(1) pp. 14–21.

Morris, E. R., Gothard, M. G. E., Hember, M. W. N., Manning, C. E. and Robinson, G. (1996) 'Conformational and rheological transitions of welan, rhamsan and acylated gellan.' *Carbohydrate Polymers*, 30(2–3) pp. 165–175.

Morris, E. R., Nishinari, K. and Rinaudo, M. (2012) 'Gelation of gellan - A review.' *Food Hydrocolloids*. Elsevier Ltd, 28(2) pp. 373–411.

Morrison, P. W. J., Connon, C. J. and Khutoryanskiy, V. V. (2013) 'Cyclodextrin-mediated enhancement of riboflavin solubility and corneal permeability.' *Molecular Pharmaceutics*, 10(2) pp. 756–762.

Moxon, S. R. (2016) *Development of Biopolymer Hydrogels As Complex Tissue Engineering Scaffolds*. University of Huddersfield.

Mythri, G., Kavitha, K., Kumar, M. R. and Jagadeesh Singh, S. D. (2011) 'Novel mucoadhesive polymers- A review.' *Journal of Applied Pharmaceutical Science* pp. 37–42.

Nasir, F., Iqbal, Z., Khan, A., Ahmad, L., Shah, Y., Khan, A. Z., Khan, J. A. and Khan, S. (2011) 'Simultaneous determination of timolol maleate, rosuvastatin calcium and diclofenac sodium in pharmaceuticals and physiological fluids using HPLC-UV.' *Journal of Chromatography B: Analytical Technologies in the Biomedical and Life Sciences*. Elsevier B.V., 879(30) pp. 3434–3443.

Nief, R. A., Tamer, M. A. and Alhammid, S. N. A. (2019) 'Mucoadhesive oral in situ gel of itraconazole using pH-sensitive polymers: Preparation, and in vitro characterization, release and rheology study.' *Drug Invention Today*, 11(6) pp. 1450–1455.

Nielsen, S. S. (2010) 'Phenol-Sulfuric Acid Method for Total Carbohydrates.' *In Food Analysis Laboratory Manual*. 2nd ed., New York: Springer, pp. 47–54.

Nirmal, H. B., Bakliwal, S. R. and Pawar, S. P. (2010) 'In-Situ gel: New trends in controlled and sustained drug delivery system.' *International Journal of PharmTech Research*, 2(2) pp. 1398–1408.

Nordqvist, D. and Vilgis, T. A. (2011) 'Rheological Study of the Gelation Process of Agarose-Based Solutions.' *Food Biophysics*, 6(4) pp. 450–460.

Okamoto, N., Ito, Y., Nagai, N., Murao, T., Takiguchi, Y., Kurimoto, T. and Mimura, O. (2010) 'Preparation of Ophthalmic Formulations Containing Cilostazol as an Anti-glaucoma Agent and Improvement in Its Permeability through the Rabbit Cornea.' *Journal of Oleo Science*, 59(8) pp. 423–430.

Ozer, B. H., Robinson, R. K., Grandison, A. S. and Bell, A. E. (1997) 'Comparison of techniques for measuring the rheological properties of labneh (concentrated yogurt).' *International Journal of Dairy Technology*, 50(4) pp. 129–133.

Pandit, J., Bharathi, D., Srinatha, A., Ridhurkar, D., Singh, S. and Singh, S. (2007) 'Long acting ophthalmic formulation of indomethacin: Evaluation of alginate gel systems.' *Indian Journal of Pharmaceutical Sciences*, 69(1) p. 37.

Papanicolaou, G. C. and Zaoutsos, S. P. (2011) 'Viscoelastic constitutive modeling of creep and stress relaxation in polymers and polymer matrix composites.' *In Woodhead Publishing Series in Composites Science and Engineering*, pp. 3–47.

Park, H., Kang, S. W., Kim, B. S., Mooney, D. J. and Lee, K. Y. (2009) 'Shear-reversibly crosslinked alginate hydrogels for tissue engineering.' *Macromolecular Bioscience*, 9(9) pp. 895–901.

Pate, D. W., Järvinen, K., Urtti, A., Jarho, P., Fich, M., Mahadevan, V. and Järvinen, T. (1996) 'Effects of topical anandamides on intraocular pressure in normotensive rabbits.' *Life Sciences*.

Pate, D. W., Järvinen, K., Urtti, A., Jarho, P. and Järvinen, T. (1995) 'Ophthalmic arachidonylethanolamide decreases intraocular pressure in normotensive rabbits.' *Current Eye Research*, 14(9) pp. 791–797.

Pate, D. W., Järvinen, K., Urtti, A., Jarho, P., Mahadevan, V. and Järvinen, T. (1997) 'Effects of topical alpha-substituted anandamides on intraocular pressure in normotensive rabbits.' *Pharmaceutical Research*, 14(12) pp. 1738–1743.

Patel, A., Cholkar, K., Agrahari, V. and Mitra, A. K. (2013) 'Ocular drug delivery systems: An overview.' *World journal of pharmacology*, 2(2) pp. 47–64.

Patel, D. M., Patel, D. K. and Patel, C. N. (2011) ‘Formulation and Evaluation of Floating Oral *In Situ* Gelling System of Amoxicillin.’ *ISRN Pharmaceutics*, 2011 pp. 1–8.

Patti, M. G., Gantert, W. and Way, L. W. (1997) ‘Surgery of the esophagus: anatomy and physiology.’ *Surgical Clinics of North America*, 77(5) pp. 959–970.

Pawar, S. N. and Edgar, K. J. (2012) ‘Alginate derivatization: A review of chemistry, properties and applications.’ *Biomaterials* pp. 3279–3305.

Pawar, V. K., Kansal, S., Garg, G., Awasthi, R., Singodia, D. and Kulkarni, G. T. (2011) ‘Gastroretentive dosage forms: A review with special emphasis on floating drug delivery systems.’ *Drug Delivery* pp. 97–110.

Peate, I. (2018) ‘Anatomy and Physiology, The gastrointestinal system.’ *British Journal of Healthcare Assistants*, 12(3) pp. 110–114.

Pelley, J. W. (2012) *Elsevier’s Integrated Review Biochemistry*. 2nd ed., Texas: Elsevier Inc.

Peppas, N. A., Bures, P., Leobandung, W. and Ichikawa, H. (2000) ‘Hydrogels in pharmaceutical formulations.’ *European Journal of Pharmaceutics and Biopharmaceutics* pp. 27–46.

Perez, S. and Kouwijzer, M. (1999) ‘Shapes and interactions of polysaccharide chains.’ *In Carbohydrates*. Springer, Dordrecht.

Picout, D. R. and Ross-Murphy, S. B. (2003) ‘Rheology of biopolymer solutions and gels.’ *TheScientificWorldJournal*, 3 pp. 105–121.

Piculell, L. and Nilsson, S. (1989) ‘Anion-specific salt effects in aqueous agarose systems. 1. Effects on the coil-helix transition and gelation of agarose.’ *Journal of Physical Chemistry*, 93(14) pp. 5596–5601.

Pineau, A., Guillard, O., Fauconneau, B., Favreau, F., Marty, M. H., Gaudin, A., Vincent, C. M., Marrauld, A. and Marty, J. P. (2012) ‘In vitro study of percutaneous absorption of aluminum from antiperspirants through human skin in the Franz^{TM} diffusion cell.’ *Journal of Inorganic Biochemistry*. Elsevier Inc., 110 pp. 21–26.

Posocco, B., Dreussi, E., De Santa, J., Toffoli, G., Abrami, M., Musiani, F., Grassi, M., Farra, R., Tonon, F., Grassi, G. and Dapas, B. (2015) *Polysaccharides for the delivery of antitumor drugs*. *Materials*.

Qian, Y., Wang, F., Li, R., Zhang, Q. and Xu, Q. (2010) ‘Preparation and evaluation of in situ gelling ophthalmic drug delivery system for methazolamide.’ *Drug Development and Industrial Pharmacy*, 36(11) pp. 1340–1347.

Qiu, Y. and Park, K. (2001) ‘Environment-sensitive Hydrogels for Drug Delivery, Adv. Drug Deliv.’ *Advanced Drug Delivery Reviews*, 53(13) pp. 321–339.

Rajinikanth, P. S. and Mishra, B. (2007) 'Preparation and in vitro characterization of gellan based floating beads of acetohydroxamic acid for eradication of H. pylori.' *Acta Pharmaceutica*, 57(4) pp. 413–427.

Rajinikanth, P. S. and Mishra, B. (2008) 'Floating in situ gelling system for stomach site-specific delivery of clarithromycin to eradicate H. pylori.' *Journal of Controlled Release*, 125(1) pp. 33–41.

Rasel, M. A. T. and Hasan, M. (2012) 'Formulation and evaluation of floating alginate beads of diclofenac sodium.' *Dhaka University Journal of Pharmaceutical Sciences*, 11(1) pp. 29–35.

Rashad, A. L., Toffler, W. L., Wolf, N., Thornburg, K., Kirk, E. P., Ellis, G. and Whitehead, W. E. (1992) 'Vaginal PO2 in healthy women and in women infected with Trichomonas vaginalis: Potential implications for metronidazole therapy.' *American Journal of Obstetrics and Gynecology*, 166(2) pp. 620–624.

Rathore, K. S., Nema, R. K. and Sisodia, S. S. (2010) 'Timolol maleate a gold standard drug in glaucoma used as ocular films and inserts: An overview.' *International Journal of Pharmaceutical Sciences Review and Research*, 3(1) pp. 23–29.

Reer, O., Bock, T. K. and Müller, B. W. (1994) 'In vitro corneal permeability of diclofenac sodium in formulations containing cyclodextrins compared to the commercial product voltaren ophtha.' *Journal of Pharmaceutical Sciences*, 83(9) pp. 1345–1349.

Reubi, J. C. (2003) 'Peptide receptors as molecular targets for cancer diagnosis and therapy.' *Endocrine Reviews* pp. 389–427.

Rismondo, V., Osgood, T. B., Leering, P., Hattenhauer, M. G., Ubels, J. L. and Edelhauser, H. F. (1989) 'Electrolyte composition of lacrimal gland fluid and tears of normal and vitamin A-deficient rabbits.' *CLAO Journal*, 15(3) pp. 222–229.

Robinson, G., Manning, C. and Morris, E. R. (1991) 'Conformation and & physical properties of the bacterial polysaccharides Gellan Welan and Rhamsan.' *In Food Polymers, Gels and Colloids*. London: Royal Soc. Chem, pp. 22–23.

Roshdy, M. N., Schwartz, J. B. and Schnaare, R. L. (2001) 'A Novel Method for Measuring Gel Strength of Controlled Release Hydrogel Tablets Using a Cone/Plate Rheometer.' *Pharmaceutical Development and Technology*, 6(1) pp. 107–116.

Ross-murphy, S. B., Wang, Q. and Ellis, P. R. (1998) 'Structure and Mechanical Properties of Polysaccharides.' *Macromol.Symp*, 127 pp. 13–21.

Rozier, A., Mazuel, C., Grove, J. and Plazonnet, B. (1989) 'Gelrite®: A novel, ion-activated, in-situ gelling polymer for ophthalmic vehicles. Effect on bioavailability of timolol.' *International Journal of Pharmaceutics*, 57(2) pp. 163–168.

Ruel-Gariépy, E. and Leroux, J. C. (2004) 'In situ-forming hydrogels - Review of temperature-sensitive systems.' *European Journal of Pharmaceutics and Biopharmaceutics*, 58(2) pp. 409–426.

Rupenthal, I. D., Green, C. R. and Alany, R. G. (2011) 'Comparison of ion-activated in situ gelling systems for ocular drug delivery. Part 1: Physicochemical characterisation and in vitro release.' *International Journal of Pharmaceutics*. Elsevier B.V., 411(1–2) pp. 69–77.

Sako, K., Nakashima, H., Sawada, T. and Fukui, M. (1996) 'Relationship between Gelation Rate of Controlled-release Acetaminophen Tablets Containing Polyethylene Oxide and Colonic Drug Release in Dogs.' *Pharmaceutical Research*, 13(4) pp. 594–598.

Salcedo, J. A. and Al-Kawas, F. (1998) 'Treatment of Helicobacter pylori Infection.' *JAMA Internal Medicine*, 158(8) pp. 842–851.

Saokham, P., Muankaew, C., Jansook, P. and Loftsson, T. (2018) 'Solubility of cyclodextrins and drug/cyclodextrin complexes.' *Molecules*, 23(5) pp. 1–15.

Schanker, L. S. (1960) 'On the Mechanism of Absorption of Drugs from the Gastrointestinal Tract.' *In* B.B., B., J.R., G., and H.S., A. (eds) *Journal of Medicinal Chemistry*. Springer, Berlin, Heidelberg, pp. 343–359.

Schramm, G. (1994) *A Practical Approach to Rheology and Rheometry*. 2nd ed., Karlsruhe: Gebrueder Haake GmbH.

Seman, A., Ekere, N. N., Ashenden, S. J., Mallik, S., Marks, A. E. and Durairaj, R. (2009) 'In-situ Non-destructive Ultrasonic Rheology Technique for Monitoring Different Lead-free Solder Pastes for Surface Mount Applications.' *In*, pp. 1448–1454.

Serrano, D. R., Ruiz-Saldaña, H. K., Molero, G., Ballesteros, M. P. and Torrado, J. J. (2012) 'A novel formulation of solubilised amphotericin B designed for ophthalmic use.' *International Journal of Pharmaceutics*, 437(1–2) pp. 80–82.

Shastri, D., Prajapati, S. and Patel, L. (2010) 'Thermoreversible mucoadhesive ophthalmic in situ hydrogel: Design and optimization using a combination of polymers.' *Acta Pharmaceutica*, 60(3) pp. 349–360.

Shelke, N. B., James, R., Laurencin, C. T. and Kumbar, S. G. (2014) 'Polysaccharide biomaterials for drug delivery and regenerative engineering.' *Polymers for Advanced Technologies*, 25(5) pp. 448–460.

Slots, J. and Rams, T. E. (1990) 'Antibiotics in periodontal therapy: advantages and disadvantages.' *Journal of Clinical Periodontology*, 17 pp. 479–493.

Smith, A. M., Shelton, R. M., Perrie, Y. and Harris, J. J. (2007) 'An initial evaluation of gellan gum as a material for tissue engineering applications.' *Journal of biomaterials applications*, 22(3) pp. 241–54.

Solari, M. (1994) 'Evaluation of the mechanical properties of a hydrogel fiber in the development of a polymeric actuator.' *Journal of Intelligent Material Systems and Structures*, 5(3) pp. 295–304.

Somani, R. H., Yang, L., Hsiao, B. S., Agarwal, P. K., Fruitwala, H. A. and Tsou, A. H. (2002) 'Shear-induced precursor structures in isotactic polypropylene melt by in-situ rheo-SAXS and rheo-WAXD studies.' *Macromolecules*, 35(24) pp. 9096–9104.

Song, H. Y., Salehiyan, R., Li, X., Lee, S. H. and Hyun, K. (2017) 'A comparative study of the effects of cone-plate and parallel-plate geometries on rheological properties under oscillatory shear flow.' *Korea Australia Rheology Journal*, 29(4) pp. 281–294.

Sood, A. and Panchagnula, R. (2001) 'Peroral route: An opportunity for protein and peptide drug delivery.' *Chemical Reviews*, 101(11) pp. 3275–3303.

Soppimath, K. S., Aminabhavi, T. M., Kulkarni, A. R. and Rudzinski, W. E. (2001) 'Biodegradable polymeric nanoparticles as drug delivery devices.' *Journal of Controlled Release*, 70(1–2) pp. 1–20.

Soppimath, K. S., Kulkarni, A. R., Rudzinski, W. E. and Aminabhavi, T. M. (2001) 'Microspheres as floating drug-delivery systems to increase gastric retention of drugs.' *Drug Metabolism Reviews* pp. 149–160.

Srividya, B., Cardoza, R. M. and Amin, P. . (2001) 'Sustained ophthalmic delivery of ofloxacin from a pH triggered in situ gelling system.' *Journal of Controlled Release*. Elsevier, 73(2–3) pp. 205–211.

Steffe, J. F. (1996) 'Introduction to rheology.' *In Rheological Methods in Food Process Engineering*. 2nd ed., Lansing, Freeman press, pp. 1–94.

Stella, V. J., Rao, V. M., Zannou, E. A. and Zia, V. (1999) 'Mechanisms of drug release from cyclodextrin complexes.' *Advanced Drug Delivery Reviews*, 36(1) pp. 3–16.

Streubel, A., Siepmann, J., Dashevsky, A. and Bodmeier, R. (2000) 'pH-independent release of a weakly basic drug from water-insoluble and -soluble matrix tablets.' *Journal of Controlled Release*. Elsevier, 67(1) pp. 101–110.

Sworn, G., Sanderson, G. R. and Gibson, W. (1995) 'Gellan gum fluid gels.' *Topics in Catalysis*, 9(4) pp. 265–271.

Szejtli, J. (1998) 'Introduction and General Overview of Cyclodextrin Chemistry.' *Chemical Reviews*, 98(5) pp. 1743–1754.

Szekalska, M., Sosnowska, K., Czajkowska-Kósnik, A. and Winnicka, K. (2018) 'Calcium chloride modified alginate microparticles formulated by the spray drying process: A strategy to prolong the release of freely soluble drugs.' *Materials*, 11(9).

Tagha, M. (2011) 'Viscocity and Oscilltory Rheology.' *In* Norton, I. T., Spyropoulos, F., and Cox, P. (eds) *Practical Food Rheology: An Interpretive Approach*. Blackwell publishing, pp. 7–22.

Tako, M. (2015) 'The Principle of Polysaccharide Gels.' *Advances in Bioscience and Biotechnology*, 6(1) pp. 22–36.

Tanaka, E., Aoyama, J., Tanaka, M., Van Eijden, T., Sugiyama, M., Hanaoka, K., Watanabe, M. and Tanne, K. (2003) 'The proteoglycan contents of the temporomandibular joint disc influence its dynamic viscoelastic properties.' *Journal of Biomedical Materials Research - Part A*, 65(3) pp. 386–392.

Tanito, M., Hara, K., Takai, Y., Matsuoka, Y., Nishimura, N., Jansook, P., Loftsson, T., Stefánsson, E. and Ohira, A. (2011) 'Topical dexamethasone-cyclodextrin microparticle eye drops for diabetic macular edema.' *Investigative Ophthalmology and Visual Science*, 52(11) pp. 7944–7948.

Tao, S. L. and Desai, T. A. (2003) 'Microfabricated drug delivery systems: From particles to pores.' *Advanced Drug Delivery Reviews* pp. 315–328.

Taylor, C., Allen, A., Dettmar, P. W. and Pearson, J. P. (2003) 'The gel matrix of gastric mucus is maintained by a complex interplay of transient and nontransient associations.' *Biomacromolecules*, 4(4) pp. 922–927.

Thomas, L. M. (2014) 'Formulation and evaluation of floating oral in-situ gel of metronidazole.' *International Journal of Pharmacy and Pharmaceutical Sciences*, 6(10) pp. 265–269.

Treuting, M. P., Arends, J. M. and Dintzis, M. S. (2017) 'Upper Gastrointestinal Tract.' *In* Treuting, P. M., Dintzis, S. M., and S.Montine, K. (eds) *Comparative Anatomy and Histology A Mouse, Rat, and Human Atlas*. 2nd ed., Academic Press, pp. 155–175.

Turgut, E. H. and Özyazici, M. (2004) 'Bioavailability File: Metronidazole.' *Fabad J. Pharm. Sci*, 29 pp. 39–49.

Uhrich, K. E., Cannizzaro, S. M., Langer, R. S. and Shakesheff, K. M. (1999) 'Polymeric Systems for Controlled Drug Release.' *Chemical Reviews*, 99(11) pp. 3181–3198.

Uyar, T., Hunt, M. A., Gracz, H. S. and Tonelli, A. E. (2006) 'Crystalline cyclodextrin inclusion compounds formed with aromatic guests: Guest-dependent stoichiometries and hydration-sensitive crystal structures.' *Crystal Growth and Design*, 6(5) pp. 1113–1119.

Valle, D. E. M. M. (2004) 'Cyclodextrins and their uses: A review.' *Process Biochemistry*, 39(9) pp. 1033–1046.

Voet, D., Voet, J. G. and Pratt, C. W. (2006) *Fundamentals of Biochemistry: Life at the Molecular Level*. John Wiley & Sons, Inc.

Wang, Q. and Cui, S. W. (2005) 'Understanding the Conformation of Polysaccharides.' *In* CUI, S. W. (ed.) *FOOD CARBOHYDRATES Chemistry, Physical Properties, and Applications*. New York: Taylor and Francis.

Warwick, R. and Williams, P. . (eds) (1973) *Gray's Anatomy*. 35th Briti, Philadelphia.

Watase, M. and Arakawa, K. (1968) ‘Rheological Properties of Hydrogels of Agar-agar. III. Stress Relaxation of Agarose Gels.’ *Bulletin of the Chemical Society of Japan*, 41(8) pp. 1830–1834.

Waters, D. J., Engberg, K., Parke-Houben, R., Ta, C. N., Jackson, A. J., Toney, M. F. and Frank, C. W. (2011) ‘Structure and mechanism of strength enhancement in interpenetrating polymer network hydrogels.’ *Macromolecules*, 44(14) pp. 5776–5787.

Wei, G., Xu, H., Ding, P. T., Li, S. M. and Zheng, J. M. (2002) ‘Thermosetting gels with modulated gelation temperature for ophthalmic use: The rheological and gamma scintigraphic studies.’ *Journal of Controlled Release*, 83(1) pp. 65–74.

Weitz, D., Wyss, H. and Larsen, R. (2007) ‘Oscillatory rheology: Measuring the viscoelastic behaviour of soft materials.’ *GIT laboratory journal Europe*, 11(3–4) pp. 68–70.

Weng, Y., Liu, J., Jin, S., Guo, W., Liang, X. and Hu, Z. (2017) ‘Nanotechnology-based strategies for treatment of ocular disease.’ *Acta Pharmaceutica Sinica B* pp. 281–291.

Whelton, H. (1996) ‘The anatomy and physiology of the salivary glands.’ *In* Edgar, W. M. and O’Mullane, D. M. (eds) *Saliva and oral health*. 2nd ed., London: British Dental Association, pp. 1–11.

Wu, Y. and Fassihi, R. (2005) ‘Stability of metronidazole, tetracycline HCl and famotidine alone and in combination.’ *International Journal of Pharmaceutics*, 290(1–2) pp. 1–13.

Wu, Y., Liu, Y., Li, X., Kebebe, D., Zhang, B., Ren, J., Lu, J., Li, J., Du, S. and Liu, Z. (2018) ‘Research progress of in-situ gelling ophthalmic drug delivery system.’ *Asian Journal of Pharmaceutical Sciences*.

Wüstenberg, T. (2014) ‘General Overview of Food Hydrocolloids, in Cellulose and Cellulose Derivatives in the Food Industry: Fundamentals and Applications.’ *In*. 25421 Pinneberg, Germany: Wiley-VCH Verlag GmbH & Co. KGaA.

Xie, J. H., Jin, M. L., Morris, G. A., Zha, X. Q., Chen, H. Q., Yi, Y., Li, J. E., Wang, Z. J., Gao, J., Nie, S. P., Shang, P. and Xie, M. Y. (2016) ‘Advances on Bioactive Polysaccharides from Medicinal Plants.’ *Critical Reviews in Food Science and Nutrition*, 56(October) pp. S60–S84.

Xiong, W., Gao, X., Zhao, Y., Xu, H. and Yang, X. (2011) ‘The dual temperature/pH-sensitive multiphase behavior of poly(N-isopropylacrylamide-co-acrylic acid) microgels for potential application in in situ gelling system.’ *Colloids and Surfaces B: Biointerfaces*. Elsevier B.V., 84(1) pp. 103–110.

Xu, Q. A. and Madden, T. L. (2010) *Analytical Methods for Therapeutic Drug Monitoring and Toxicology*. *Analytical Methods for Therapeutic Drug Monitoring and Toxicology*. New Jersey: John Wiley & Sons, Inc.

Young, K. A., Wise, J. A., DeSaix, P., Kruse, D. H., Poe, B., Johnson, E., Johnson, J. E., Korol, O., Betts, J. G. and Womble, M. (2013) ‘The Digestive System.’ *In Anatomy & Physiology*. Houston: OpenStax College, pp. 1022–1056.

Youssef, N. A. H. A., Kassem, A. A., El-Massik, M. A. E. and Boraie, N. A. (2015) 'Development of gastroretentive metronidazole floating raft system for targeting Helicobacter pylori.' *International Journal of Pharmaceutics*, 486(1–2) pp. 297–305.

Yuguchi, Y., Thu Thuy, T. T., Urakawa, H. and Kajiwara, K. (2002) 'Structural characteristics of carrageenan gels: Temperature and concentration dependence.' *Food Hydrocolloids*, 16(6) pp. 515–522.

Zatz, J. L. and Woodford, D. W. (1987) 'Prolonged release of theophylline from aqueous suspensions.' *Drug Development and Industrial Pharmacy*, 13(12) pp. 2159–2178.

Zhang, J., Wang, L., Gao, C., Zhang, L. and Xia, H. (2008) 'Ocular Pharmacokinetics of Topically-Applied Ketoconazole Solution Containing Hydroxypropyl Beta-Cyclodextrin to Rabbits.' *Journal of Ocular Pharmacology and Therapeutics*, 24(5) pp. 501–506.